Ministério da Saúde

FIOCRUZ
Fundação Oswaldo Cruz

INSTITUTO OSWALDO CRUZ
Pós-Graduação em Biologia Celular e Molecular

Ilya Violeta Llanos Salamanca

MOLECULAR INSIGHTS INTO THE INNATE IMMUNE RESPONSES OF *LUTZOMYIA LONGIPALPIS* TO *LEISHMANIA* AND VIRUS.

Tese apresentada ao Instituto Oswaldo Cruz como parte dos requisitos para obtenção do título de Doutor em Biologia Celular e Molecular

Orientadora: Dra. Yara Maria Traub-Csekö

RIO DE JANEIRO
2018

LLANOS SALAMANCA, ILYA VIOLETA.

MOLECULAR INSIGHTS INTO THE INNATE IMMUNE RESPONSES OF LUTZOMYIA LONGIPALPIS TO LEISHMANIA AND VIRUS. / ILYA VIOLETA LLANOS SALAMANCA. - Rio de janeiro, 2018.
158 f.

Tese (Doutorado) – Instituto Oswaldo Cruz, Pós-Graduação em Biologia Celular e Molecular, 2018.

Orientador: Yara Maria Traub-Csekö.

Bibliografia: f. 93-117

1. Lutzomyia longipalpis. 2. Imunidade inata. 3. Resposta antiviral. 4. Exossomos. 5. Leishmania RNA Virus. I. Título.

Ministério da Saúde

FIOCRUZ
Fundação Oswaldo Cruz

INSTITUTO OSWALDO CRUZ

Pós-Graduação em Biologia Celular e Molecular

AUTOR: Ilya Violeta Llanos Salamanca

MOLECULAR INSIGHTS INTO THE INNATE IMMUNE RESPONSES OF *LUTZOMYIA LONGIPALPIS* TO *LEISHMANIA* AND VIRUS.

ORIENTADORA: Dra. Yara Maria Traub-Csekö

Aprovada em: 31/ 10/ 2018

EXAMINADORES:

Prof. Dr. Elisa Cupolillo – IOC/FIOCRUZ **- Presidente**
Prof. Dr. Mauricio Roberto Viana Sant'Anna – UFMG/MG
Prof. Dr. André Nobrega Pitaluga – IOC/FIOCRUZ
Prof. Dra. Rafaela Vieira Bruno – IOC/FIOCRUZ
Prof. Dr. Carlos Roberto Alves – IOC/FIOCRUZ

Rio de Janeiro, 31 de Outubro de 2018

ACKNOWLEDGEMENTS

First, I must acknowledge my supervisor, Dr Yara M. Traub-Csekö, who four years ago gave me the chance to be part of her renowned research group and laboratory, and opened the door for such a great experience that this PhD has been. I thank her immensely for the advice, guidance, and support, not only in research and work matters but also at personal level. It was truly an honour and a privilege to have you as my supervisor.

Countless thanks go to Erich Telleria; without your help, advice and numerous conversations about experiments, results and how to make the best of my time in the lab, my PhD certainly would have been much harder. I would also take the chance here to recognize, that your support, advice and company transcended the lab environment and help me at a personal level and I consider you one of my most valuable friends. Also many thanks for always welcoming David and I at your house and giving us the chance to have family moments, while we were away from our own for such a long time. For all that and more, muchas gracias Erich!.

I would also like to thank to Dr. Antonio Tempone, who was always ready to offer suggestions and advice about my project, enriching with questions and analysis my results throughout my time at the lab.

To Andrea Martins, many thanks for introducing me into the project techniques and experimental protocols when I started at the lab, for your friendship and advice in those moments that were most needed.

I also extend my gratitude to Dr Fabricio Marchini and Michel Batista from the Proteomic Platform at Carlos Chagas Institute in Curitiba, for the opportunity to develop part of my research project at their institute, for their continuous help in my data analysis and support.

To Dr Elisa Cupolillo, thanks for providing *L. (V.). guyanensis* strains, information and help in the development of the experiments with these strains.

To all the students in the lab, some of them already gone, Tati, Andrés, Daniel, João, Guilherme, Lívia, Gabriel, Daisy, thank you for all your help, contributions and kind words, to Marina my immense gratitude for helping me to find a place to live during my first week in Rio and showing me the city. Special thanks to Thais and Monique for your help in the lab, especially in these last months, your support and cheering words to keep the mood up. To Bianca and Daiana many thanks; my project would not have been possible without the good care you provided to our colony. To Professor Marcelo Riveiro-Alves for his valuable statistical advice about my data. To Dona Marissa and Sinara, that always had a nice word and a smile to offer every morning, even if

it was 6a.m. Their kindness, blessings and encouraging words towards David and me, is something I will miss.

I also extend my gratitude to the people of the post-graduation secretary, particularly Julimar and Clarissa, for helping with all the bureaucratic problems throughout these four years.

I am extremely grateful for the financial support provided by CNPq during my PhD, none of this could have been possible without their support.

And last, but not least, to my family, even though I only had the chance to visit them once during these four years, my family has always been there with me, their support, advice and video calls were invaluable. And the utmost "thank you" of all goes to David, my husband, friend and confidant. These four year have definitely change me in many ways and I believe that a lot of that is thanks to you. You have helped me to be a better person, to know myself better and to grow up. Thank you for your infinite patience and encouraging words in my hard times. Thank you for being with me. I love you.

Thank you all!...

MOLECULAR INSIGHTS INTO THE INNATE IMMUNE RESPONSES OF *LUTZOMYIA LONGIPALPIS* TO *LEISHMANIA* AND VIRUS.

ABSTRACT

Phlebotomine sand flies are well known vectors of leishmaniasis. One severe manifestation of this disease is visceral leishmaniasis (VL). In the Americas approximately 96% of the cases are concentrated in Brazil, making it an important public health issue. In Brazil the agent for VL is *L. infantum (syn. chagasi)* and *L. longipalpis* its principal vector. *L. longipalpis* can also transmit bacteria and virus, and research on basic immune systems and responses to different pathogens is important to better understand vector-pathogen interactions, that could provide tools for alternative vector control and transmission blocking approaches.

Previous studies in our laboratory identified a non-specific antiviral response in the *L. longipalpis* cell line LL5 after stimulation with dsRNA. To further understand the mechanisms of this immune response, proteomic analysis of exosomes from Poly(I:C) -dsRNA mimic- and mock transfected cells was carried out, and a relative gene expression of several immune genes in the cells was assessed by qPCR. Exosomes from Poly(I:C) transfected cells have 40 exclusive proteins, several associated to a non-specific antiviral response similar to INF response in mammals and that canonical innate immune pathways are not involve in the response. These results, are in line with a recent proteomic study on the conditioned media of Poly(I:C) stimulated LL5 cells.

Previous studies from our laboratory showed that silencing of cactus – the major negative regulator of the Toll pathway - in LL5 cells elicits an activation of the pathway. Nevertheless, the opposite result was observed when cactus was silenced in adult sand flies. The existence of a negative regulatory loop involving WntD gene was proposed. The silencing of cactus and/or WntD in adult sand flies was carried out, showing that in cactus silenced flies AMPs, as well as dorsal expression, was reduced, but not significantly. WntD silenced flies had no significant modulation of AMPs or dorsal. Curiously, a synchronicity between cactus and dorsal expression was observed, leading to the *in silico* identification of four transcription factor binding sites for NF-kB in the upstream region of cactus gene, indicating possible auto-regulation through dorsal. The Toll pathway regulation appears to be complex in adult *L. longipalpis*.

In the last decade, the severity of cutaneous/mucocutaneous leishmaniasis in the Americas was linked to the presence of a viral endosymbiont, Leishmania RNA Virus 1 (LRV1), in some *Leishmania* species. The effect of LRV1 presence in *L. guyanensis* on *L. longipalpis* infection was evaluated. Both LL5 cells and adult females were exposed to parasites containing or not LRV1. *In vitro* experiments showed that the presence of LRV1 down regulates molecules from canonical immune pathways and modulate some non-specific antiviral response related molecules that could favour survival of the LRV1+ parasite. In female insects, LRV1+ parasites had a significantly increased parasite load. Only one molecule, defensin1, was downregulated in the presence of LRV1. Also, despite increased parasite numbers none of the pathways evaluated showed important activation, suggesting that retention of LRV1 in *L. guyanensis* could also provide advantages in the insect host but by impairing any exacerbated response from the insect and improving its replication rate or survival. We expect that these data lead to a better understanding of sand fly immunity and its interaction with other pathogens.

MOLECULAR INSIGHTS INTO THE INNATE IMMUNE RESPONSES OF *LUTZOMYIA LONGIPALPIS* TO *LEISHMANIA* AND VIRUS.

RESUMO

Os flebotomíneos são vetores das leishmanioses. Uma manifestação grave da doença é a leishmaniose visceral (LV). Nas Américas, aproximadamente 96% dos casos estão concentrados no Brasil, tornando-se um importante problema de saúde pública. No Brasil, o principal agente da LV é *L. infantum (Sin. chagasi)* e *L. longipalpis* seu vetor. *L. longipalpis* também pode transmitir bactérias e vírus. Pesquisas sobre sistemas imunológicos básicos e respostas a diferentes patógenos são importantes para entender melhor as interações vetor-patógeno, que podem fornecer ferramentas alternativas para controle de vetores e novas abordagens de bloqueio de transmissão.

Estudos anteriores em nosso laboratório identificaram uma resposta antiviral não específica na linhagem de células LL5 de *L. longipalpis* após estímulo com dsRNA. Para entender melhor os mecanismos dessa resposta imune, procedeu-se à análise proteômica de exossomos de células transfectadas com Poly (I:C) -mimetizante de dsRNA- e "mock"-transfectadas. A avalição transcricional de genes de imunidade das células foi realizada por qPCR. Os exossomos das células transfectadas com Poly (I:C) possuem 40 proteínas exclusivas, várias associadas a uma resposta antiviral não específica semelhante à resposta ao interferon em mamíferos. As vias imunes inatas canônicas não parecem estar envolvidas na resposta. Estes resultados estão de acordo com um estudo proteômico recente sobre o meio condicionado de células LL5 estimuladas com Poly (I:C).

Estudos anteriores do nosso laboratório mostraram que o silenciamento de cactus - o principal regulador negativo da via do Toll - nas células LL5 desencadeia uma ativação da via. No entanto, o resultado oposto foi observado quando cactus foi silenciado em flebotomíneos adultos. A existência de uma alça regulatória negativa envolvendo o gene WntD foi proposta. O silenciamento de cactus e/ou WntD em flebotomíneos adultos foi realizado, mostrando que em insetos silenciadas, os AMPs, assim como a expressão de dorsal, foram reduzidos, mas não significativamente. Flebotomíneos silenciados para WntD não tiveram modulação significativa de AMPs ou dorsal. Curiosamente, foi observada uma sincronicidade entre a expressão de cactus e dorsal, levando à identificação in silico de quatro sítios de ligação para o fator de transcrição NF-kB na região a montante do gene do cactus, indicando possível auto-regulação através do dorsal. A regulação da via Toll parece ser complexa em *L. longipalpis* adulta.

Na última década, a gravidade da leishmaniose cutânea/mucocutânea nas Américas foi associada à presença de um endossimbionte viral, o Leishmania RNA Virus 1 (LRV1), em algumas espécies de *Leishmania*. O efeito da presença de LRV1 em *L. guyanensis* na infecção por *L. longipalpis* foi avaliado. Tanto as células LL5 quanto fêmeas foram expostas a parasitas contendo ou não LRV1. Experiências *in vitro* mostraram que a presença de LRV1 regula moléculas de vias imunes canônicas e modula algumas moléculas não específicas relacionadas à resposta antiviral que poderiam favorecer a sobrevivência do parasita LRV1+. Em fêmeas, os parasitas LRV1+ tiveram um aumento significativo da carga parasitária. Apenas a defensina 1, foi diminuída na presença de LRV1. Apesar do aumento do número de parasitas, nenhuma das vias avaliadas mostrou ativação importante, sugerindo que a retenção de LRV1 em *L. guyanensis* também poderia dar vantagens ao parasita no inseto, diminuindo uma resposta exacerbada do inseto e melhorando sua taxa de replicação ou sobrevivência. Esperamos que esses dados levem a um melhor entendimento da imunidade de flebotomíneos e sua interação com outros patógenos.

INDEX

LIST OF ABREVIATIONS AND SIMBOLS

AMP	Antimicrobial peptide
AP-1	Activator protein 1
BLAST	Basic Local Alignment Search Tool
bp	Base pairs
cDNA	Complementary DNA
CHPV	Chandipura virus
CL	Cutaneous leishmaniasis
CrPV	Cricket paralisis virus
DCV	Drosophila C Virus
DENV	Dengue virus
Dl	Dorsal
DMSO	Dimethyl sulfoxide
DNA	Deoxyribonucleic acid
dNTP	Deoxyribonucleotide triphosphate
dsRNA	Double strand RNA
FBS	Foetal bovine serum
Hsp	Heat shock protein
IAV	Influenza A virus
IFN	Interferon
IMD	Immune deficiency
ISFV	Isfahan virus
JAK/STAT	Janus kinase/signal transducers and activators of transcription
JNK	c-Jun N-terminal Kinase
kb	Kilobase
kDa	Kilodalton
L	Litre
LC-MS/MS	Liquid chromatography tandem-mass spectrometry
LCAT	Lecithin cholesterol acyltransferase
Lg(LRV1+)	Leishmania guyanensis positive for LRV1
Lg(LRV1+)	Leishmania guyanensis negative for LRV1
LL5	Lutzomyia longipalpis embryonic cell line

LRR	Leucin rich repeat
LRV1	Leishmania RNA virus 1
LTQ	Linear Trap Quadrupole
M	Molar
M	Mock
MCL	Mucocutaneous leishmaniasis
MDA5	Melanoma Differentiation-Associated protein 5
Min	Minute(s)
mL	Millilitre
mM	Millimolar
mm	Millimetre
NF-kB	Nuclear factor kappa-light-chain-enhancer of activated B cells
ng	Nanogram
nM	Nanomolar
ºC	Degrees Celsius
PAMP	Pathogen-associated molecular pattern
PBS	Phosphate Buffered Saline
PCA	Principal component analysis
PCR	Polymerase Chain Reaction
PGRP	Peptidoglycan recognition protein
PM	Peritrophic matrix
Poly (I:C)	Polyinosinic:polycytidilic acid
PRR	Pattern recognition receptor
qPCR	Quantitative PCR
qRT-PCR	Quantitative reverse transcriptase PCR
RIG-I	Retinoic acid inducible gene I
RLR	RIG-I like receptor
RNA	Ribonucleic acid
RNAi	RNA interference
rpm	Revolutions per minute
SFNV	Sand fly fever Naples virus
SFSV	Sand fly fever Sicilian virus

SHP-1	Src homology-2 containing protein tyrosine phosphatase 1
SINV	Sindvis Virus
Spz	Spätzle
ssRNA	Single strand RNA
STAT	Signal transducers and activators of transcription
T	Transfected
TFBS	Transcription Factor Binding Site
TLR	Toll-like receptor
TNF	Tumour necrosis factor
TOSV	Toscana virus
TPB	Tryptose phosphate broth
TRANSK	Transketolase
U	Unit
Upd	Unpaired
VIR-1	Virus induced RNA-1
VL	Visceral leishmaniasis
VLP	Virus-like particle
VSV	Vesicular stomatitis virus
WHO	World Health Organization
WntD	Wnt inhibitor of Dorsal
WNV	West Nile virus
xg	Times gravity
βGal	Beta galactosidase
µ	Micro
µg	Microgram
µL	Microlitre
µM	Micromolar

FIGURE INDEX

TABLE INDEX

1 GENERAL INTRODUCTION

1.1 SAND FLIES

Sand flies are included in the order Diptera, suborder Nematocera, family Psychodidae, and subfamily Phlebotominae. The classification system from Young and Duncan (Young and Duncan 1994) and Galati (Galati et al. 2003) are generally used, although many have been described (reviewed in Akhoundi et al. 2016). Galati published a new revision on her work, where Phlebotomini tribe included 931 existent species (916 valid species and 15 with uncertain taxonomic status) (Galati 2014). Presently, the subdivision of the Phlebotominae into six genera is widely used: three of them from the Old World (*Phlebotomus, Serentomyia* and *Chinius* and three form the New World (*Lutzomyia, Brumtomyia* and *Warileya*) (Lane 1993; Young and Duncan 1994). Phlebotomines are found in the subtropical and tropical regions with some species spread into temperate regions and are completely absent in New Zealand and Pacific islands. Sand flies occur in a very wide range of habitats, from sea level to altitudes of 2800 m or more in the Andes and Ethiopia, and from hot dry deserts, through savannas and open woodland to dense tropical rain forest. In general, every species has rather specific ecological needs and in a few cases these involve the conditions in and around the dwellings of man or his domestic animals (Lane 1993; Akhoundi et al. 2016). The genus *Lutzomyia* (França and Parrot 1921), contains nearly 434 species and several sub-genera, making it more diverse than the Old World genera. *Lutzomyia* is the most important genus in terms of diversity and medical impact and presents a wide distribution area (Akhoundi et al. 2016). *L. longipalpis* was originally described by Lutz and Neiva (1912) from specimens collected in the state of São Paulo and Benjamin Constant (Minas Gerais) Brazil. *L. longipalpis* has a geographical distribution that extends from Mexico to Argentina. Although distribution pattern is more patchy than continuous, sand flies are mainly associated to dry habitats in Central and northern South America. Nevertheless, it is also related to humid forest in the Amazon river basin (Lainson et al. 1985; Lanzaro et al. 1993; Dujardin et al. 2008). Lanzaro et al. (1993) suggested that genetic divergence caused by genetic drift and/or selection may affect vectorial capacity resulting in some populations being more efficient vectors than others. Variability among populations of *L. longipalpis* has been observed at numerous levels including morphological, molecular and biochemical (reviewed in Bauzer et al. 2007).

Phlebotomines are mostly known as vectors of *Leishmania*, protozoan parasites which cause leishmaniasis in humans. However, they also transmit the bacteria that causes bartonellosis and several viral agents.

1.2 PATHOGENS TRANSMITTED BY SAND FLIES.

1.2.1 Bacteria (Bartonella)

For a long time there was only one recognized Bartonella species (*Bartonella bacilliformis*), although there are now over 36 known species, of which 17 have been associated with an expanding spectrum of animal and human diseases. Recent advances in diagnostic techniques have facilitated documentation of chronic bloodstream and dermatological infections with Bartonella spp. (Breitschwerdt 2017).

B. bacilliformis is a small Gram-negative, facultative intracellular, aerobic coccobacillus which is a member of the alpha-proteobacteria group (order Rhizobiales, family Bartonellaceae) along with Rickettsia and Brucella. Bartonella organisms are widely dispersed in nature (Maguiña and Gotuzzo 2000; Sanchez Clemente et al. 2012; Silaghi et al. 2016). *B. bacilliformis* is responsible for one disease, that despite its limited distribution, has been given a multitude of names including bartonellosis, Carrion's disease, Oroya fever, Guaytara fever and verruga peruana. The disease is restricted to the Andean cordillera in Peru, Ecuador, and Colombia (Maguiña and Gotuzzo 2000; Sanchez Clemente et al. 2012).

In the Andean region, *B. bacilliformis* is naturally transmitted by sand flies belonging to the *Lutzomyia* genus, mainly *Lutzomyia verrucarum*, but also *Lutzomyia peruensis*. These sand flies are present in the inter-Andean valleys, although the illness is also present in areas where these vectors are absent, suggesting the presence of vectors not reported yet. Additionally, since the late 1990s, a continuous expansion of the illness to areas previously considered free, including coastal and high jungle areas, has been evident. This spread has been associated with climate change, which, together with human activities, is probably affecting vector distribution and expansion (Pons et al. 2016). Moreover, the possibility that *Lutzomyia* spp. living in non-endemic areas could become competent vectors of *B. bacilliformis* should be kept in mind, (Minnick et al. 2014; Pons et al. 2016).

Once a susceptible person is bitten by a *Bartonella* infected sand fly, infection may be asymptomatic, or the person may experience mild to severe disease. The disease has two stages, anaemic (Oroya fever) and eruptive (Peruvian wart), with an asymptomatic intermediate period. After an incubation period in average of about 60 days, acute infection results in bacteraemia (Oroya fever) with symptoms that include malaise, fever and headache, having a reported mortality of 44% to 88% in untreated individuals (Maguiña and Gotuzzo 2000; Maguiña et al. 2009). In the following phase, which may occur weeks to months after the acute illness, *B. bacilliformis* induce

endothelial cell proliferation, producing skin lesions called Peruvian warts with very low lethality (Sanchez Clemente et al. 2012; Minnick et al. 2014). Additionally, the presence of asymptomatic carriers is frequent, although the real numbers remain uncertain because of the difficulty in detecting these subjects (Minnick et al. 2014; Pons et al. 2016).

To date, no single treatment is effective for all Bartonella-associated diseases. In the absence of systematic reviews, treatment decisions for Bartonella infections are based on case reports that test a limited number of patients (Angelakis and Raoult 2014; Breitschwerdt 2017).

1.2.2 Leishmania

Leishmania parasites belong to the Order Trypanosomatida (Saville-Kent 1880), Family Trypanosomatidae (Döflein 1901), Subfamily Leishmaniinae (Jirků et al. 2012), and Genus *Leishmania* (Ross 1903). *Leishmania* species are heteroxenous, meaning that they required more than one host to complete the life cycle. They live in the phagocytes of the reticulum-endothelial system of mammals and in the intestinal tract of phlebotomine sand flies. Mammalian *Leishmania* species exhibit a worldwide distribution. They are present in tropical and subtropical areas, including North, Central, and South America, as well as in the Mediterranean basin, Southeast Europe, the Middle East, Central and Southeast Asia, the Indian subcontinent, Africa, and recent reports also demonstrate their presence in Australia (Akhoundi et al. 2016).

New classification for *Leishmania* has been proposed based on combined molecular data, which divides *Leishmania* species into two major phylogenetic lineages referred to as sections Euleishmania and Paraleishmania (Cupolillo et al. 2000). The section Euleishmania comprises four subgenera: *L.* (*Leishmania)* (type strain: *Leishmanina donovani*), *L.* (*Viannia)* (type strain: *Leishmania braziliensis*), *L.* (*Sauroleishmania)* (type strain: *Leishmania tarentolae*), and *Leishmanaia enriettii* complex (type strain: *Leishmania enriettii*). Section Paraleishmania includes *Leishmaia hertigi, Leishmania deanei, Leishmania herreri, Leishmania equatorensis*, and *Leishmania colombiensis* as well as the former *Endotrypanum* genus. Of this group, only *L. colombiensis* was found to be pathogenic to humans (Akhoundi et al. 2016).

The subgenus *Viannia* is limited to the Neotropics, while the subgenus *Leishmania* occurs in both the New and Old World. Fifty-three named species (without synonyms, including all five subgenera and complexes: *L.* (*Leishmania), L. (Viannia), L. (Sauroleishmania), L. enrittii* complex, and Paraleishmania) are recognized, 29 of which are present in the Old World, 20 in the New World, three species *("Leishmania siamensis", Leishmania martiniquensis, and Leishmania infantum*) in both Old and New World, and one species in Australia ("*Leishmania australiensis")*.

Names in quotation marks indicate that their taxonomic validity is under discussion (Akhoundi et al. 2016). Amongst these recognized species, 20 (without synonyms) are known to infect humans (Maroli et al. 2013).

Most *Leishmania* transmission, in the Old World, occurs peri-domestically in semiarid areas altered by humans, while New World parasites are frequently associated with sylvatic habitats, though some species exhibit predominately peri-domestic transmission. Host preference is also a main factor that affects the modality of *Leishmania* transmission by vectors that prefer feeding in areas with wild animals (sylvatic), or with animals and people (peridomestic), or only people (urban) (Alvar et al. 2012).

Incrimination of sand flies as proven or potential vectors of *Leishmania* is a controversial and debated matter. Killick-Kendrick et al. (1986) specified five criteria as a requirement to incriminate a particular sand fly species as a vector, which include the observation of epidemiological data, feeding behaviour of the sand flies on the intermediate host, the isolation of promastigote parasites from the sand flies, the existence of the complete life cycle of the parasite in its putative vector and experimental transmission of the parasite through the bite of the infected species; recently detection of *Leishmania* DNA by PCR in the insect was included (Akhoundi et al. 2016).

Approximately 166 sand fly species have been reported to be proven or potential vectors of different *Leishmania* species in the Old and New World. Among these species, 78 are reported as confirmed vectors of *Leishmania*. In the Old World, *Leishmania* parasites are transmitted by sand flies from the *Phlebotomus* genus (49 species, 31 are reported as proven). In the New World, *L. (Leishmania), L. (Viannia)* and *Endotrypanum* species are transmitted by sand flies from the *Lutzomyia* genus (118 species, 47 are reported proven) (Akhoundi et al. 2016). Demonstration of *L. longipalpis* as a vector for New World *Leishmania infantum* (syn. *chagasi*) was made by Lainson et al. (1977).

1.2.2.1 *Leishmania* life cycle

The female sand fly regurgitates infective promastigotes into a susceptible mammal during blood feeding. These promastigotes are quickly taken by resident phagocytes, transformed into tissue-stage amastigotes, and divide through simple division in the parasitophorous vacuole (Figure 1.2-1). Depending on host and parasite factors, the parasite infects additional phagocytic cells either at the site of cutaneous infection or in secondary lymphoid organs, with subsequent parasitaemia. Sand flies become infected through feeding on a host either with an active skin lesion in cutaneous

leishmaniasis or with parasitaemia in visceral leishmaniasis (Esch and Petersen 2013). See Figure 1.2-1 for complete representation of the *Leishmania* life cycle.

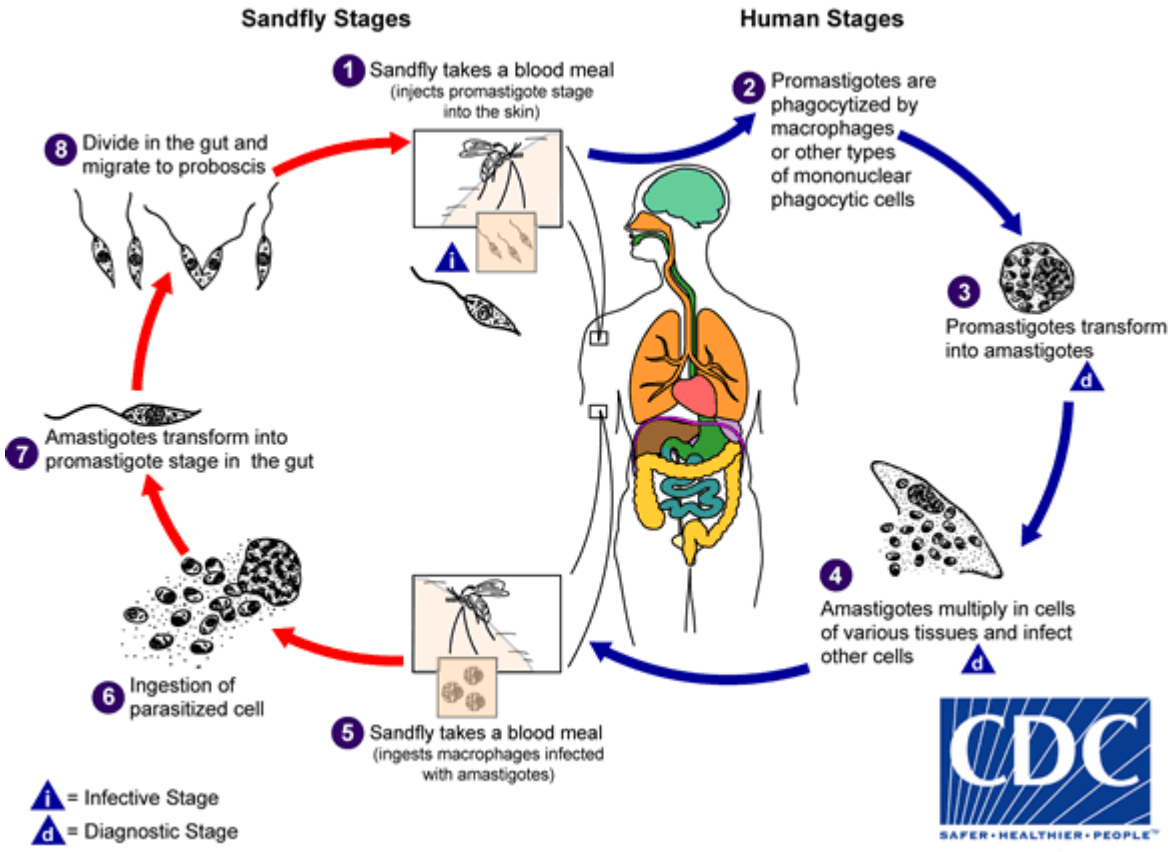

Figure 1.2-1 *Leishmania*sis is transmitted by the bite of infected female phlebotomine sand flies. For detailed description refer to text. Taken from https://www.cdc.gov/parasites/leishmaniasis/biology.html

Leishmania development in the sand fly vector is confined to the digestive tract of the insect. This tract consist of three major parts, foregut (stomodeum), midgut (mesenteron) and hindgut (proctodeum) (Figure 1.2-2A). Promastigotes of the subgenus *L.* (*Leishmania)* develop exclusively in the midgut (and eventually in the foregut), and have thus been called Suprapylaria (reviewed in Killick-Kendrick 1979). In contrast, promastigotes of parasites from the subgenera *L.* (*Vianni)a* and *L.* (*Sauroleishmania)* move posteriorly and attach to the chitin lining of the pylorus region (as haptomonads), (Lainson et al. 1977b; Walters et al. 1993). The infective blood meal containing *Leishmania* amastigotes is passed into the abdominal midgut, where water is removed and blood is retained inside the peritrophic matrix (PM). The amastigotes ingested along with the blood meal transform first in procyclic promastigotes and remain short, ovoid and only slightly motile. During blood digestion intense replication of these forms occur accompanied by the transformation of the promastigotes to a long, slender, highly motile form called nectomonads (Sacks and Kamhawi 2001). At the end of the digestion process, which happens approximately 72h

after blood meal, sand fly chitinases (Ramalho-Ortigão and Traub-Csekö 2003; Ramalho-Ortigão et al. 2005) disintegrate the PM (Sádlová and Volf 2009). The kinetics of PM synthesis and disintegration differs between sand fly species (Walters et al. 1993; Pruzinova et al. 2015) as does the period between PM breakdown and defecation. After the PM disintegrates, the nectomonads must attach themselves to the midgut wall to avoid being expelled with the blood meal remnants (Dvorak et al. 2018). The next parasite stage are replicative short nectomonads called leptomonads that accumulate in large numbers in the thoracic part of the midgut and produce promastigote secretory gel (PSG) (Stierhotf et al. 1999). This PSG, together with parasite masses, obstruct the gut creating a gel-like plug (Rogers et al. 2002). Leptomonads transform either to metacyclics or haptomonads. Metacyclic parasites are small and highly motile forms with long flagella, and are highly infective for vertebrate hosts (Perkins and Sacks 1985; Rogers et al. 2002). Haptomonads attach to the cuticular lining of the stomodeal valve causing damage to the structure, interfering with its function and facilitating reflux of parasites from the midgut (Figure 1.2-2A) (Schlein et al. 1992). Recently, Serafim et al. (2018) revealed how *Leishmania* infections in the sand fly gut are massively amplified following successive blood meals and identified a new stage in the life cycle that is responsible for this amplification. The key finding reported by the group is that metacyclic promastigotes are capable of de-differentiation in the sand fly (into retroleptomonads), enhancing population growth of parasites in a second blood meal, and leading to a sand fly with an even greater potential to transmit disease than following a first infected blood meal (Figure 1.2-2B).

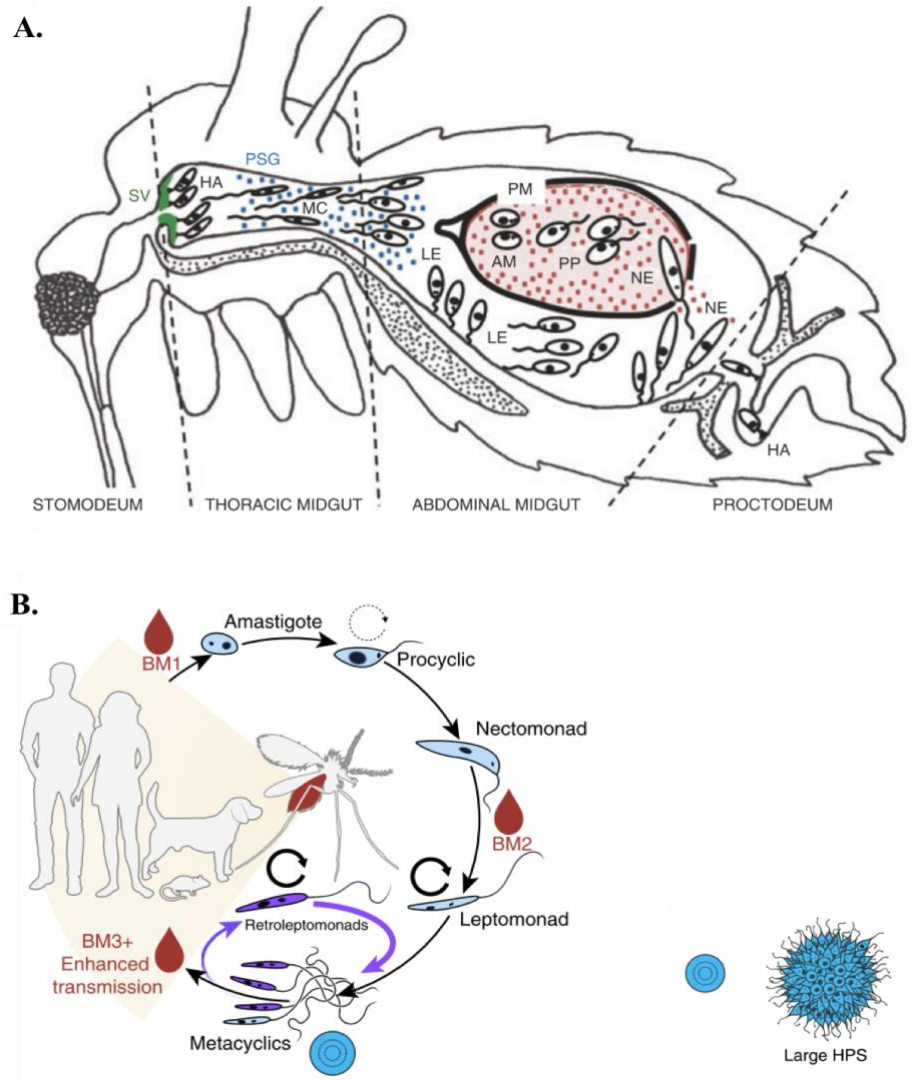

Figure 1.2-2 Sand fly digestive tract and *Leishmania* development in the vector. A) For detailed description of *Leishmania* development in the fly gut refer to the text. Amastigotes (AM), peritrophic matrix (PM), procyclic promastigotes (PP), nectomonads (NE), leptomonads (LE = short nectomonads), haptomonads (HA), promastigote secretory gel (PSG), metacyclics (MC), stomodeal valve (SV). Taken from (Dvorak et al. 2018). B) Subsequent blood meals promote *Leishmania* establishment by triggering metacyclic dedifferentiation into multiplicative retroleptomonads amplifying their numbers. Circular arrows depict a multiplicative stage. Blue circles represent the HPS (Haptomonasformation and development in each scenario. Taken from (Serafim et al. 2018)

1.2.2.2 ***Leishmania*sis**

Out of the 53 *Leishmania* species that have been described, 31 species are known to be parasites of mammals and 20 species are pathogenic for humans. *Leishmania* parasites cause four main clinical forms of the disease – according to the location of the parasite in mammalian tissues – indicated as visceral, cutaneous, diffuse cutaneous and mucocutaneous leishmaniasis (Akhoundi et al. 2016; WHO 2017).

*Cutaneous leishmaniasis (CL):*it is a zoonotic disease, including various wild animals and humans as vertebrate hosts and different sand fly species as vectors playing a part in *Leishmania* transmission. CL is the most common form of the disease and the countries of Afghanistan, Algeria,

Colombia, Brazil, Iran, Syria, Ethiopia, North Sudan, Costa Rica, and Peru together account for 70% to 75% of the global estimated CL incidence (Figure 1.2-3) (Alvar et al. 2012). From 2001 to 2016, 892,846 new CL cases distributed in 17 of the 18 endemic countries in the Americas were reported to PAHO/WHO. In 2016 alone, endemic countries reported 48,915 CL/ML cases, the highest numbers were registered by Brazil (12,690), Colombia (10,966), Nicaragua (5,423) and Peru (7,271), which together account for 74.3% of the total number of cases in the region (Figure 1.2-4) (PAHO/WHO 2018). Generally, this form of the disease produces ulcers on the unprotected parts of the body, including the face, arms and legs. *Leishmania* species that are accountable for CL vary between the Old and New World. Etiological agents of CL in the Old World involve *L. tropica, L. major,* and *L. aethiopica,* while New World CL is caused by parasites of the *Leishmania mexicana* complex *(L. mexicana, L. amazonensis, L. pifanoi, L. garnhami,* and *L. venezuelensis)* or the subgenus *L. (Viannia) (L. braziliensis, L. guyanensis, L. panamensis, L. naiffi, L. shawi, L. lainsoni,* and *L. peruviana*) (Akhoundi et al. 2016).

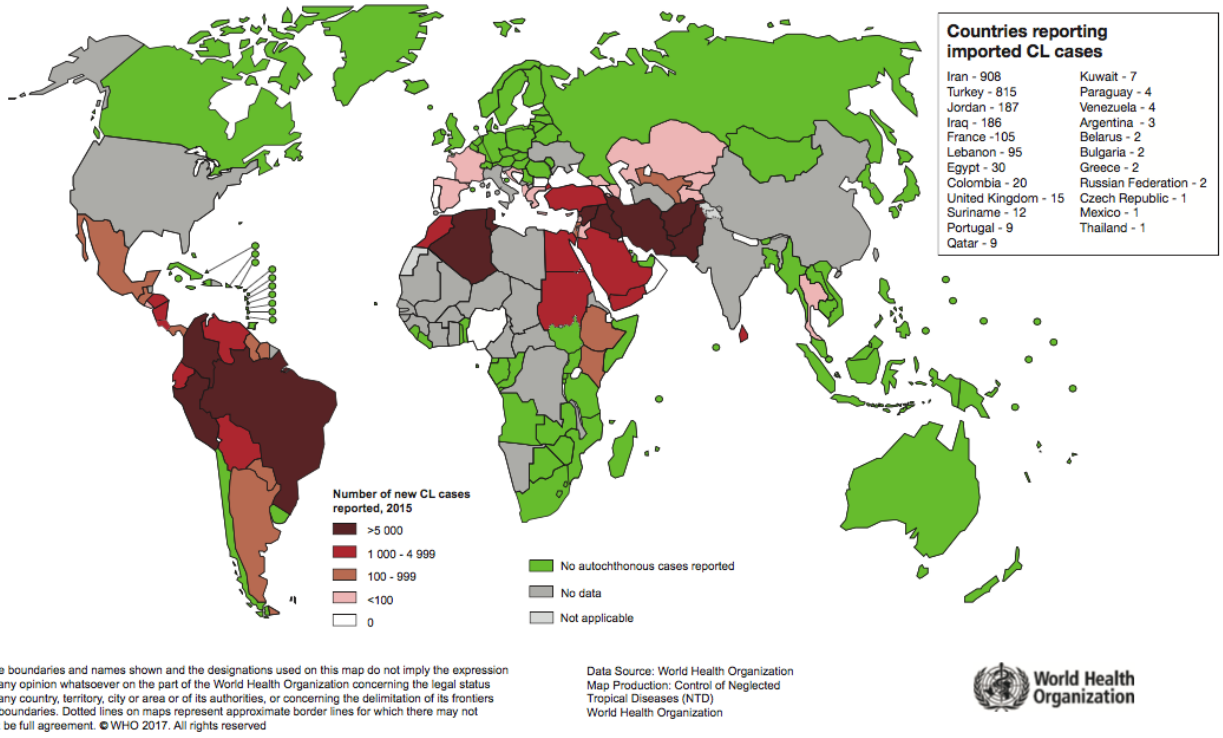

Figure 1.2-3 Status of endemicity of Cutaneous *Leishmania*sis worldwide, 2018. From WHO, 2018. http://www.who.int/leishmaniasis/burden/en/

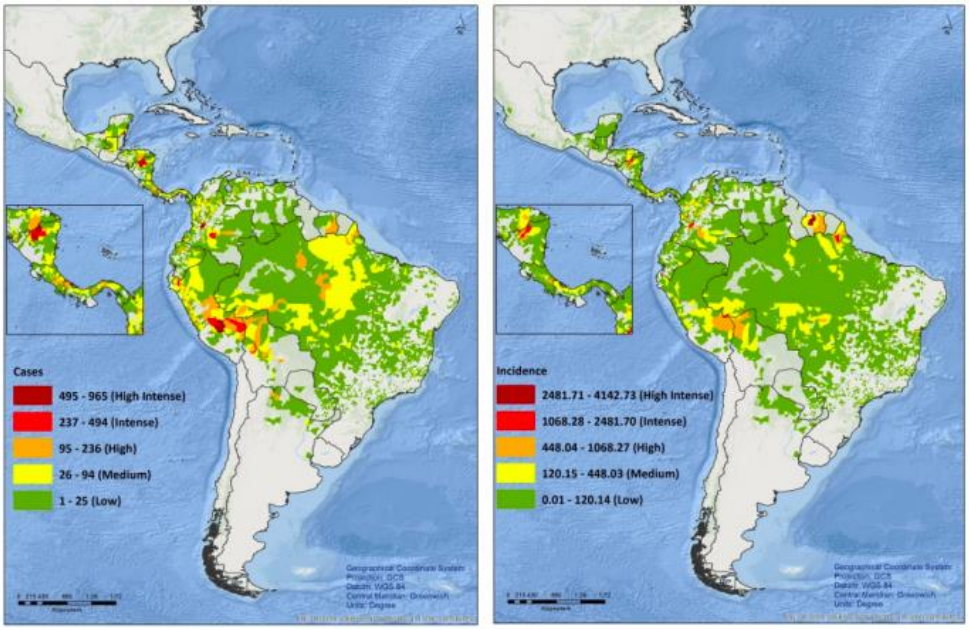

Figure 1.2-4 Cutaneous *Leishmania*sis Cases and incidence stratified by risk of transmission, Americas 2016. Source: SisLeish – PAHO/WHO: Data reported by the National *Leishmania*sis Programs / Surveillance Services. Adapted from (PAHO/WHO 2018)

Diffuse cutaneous leishmaniasis (DCL): this form of the disease was first reported in Kenya in 1969. DCL is characterized by the presentation of a large number of lesions at various anatomic sites. Lesions include papules, nodules and areas of diffuse infiltration that do not ulcerate and bear abundant parasites on histopathological examination (Bryceson 1969). DCL is a long-lasting disease due to a deficient cellular-mediated immune response in the host, lesions never heal spontaneously and the disease is subject to relapse after treatment with any of the currently available drugs (Desjeux 2004). The causative agent is *L. aethiopica*, which is transmitted by *Phlebotomus pedifer* and *Phlebotomus longipes*. Nonetheless, in the New World DCL has also been reportedly caused by *L. amazonensis*, transmitted by *Lutzomyia*-group Olmeca (Akhoundi et al. 2016).

Mucocutaneous leishmaniasis (MCL), also called espundia, happens exclusively in South America, presenting a higher incidence in Perú, Bolivia, Paraguay, Ecuador, Colombia, Brazil and Venezuela (Akhoundi et al. 2016). Classical mucosal lesions occurring are highly destructive, severely disfiguring, and potentially deadly. Typical lesions are ulcerated and often lead to septum perforation (Strazzulla et al. 2013). The nasal and oral cavities are especially affected; ulcerative lesions may spread into the oropharynx and trachea (Goihman-Yahr 1994). Cutaneous lesions precede ML in 5–20% of cases (Lella et al. 2006). These lesions can be clinically manifested or healed, from days to decades before mucosal involvement (Goto and Lindoso 2010). High number of cutaneous lesions and mistreatment are risk factors for evolution towards MCL (Camuset et al.

2007). The percentage of cases of MCL in endemic areas can range from 3 to 20% (Handler et al. 2015). In the latest PAHO/WHO report (2018), the clinical form of the disease was reported in 98% (47,947) of the cases. Of the total, 1,940 (3.9%) of the cases were of the mucosal/muco-cutaneous form. The countries that reported 85.5% of the MCL cases were: Brazil (762), Peru (547) and Bolivia (349); Paraguay registered the highest proportion of MCL cases (47.8%) (PAHO/WHO 2018). *L. (Viannia) braziliensis* is the principal causative agent and in a smaller proportion, *L. (V.) guyanensis*, *L. (V.) panamensis*, and *L. (L.) amazonensis* have also been implicated in MCL cases. The vectors of this disease mainly belong to the subgenus *Psychodopygus* (Strazzulla et al. 2013).

Visceral leishmaniasis (VL) also known as kala-azar is commonly a systemic disease that affects internal organs, especially the spleen, liver and bone marrow. If the disease is not treated, the fatality rate in developing countries can be as much as 100% within 2 years (WHO, 2018). VL is distributed in 76 countries, being endemic in 12 countries of the Americas (Figure 1.2-5). Approximately 96% of the cases registered in the Americas are concentrated in Brazil (Figure 1.2-6); however, there has been a geographic expansion in Argentina, Colombia, Paraguay and Venezuela. During 2001-2016, 55,530 human VL cases were reported in the Americas, with an annual average of 3,457 cases. The number of deaths by this disease has increased since 2012 and the fatality rate of the Americas has reached 7.9% in 2016, which is the highest rate compared to other continents (Figure 1.2-6 B) (PAHO,2018). *L. (L.) donovani* and *L. (L.) infantum* are the agents responsible for Old World VL, while *L. (L.) infantum* (*syn. chagasi*) is responsible for New World VL. Some VL cases caused by *L. tropica* or *L. amazonensis* have also been reported (Alborzi et al. 2006). The vectors involved in the transmission of American VL belong to the *Lutzomyia* sensu stricto, *Migonemyia, Nyssomyia, Pifanomyia, Psychodopygus*, and *Verrucarum* subgenera (Ready 2014).

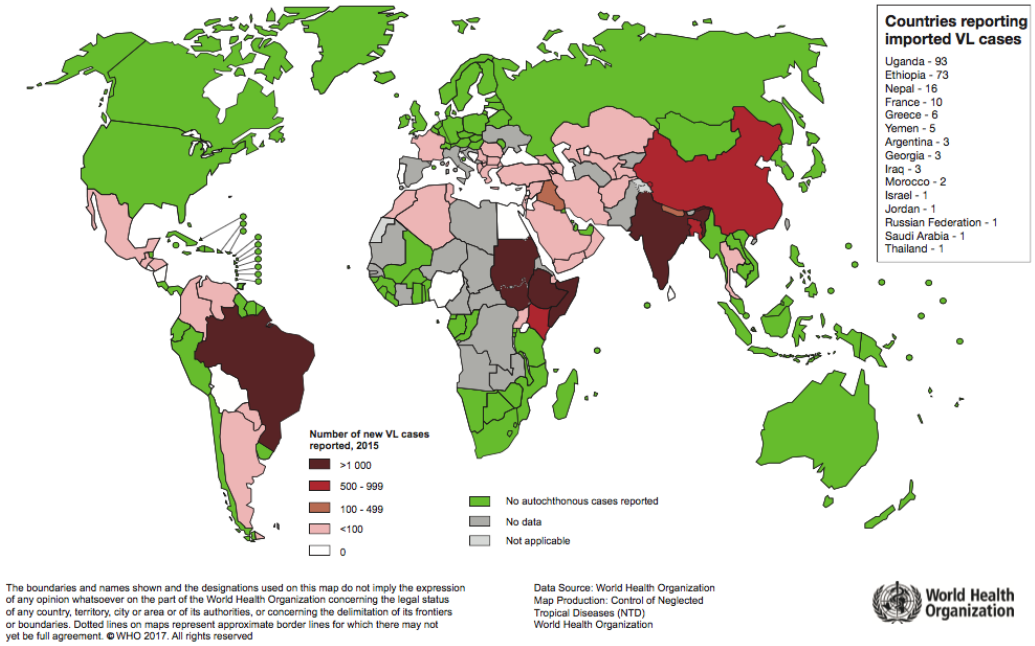

Figure 1.2-5 Status of endemicity of Visceral *Leishmania*sis worldwide, 2018. From WHO, 2018. http://www.who.int/leishmaniasis/burden/en/

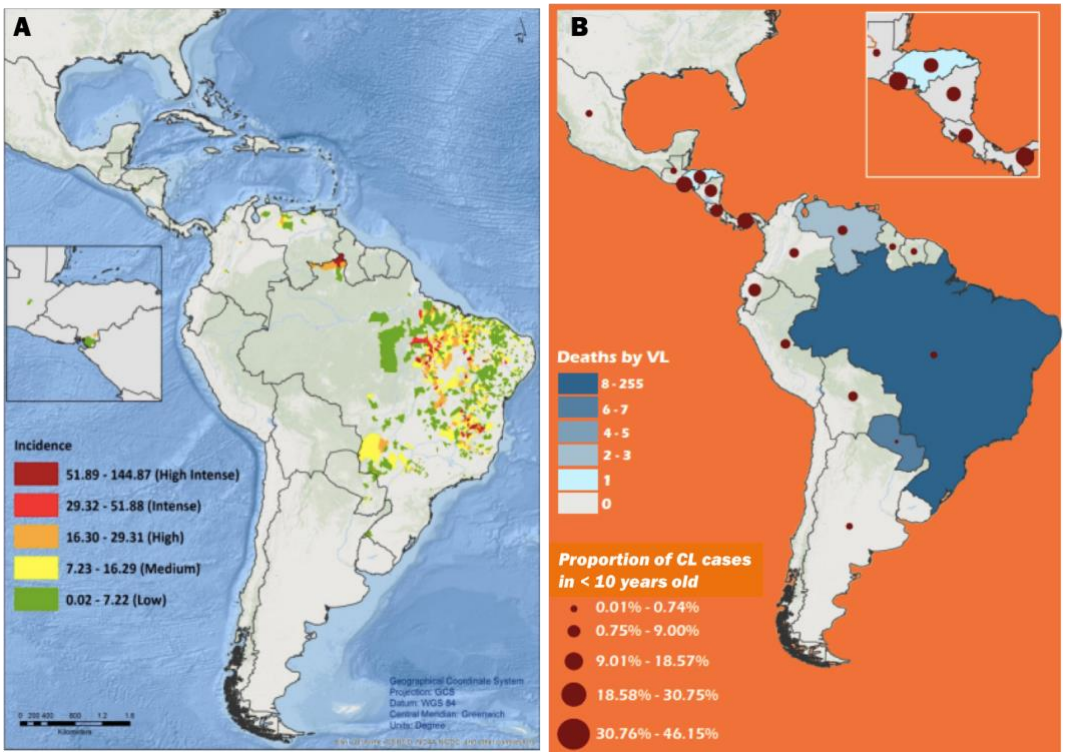

Figure 1.2-6 Visceral *Leishmania*sis in the Americas, 2016. A) Incidence per 100.000 population. B) Number of deaths due to VL. Source: SisLeish – PAHO/WHO: Data reported by the National *Leishmania*sis Programs / Surveillance Services. Adapted from (PAHO/WHO 2018)

1.2.3 Viruses

Insects are host to a large variety of viruses. From the vector-borne diseases, the arboviruses like Chikungunya, Dengue and Zika are among the ones with higher impact in human population.

Even though viral infections are very well studied in mosquito vectors and the model organism *Drosophila*, little is known about the viruses transmitted by phlebotomine sand flies and they can be considered as neglected pathogens (Depaquit et al. 2010).

Phlebotomine sand flies are involved in the transmission of many viral agents. The most important are classified into the *Phlebovirus* genus (family Bunyaviridae), that includes the sand fly fever Sicilian virus(SFSV) and Toscana virus (TOSV), and the Vesiculovirus genus (family Rhabdoviridae), which includes Vesicular stomatitis (VSV), Chandipura (CHPV) and Isfahan (ISFV) viruses (Maroli et al. 2013). During the last decade, new phleboviruses have been discovered, but are still unclassified (Ayhan and Charrel 2017).

The risk for infection with sand fly-transmitted phleboviruses has been shown to affect very extended areas of the Old World (southern Europe, Africa, the Middle East, central and western Asia) in association with the presence of sand fly vectors (Tesh 1988; Moriconi et al. 2017). SFSV and SFNV cause a typical "three-day fever" or "pappataci fever," while TOSV displays a strong neurotropism responsible for acute meningitis and meningoencephalitis (Depaquit et al. 2010). In the Old World, at least 250 million people are exposed to Phlebovirus infections. Chandipura encephalitis virus and Isfahan virus are endemic in the Old World in some parts of India (Basak et al. 2007), Iran (Tesh et al. 1977), and Turkmenistan and other central Asian republics (Gaidamovich et al. 1978).

Vesicular stomatitis viruses causing stomatitis in humans and domestic livestock are largely endemic in the New World, including Mexico, Central America, northern South America and eastern Brazil, as well as in limited areas of the south-eastern U.S.A. (Letchworth et al. 1999). Most of the studies about viruses transmitted by phlebotomine sand flies in the Americas are from the decades between 70-90's. Studies report isolation of several serotypes of vesicular stomatitis virus and other virus types from *Lutzomyia* spp. in Colombia (Tesh et al. 1987), Panamá (Peralta et al. 1974) and U.S.A (Nettles et al. 1990).

Between 1961 and 1995, 69 arbovirus serotypes were isolated from sand flies in several areas of the Brazilian Amazon (Figure 1.2-7) (reviewed in Shaw et al. 2018). From the 39 recognized serotypes of phleboviruses, 25 have been isolated in the New World (Vasconcelos et al 2001). The prevalence of serotypes in the New World is probably a reflection of the large diversity of sand flies in the Americas (Shaw et al. 2018). Ten phleboviruses have been associated with disease in humans, that become infected when in contact with the sand flies' ecological niche. In the New World, this tangential mode of infection results in limited and sporadic numbers of cases, usually in people living near or in forested areas (Rodrigues et al. 1998).

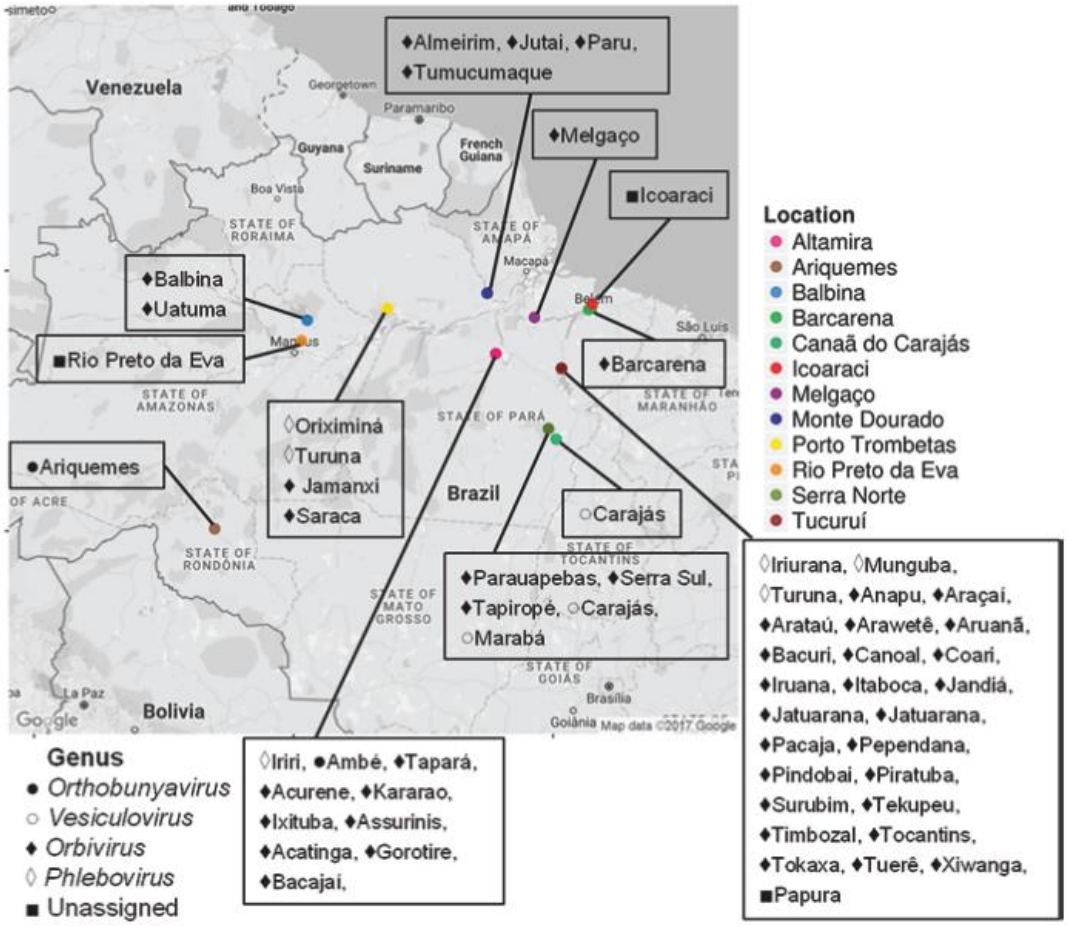

Figure 1.2-7 Map of the Brazilian Amazonian region showing the localization of the capture sites of the sand flies from which viruses were isolated. (Shaw et al. 2018)

1.3 INSECT DEFENCE AGAINST PATHOGENS

Insects are exposed to microorganisms like bacteria, viruses and fungi as well as parasites on a regular basis; this risk is greater in hematophagous insects during infected blood meals. To survive infection insects developed several defence mechanisms. The exoskeleton is a first line of defence to offer an effective physical and chemical barrier against attachment and infiltration of pathogens. The digestive tract, which is a principal route of invasion, is protected after blood feeding by a chitinous membrane called peritrophic matrix. Additionally, the hostile environment of digestive enzymes and acids in the midgut is able to inactivate and digest many viruses and bacteria. In the majority of cases these physical and chemical barriers are sufficient to protect insects against pathogens, which produce disease only when the integument has been injured. Once pathogens invade the hemocoel of the host or interact with the midgut epithelium, they confront a complex system of innate defence mechanisms involving cellular and humoral responses (Jiravanichpaisal et al. 2006).

1.3.1 Cell response in insects

The most common types of haemocytes described from species of diverse orders including Lepidoptera, Diptera, Orthoptera, Blattaria, Coleoptera, Hymenoptera, Hemiptera, and Collembola are Granular Cells (GC), plasmatocytes, spherule cells, and oenocytoids. The haemocytes described from *Drosophila*, which is one of the primary models for insect and human immunity studies, are named differently and commonly contain the three types of haemocytes: plasmatocytes, crystal cells and lamellocytes (Lanot et al. 2001; Wertheim et al. 2005). Plasmatocytes function as professional phagocytes and are strongly adhesive in vitro. Cristal cells play an important role in defence-related melanisation and are non-adhesive cells. Lamellocytes are large, flat, adhesive cells; their principal function is encapsulating parasitoids and other large invaders (Strand 2008). Less is known about haemocytes produced by other insects including several species of economic and health importance. Castillo et al. (2006) study in haemolymph from *An. gambiae* and *Ae. aegypti* adult females showed that it contains three haemocyte types (granulocytes, oenocytoids and prohemocytes). Identification was done using a combination of morphological and functional markers, granulocytes being the most abundant cell type. All these types of haemocytes were found in all life cycle stages.

The principal defence responses involving haemocytes against invaders are phagocytosis, nodulation and encapsulation. Haemocytes also react to external injury by contributing in clot reaction. Phagocytosis means the engulfment of entities by an individual cell, it is the most widely conserved of the above mentioned responses, found in protozoa and all metazoan phyla (Jiravanichpaisal et al. 2006). Encapsulation or nodulation is a cellular immune response that appears to be restricted to invertebrates in response to external bodies too large for phagocytosis by individual haemocytes (Kounatidis and Ligoxygakis 2012). Nodulation refers to multicellular haemocytic aggregates, which capture a big number of bacteria in an extracellular material, and larger nodules may ultimately be encapsulated. Encapsulation refers to the attachment of haemocytes to bigger targets like parasites or nematodes in a multilayer manner, that ends in melanisation of the structure and ultimately the killing of the parasite inside the capsule (Ratcliffe and Gagen 1977; Wertheim et al. 2005). Melanisation has been of considerably interest in antiparasitic responses in mosquitos and for some species even against bacteria. This response had been reported against *Plasmodium* ookinetes in the midgut and filarial worms in the Malpighian tubule cells (Christensen et al. 2005).

1.3.2 Humoral response in insects.

Humoral defences in insects include the production of antimicrobial peptides (AMPs) through activation of immune pathways, reactive intermediates of oxygen or nitrogen and the complex enzymatic cascade that regulate clotting or melanisation of haemolymph (Jiravanichpaisal et al. 2006). In this section, the focus will be on the major insect immune signalling pathways, namely the Toll, immune deficiency (IMD), and Janus kinase/signal transducers and activators of transcription (JAK/STAT) pathways (Figure 1.3-1), since they are a central part of this project.

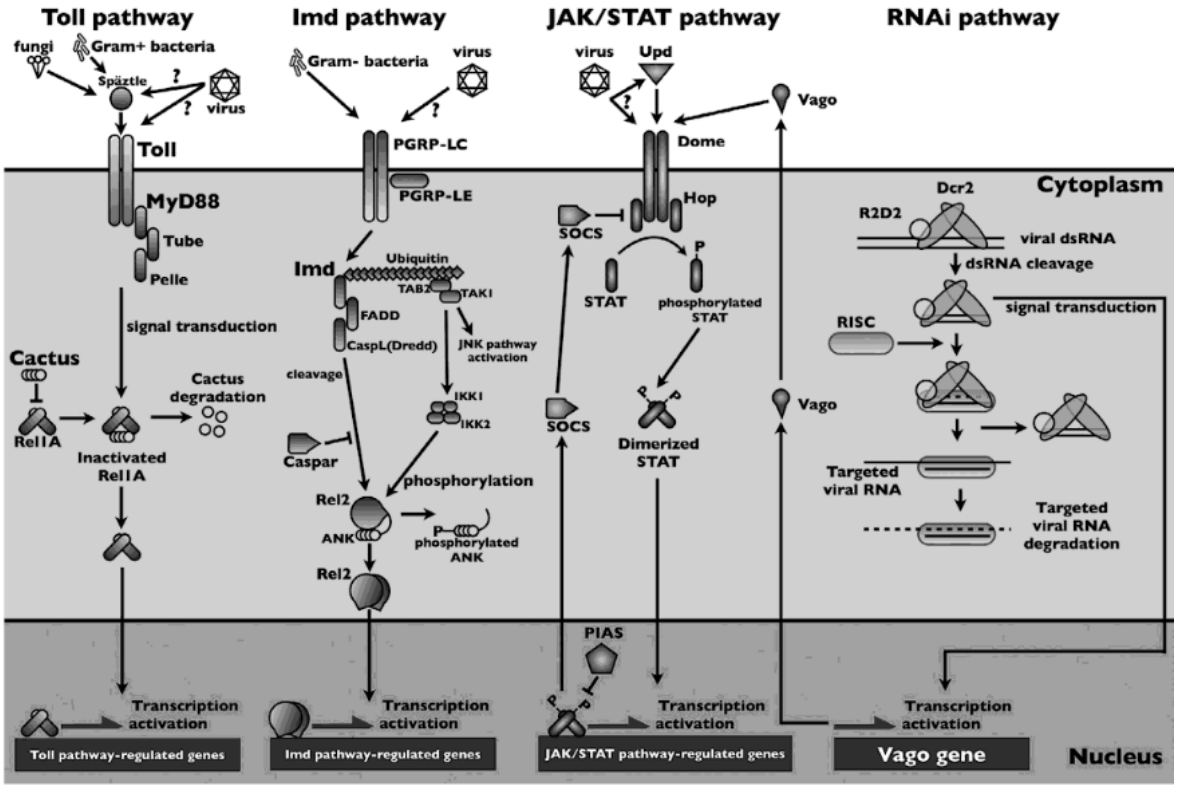

Figure 1.3-1 Summary of the insect Toll, IMD, JAK/STAT, and RNAi pathways (based on Drosophila and mosquito model). Three classical immune pathways are specifically activated upon recognition of PAMPs by receptors on the cell surface. The recognition trigger signalling cascades that results in the activation of transcription factors that control expression of AMPs and other immune factors. The RNAi serves as an intracellular PRR and immune defence mechanism. The RNAi pathway can also activate the JAK/STAT pathway and provide systemic protection against arbovirus infection. For detailed description refer to the text. Taken from (Jupatanakul and Dimopoulos 2016)

1.3.2.1 Recognition

When a pathogen invades an insect, it confronts many host-derived molecules that interact with these external agents depending on their structure and surface molecules. These host-derived molecules are called pattern recognition receptors (PRRs), that can bind to pathogen-associated molecular patterns (PAMPs). PRRs are generally, secreted proteins that are located in different parts of the insect's midgut and hemocoel (Kumar et al. 2018). Activation of immune responses can either occur directly through phagocytosis and melanisation, or indirectly, through intracellular

immune-signalling pathways that initiate the transcriptional activation of appropriate AMPs and other immune effector genes (Dimopoulos 2003; Christophides et al. 2004; Osta et al. 2004).

A very well known PRR is peptidoglycan recognition protein (PGRP), that recognizes one of the abundant and typical bacterial elements, peptidoglycan, and activate a proteases cascade that involves serine-protease and serpins. A transcriptomic study by Pitaluga et al. (2009) identified in the gut of *L. longipalpis* infected with *Leishmania* some representatives of serine-proteases, serpins and PGRP-s class that could be involved with immune system activation.

As mentioned previously, there are three canonical signalling pathways in innate immunity in insects, Toll, IMD and JAK/STAT pathways, that are responsible for AMPs and other effector genes expression.

1.3.2.2 Toll pathway.

This pathway was initially identified in the context of embryonic development in *Drosophila melanogaster*, later it was found to have an important role in defence against fungi, Gram-positive bacteria and viruses (Lemaitre et al. 1996; Rutschmann et al. 2002; Zambon et al. 2005). Recognition of PAMPs by PRRs activates a proteolytic cascade that ends in cleavage of the cytokine Spätzle (DeLotto and DeLotto 1998). Spätzle binds to and activate the transmembrane Toll receptor (Weber et al. 2003), initiating signalling through associated adaptor proteins MyD88 and Tube and the kinase Pelle. This activation promotes phosphorylation and degradation of the negative regulator cactus (Nicolas et al. 1998; Fernandez et al. 2001), which in absence of stimuli binds and retains the NF-kB-like transcription factor dorsal (Rel1 in mosquitoes) in the cytoplasm. Cactus degradation permits dorsal's translocation to the nucleus and following transcription of effector genes such as AMPs (Hoffmann 2003; Lemaitre and Hoffmann 2007) (Figure 1.3-1). The Toll pathway is conserved in mosquitoes and also plays a role in antiviral defence in these insects (Sim et al. 2014). In *L. longipalpis* some elements of this pathway have been identified (Dillon et al. 2006) and shown to respond to bacterial and parasite challenges *in vitro* using the embryonic *L. longipalpis* cell line LL5 (Tinoco-Nunes et al. 2016).

1.3.2.3 The immune deficiency pathway

The immune deficiency (IMD) pathway is involved in antibacterial response in insects. Like the Toll pathway, the IMD pathway was initially identified and described in *Drosophila* (Rutschmann et al. 2000; Georgel et al. 2001; Lu et al. 2001). This pathway has molecules that also

participate in the Toll pathway in eliciting an immune response. Activation of the IMD pathway is also initiated by PRR-mediated recognition of PAMPs (Sim et al. 2014). Intracellular signalling is then passed through the adaptor protein IMD and several cascade-like proteins and kinases, then takes to a functional separation in the pathway into two downstream branches (Georgel et al. 2001; Silverman et al. 2003; Kleino et al. 2005). One branch, comparable to the mammalian c-Jun/JNK pathway, activates the transcription factor AP-1 via JNK signalling (Sluss et al. 1996; Chen et al. 2002), while the other branch ends in the processing and activation of the NF-kB transcription factor Relish (Rel2 in mosquitoes) via caspase mediated cleavage of its carboxy-terminal end (Rutschmann et al. 2000; Lu et al. 2001). After activation, Relish is translocated to the nucleus to stimulate the transcription of antimicrobial effectors like AMPs (Leulier et al. 2000; Stöven et al. 2003). Caspar is the negative regulator of the pathway, possibly by interfering with the enzymes involved in cleavage of Relish (Kim et al. 2006) (Figure 1.3-1). In mosquitoes, the IMD pathway is also important in the antibacterial defence, and also directs immune responses against *Plasmodium* parasites (Meister et al. 2005; Dong et al. 2011; Garver et al. 2012). This pathway has also been linked to antiviral response. Studies in flies have shown active participation against SINV and cricket paralysis virus (CrPV) infections (Avadhanula et al. 2009; Costa et al. 2009). In mosquitos up-regulation of IMD components in DENV and SINV infections has also been observed (Xi et al. 2008; Luplertlop et al. 2011). Studies in *L. longipalpis* have shown the importance of the IMD pathway in controlling *Leishmania* infection in the vector, since silencing of a Caspar-like homolog impaired parasite establishment in the midgut (Telleria et al. 2012). Activation of the IMD pathway in the *L. longipalpis* LL5 cell line when stimulated with heat-killed bacteria and yeast, and live parasites has also been reported (Tinoco-Nunes et al. 2016).

1.3.2.4 JAK/STAT Pathway

The Janus kinase/signal transducers and activators of transcription (JAK/STAT) pathway is known to be a main signalling pathway induced by interferons and plays a key role in antiviral immunity in mammals. This pathway is conserved in invertebrates and was first identified in *Drosophila* while studying developmental aspects, being later identified as in important part of the antiviral response in *Drosophila* (Dostert et al. 2005). The JAK/STAT pathway in *Drosophila* is activated by the binding of Unpaired (Upd) peptide ligand to the transmembrane receptor Dome. Ligand recognition leads to dimerization of Dome, followed by self-phosphorylation of the receptor-associated Janus kinases (JAKs). Activated JAKs then phosphorylate the C-terminal side of the receptor dimers, producing binding pockets for STAT proteins. The recruited STATs are

then phosphorylated by the Dome/JAK activated complex, which results in the activation and dimerization of the STAT proteins. Activated STAT dimers are translocated to the nucleus and induce the expression of effector genes (Figure 1.3-1) (Agaisse et al. 2004; Arbouzova and Zeidler 2006). The JAK/STAT pathway has also been found to be activated under bacterial challenge in the malaria vector *An. gambiae* (Barillas-Mury et al. 1999). Later, it was associated with antiviral response in *Drosophila* infected with *Drosophila* C virus (DCV) (Dostert et al. 2005) and in *Ae. aegypti* infected with Dengue virus (DENV), suggesting an evolutionarily conserved antiviral mechanism in insects and humans (Souza-Neto et al. 2009).

1.3.2.5 AMPs

Insects produce a larger collection of AMPs than any other taxonomic group, and the number of individual AMPs produced by each species fluctuates considerably (Mylonakis et al. 2016). AMPs are short immunity-related proteins that can act against bacteria, fungi, viruses or parasites. In insects they are secreted from cells and tissues that participate in host innate immunity like haemocytes or the fat body (Bulet et al. 2004; Vale et al. 2014). The functional classification of insect AMPs tends to be based on target pathogen range rather than any specific mechanism of action. Some have a wide range, while others show varying degrees of specificity to Gram-positive or Gram-negative bacteria, fungi, parasites or viruses (Vilcinskas 2011; Pretzel et al. 2013).

The majority of insect AMPs have a net positive charge and contain up to 50% hydrophobic residues (Bulet et al. 2004; Bulet and Stocklin 2005; Wiesner and Vilcinskas 2010). These characteristics lead to interaction of those AMPs with the negatively charged and lipophilic membranes of bacterial cells (Brown and Hancock 2006), which means that AMPs are electrostatically attracted to bacterial cell membranes, and when the contact is established the hydrophobic residues promote integration, causing the outer leaflet of the membrane to expand and become thinner, eventually creating pores or even causing lysis (Mylonakis et al. 2016).

According to their structures or unique sequences, AMPs can be organized into four families: the α- helical peptides (cecropin and moricin), cysteine-rich peptides (insect defensin and drosomycin), proline-rich peptides (apidaecin, drosocin and lebocin), and glycine-rich peptides/proteins (attacin and gloverin). Amongst insect AMPs, defensins, cecropins, proline-rich peptides and attacins are common, whereas gloverins and morticians have been identified only in Lepidoptera. The majority of AMPs are synthesized as inactive precursor proteins or pro-proteins, and active peptides (20-50 residues) are produced by limited proteolysis. However, active gloverins (~14kDa) and attacins (~20kDa) are large proteins (Yi et al. 2014).

Insect defensins are small cationic/basic peptides of 34–51 residues with six conserved cysteines identified in nearly all living organisms suggesting they may have derived from a common ancestor gene. Insect defensins are active primarily against Gram-positive bacteria (Yi et al. 2014). Cecropins are a family of cationic antimicrobial peptides of 31–39 residues. They are synthesized as secreted proteins and become mature active cecropins after removal of signal peptides. Cecropins have a wide range of activity against Gram-negative and Gram-positive bacteria, as well as fungi (Moore et al. 1996; Ekengren and Hultmark 1999; Vizioli et al. 2000). Attacins are synthesized as pre-pro-proteins containing a signal peptide, a pro-peptide (P domain), and an N-Terminal attacin domain, followed by two glycine-rich domains (G1 and G2 domains) (Sun et al. 1991; Hedengren et al. 2000). Mature attacins are produced after processing of pro-attacins by burin-like enzymes. Most attacins are active against *E. coli* and some particular Gram-negative bacteria (Hultmark et al. 1983).

2 OBJECTIVES

2.1 GENERAL OBJECTIVE

To investigate aspects of immune responses in *Lutzomyia longipalpis*.

2.1.1 Specific objectives

-To investigate the mechanisms of non-specific antiviral response in *L. longipalpis* LL5 embryonic cells response to synthetic dsRNA exposure (Chapter 1).

-To investigate *L. longipalpis* immunity in relation to *Leishmania infantum (Syn. chagasi)* infection with specific focus on the Toll pathway (Chapter 2).

-To investigate the immune responses of *L. longipalpis* to infection by *Leishmania (V.) guyanensis* containing or not the endosymbiont *Leishmania* virus 1 (LRV1) (Chapter 3).

3 CHAPTER 1. NON-SPECIFIC ANTIVIRAL RESPONSE IN LL5 CELLS.

3.1 INTRODUCTION

A study by Pitaluga et al (2008) in the sand fly cell line LL5 where virus-like particle (VLPs) of West Nile virus (WNV) that could transduce self-replicating RNA genome encoding Luc gene to infect LL5 cells, showed that treatments with Luc specific dsRNA, dsRNA from unrelated genes and even ssRNA were able to suppress the expression of VLP in infected cells. Additionally, it was reported that dsRNA treatment of LL5 cells reduced the number of cells that became infected with WNV VLPs encoding a β-Gal reporter, reinforcing the discovery of a nonspecific, innate antiviral immune response in LL5 cells (Pitaluga et al. 2008). This was the first report of this type of response in cells from an insect. Later, (Martins-da-Silva et al. 2018) showed that proteins in the secretome of LL5 cells that were stimulated with polyinosinic:polycytidilic acid (Poly(I:C)) -a synthetic molecule that mimics dsRNA structure- were associated to Interferon (INF)-like response and not to canonical pathways. Also very few proteins had the same profile at mRNA and protein levels.

Antiviral response in insects and other invertebrates is commonly controlled by the RNAi pathway, nevertheless new studies like those previously described have shown that new types of antiviral responses are still unknown.

3.1.1 The RNA interference (RNAi) pathway in insects

Antiviral response in insects as part of the innate immunity is mainly regulated by the RNAi pathway. RNAi is a conserved sequence-specific gene-silencing mechanism that controls numerous functions in keeping cellular homeostasis during pathogen infections. This pathway is a primitive immune response elicited by the presence of foreign nucleic acid and has been described in both vertebrates and invertebrates, including algae, plants and fungi, but not bacteria (Agrawal et al. 2003). The RNAi pathways includes the production of small RNA molecules of different characteristics, such as small endogenous interfering RNAs (siRNAa), microRNAs (miRNAs), and P element-induced wimpy testis (PIWI)-interacting RNAs (piRNAs), and interaction of these molecules with the RNA silencing complex (RISC) to elaborate a defence response (Kumar et al. 2018). Viral infection primarily activates the siRNA pathway in insects. This response is triggered when long, virus-derived double-stranded RNA (dsRNA) in the cytoplasm of infected cells is identified and cleaved by Dicer-2 (Dcr2) into siRNAs, typically 21 base pairs (bp) in length. Then, siRNAs are loaded on the multi-protein RNA-induced silencing complex (RISC), which untwist

the duplex RNA and degrades one of the siRNA strands, using the remaining strand for targeted degradation of single-stranded viral RNA with sequence complementary to the siRNA (review in (Sanchez-Vargas et al. 2004)), (Figure 1.3-1). Initially, RNAi was shown to influence RNA virus replication in *D. melanogaster* (Wang et al. 2006; Zambon et al. 2006), and more recently it has been proven to be an antiviral mechanism in mosquitoes also, (Campbell et al. 2008; Sánchez-Vargas et al. 2009).

3.1.2 IFN-mediated antiviral response

In mammals RNAi-mediated sequence-specific antiviral mechanisms and INF system-mediated non-specific antiviral response are analogous antiviral pathways involved in the identification of nucleic acids produced by viral replication (Sagan and Sarnow 2013). The IFN system is a very powerful antiviral response that can control the majority of virus infections in a situation where the adaptive immunity is deficient (Randall et al. 2008) and it is the predominant system in mammal innate antiviral immunity. After viral infections, viral nucleic acids (include ssRNA, dsRNA, and DNA) can be recognized by several PRRs, like Toll-like receptors (TLRs) and retinoid acid-inducible gene (RIG)-I-like receptors (RLRs).

Four TLRs, TLR3, TLR7, TLR8 and TLR9, that are localized on endosomes and lysosomes have been associated with nucleic acid recognition (Barbalat et al. 2011) (Figure 3.1-1). The dsRNA can be produced during viral infection as an intermediate in ssRNA viruses replication or as a by-product of symmetrical transcription in DNA viruses (Akira et al. 2006). dsRNA is a common viral PAMP and a strong inducer of type I IFNs. The dsRNA and its synthetic equivalent, Poly(I:C), are recognized by TLR3. This receptor has been connected to host response to ssRNA, dsRNA and DNA viruses (Akira et al. 2006; Barbalat et al. 2011; Wang et al. 2015).

Other type of receptors detect nucleic acids in the cytosol. RIG-I and MDA5 can recognise cytosolic dsRNA. The long (>2kb) polymers of dsRNA mimic Poly(I:C) are specially recognized by MDA5, while smaller polymers (as short as 70bp) are recognized by RIG-I (Figure 3.1-1) (Akira et al. 2006; Barbalat et al. 2011; Wang et al. 2015)

Identification of viral nucleic acids triggers the production of pro-inflammatory cytokines, chemokines, and IFNs through the activation of NF-kB and IRF3/7 pathways, inducing inflammation and IFN responses, which are characteristic of host innate antiviral immunity (Akira et al. 2006). INF can bind their associated receptors and induce the expression of hundreds of interferon-stimulated genes (ISGs) through the JAK/STAT pathway. Activation of transcription of

these ISGs can target multiple stages in the virus life cycle and facilitate the inhibition of viral replication (Schoggins and Rice 2011).

Information on the PRRs of nucleic acids and the main elements of the IFN sites in invertebrates has not been updated (Wang et al. 2013). Nevertheless, some groups have found that viral infections or nucleic acid challenges can trigger non-specific antiviral immunity in some invertebrate species, that shows similarities with characteristics of the mammalian IFN responses (Deddouche et al. 2008; Pitaluga et al. 2008; Takeuchi and Akira 2008; Paradkar et al. 2012; Green and Montagnani 2013; Wang et al. 2013)

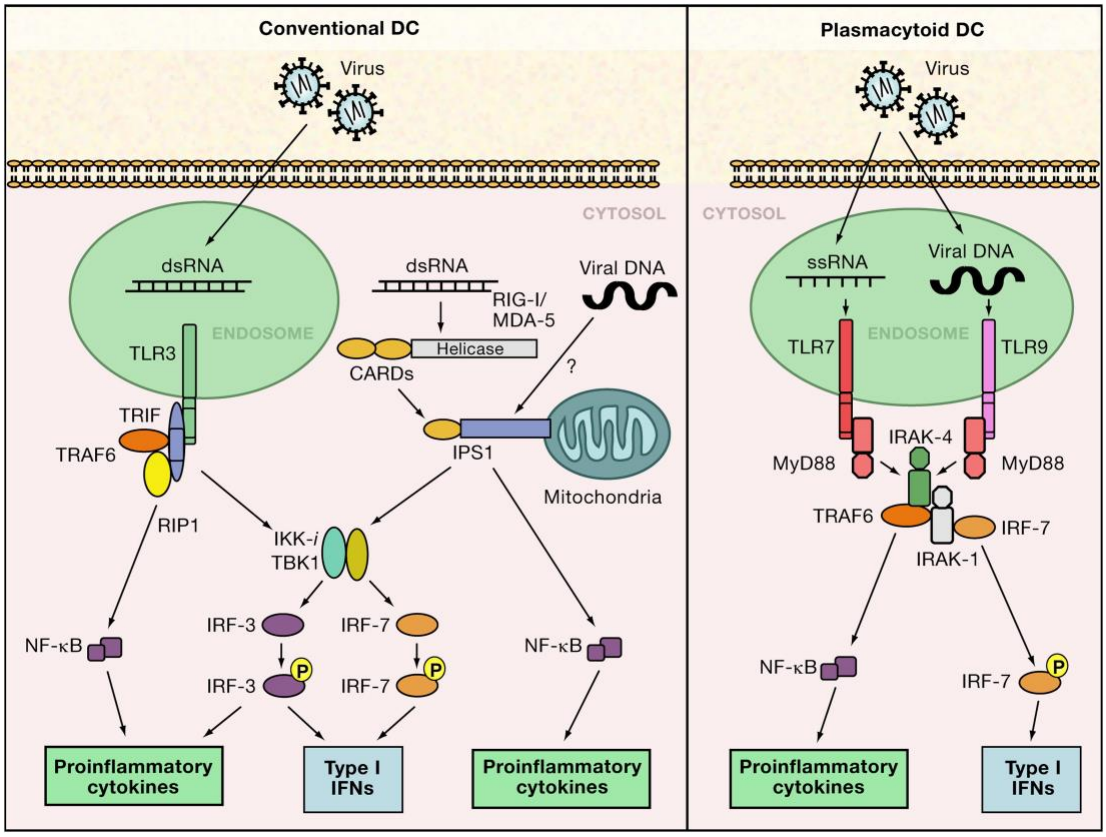

Figure 3.1-1 TLR3-dependent and RIG-I-dependent pathways operate to detect viral infection. In cDCs (conventional dendritic cells). Recognition of dsRNA by TLR3 in the endosomal membrane recruits TRIF to the receptor, which induces proinflammatory cytokines and type I IFNs via the RIP1/TRAF6-NF-kB pathway and the TBK1/IKK-i-IRF-3/IRF-7 pathway, respectively. In contrast, detection of dsRNA in the cytoplasm by RIG-I activates TBK1/IKK-i through IPS-1, which is localized on the mitochondrial membrane. In pDCs (plasmacytoid dendritic cells), TLR7 and TLR9 recognize viral ssRNA and DNA, respectively. Stimulation with TLRs recruits a complex of MyD88, IRAK-4, IRAK-1, TRAF6, and IRF-7. Phosphorylated IRF-7 translocate into the nucleus and upregulates the expression of type I IFN genes. Taken form (Akira et al. 2006)

3.1.3 INF-Like response in invertebrates

In *Drosophila*, infection by DCV and Sindbis virus not only induce RNAi-mediated antiviral response but also active the expression of some genes similar to mammals (Deddouche et al. 2008; Takeuchi and Akira 2008). Vago was recognized as a viral inducible gene. Vago expression is dependent on Dicer-2 activity but does not need the other proteins involved in RNAi

pathway. In *Culex* sp. mosquitoes, an analogous Dicer-2-Vago signalling pathway was found. The study reported that Vago was secreted from WNV (West Nile virus) infected cells and induced an antiviral state in uninfected cells. Secreted Vago constrains WNV infection in *Culex* cells by activation the JAK/STAT pathway and up-regulates the expression of the STAT-dependent virus-inducible gene vir-1. Vago appears to function as a cytokine that works like mammalian IFNs (Figure 3.1-2) (Paradkar et al. 2012). Studies in honey bee have showed that challenge with dsRNA, regardless of sequence, can generate an antiviral response that controls viral infection in adult bees. This was the first report of the non-specific antiviral response in adult insects (Flenniken and Andino 2013). Response to viral infection or dsRNA challenge in honey bee was evaluated at transcriptional level by microarrays, indicating that the majority of canonical immunity genes were not regulated by dsRNA, and those genes that presented up-regulation were not recognized immune genes. This study reveals that dsRNA-mediated antiviral response in honey bees may involve unique genes and signal transduction cascades that are RNAi-independent mechanisms (Flenniken and Andino 2013). This type of non-specific antiviral response that are induced by dsRNA and that resemble type I IFN response in mammals, have also been reported in bumblebees (Piot et al. 2015) and other invertebrates like shrimp (Robalino et al. 2004, 2005) and Pacific oysters (Green and Montagnani 2013).

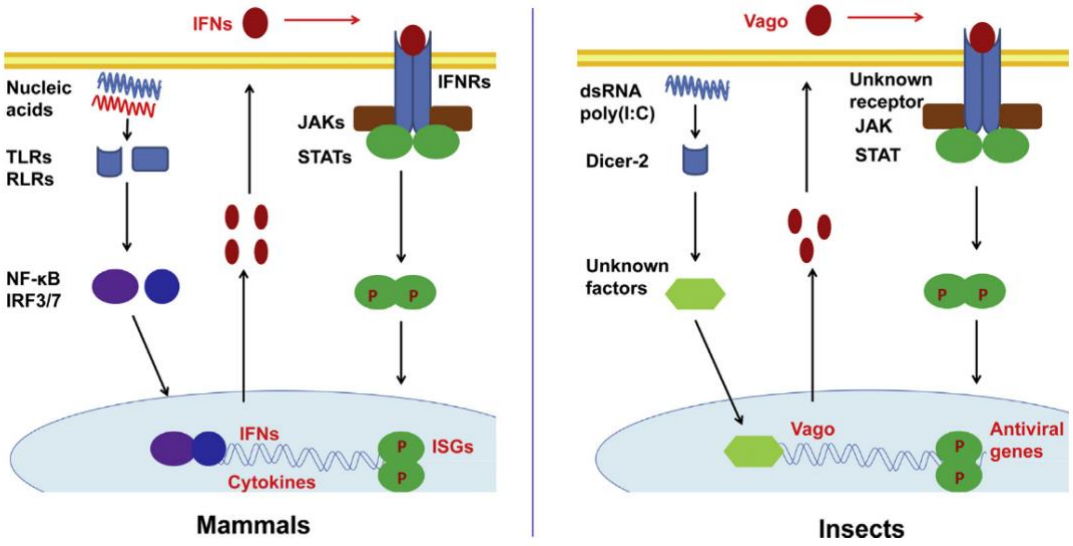

Figure 3.1-2 Nucleic acid-induced antiviral immunity in mammals and insects. In mammals (left), nucleic acids generated by virus replications can be sensed by TLRs and RLRs, triggering the release of inflammatory cytokines and type I IFNs through the activation of NF-jB and IRF3/7 pathways. Subsequently, the cytokines and IFNs bind their cognate receptors and induce the expression of hundreds of ISGs through the JAK-STAT pathway, inducing the host antiviral state (Akira et al., 2006; Randall and Goodbourn, 2008; Schoggins and Rice, 2011). In insects (right), Dicer-2, which is the functional equivalent of mammalian RLRs, can recognize the viral dsRNA and unregulate the expression of Vago, a cytokine that acts similar to mammalian IFNs. Vago activates the JAK/STAT pathway and induces the expression of antiviral genes, e.g., vir-1 (Deddouche et al., 2008; Kingsolver and Hardy, 2012; Paradkar et al., 2012; Takeuchi and Akira, 2008). Taken from (Wang et al. 2015)

3.1.4 Exosomes

Previous studies in our laboratory showed that conditioned medium from LL5 cells challenged with Poly(I:C) reduced virus like particles (VLP) replication in unchallenged cells. Also, purified exosomes from Poly(I:C) transfected cells conditioned medium had similar effect of protecting naïve cells from VLP replication (unpublished results). Exosomes are vesicles of endocytic origin released in the extracellular space by different types of cells (Simpson et al. 2008) (Figure 3.1-3), and are capable of transporting miRNAs (Lim et al 2003) and other regulatory molecules. Exosomes also have an important role in infection with pathogens, including *Leishmania* (Silverman et at 2010, Silverman & Reiner 2011). These vesicles can be generated from the pathogens or the cells they infected. A recent study reported that exosomes from mammalian cells mediated intercellular transmission of an antiviral response induced by IFN (Li, et al 2013b). In the Martins-da-Silva et al. (2018) study of the secretome of LL5 cells stimulated with Poly(I.C), it was found that an important number of proteins lack a signal peptide (SP) which suggested that this proteins could be secreted through an alternative pathway, like exosomes. In this chapter the role of LL5 exosomes in the non-specific innate antiviral response is investigated.

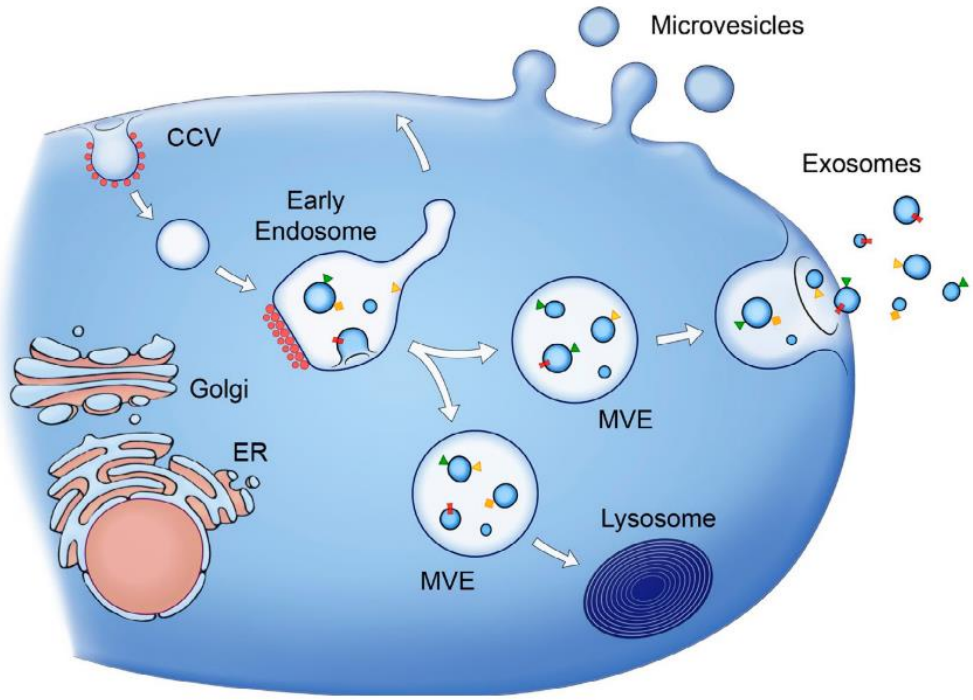

Figure 3.1-3 Release of MVs and exosomes. MVs bud directly from the plasma membrane, whereas exosomes are represented by small vesicles of different sizes that are formed as the ILV by budding into early endosomes and MVEs and are released by fusion of MVEs with the plasma membrane. Other MVEs fuse with lysosomes. The point of divergence between these types of MVEs is drawn at early endosomes, but the existence of distinct early endosomes feeding into these two pathways cannot be excluded. Red spots symbolize clathrin associated with vesicles at the plasma membrane (clathrin-coated vesicles [CCV]) or bi-layered clathrin coats at endosomes. Membrane-associated and transmembrane proteins on vesicles are represented as triangles and rectangles, respectively. Arrows represent proposed directions of protein and lipid transport between organelles and between MVEs and the plasma membrane for exosome secretion. Taken from (Raposo and Stoorvogel 2013).

3.2 CHAPTER 1 SPECIFIC OBJECTIVES

-Characterize exosomes from LL5 cells challenged with Poly (I:C).

-Evaluate gene expression of molecules from canonical immunity pathways (Toll, JAK/STAT and IMD) that could be potentially involved with antiviral response.

3.3 METHODS

3.3.1 Cell culture

L. longipalpis embryonic LL5 cells were maintained at 30ºC in L15 medium (SIGMA-Aldrich) supplemented with 10% foetal bovine serum (FBS) (Econolab), 10% Tryptose Phosphate Broth (TPB) and 1% antibiotics (penicillin 100U/ml and streptomycin 100mg/ml -Sigma).

3.3.2 Transfection with Poly (I:C)

Transfections were performed using the lipid reagent Lipofectamine 2000 (Invitrogen) following manufacturer's instructions. Briefly, a first mix was prepared containing 1,6µL of polyinosinic:polycytidilic acid (Poly (I:C)) at 1µg/µL, a synthetic analogue of double-stranded RNA (Invitrogen) and 78,4µL of L15 medium without serum; a second mix contained 6,4µL of Lipofectamine 2000 (at 1mg/mL) and 153,6µL of L15 medium 20% TPB. Following 45 min incubation at room temperature the mixtures were put together and 760µL of L15 medium 20%TPB was used to complete a final volume of 1ml. From this final mix, 500µL were added into each of two wells (in a 24 well plate) already containing $5x10^5$ cells/well seeded the day before. For the mock-transfected cells the same protocol was followed using medium without Poly (I:C). Cells were incubated at 30ºC for 24h, the medium was removed, cells were washed twice using L15 medium and 500µL of L15 medium 20%TPB without FBS was added to each well (this was considered time zero).

The previous protocol was adjusted to 10ml final volume for $75cm^2$ canted neck flasks used for exosome collection experiments.

3.3.3 Exosomes purification

Exosome collection was performed according to Théry et al. (2006) Medium from transfected and mock-transfected cells at 0, 24 and 48 hours post transfection was collected and processed immediately at each time point. Briefly, the collected supernatant was transferred to clean 50ml falcon tubes and centrifuged at 300xg for 10min for discarding the cell pellet, then 2000xg for 10 min for discarding pellet of dead cells and 10000xg for 30min discarding pellet of cell debris. Lastly supernatant was transferred to clean polyallomer clear 25x89mm tubes for ultracentrifugation at 100,000xg for 70mins using a SW 32Ti swinging-bucket rotor to pellet exosomes. Pellet was resuspended in PBS and the ultracentrifugation was repeated as a washing

step. Pellet was resuspended in 100µL PBS and stored at -80ºC until use. See Figure 3.3-1. for flow chart on protocol description.

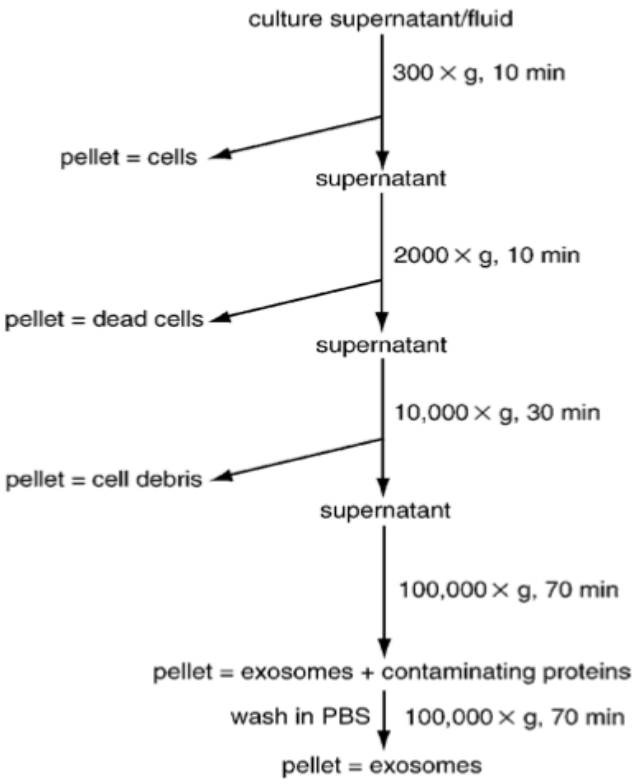

Figure 3.3-1 Flow chart for the exosome purification procedure based on differential ultracentrifugation. The speed and length of each centrifugation are indicated to the right of the arrows. After each of the first three centrifugations, pellets (cells, dead cells, cell debris) are discarded, and the supernatant is kept for the next step. In contrast, after the two 100,000 ×g centrifugations, pellets (exosomes + contaminant proteins, exosomes) are kept, and supernatants are discarded. From (Théry et al. 2006).

3.3.4 Mass spectrometry

The peptides were analysed in triplicate by liquid chromatography tandem-mass spectrometry (LC-MS/MS) in a Thermo Scientific Easy-nLC 1000 system coupled to a LTQ Orbitrap XL ETD (mass spectrometry facility RPT02H/Carlos Chagas Institute–Fiocruz, Curitiba, PR, Brazil), using sample preparation and parameter of analysis were done as described in Martins-da-Silva et al.(2018).

3.3.5 In Silico analyses

Protein identification was performed with MaxQuant algorithm [29,30] version 1.5.5.1. Parameters of the software as previously described in Martins-da-Silva et al.(2018) were used for analysis. Proteins were searched against an *L. longipalpis* protein sequence database (containing

10,110 protein sequences from the VectorBase protein database + NCBI data base, downloaded on 6 March 2016). Identified exosome proteins were subjected to descriptive analyses (Pearson correlation and Principal component analysis (PCA)) using Perseus 1.5.3.2 program, then were annotated by homology using the tool blastp in the NCBI database and VectorBase database for domain identification. Next, exosomal markers were identified using Exocarta (http://www.exocarta.org/) reference list of most frequent markers across species.

3.3.6 RNA extraction from LL5 cells and cDNA synthesis

RNA extraction from LL5 cells was performed using TRIzol Reagent (Ambion), following manufacturer's instructions. Cells from 2 wells from a 24-well plate, were homogenized in 1ml of TRIzol and incubated for 5min at room temperature. Then 200μL of chloroform was added to each sample, mixed vigorously by inversion for 15 secs and incubated at room temperature for 5mins. Next, all samples were centrifuged at top speed (12.000 rpm) for 15min/4ºC. The aqueous phase was transferred to a new 1,5ml tube, 500μL of isopropanol and 2μL of Glycoblue (Ambion) were added and mixed by pipetting, and the mixture was incubated for 10 mins at room temperature. The samples were centrifuged at top speed for 15mins and the supernatant was discarded. Each RNA pellet was washed with 150μL of 75% ethanol (cold) and centrifuged at top speed for 5mins. The ethanol was discharged and pellets were dried upside down for 20-25mins, certifying that no residue of ethanol remained before resuspending each pellet in 20μL of RNase-free water.

RNA samples were treated with DNA-free Kit (Ambion) to remove contaminant DNA. Confirmation of complete DNA absence was checked by PCR using histone primers (ANNEX-A) which produces a 1500bp band (Figure 3.3-2). All RNA was quantified in Thermo Scientific NanoDrop TM ND-1000 spectrophotometer and stored at -20ºC.

cDNA was synthesized from 5μg of total RNA using SuperScript III First- Strand Synthesis kit (Invitrogen) following manufacturer's instructions. Briefly, the first reaction was performed using 250ng of random primers, 1μL of 10mM dNTP, 1.5-2μg of RNA in a final volume of 13μL. The mixture was heated to 65ºC for 5 mins and incubated in ice for 1 min. Afterwards, 4μL of First-Strand buffer 5X, 1μL of 0.1M DTT, 1μL of Super Script^{TM} III RT (200U/μL) and 1μL of water were added to each sample. All samples were incubated at 25ºC for 5mins, followed by 50 mins at 50ºC and finally 15mins at 70ºC.

Successful synthesis was checked by PCR using Rp49 primers (See Figure 3.3-3, ANNEX-A) which only amplifies with cDNA template. cDNA was diluted 1:10 for further use in qPCR reactions.

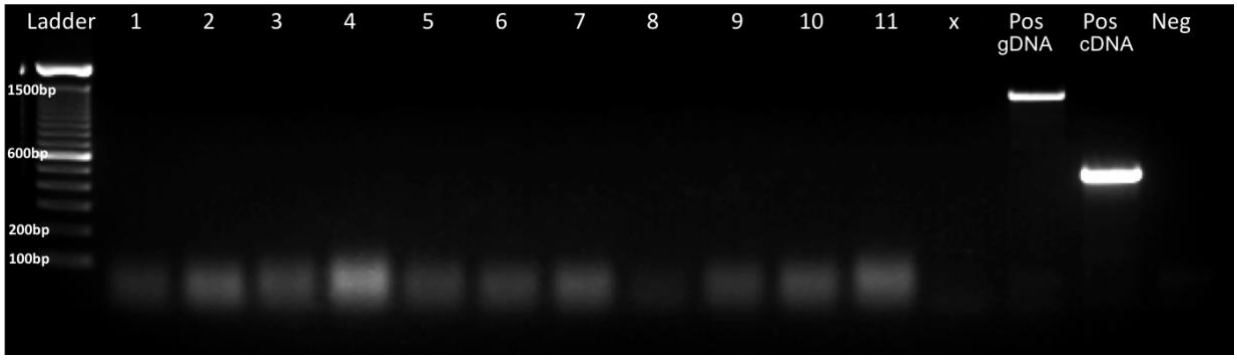

Figure 3.3-2 Electrophoresis of histone amplification from RNA samples (example). Lanes numbered from 1-11 are PCR reactions of RNA samples free of gDNA contamination. Lane x is an empty well, Neg = negative control, Pos gDNA= positive control using LL5 gDNA as template, Pos cDNA= positive control using LL5 cDNA as template.

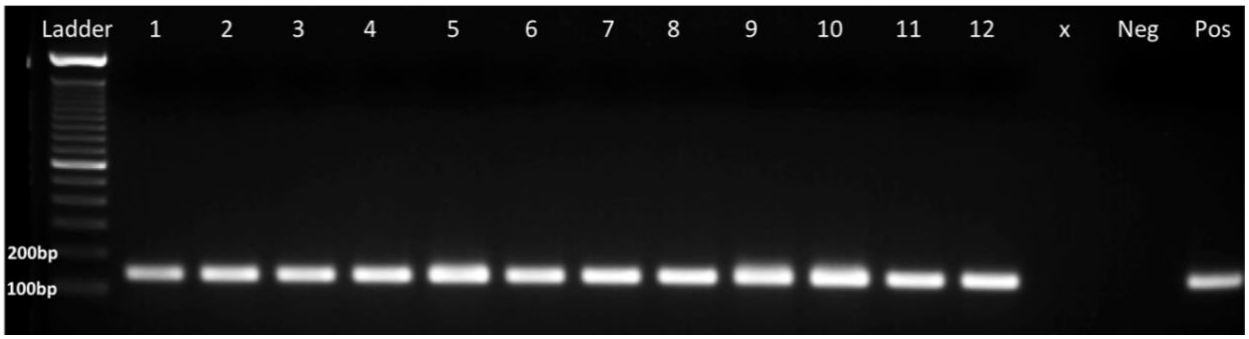

Figure 3.3-3 Electrophoresis of rp49 amplification from cDNA samples (example). Lanes numbered from 1-12 are amplification of rp49 150bp band from synthesised cDNA. Lane x is an empty well, Neg = negative control, Pos= positive control.

3.3.7 qPCR analysis

Mix reactions for qPCR were prepared using Power SYBR Green supermix (Applied Biosystems) following manufacturer's instructions and run in an Applied Biosystems® 7500 Real-Time PCR Systems machine. Gene expression was normalised by Rp49 or GAPDH housekeeping genes using the Pfaffl method (Pfaffl 2001) where correction for real-time PCR efficiency of each pair of primers is used. Graphs and statistical analysis were made using normalized values transformed to Log2(x). Statistical analyses were done using GraphPad Prism 7 software, version 7.0a (GraphPad Software, Inc., San Diego, CA, USA). Comparison of transfected and mock samples at different times after transfection, an unpaired two-tailed Student's t test was performed for each time point, with Welch's correction without assumption of equal standard deviations. * $p \leq 0.05$, ** $p \leq 0.01$, *** $p \leq 0.001$.

3.4 RESULTS

3.4.1 Proteomic profile of exosomes from LL5 embryonic cells treated or not with Poly(I:C)

Mass spectrometry peptide raw data was initially analysed in MaxQuant 1.5.5.1 program to identify proteins detected in all exosome samples. For better identification percentage one FASTA file was assembled containing protein sequences from VectorBase and NCBI databases. This new database was used as a frame for protein identification in MaxQuant program. There were 3964 peptides identified (short segments generated by trypsin digestion) and 525 proteins in total (can be identified by one or more peptides) without contaminants, with an MS2 (second round of mass spectrometry reading) percentage identification (%MS2) of 10,36%.

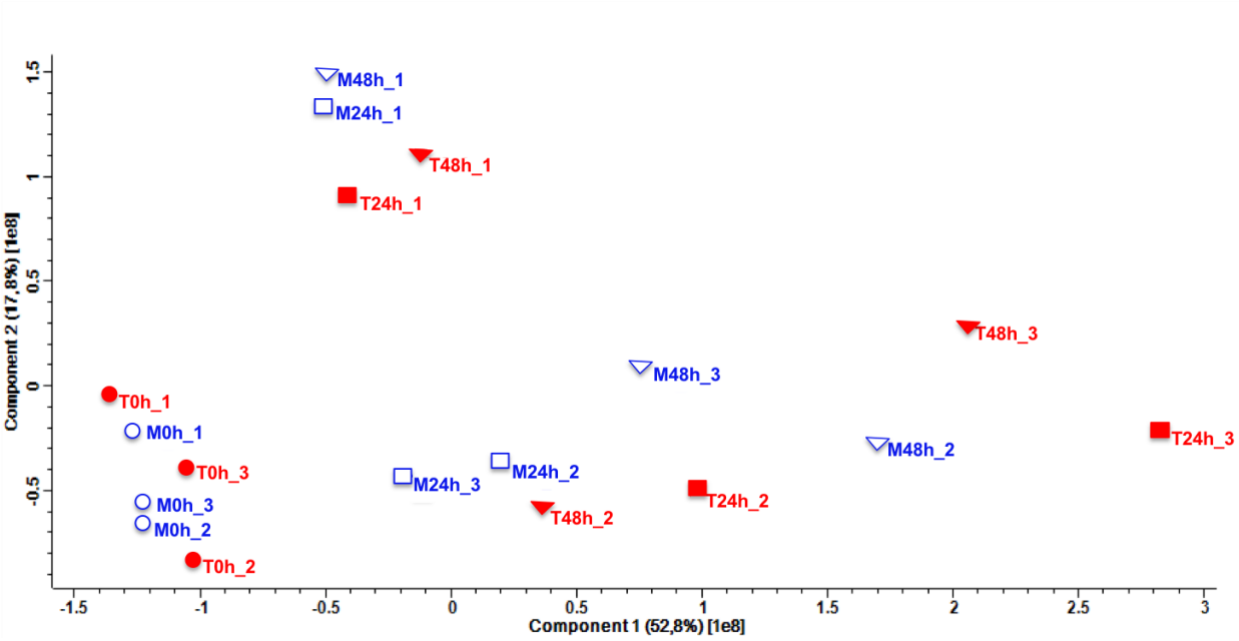

Figure 3.4-1 Principal component analysis (PCA) of exosome samples. Samples from mock transfected cells (M) at timepoints 0, 24 and 48 hours are represented in blue, the number after indicates the biological replicate (1-3); Samples from Poly (I:C) transfected cells (T) are represented in red, for the same timepoints and replicates as M. Graph generated in Perseus 1.5.3.2 program.

The list of identified proteins were then analysed in Perseus 1.5.3.2. Initially a principal component analysis (PCA) was carried out to visualize variance between samples, as seen in Figure 3.4-1, the distribution of samples in 2D show a higher variability in the late time points for both groups M and T. For the time point 0h variability is lower yet it is not possible to differentiate each group as separate cluster. Subsequently, a Pearson correlation analysis was made to measure the strength of the association between replicates as a form to evaluate reproducibility between experiment. Figure 3.4-2 and Figure 3.4-3 show scatter plots of samples correlation and Pearson correlation coefficient as a number in blue each comparison inside group M and T respectively. Samples from group T are less related between them as seen with lower values for Pearson's

coefficient especially in later time points. Group M show slightly higher values for Pearson's coefficient yet decreasing at the last time point like group T. Due to lack of clustering pattern in the PCA that could indicate that group T and M protein profile are different at any time point, we decide to do further analyses grouping all time points, therefore only comparing group T and M as a whole without subdivision by time points. When comparing the set of proteins identified in group T and group M, we found that from 525 total proteins, 425 where shared between groups, 40 where identified only in group T and 60 only in group M (Figure 3.4-4).

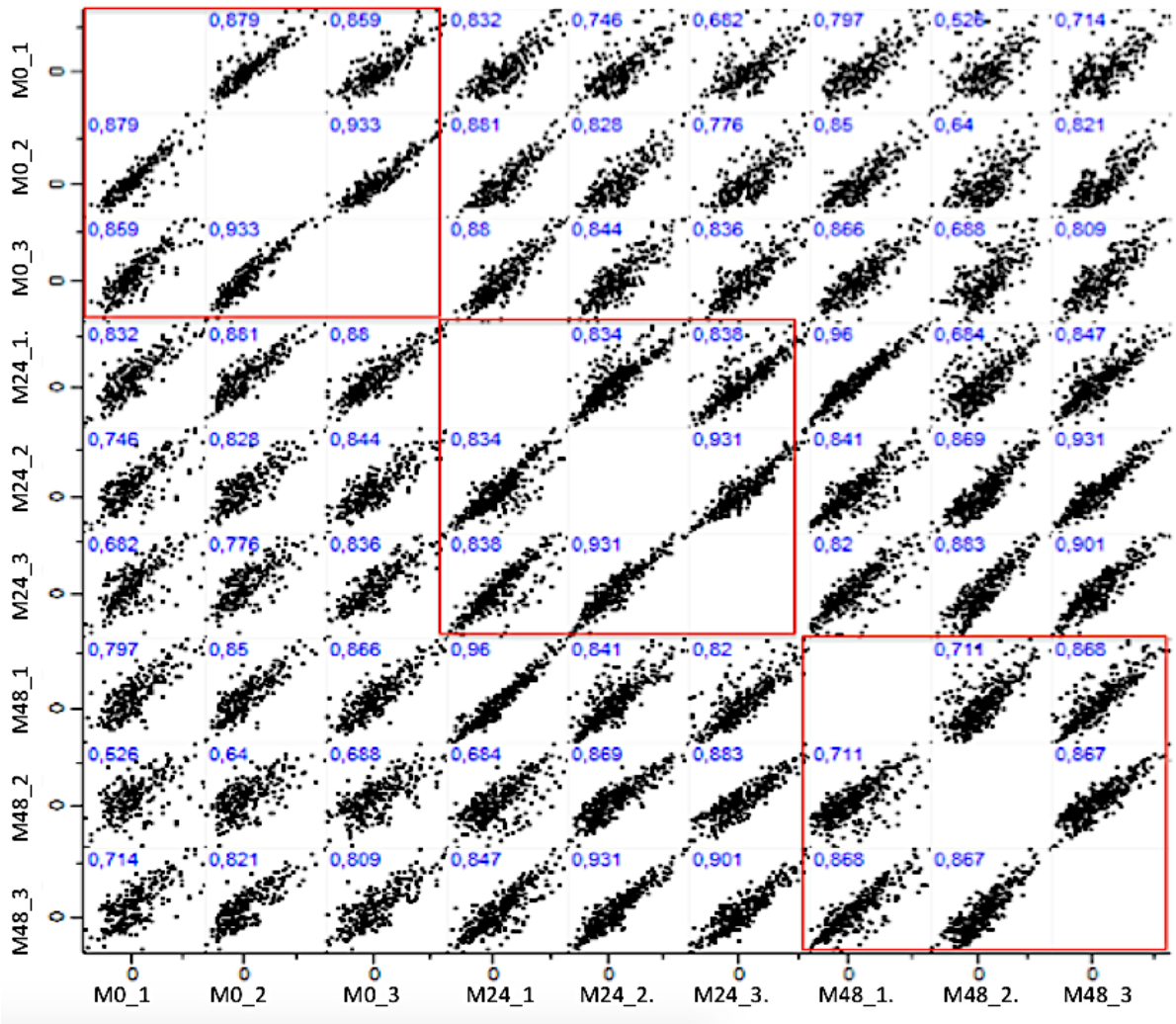

Figure 3.4-2 Pearson Correlation between biological replicates from Mock transfected cells (group M). Each three columns represent a timepoint, 0, 24 and 48 hours after. R values are shown in blue. Graph generated in Perseus 1.5.3.2 program.

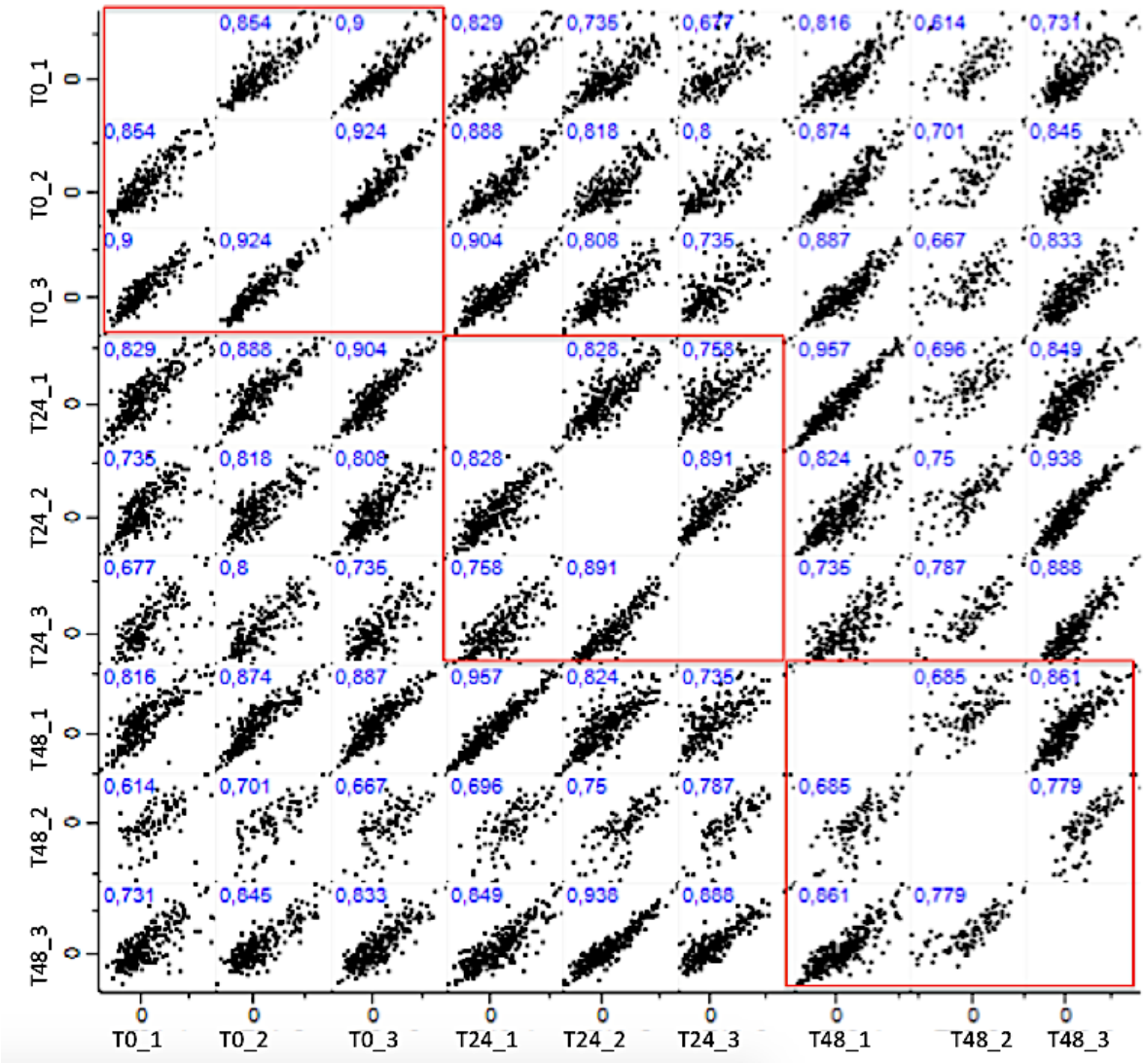

Figure 3.4-3 Pearson Correlation between biological replicates from Poly (I:C) transfected cells (group T). Each three columns represent a timepoint, 0, 24 and 48 hours after. R values are shown in blue. Graph generated in Perseus 1.5.3.2 program.

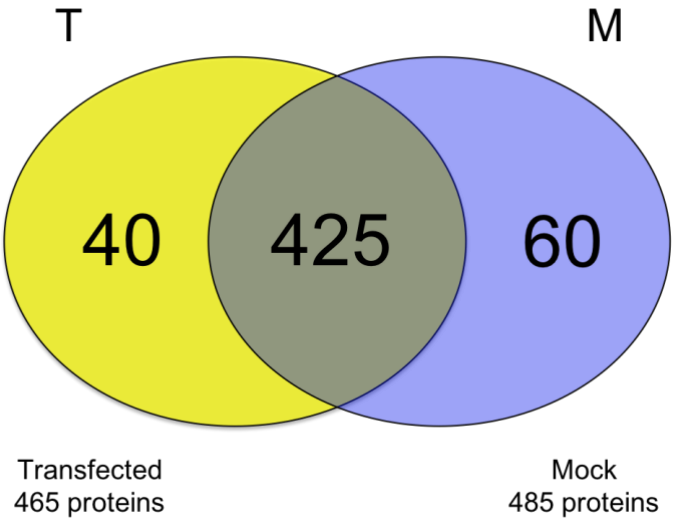

Figure 3.4-4 Venn diagram of total proteins identified. T = Poly (I:C) transfected cells (all time points included), M = Mock transfected cells (all time points included).

In order to confirm that our samples were composed by exosomes, a search was performed for exosomal markers reported in Exocarta (http://www.exocarta.org/) -an exosome database. The database rank order 100 exosomal markers according to the frequency they were found in exosomes across all studies and species, from the top 35 most frequent we found 21 in the list of shared proteins between groups. This markers are listed in Table 3.4-1 and visualized in Figure 3.4-5 both organized in a descendant order by mass spectrometry protein intensity.

To understand better the proteomic profile of exosomes from Poly (I:C) transfected cells, we annotated by homology all 40 proteins detected exclusively in this group and rank order in a descendant manner by mass spectrometry protein intensity (Figure 3.4-6 and Table 3.4-2).

Protein Ids	Name	Pfam
LLOJ009270-PA	**Actin-4**	Actin family
LLOJ004330-PA	**Histone deacetylase 3**	Histone deacetylase domain/14-3-3 domain superfamily
LLOJ001225-PA	**Annexin**	Chaperonin Cpn60/TCP-1 family/TCP-1-like chaperonin intermediate domain superfamily
LLOJ003303-PA	**Annexin**	Actin family
LLOJ008981-PA	**Elongation factor 1-alpha**	dUTPase-like
LLOJ003112-PA	**Aldo: fructose biphosphate aldolase**	Fructose-bisphosphate aldolase, class-I
LLOJ008989-PA	**Tetraspanin**	Immunoglobulin-like domain superfamily
LLOJ004224-PA	**Hsp83: heat shock protein 83**	Apyrase
LLOJ001891-PA	**GAPDH**	Glyceraldehyde 3-phosphate dehydrogenase, NAD(P) binding domain
LLOJ005152-PA	**Ras-like protein 3**	Small GTPase superfamily, Ras-type
LLOJ000219-PA	**Putative enolase**	Histone deacetylase domain
LLOJ000130-PA	**Tubulin alpha chain**	Tubulin/FtsZ, GTPase domain
LLOJ008678-PA	**Phosphoglycerate kinase**	Phosphoglycerate kinase
LLOJ004308-PA	**Tpi: triosephosphate isomerase**	NADP-dependent oxidoreductase domain
LLOJ006091-PA	**Proliferating cell nuclear antigen**	14-3-3 domain superfamily
LLOJ009711-PA	**Endoplasmin**	Tetraspanin/Peripherin
LLOJ006488-PA	**Hsp70A: heat shock protein 70A**	Serpin superfamily
LLOJ008460-PA	**Prdx1: thioredoxin peroxidase**	Alkyl hydroperoxide reductase subunit C/ Thiol specific antioxidant
LLOJ002807-PA	**Tumor susceptibility gene 101**	Ubiquitin E2 variant, N-terminal
LLOJ006270-PA	**Peptidyl-prolyl cis-trans isomerase**	Trypsin Inhibitor-like, cysteine rich domain/von Willebrand factor, type D domain
LLOJ002484-PA	**Clathrin heavy chain**	Clathrin, heavy chain/VPS, 7-fold repeat

Table 3.4-1 Exosomal markers organized in descendant order by their intensity. Protein Ids = Protein identification code from VectorBase Database; Name = Protein name by homology (NCBI Database); Pfam= Protein family.

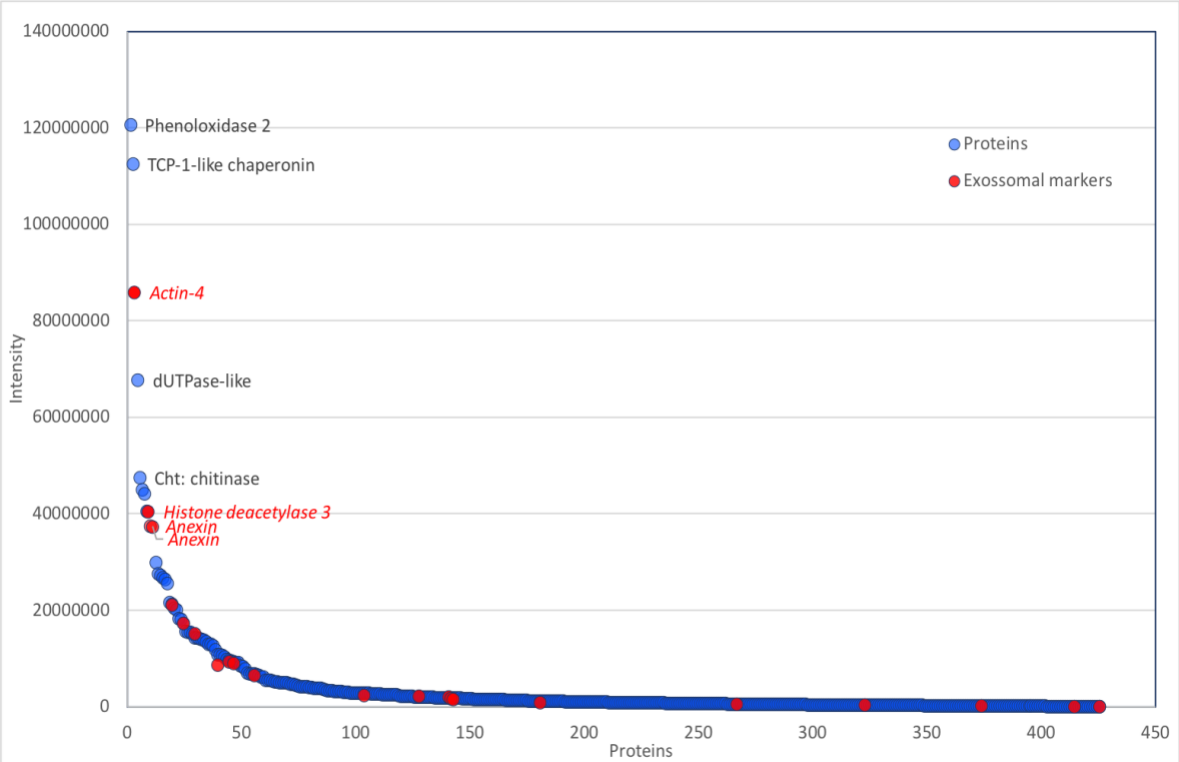

Figure 3.4-5 Shared proteins between T and M groups, organized by mass spectrometry protein intensity. Red dots mark the proteins identified as exosomal markers. For detailed information see ANNEX-D

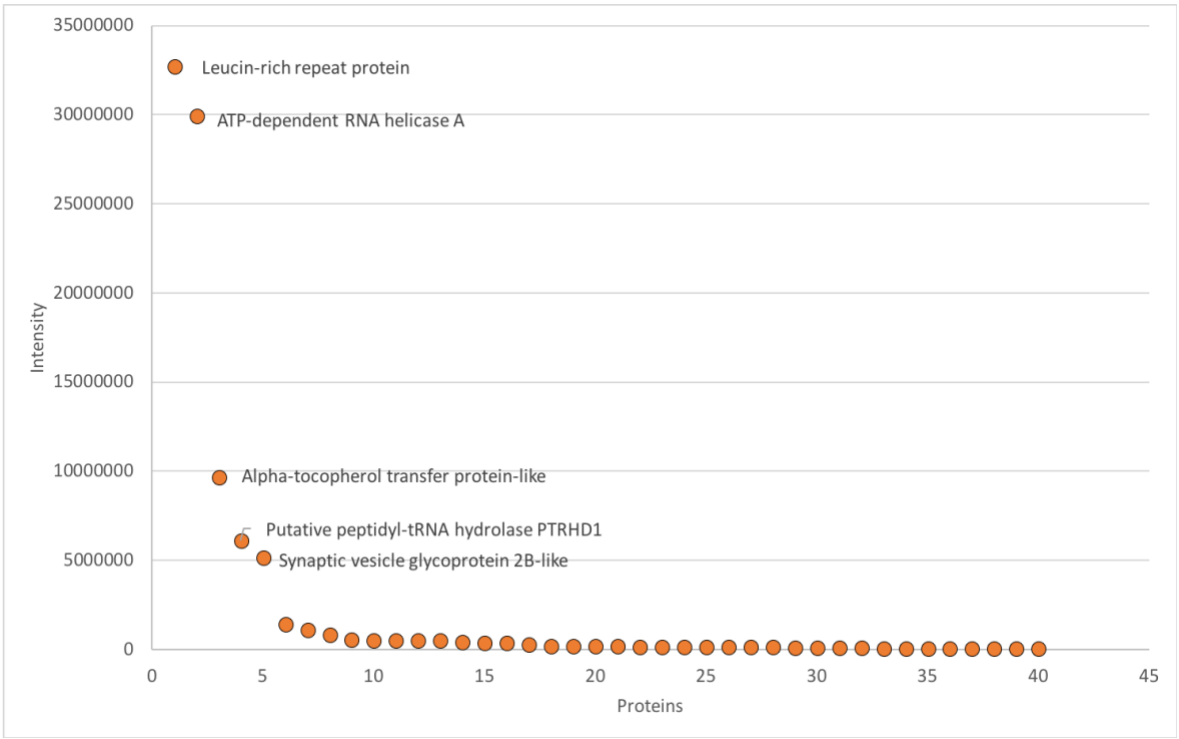

Figure 3.4-6 Proteins found only in Poly (I:C) transfected group (T) organized by mass spectrometry protein intensity. For more detail see Table 3.4-2 and ANNEX-B.

Protein Ids	Name	Pfam
LLOJ001758-PA	**Leucin-rich repeat protein**	Leucine-rich repeat
LLOJ006761-PA	**ATP-dependent RNA helicase A**	DEAD/DEAH box helicase domain/Zinc finger, CCCH-type
LLOJ000307-PA	**Alpha-tocopherol transfer protein-like**	CRAL-TRIO lipid binding domain
LLOJ005291-PA	**Putative peptidyl-tRNA hydrolase PTRHD1**	Peptidyl-tRNA hydrolase, PTH2
LLOJ001309-PA	**Synaptic vesicle glycoprotein 2B-like**	Major facilitator, sugar transporter-like
LLOJ009642-PA	**Leucine zipper putative tumor suppressor 2 homolog**	Family Fez1 (contains a leucine-zipper region)
LLOJ003029-PA	**Elongation factor Tu, mitochondrial**	Transcription factor, GTP-binding domain/Superfamily Translation elongation factor EF1A
LLOJ007948-PA	**Protein unc-80 homolog**	Cation channel complex component UNC80, N-terminal
LLOJ007947-PA	**Myosin light chain alkali**	Myosin light chain alkali
LLOJ005689-PA	**Isovaleryl-CoA dehydrogenase, mitochondrial**	Acyl-CoA dehydrogenase, conserved site/ Isovaleryl-CoA dehydrogenase/ Proteasome beta-type subunit
LLOJ007856-PA	**Glutamate synthase**	Dihydroprymidine dehydrogenase domain II/FAD/NAD(P)-binding domain/Glutamate synthase, alpha subunit, C-terminal
LLOJ000817-PA	**E3 ubiquitin-protein ligase RNF13**	PA domain/Zinc finger, RING-type
LLOJ001625-PA	**60S ribosomal protein L11**	Ribosomal protein L5 domain superfamily
LLOJ001875-PA	**Cell division cycle 37 (CDC37)**	Cdc37, Hsp90 binding
LLOJ006348-PA	**Arf3: ADP-ribosylation factor 3**	Small GTPase superfamily, ARF/SAR type
LLOJ009369-PA	**S-adenosylhomocysteine hydrolase-like protein**	Adenosylhomocysteinase-like
LLOJ008241-PA	**Sphingomyelin phosphodiesterase**	Calcineurin-like phosphoesterase domain, ApaH type/Sphingomyelin phosphodiesterase
LLOJ001189-PA	**Vesicle transport v-SNARE 12**	Family V-SNARE_C (SNARE region achored in the vesicule membrane c-terminus)
LLOJ003622-PA	**Flavin reductase (NADPH)**	NAD(P)-binding domain
LLOJ004428-PA	**Protein NPC2 homolog**	MD-2-related lipid-recognition domain
LLOJ001307-PA	**Ankyrin-3 isoform**	Death domain
LLOJ001204-PA	**DNAJ-like protein 2**	Chaperone DnaJ/Heat shock protein DnaJ, cysteine-rich domain
LLOJ005349-PA	**Acuolar protein sorting-associated protein 37B**	Modifier of rudimentary, Modr/Vacuolar protein sorting-associated protein 37
LLOJ000061-PA	**Ionotropic receptor 21a-like**	Leucine-reach repeat (LRR) domain superfamily
LLOJ006682-PA	**Golgi phosphoprotein 3 homolog sauron**	Golgi phosphoprotein 3-like
LLOJ004857-PA	**Guanylate kinase**	Guanylate kinase/L-type calcium channel beta subunit
LLOJ009131-PA	**SH3 domain-binding glutamic acid-rich protein**	SH3-binding, glutamic acid-rich protein
LLOJ003521-PA	**V-type proton ATPase proteolipid subunit**	V-ATPase proteolipid subunit C-like domain
LLOJ009718-PA	**integrin alpha-PS1**	Integrin alpha-2
LLOJ000883-PA	**coactosin-like protein**	Actin-depolymerising factor homology domain
LLOJ008434-PA	**putative nuclear transport factor 2**	Nuclear transport factor 2
LLOJ001580-PA	**Ubqn: ubiquilin**	Ubiquitin domain
LLOJ009328-PA	**Probable isoaspartyl peptidase**	Peptidase T2, asparaginase 2
LLOJ005310-PA	**Vacuolar ATPase subunit C**	ATPase, V1 complex, subunit C
LLOJ005181-PA	**Elongin-C**	SKP1 component, POZ domain (tetramerisation domain)
LLOJ003536-PA	**Camp-dependent protein kinase catalytic subunit**	Phosphorilase kinase; domain1.
LLOJ000658-PA	**26S proteasome non-ATPase regulatory subunit 7**	JAB1/MPN/MOV34 metalloenzyme domain
LLOJ007054-PA	**Uncharacterized protein**	PDZ domain/Sterile alpha motif domain
LLOJ001587-PA	**Sorting nexin**	Sorting nexin Vps5-like, C-terminal/Phox homologous domain
LLOJ005056-PA	**Lamin**	Ribosome binding protein-1

Table 3.4-2 Proteins present only in group T exosomes organized in descendant order by their intensity. Protein Ids = Protein identification code from VectorBase Database; Name = Protein name by homology (NCBI Database); Pfam= Protein family. Table in ANNEX-B, include intensity and molecular weight values.

3.4.2 Gene expression in LL5 cells transfected with Poly(I:C)

3.4.2.1 Toll and IMD pathway

In order to asses if Toll and IMD pathways were activated in response to Poly(I:C) challenge, gene expression of positive regulators and AMPs were evaluated at different time points. Time point zero was taken at the end of the 24h transfection reaction. Gene expression of transcription factors dorsal (Toll pathway) and Relish (IMD pathway) was very close to control groups with no significant difference to control at any time point (Figure 3.4-7A, B). attacin, cecropin and Defensin 4 expression in Poly(I:C) challenged cells did not vary significantly from mock transfected cells at any time point (Figure 3.4-7C).

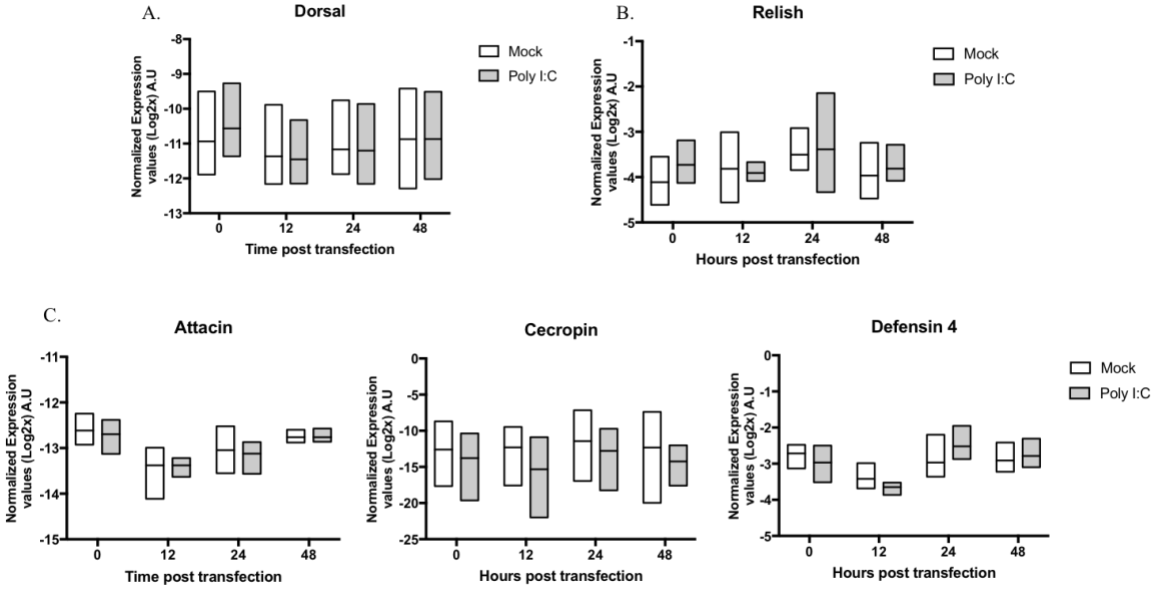

Figure 3.4-7 Transcriptional profile of Toll and IMD pathway molecules in LL5 cells transfected with Poly(I:C). (A-B) mRNA levels in LL5 cells of Toll pathway transcription factor dorsal and IMD pathway transcription factor Relish, at different timepoints after transfection with Poly(I:C) and mock transfection. (C) mRNA level of three AMPs at the same timepoints. All graphs Y-axis represent log2(x) of normalized by reference gene (GAPDH) expression values from qPCR data. The X-axis represent timepoints of sample collection at 0, 12, 24 and 48 hours after transfection reaction. Boxes represent mean with maximum and minimum values. A Student's T test with Welch's correction was performed for each timepoint.

3.4.2.2 JAK/STAT pathway

To evaluate if the JAK/STAT pathway was modulated in response to Poly(I:C) challenge, gene expression of regulatory molecules and effectors was assessed. Gene expression of transcription factor STAT and negative regulator Pias were close to control group with no significant difference at any time point (Figure 3.4-8A and B respectively). One of the effector genes of this pathway and related to antiviral response is vir-1, yet this gene showed no difference

in gene expression when compared to control group across all time points (Figure 3.4-8C). It has been reported in the literature that insects have a IFN-like molecule, Vago, that is also related to antiviral response and possibly linked to activation of the JAK/STAT pathway (Paradkar et al. 2012), therefore *L. longipalpis* Vago2 molecule was tested. Results showed significant down regulation of Vago2 at 12h time point only, while gene expression of other time points remains not significant in relation to control (Figure 3.4-8D).

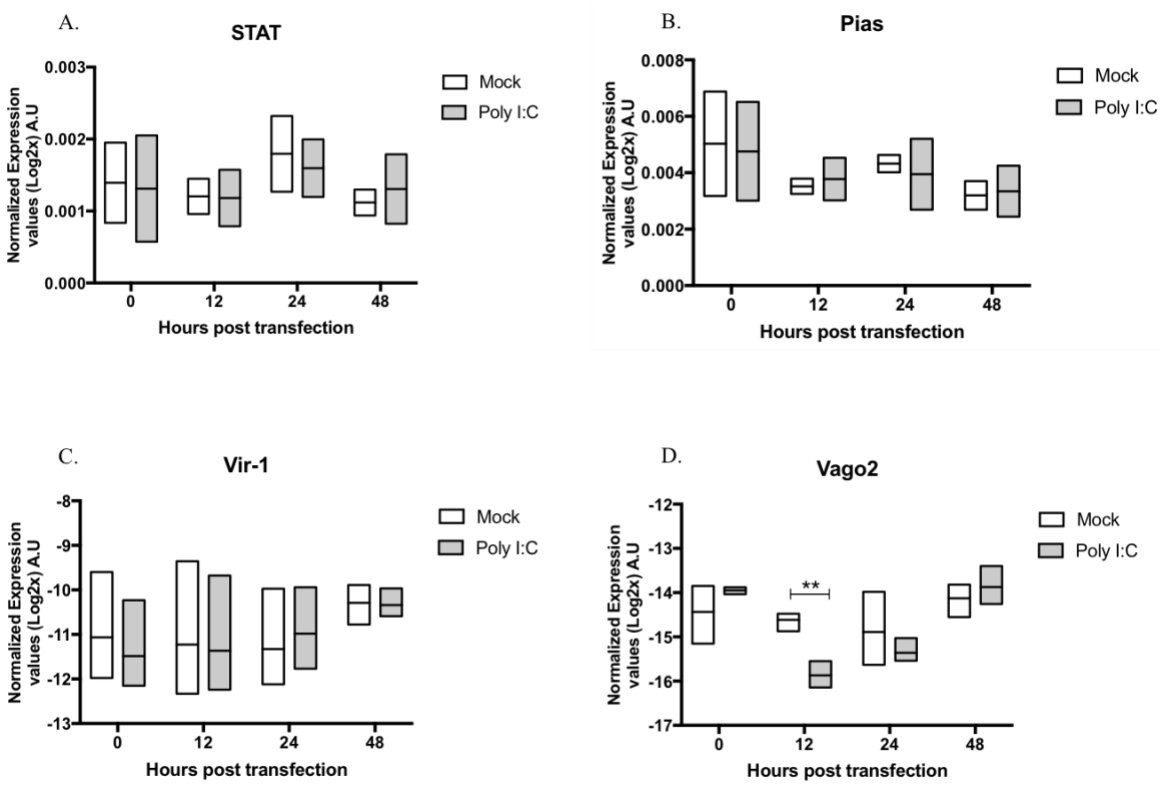

Figure 3.4-8 Transcriptional profile of JAK/STAT pathway molecules in LL5 cells transfected with Poly(I:C). (A) mRNA levels in LL5 cells of transcription factor STAT, at different timepoints after transfection with Poly(I:C) and mock transfection. (B) mRNA levels of JAK/STAT pathway's negative regulator Pias at the same timepoints. (C-D) mRNA expression levels of vir-1 and Vago, two effector genes related to JAK/STAT pathway. All graphs Y-axis represent log2(x) of normalized by reference gene (GAPDH) expression values from qPCR data. The X-axis represent timepoints of sample collection at 0, 12, 24 and 48 hours after transfection reaction. Boxes represent mean with maximum and minimum values. A Student's T test with Welch's correction was performed for each timepoint. **$p \leq 0.01$.

3.5 DISCUSSION

3.5.1 Protein profile of exosomes from Poly (I:C) stimulated LL5 cells

PCA results show that samples from group M and T do not group in separate clusters either by type of stimuli (Poly (I:C) or Mock) or by time point, indicating that protein profiles present a high variability between them. It is possible to distinguish that samples from time point 0h seem to group together better that the rest yet there is no distinction between groups M and T. From this observation we suggest the protein profile in the first time point is more conservative than late time points, with an increase in variability between groups and inside group samples becoming more apparent as time progresses. Results from Pearson correlation confirm that similarity between replicates of the same group and time point is not very high. Considering these results we decided to analyse the data in a more descriptive manner in order to characterize and understand the proteomic profile of exosomes after Poly(I:C) challenge.

Exosome composition varies depending on cell type of origin, but they share certain characteristic proteins, usually proteins like tubulin, actin (and actin ligation proteins), annexing and Ras protein as well as transduction signal proteins like kinases. They also contain heat shock proteins Hsp70 and Hsp90 (Simpson et al. 2008). Comparison results from the list of shared proteins between groups and list of protein exosomal markers reported in Exocarta confirm that all samples obtained through serial centrifugation were indeed exosomes, since 21 of the top 35 most frequent markers were found (Table 3.4-1). These proteins are generally related to structure, ligation and transport of exosomes.

dsRNA is a universal viral PAMP and a potent inducer of type I IFNs. The dsRNA and its synthetic analogue Poly (I:C) are recognized by TLR3 that are localized in endosomes and lysosomes, and by RIG-I and MDA5 that are located in the cytosol. TLR3 has been implicated in the host response to ssRNA, dsRNA, and DNA viruses (Akira et al. 2006; Barbalat et al. 2011). After detection of viral nucleic acids either by TLRs or cytosolic RNA sensors, IFN type I is induced and other inflammatory genes according to each detector (Akira et al. 2006; Barbalat et al. 2011). Several studies have reported that nucleic acid mimics, especially Poly(I:C), can strongly induce non-specific antiviral immune responses in insects, sand fly (Pitaluga et al. 2008) and honeybee (Flenniken and Andino 2013), shrimp (Robalino et al. 2004, 2005), and oyster (Green and Montagnani 2013).

From the list of proteins identified exclusively in exosomes derived from Poly (I:C) transfected cells (Table 3.4-2) it is possible to highlight six that are related to immune (antiviral)

responses. *Leucine-rich repeats protein (LRR)* contain 20-29 residue sequence motifs and present diverse functions that are involved in a variety of biological processes, including signal transduction, cell adhesion, DNA repair, RNA processing, disease resistance, apoptosis and the immune response (Kobe and Kajava 2001). The principal function of these motifs appears to be to provide a versatile structural framework for the formation of protein-protein interactions (Kobe and Kajava 2001). One of the best-known examples is the toll-like receptor that possesses 19-25 tandem copies of LRR motifs which serve to bind pathogen and danger-associated molecular patterns (Akira and Kiyoshi 2004).

The second most abundant protein in this group was an *ATP-dependent RNA helicase A*. RNA helicases catalyse the ATP-dependent unwinding of RNA duplexes and structural rearrangements of RNAs and RNA-protein complexes (RNPs) in a large number of processes; they also play a crucial role in viral infection. In vertebrates RNA helicases sense RNAs and mediate the antiviral immune response (Steimer and Klostermeier 2012). The RIG-I-like (retinoid acid inducible gene) receptors, MDA-5 (melanoma differentiation-associated gene 5) and LGP2 are cytoplasmic DEx/H box helicases that trigger the innate immune response to RNA virus infections of vertebrates (Yoneyama et al. 2005). RIG-I and MDA-5 stimulate antiviral responses through the same pathway but they detect different RNAs. RIG-I senses positive and negative strand RNA viruses while MDA-5 detects different positive strand and dsRNA viruses (review in Wilkins and Gale 2010). MDA-5 is an early response gene inducible by IFN and tumour necrosis factor-α (Kang et al. 2002). Later studies showed that LGP2 was essential for type I IFN production in response to picornaviridae infection in mice (Satoh et al. 2010).

Synaptic vesicle protein-2 (SV2) gene was found to be up regulated significantly in virus infected mosquitoes (Sanders et al. 2005). SV2 is involved in regulation of vesicle transport, mediating vesicle docking to the plasma membrane and subsequent fusion of the two membranes, and is also involved in the control of calcium-mediated exocytosis (Detrait et al. 2014). These genes are homologs of the mammalian SV2, a transporter like proteins family that are located in synaptic neurotransmitter-containing vesicles in mammals. These have structural similarities with the major facilitator (MF) family of small molecule transporters, including glucose transporters (GLUTs) (Bartholome et al. 2017).

Another interesting protein is *E3 ubiquitin protein ligase RNF13*. The RING-domain E3 ligases (RING E3s) contain one or two RING finger domains, and are an extended family of ligases present in various organisms from animals to plants and viruses. They are involved in several cellular processes such as cell proliferation, immune regulation, and apoptosis among others. In

mammalian hosts, a considerable number of the RING E3s have been implicated in viral replication inhibition through immune response regulation, including activation and inhibition of RIG-I-like receptors (RIG-I, MDA-5 and LGP2), toll-like receptors and DNA receptor signalling pathways among others (Zhang et al. 2018). IFN signalling is tightly regulated by several mechanisms, and one such mechanism is ubiquitination (Oshiumi et al. 2012).

RING finger protein 13 (RNF13) is a highly regulated ubiquitin ligase anchored in endosomal membranes. The cytoplasmic half of the protein is released from the membrane by regulatory proteases and therefore has the potential to mediate ubiquitination at distant sites independent of the full-length protein (Bocock et al. 2011).

Protein Cdc37 (cell division cycle 37) is a molecular chaperone with specific functions in cell signal transduction and has been shown to form complexes with heat shock protein Hsp90 (Calderwood 2015). Van der Lee et al. (2015) carried out an integrative genomic-based discovery of novel regulators of RIG-I-like receptor (RLR) pathway, which is essential for detecting cytosolic viral RNA to trigger type I interferon response and initiate innate antiviral response in mammals. Validation RNAi knockdown experiments identified with high prediction accuracy 94 genes among 187 candidates tested (~50%) that affected viral RNA-induced production of IFNβ, one of these genes being Cdc37. Previous studies already linked Cdc37 to antiviral responses. Lee et al. (2013) used integrative approach studies which combined quantitative proteomics and genomics to identify genes involved in viral DNA detection and type I interferon production. They found that Cdc37 regulates stability of TBK1 via Hsp90, allowing for induction of INFβ in response to viral DNA and retroviral infections.

DNAJ-like protein 2 belongs to the DNAJ/Hsp40 (heat shock protein 40) group, evolutionarily conserved proteins important for translation, folding, unfolding, translocation and degradation, primarily by stimulation the ATPse activity of chaperone proteins like Hsp70s (Qiu et al. 2006). A genome-wide study to identify dsRNA-activated genes (DRAGs) by microarray and qRT-PCR analyses in filamentous fungus *Neurospora crassa* revealed that additional RNAi components and homologs of antiviral and interferon-stimulated genes were involved in this response and independent from Dicer proteins and siRNA (Choudhary et al. 2007). One of the major functional groups of DRAGs found were stress response and protein degradation, where DNAJ-like protein was upregulated upon dsRNA challenge along with proteins involved in peroxisome function and proteasome regulation (Choudhary et al. 2007).

Our proteomic results show that exosomes from LL5 challenged with Poly (I:C) contain exclusive proteins, where some molecules discussed previously have been associated with IFN

response, reinforcing the hypothesis already suggested by Pitaluga et al. (2008) and Martins-da-Silva et al. (2018), that LL5 non-specific antiviral response could be comparable to mammalian-like type I interferon response.

3.5.2 Analysis of some immune-related genes of Poly (I:C) stimulated LL5 cells

It has also been shown that other antimicrobial innate immune pathways like IMD, Toll and JAK/STAT could also participate in antiviral immunity (Kingsolver et al. 2013). Studies in mosquito cells showed that pre-activation of the IMD pathway reduced SFV (Semliki Forest Virus) viral replication and, experiments with *Drosophila* mutants for components of IMD pathway presented an increase in viral replication when infected with virus like Sindbis Virus (SINV), SFV and Ross River, suggesting an antiviral role for this pathway in those insects (Fragkoudis et al. 2008; Huang et al. 2013). Research on insect vectors like *Ae. aegypti* has revealed the participation of the Toll pathway in reducing the viral titre of Dengue virus in laboratory and field tests (Xi et al. 2008; Ramirez and Dimopoulos 2010). In contrast, our gene expression results for Toll and IMD pathways did not show any significant regulation (Figure 3.4-7) which could indicate that these pathways do not participate in the response to Poly (I:C).

The JAK/STAT pathway has also been reported to be involved in antiviral response in insects (Souza-Neto et al. 2009; Paradkar et al. 2012). Our results obtained for JAK/STAT molecular components (Figure 3.4-8) including STAT, Pias and vir-1, an effector gene, did not vary significantly in relation to the control group, which indicates that this pathway also may not be involved in the response to Poly(I:C) challenge.

It has been reported that crosstalk between the JAK/STAT and RNAi pathways exists during viral infection in mosquito cells through Vago. Basically, viral infection up-regulates Dicer-2 of the RNAi pathway, which activates Vago transcription and therefore increases levels of secreted Vago; consequently this induces the JAK/STAT antiviral immunity in a mode similar to mammalian interferon (Paradkar et al. 2012, 2014). Nonetheless, the role of Vago in other insects during viral infections is not well understood (Sheldon et al. 2007; Paradkar et al. 2012, 2014). We evaluated transcription levels of a putative homologue, Vago2, in LL5 cells, which surprisingly presented a significant down regulation at 12h post challenge with Poly(I:C). Down regulation of Vago/Vago-like molecule in response to viral infection has only been reported before in the bumblebee (*Bombus terrestris*) -which also has a non-specific antiviral response (Piot et al. 2015)- upon infection by the virulent Israeli acute paralysis virus (IAPV) but not with Slow bee paralysis virus (SBPV). The study proposed that in their case Vago expression could be related to the

virulence of the virus (Niu et al. 2016). Similar results were obtained in later experiments with IAPV (Wang et al. 2017). Additionally, studies in *Drosophila* have shown that Vago is induced after viral infection with DCV (*Drosophila* C virus) and Sindbis virus, but not with Flock house virus (Deddouche et al. 2008). These evidence suggest that expression of Vago (up, down or constant) may be depend on the virus species and/or variables in the virus/host interaction (Niu et al. 2016). In the study by Paradkar et al. (2012), only WNV (West Nile Virus) was able to trigger Vago production, and Poly(I:C) and Bluetongue virus dsRNA did not cause variation in Vago expression, showing one more time that stimulation either by a virus or by a dsRNA mimic could generate efferent profiles of Vago gene expression that could be specific to each case.

Another gene that is regulated in a positive manner by the JAK/STAT pathway is vir-1, although its specific function is not fully understood. However it is known that vir-1 gene regulation is specific for viral infection (Dostert et al. 2005). Other studies showed that experiments using inactivated virus or only viral dsRNA did not produce up regulation of vir-1, suggesting that active viral replication may be necessary for activation of this gene, even though vir-1 does not have an apparent direct effect on production or viral replication (Hedges and Johnson 2008). These findings are in line with our results (Figure 3.4-8) showing that vir-1 regulation in LL5 cells could depend on viral replication, therefore Poly(I:C) challenge by itself should not up regulate this gene.

The negative regulator Pias and transcription factor STAT did not vary when compared to the control group (Figure 3.4-8), reinforcing the theory that JAK/STAT pathway has very low to no participation in the non-specific antiviral response investigated in this work. It is important to mention that antiviral response studies have shown that individual genes are not representative of immune activation in each scenario (Kingsolver et al 2013). This has been proven clearly in *Drosophila* research when comparing different viral infection transcriptome profiles, revealing that a majority of regulated genes are different among infections, particularly, the JAK/STAT pathway regulated genes (Kemp et al 2013).

Taking together our proteomic and transcriptional analysis results seems to indicate that this non-specific antiviral response is in a way similar to an interferon-like response as previously by Martins da Silva et al. (2018).

3.6 CONCLUSIONS

-Exosomes from LL5 cells contain 21 of the most frequent exosomal markers reported across all cell types.

-Exosomes derived from Poly(I:C) stimulated LL5 cells contained several proteins that are related to antiviral response and antiviral INF-like response.

-None of the canonical immune pathways (Toll, IMD, JAK/STAT) are activated in response to Poly(I:C) challenge.

4 CHAPTER 2. THE TOLL PATHWAY IN *L. LONGIPALPIS*

4.1 INTRODUCTION

The recognition of pathogens and subsequent activation of signal transduction pathways stimulate humoral responses and leads to the production of factors with antimicrobial activity and the potentiation of effector mechanisms. The three best characterized immune signalling pathways in insects are the Toll pathway, the IMD pathway, and the JAK/STAT pathway (Figure 1.3-1) (Hillyer 2016).

4.1.1 Toll pathway in insects

The identification of the *Drosophila melanogaster* Toll pathway cascade and consequent description of TLRs (Toll-like receptors) have contributed greatly to the understanding of the immune system in insects and mammals. Since then, NF-kB signalling in *D. melanogaster* has been studied actively. In general, Toll receptors in flies are important for embryonic development and immunity (Lemaitre et al. 1996; Valanne 2014) .

The Toll pathway in *D. melanogaster* responds to Gram-positive bacterial and fungal infections (Lemaitre et al. 1996). *Drosophila* TLRs are cytokine receptors which do not bind pathogens or pathogen-derived molecules directly and instead are activated by a cytokine molecule, in this case by Spätzle (Spz). Extracellular recognition factors start protease cascades that lead to the activation of Spätzle, by conformational changes that expose elements that are critical for binding to the Toll receptor (Aggarwal and Silverman 2008; Arnot et al. 2010). Bacteria and fungi recognition involve three distinct pathways that converge on Spätzle cleavage (Figure 4.1-1) (Aggarwal and Silverman 2008). Until now, two models have been proposed for the binding of Spz to Toll, the first one implies that one Spz dimer binds to two Toll receptors (Weber et al. 2005) and the second one, suggests that two Spz dimers, each binding to the N terminus of one of the two Toll receptors, generate a conformational change in the receptors to activate downstream signalling (Gangloff et al. 2008).

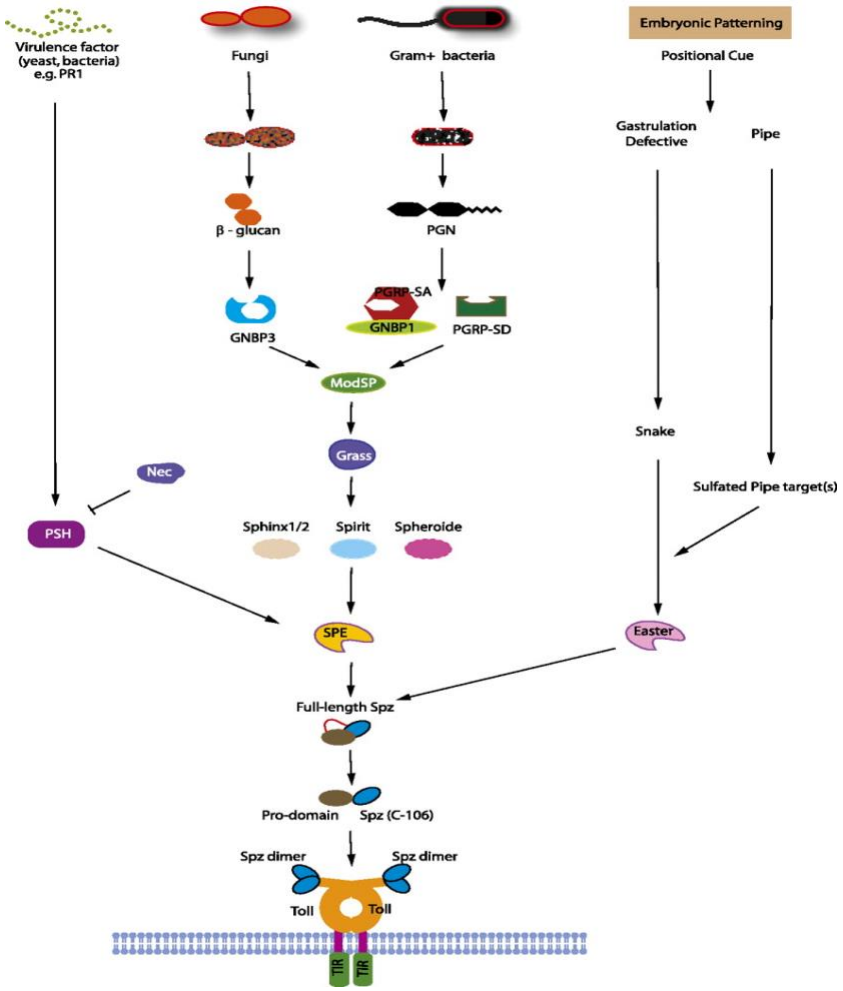

Figure 4.1-1 Extracellular cleavage of Spz leading to Toll pathway activation. In the immune response, three protease cascades lead to the activation of SPE to cleave full-length Spz; the Persephone (PSH) cascade senses virulence factors and is activated by live Gram- positive bacteria and fungi. The other two cascades are activated by pattern recognition receptors binding cell wall components from Gram-positive bacteria and fungi, respectively. Upon proteolytical processing, the Spz pro-domain is cleaved, exposing the C-terminal Spz parts critical for binding of Toll. Spz binding to the Toll receptor initiates intracellular signalling.(Valanne et al. 2011)

When the processed Spz binds to the Toll receptor, it induces Toll dimerization which is believed to recruit the adaptor protein MyD88 via intracellular TIR domains (Horng and Medzhitov 2001; Sun et al. 2002; Tauszig-Delamasure et al. 2002). After this interaction, a second adaptor protein, Tube, and the kinase Pelle are recruited to form MyD88-Tube-Pelle heterotrimeric complex through death domain (DD)-mediated interactions (Xiao et al. 1999; Sun et al. 2002; Moncrieffe et al. 2008). After the MyD88-tube-pelle complex is formed, the signal advances to the phosphorylation and ubiquitin/proteasome-mediated degradation of cactus, *Drosophila* IκB homolog (Figure 4.1-2) (Fernandez et al. 2001). In the absence of signalling, cactus is bound to the NF-kB transcription factor(s) dorsal and/or Dif in a context-dependent manner, inhibiting their activity and nuclear localization. Therefore, the nuclear translocation of both dorsal and Dif requires cactus degradation (Wu and Anderson 1998). In order to be degraded, cactus needs to be

phosphorylated, and while it has not been directly demonstrated, it is possible that this is accomplished by pelle, since its kinase activity is essential for cactus phosphorylation. Different laboratories have failed to identify any kinase other than pelle that functionally links Toll to cactus (Towb et al. 2001; Kuttenkeuler et al. 2010; Valanne et al. 2010). Following phosphorylation, nuclear translocation of dorsal/Dif leads directly to transcriptional induction of many immune responsive genes such as those for AMPs (Figure 4.1-2) (Reichhart et al. 1993; Wu and Anderson 1998).

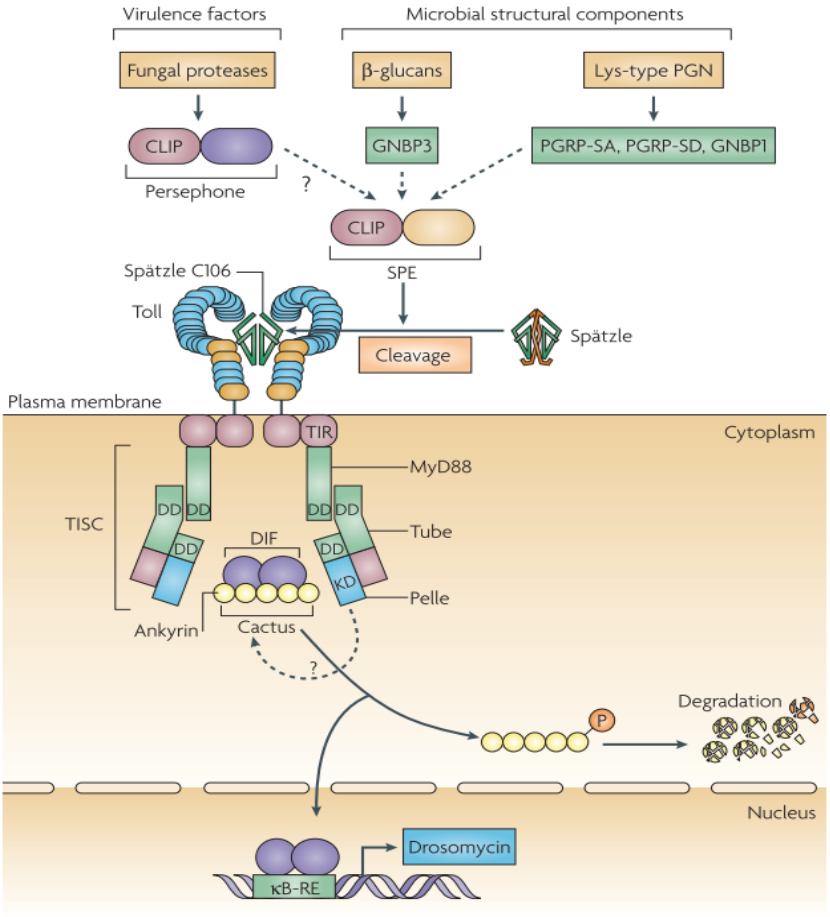

Figure 4.1-2 Intracellular cascade of the Toll pathway. The Toll pathway is activated upon dimeric Spätzle-C106 binds with Toll receptor to induce Toll- induced signalling complex (TISC), which is composed of three death-domain (DD)-containing proteins, MyD88 (myeloid differentiation primary-response gene 88), Tube and Pelle. Cactus may be phosphorylated by Pelle, phosphorylated Cactus is rapidly polyubiquitylated and degraded, allowing for the nuclear translocation of DIF, and binding to NF-κB response elements (κB-RE), which in turn induces the expression of genes encoding antimicrobial peptides, such as Drosomycin (Ferrandon et al. 2007)

4.1.2 Negative Regulators.

Innate immune pathways generate a variety of molecules that target all kinds of pathogens to diminish any risk of mortality by infection. Nevertheless, excessive or constitutive activation of those pathways results in uncontrolled tissue damage and thus present a fitness cost. For instance, hyper-activation of the Toll or IMD pathways impairs insect viability over time (Gordon et al.

2005, 2008; Lamiable et al. 2016a). Many distinct regulatory mechanisms that operate at different molecular levels have evolved to negatively control immune signalling.

Several studies in *Drosophila* negative regulation have identified the presence of signal inactivators at every step of signal transduction in the Toll pathway. The extracellular activation signals transduced by serine protease cascade is inhibited by serpin (SPN) (Reichhart 2005; Meekins et al. 2017). Various immune-related serpins have been identified in different insects like *Tenebrio molitor* (beetle) (Jiang et al. 2009), *Manduca sexta* (moth) (An and Kanost 2010), *Apis mellifera* (bee) and *Anopheles gambiae* (mosquito) (Meekins et al. 2017), some of these insects have fewer serpin genes implying considerable plasticity in the regulation of the cascade reactions (Wang and Xia 2018).

The intracellular part of Toll signalling is frequently regulated by the ubiquitination status of signalling molecules. The molecule Pellino associates with the C-terminal phosphoinositide-binding domain of MyD88 and marks it for ubiquitination and degradation (Ji et al. 2014). The enzyme Ubc9 (ubiquitin-conjugation enzyme 9), has been shown to regulate the expression of AMPs drosomycin and cecropin, in the fruit fly (Chiu et al. 2005). Its inhibitory mechanism is unknown but it has been proposed that dUbc9 conjugates SUMO (an ubiquitin-like modifier) to cactus and protects it from phosphorylation and degradation, therefore preventing translocation of dorsal/Dif to the nucleus. (Wang and Xia 2018). A deubiquitinase, (USP34)/Puf (Puffyeye), can also prevent the constitutive expression of drosomycin which has been specifically related to Toll signalling, while it seems to be needed for induction of other AMPs regulated by the IMD pathway in response to bacterial infection (Figure 4.1-3) (Engel et al. 2014). β-arrestins can also play a role in the Toll pathway regulation; in *Drosophila*, the β-arrestin Kutz inhibits MAPK during development and it was later demonstrated that Kutz and Ulp1 (SUMO protease) work together to regulate this immune pathway (Tipping et al. 2010). In shrimp (*Marsupenaeus japonicus*) two β-arrestins were found to interact with cactus and dorsal, forming a β-arr-cactus-dorsal complex, preventing cactus phosphorylation and degradation, as well as dorsal translocation to the nucleus. These β-arrestins also have a secondary method of regulation, by preventing ERK phosphorylation and consequently dorsal translocation and phosphorylation (Sun 2016).

Interestingly, Wnt inhibitor of dorsal (WntD) was initially described as a feedback inhibitor of Toll signalling in *Drosophila* embryos. Activation of the Toll pathway leads to the transcription of WntD, than consequently inactivate the pathway (Ganguly et al. 2005; Gordon et al. 2005). More recently, it was shown that the mechanism by which WntD blocks the nuclear translocation of

dorsal is through association with its receptor Frizzled4, by preventing that the extracellular Toll domain adopt the productive conformation required for the recruitment of downstream molecules (Figure 4.1-4) (Rahimi et al. 2016). WntD can also regulate systemic activation of the IMD pathway in *Drosophila* (Lamiable et al. 2016b).

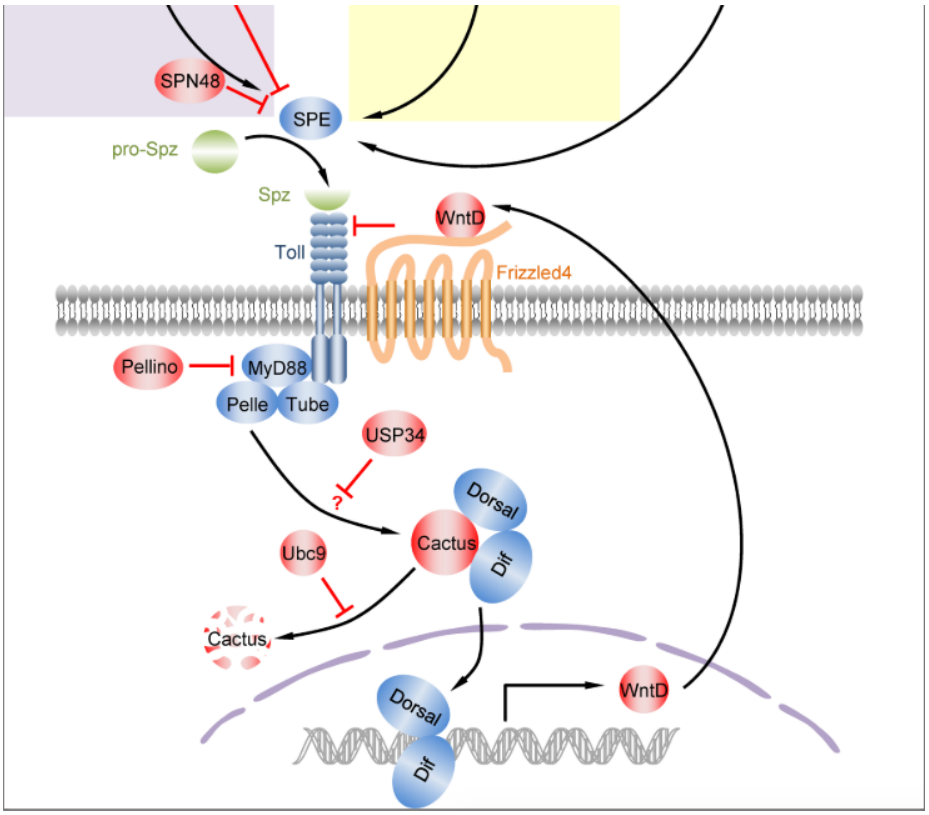

Figure 4.1-3 Negative regulation of the Toll pathway in *Drosophila*. The negative regulators (red) target the signalling components (blue) in the Toll pathway at every step of signal transduction. Question mark indicates the target has not been determined. Adapted from Wang & Chia, 2018

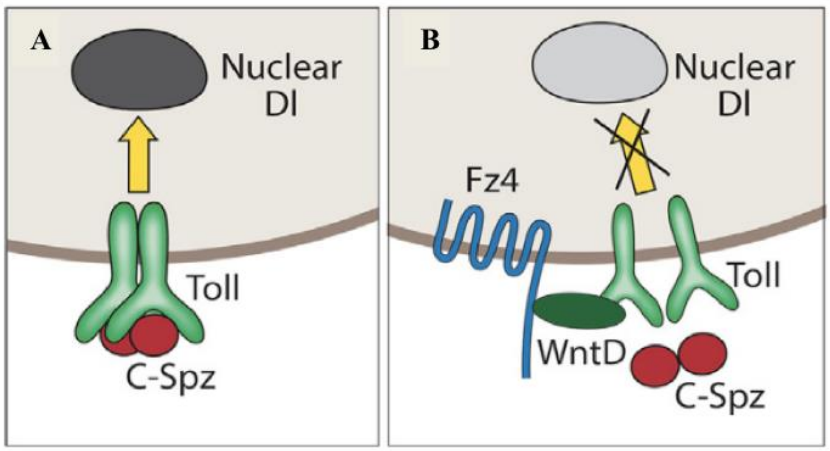

Figure 4.1-4 Schematic representations of Toll signalling and the mechanism of WntD/Fz4 inhibition. (A) Binding of C-Spz to Toll triggers Dl nuclear localization. (B) WntD binds Fz4 and is presented to the extracellular domain of Toll, to block its association with C-Spz or dimerization, thus interfering with signalling in the embryo. From Rahimi et al, 2016.

4.1.3 Toll Pathway in L. longipalpis

In comparison to the several studies on other insect immune response to parasites, not much is known about the sand fly response to infections with *Leishmania* (reviewed in Telleria et al. 2018) and more specifically on the role of the Toll pathway. Studies in sand fly transcriptome have identified some components of the canonical innate immunity pathways, including molecules known to participate in the Toll pathway like Tube, Spz, cactus and other genes that could be related like defensins and serpins, some of which were modulated during *Leishmania* infection (Dillon et al. 2006; Pitaluga et al. 2009). More recently, RNAi studies carried out by our research group in LL5 *L. longipalpis* embryonic cells, have shown upregulation of AMPs after cactus silencing and modulation of Toll and IMD components after several challenges, including *Leishmania* (Tinoco-Nunes et al. 2016). Initial studies in our laboratory about the Toll pathway regulation in *L. longipalpis* adult females indicate that regulatory processes could be more complex than what is known in LL5 cell line. Upregulation of cactus and AMPs two and three days after the sand fly infection with *Leishmania* was observed by Tinoco-Nunes (2014) indicating a possible modulation of the Toll pathway by the parasite and therefore probable participation on infection establishment. The possibility of a negative regulatory loop by WntD molecule has also been suggested. In female sand flies without stimuli, after RNAi silencing of the negative regulator cactus, downregulation of AMPs and upregulation of dorsal and WntD molecule were observed (Tinoco-Nunes 2014).

Understanding the defence mechanisms of *L. longipalpis* or any other vector could contribute toward controlling transmission of many pathogens. Not only in the identification of new genes that participate in important steps in phlebotomine immunity, but also understanding their role in the pathway and during infection will help us improve our comprehension of recognition and protection mechanisms against pathogens in sand flies. These mechanisms can directly influence the permissiveness and vector capacity and also benefit strategies based on blocking parasite transmission.

4.1.4 Microbiota in L. longipalpis

The microbiota has a fundamental role in the induction, maturation and function of the host immune system, which can modulate host protection from pathogens and infectious diseases, and in the same way that ingested food can influence gut microbiota in larvae, it can influence gut microbial content of adults as well (Telleria et al. 2018). There are several studies comparing microbiota diversity between different populations of *L. longipalpis*, and between field and

laboratory reared flies (Oliveira et al. 2000; de Oliveira et al. 2001; Gouveia et al. 2008) showing that even though composition of microbiota varies greatly, there are some genera that are shared between conditions. Additionally, it has been demonstrated that microbial diversity in *L. longipalpis* (from field or laboratory) decreased after blood feeding and that after blood digestion contents were eliminated the bacterial diversity recovered to previous sugar fed insect levels (Kelly et al. 2017; Pires et al. 2017). It is important to mention that although bacterial diversity decreases after a blood meal, bacterial numbers actually increase. This might be due to some bacteria overgrowing others in a nutrient-rich environment (Volf et al. 2002).

Bacteria that are common among *L. longipalpis* field and laboratory-reared insects belong mostly to the Proteobacteria phylum including *Pantoea, Serratia, Stenotrophomonas* and *Erwinia* genera. These are known to have an impact on *L. longipalpis* or other insects immunity (Boulanger et al. 2004; Telleria et al. 2013; Booth et al. 2015; Heerman et al. 2015; Husseneder et al. 2016; Keita et al. 2017).

It has also been shown that there is a close interaction between microbiota and *Leishmania* infection in the vector, *L. longipalpis*. Sant'Anna et al. (2014) reported a protective role of *Leishmania* in bacterial infections. The nuance of these interactions was revived in detail by Telleria et al. (2018). Microbiota studies in *L. longipalpis* and other sand flies shows the importance of this microbiome and its homeostasis over the insects immune system, interaction with other pathogens and influence in vector viability.

4.2 CHAPTER 2 SPECIFIC OBJECTIVES

-Silence cactus and WntD genes, negative regulators of Toll pathway, independently and in conjunction in *L. longipalpis* adult females.

-Evaluate the effects of silencing these genes on the Toll pathway modulation by investigating AMPs expression.

-Assess microbiota load of female sand flies under cactus and WntD gene silencing, independently and in combination.

-Evaluate the effects of silencing these genes on *L. infantum (Syn. chagasi)* survival in the vector.

4.3 METHODS

4.3.1 Parasite Culture

L. infantum (Syn. chagasi) (MHOM/BR/1974/PP75) obtained from the *Leishmania* collection of Instituto Oswaldo Cruz (CLIOC) was maintain at 26ºC in 199 Medium (Gibco-Life Technologies) supplemented with 10% foetal bovine serum (FBS) (Econolab), HEPES 40Mm, adenine 100µM, hemin 2,5µg/ml and 1% antibiotics (penicillin 100U/ml and streptomycin 100mg/ml -Sigma). Passages were performed every two - five days.

4.3.2 Insects

All of the experiments were performed using sand flies from our laboratory colony of *L. longipalpis* established from sand flies caught in Jacobina (Bahia, Brazil). The insects were fed on 70% sucrose *ad libitum* and maintained at 27±1ºC, humidity of 80-95%.

4.3.3 L. longipalpis infection with Leishmania

Blood preparation: defibrinated rabbit blood was placed in 1,5mL Eppendorf tubes and centrifugated at 3000 rpm for 8 mins at 4ºC. Plasma layer (supernatant) was collected in a different tube and incubated at 57ºC for 1 hour to inactive the complement system. After inactivation, plasma was allowed to cool down at room temperature and carefully mixed with the blood cells. The blood cell phase was washed with PBS 1X 2 to 3 times and centrifuged at 3000 rpm/10min/4ºC, always using cut tips and kept on ice in between manipulation times. After plasma and blood cell treatment, *Leishmania* ($1x10^7$ parasites per 1ml of reconstituted blood) were mixed with plasma first and then with blood cells.

Parasite preparation: 2-3 mL from a parasite culture in exponential growth phase were centrifuged at 1500xg/10min/4ºC. Supernatant was discarded, pellet resuspended in 10mL fresh medium and centrifuged again with same set up for a second wash. The pellet was resuspended in 1.5-2mL M199 media, counted in a Neubauer chamber, and $1x10^7$ parasites were transferred to a new tube, pelleted and the supernatant was discarded. The parasite pellet was resuspended in blood serum as mention above, and then fed to *L. longipalpis* females through a chick skin membrane.

4.3.4 dsRNA synthesis

Double stranded RNA (dsRNA) samples were synthetized in vitro using templates that were amplified from LL5 cDNA, followed by addition of bacteriophage T7 DNA-dependent RNA

polymerase promoter by PCR, as shown in schematic Figure 4.3-1. Briefly, two PCR runs were carried out, where in the first run specific primers for target genes, cactus (LLOJ004612), WntD (LLOJ004743), and βGal containing adaptor sequence at the 5' end were used (ANNEX-A). The first PCR reaction was used as a template for the second PCR reaction using primers for adaptor sequence containing promotor T7 (Figure 4.3-1 and ANNEX-A). In detail, PCR conditions were 95ºC for 3 minutes, 35 cycles of 95ºC for 30 seconds, 57ºC for 45 seconds and 72ºC for 45 seconds, followed by 72ºC for 7 minutes. Secondly the PCR product was purified with Wizard® SV Gel and PCR Clean Up System and quantified in Thermo Scientific NanoDrop TM ND-1000 spectrophotometer. In vitro transcription was carried out using MEGAscript® Kit following manufacturer's instructions. An example of unique bands from dsRNA synthesis before and after purification process can be seen in Figure 4.3-2.

The resulting dsRNA lengths were: dsCactus 576bp, ds βGal 503bp, dsWntD 394bp.

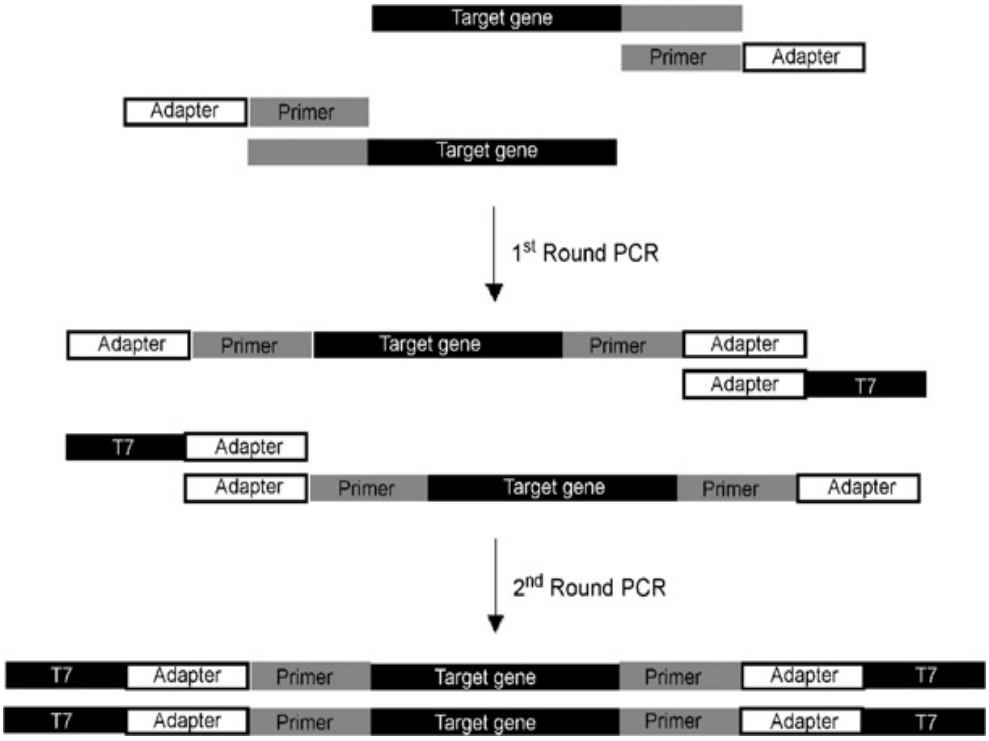

Figure 4.3-1 Flowchart of the method used to produce templates to transcribe the dsRNA molecules used in this study. From Pitaluga at al 2007

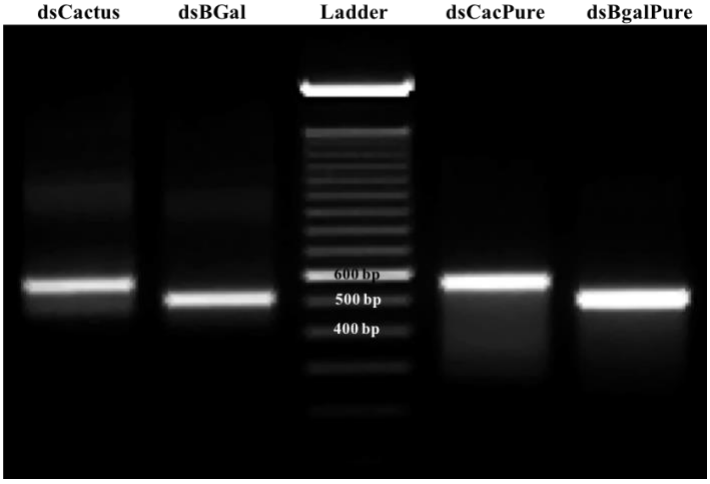

Figure 4.3-2 Electrophoresis of dsRNA before and after purification. All samples show 1/400th of the dsRNA reaction. They were run in 1,5% agarose gel with ethidium bromide and visualized under UV light.

4.3.5 Sand-fly silencing by microinjection

Microinjections were carried out as described in Sant'Anna et al. (2008) and in Figure 4.3-3 for schematic representation of the setup. Female sand flies 2-3 days old were injected with 32nl of dsRNA at 4,5μg/μL of either target gene or β-Galactosidase (β-Gal) as control group. After injection insects were kept at 26ºC, 80-90% humidity and 70% sucrose solution ad libitum, except for groups that were going to be infected, in which case the sucrose source was removed at least 12h before the infected blood meal was offered.

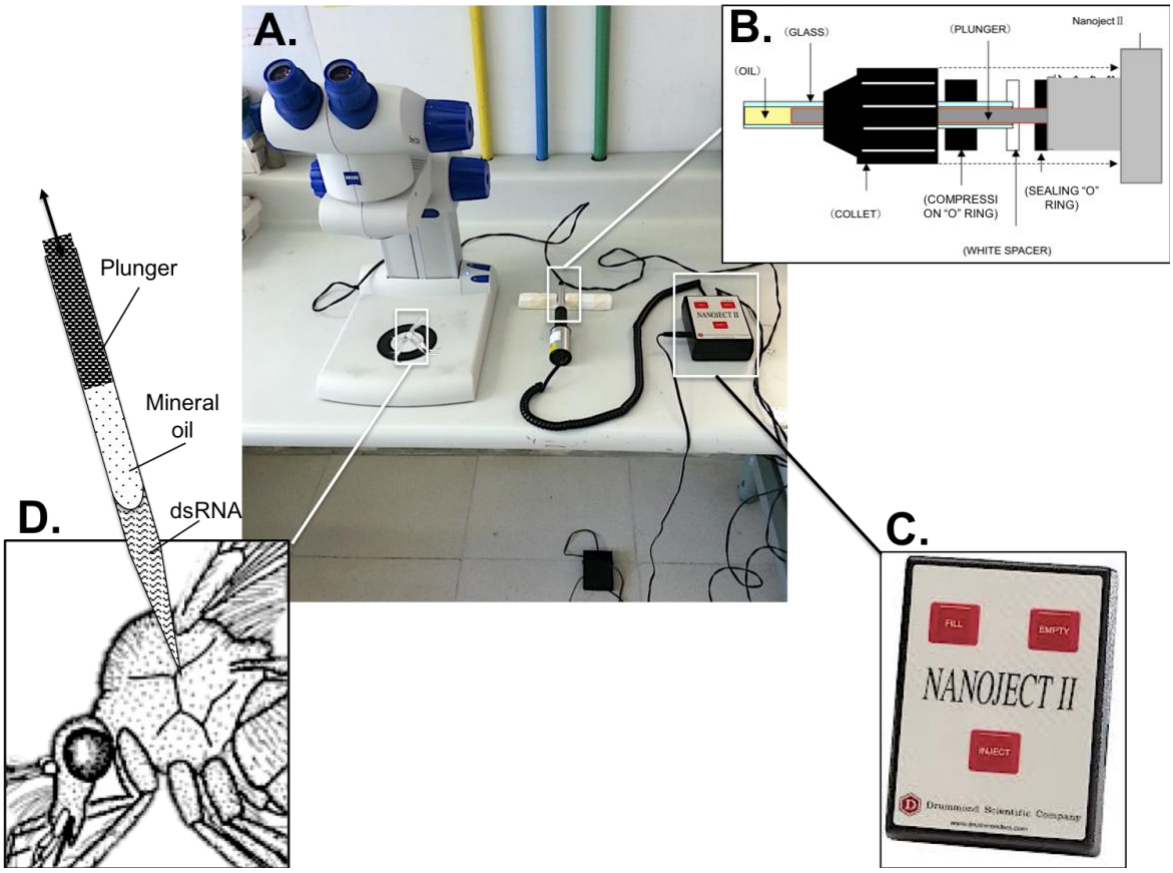

Figure 4.3-3 Representation of microinjection setup. A. General setup for microinjection using microinjector Nanoject II and stereoscope; B. Detail of micropipette parts; C. Detail of command keypad with Fill, Empty and Inject buttons; D. Schematic representation of injection site in sand fly thorax and detail of content in needle. Adapted from https://www.drummondsci.com/product.cfm?cat=microinjection&prod=nanoject-II-auto-nanoliter-injector

4.3.6 RNA extraction and cDNA Synthesis from insects

RNA extraction from *L. longipalpis* females was performed using TRIzol Reagent (Ambion), following manufacturer's instructions. Each pool of 10 insects was macerated in 300µL of TRIzol and centrifuged at top speed (12.000-13.000rpm) for 10min/4ºC, the supernatant was transferred to a new microtube and then incubated at room temperature for 5mins. Next, 60µL of chloroform were added to each sample, shaken vigorously by inversion for 20 seconds, and subsequently incubated for 10mins at room temperature. After this, samples were centrifuged at top speed for 15min/4ºC. The aqueous phase was carefully transferred to a new 1,5mL tube, avoiding disturbing the interphase. Afterwards, 150µL of RNAse-free water, 300µL of isopropanol and 1,5µL Glycoblue (Ambion) were added to each sample and incubated for 10mins at room temperature. Later, samples were centrifuged at top speed for 15min and the supernatant was discharged. Each RNA pellet was washed with 150µL of 75% ethanol (cold) and centrifuged at top speed for 5min. The ethanol was discharged, and pellets were allowed to air dry upside down for

20-25mins, certifying that no residue of ethanol remained, before resuspending each pellet in 20μL of RNase-free water.

RNA samples were treated with DNA-free Kit (Ambion) to remove contaminant DNA, confirmation of complete gDNA degradation was checked by PCR using histone primers (ANNEX-A) which produces a 1500bp band (Figure 3.3-2_in Chapter 1). All RNA was quantified using a Thermo Scientific NanoDrop TM ND-1000 spectrophotometer and stored at -20ºC.

cDNA was synthesized from 1-2μg of total RNA using SuperScript III First- Strand Synthesis kit (Invitrogen) following manufacturer's instructions, in all cases random primers were used. Temperature cycles were described above in Chapter 1, section 3.3.6.

Successful synthesis was checked by PCR using rp49 primers (Figure 3.3-3_in Chapter 1) which only amplify the cDNA template. cDNA was diluted 1:10 with ddH_20 for later use in qPCR reactions.

4.4 RESULTS

4.4.1 Cactus and WntD silencing.

In order to further evaluate the hypothesis proposed by Tinoco-Nunes (2014) of the possible existence of a negative loop regulation for Toll pathway in *L. longipalpis* adult females, experiments of single silencing were repeated using sequence specific dsRNA fragments for cactus gene and new experiments using dsRNA for WntD gene. Several genes that are well known to be involved in the Toll pathway were analysed to assess their variation in an environment with reduced cactus or WntD mRNA. After cactus dsRNA (dsCactus) microinjection a significant reduction in mRNA levels for this gene at 24 and 72 hours post-injection was observed, with cactus transcript levels recovering 48 hours post-injection compared to the control group (Figure 4.4-1, A). Among known AMPs in *L. longipalpis* are: attacin, cecropin and defensin 4. Although the direct connection that each one of them have with a particular immune pathway is yet unknown, it is clear that they are effector genes of innate immunity and for this reason their expression levels were evaluated. Figure 4.4-1C shows a tendency to downregulation in all three AMPs at 24 and 72 hours, when cactus transcripts were silenced. This trend is in line with previous results reported for Tinoco-Nunes (2014); due to variation across biological replicates no significant difference was found at any time point in the present experiments. The transcription factor dorsal seems to follow the same tendency of expression as cactus, but no significant statistical reduction in transcript levels was observed at any time point (Figure 4.4-1, B). *L. longipalpis* WntD gene expression was also evaluated upon cactus silencing. Even though its expression tends to increase in the first 24 hours and then decrease in the next two days when compared to control, there was no statistical difference (Figure 4.4-1,D). An important part of maintaining the homeostasis in insects is to protect and regulate microbiota. In order to estimate the consequences of cactus silencing over general bacterial load, expression of gene 16S was measured, showing significant reduction at 24 and 72 hours post-injection and an increase trend at 48 hours. No significant difference was found at this time point due to variations between biological replicates, (Figure 4.4-1, E).

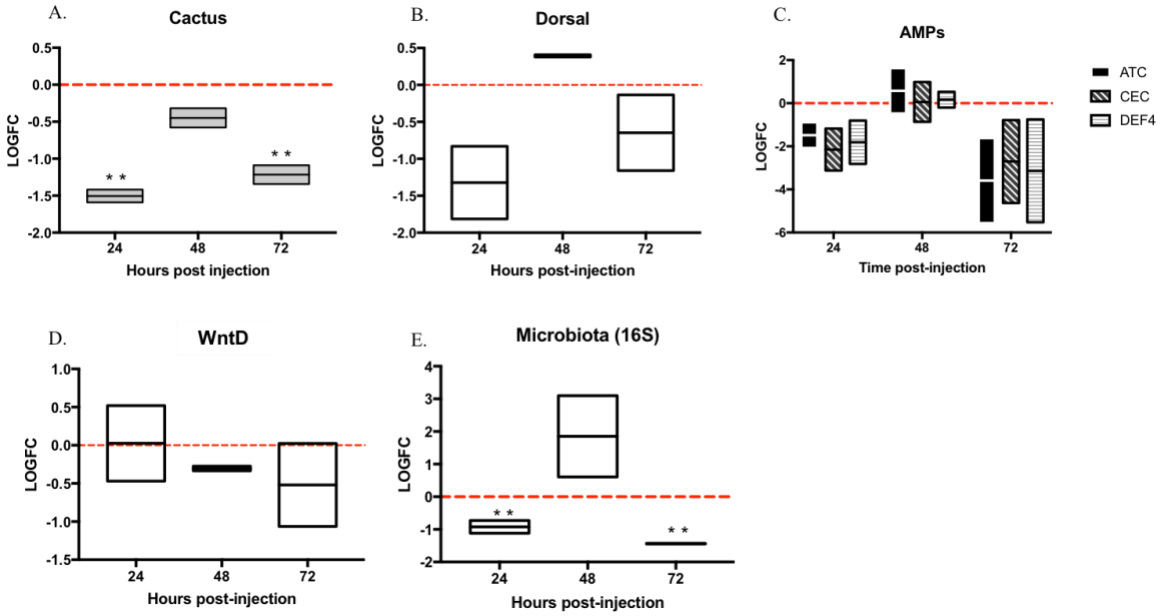

Figure 4.4-1 cactus silencing in *L. longipalpis* females. (A) Log fold change of cactus gene expression in female *L. longipalpis* at different timepoints after injection with cactus dsRNA (B) Log fold change of transcription factor dorsal (C) Log fold change of gene expression of three AMPs (D)Log fold change of WntD. (E) Log fold change of microbiota load represented by gene expression of bacterial 16S. All graphs Y-axis represent log2(x) of fold change between test group injected with dsCactus versus control group injected with dsβGal, both previously normalized by reference gene (GAPDH) expression values from qPCR data. The X-axis represent timepoints of sample collection 24, 48 and 72 hours after injection with dsRNA. Boxes represent mean with maximum and minimum values from three biological replicates. Student's T test with Welch's correction was performed using log2(x) data from each group for each timepoint. **p≤0.01.

In sand flies microinjected with WntD dsRNA (dsWntD) it was possible to observe a decrease in transcript levels for this gene at 24 hours post-injection with statistical significance. WntD mRNA levels start to recover close to those in control groups from 48 hours post-injection (Figure 4.4-2, A). Transcription factor dorsal increased in the first 24 hours and then decreased in the next two days when compared to controls, however it was not possible to find statistical difference at any time point (Figure 4.4-2, B). Gene expression of cactus – the main negative regulator of the pathway - was also evaluated. Its expression follows a pattern similar to dorsal, where mRNA levels increase in the first 24 hours and then decrease in the next days. No statistical significant difference was observed between test and control groups (Figure 4.4-2, D). In these experiments attacin, cecropin and defensin 4 were also evaluated. Figure 4.4-2C shows a tendency of downregulation in all three AMPs at 24 and 72 hours and expression levels comparable to control groups at 48 hours post-injection, with an increase of attacin and cecropin expression at this time point. Due to variation across biological replicates no significant difference was found. Expression of gene 16S (microbiota) shows a tendency to increase at 24 and 72 hours post-injection and to decrease at 48 hours, but there is no significant difference at any time point due to variation between biological replicates (Figure 4.4-2, E).

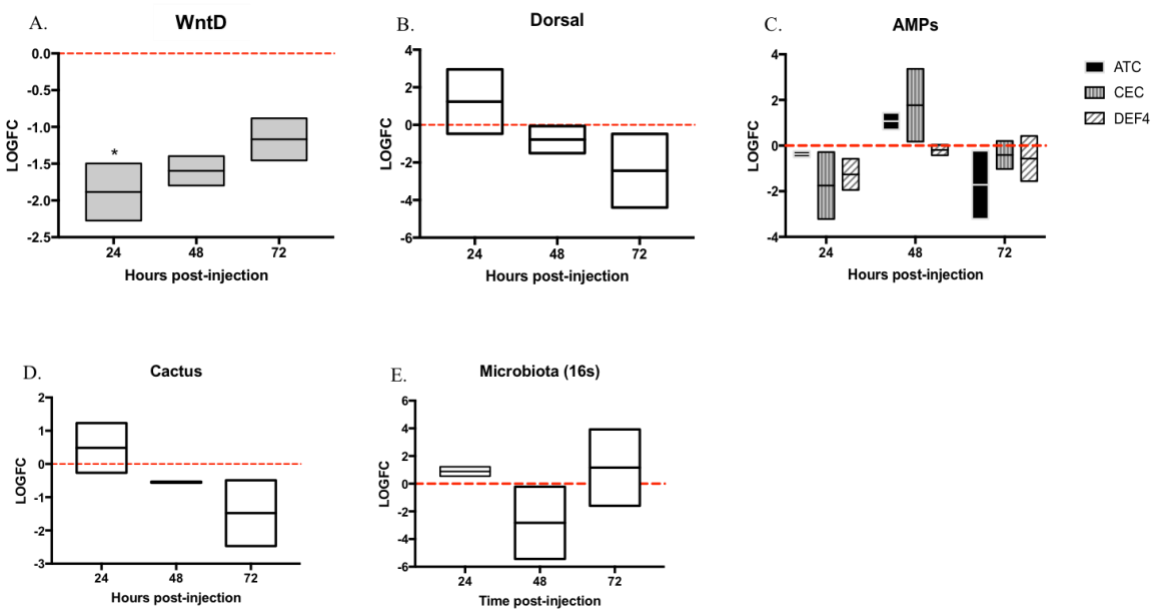

Figure 4.4-2 WntD silencing in *L. longipalpis* females. (A) Log fold change of WntD gene expression in female *L. longipalpis* at different timepoints after injection with dsWntD dsRNA, (B) Log fold change of transcription factor dorsal (C) Log fold change of gene expression of three AMPs, (D)Log fold change of cactus, (E) Log fold change of microbiota load represented by gene expression of bacterial 16S. All graphs Y-axis represent log2(x) of fold change between test group injected with dsCactus versus control group injected with dsβGal, both previously normalized by reference gene (GAPDH) expression values from qPCR data. The X-axis represent timepoints of sample collection 24, 48 and 72 hours after injection with dsRNA. Boxes represent mean with maximum and minimum values from three biological replicates. Student's T test with Welch's correction was performed using log2(x) data from each group for each timepoint. *p≤0.05.

4.4.2 Cactus silencing and Leishmania infection

With the purpose to evaluate Toll pathway gene expression in relation to parasite challenge in conditions of low cactus mRNA level, female sand flies were injected with dsRNA cactus or βgal and 24h later were fed on blood seeded with *L. infantum (Syn. chagasi).* In order to verify the transcript state of the pathway before the challenge, a time point 1 hour before blood feeding was taken (represented in graphs as -1h time point, Figure 4.4-3), this time point is equivalent to 24 hours post-injection of previous experiments. Despite the fact that cactus transcript levels were diminished before feeding, there is no statistical difference at any time point (Figure 4.4-3, A). *Leishmania* load seems to increase 48 hours post-infection and decrease at 72h, which is in line with the end of digestion (Figure 4.4-3, B). Expression of the secondary negative regulator WntD appears to be reduced 1hour before and increased 24 hours after infection and at 48 and 72 hours remains closer to control mRNA levels (Figure 4.4-3, D). Gene expression of the transcription factor dorsal remains very similar to control at all time points (Figure 4.4-3, C). This same pattern is visualized for general microbiota load, expressed as mRNA levels of 16S bacterial gene (Figure 4.4-3, E). Neither dorsal, nor WntD and microbiota showed significant modulation prior to or during parasite infection. Out of the three AMPs assessed only cecropin and defensin 4 had

statistically significant transcript augmentation 24 hours post infection. At this same time point attacin expression also has a tendency to increase but with no significance; at all other time points transcription of AMPs vary close to those of control group (Figure 4.4-3, F).

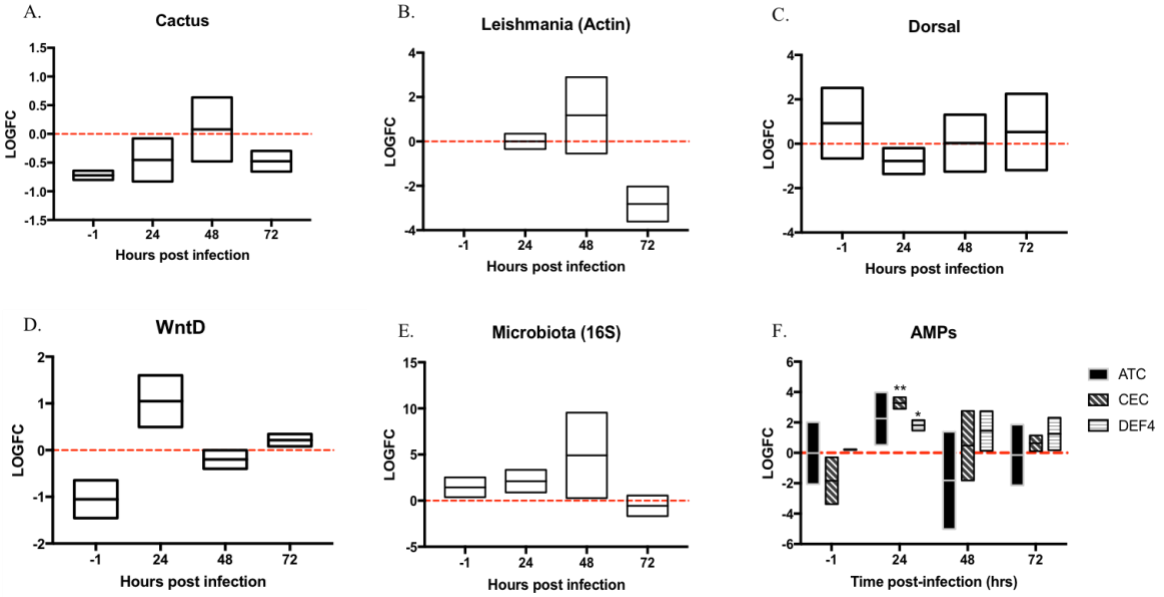

Figure 4.4-3 Gene expression of Toll pathway molecules after dsCactus injection and *L. infantum (Syn. chagasi)* infection in female sand flies. (A) Log fold change of cactus gene expression in female *L. longipalpis* at different timepoints during infection with *L. infantum (Syn. chagasi)* (B)Log fold change of parasite load represented by gene expression of *Leishmania* actin during infection. (C, D) Log fold change of WntD and transcription factor dorsal respectively at different time points during infection. (E) Log fold change of microbiota load represented by gene expression of bacterial 16S during infection (F) Log fold change of gene expression of three AMPs at the same timepoints. All graphs Y-axis represent log2(x) of fold change between test group injected with cactus dRNA versus control group injected with βGal dsRNA, both previously normalized by reference gene (GAPDH) expression values from qPCR data. The X-axis represent timepoints of sample collection at -1h, as time point before infection, and 24, 48, 72 hours after infected blood feed. Boxes represent mean with maximum and minimum values. Student's T test with Welch's correction was performed using log2(x) data from each group for each timepoint. *p≤0.05, **p≤0.01.

4.4.3 Micro-injection of mixed WntD and cactus dsRNA

In the attempt to fully activate the Toll pathway, female sand flies were microinjected with a 1:1 mix of cactus and WntD dsRNA and gene expression of the pathway molecules were calculated. Only WntD showed a slight trend to reduction of its transcript levels at 24 to 72 hours post-injection when compared with control group; cactus transcripts were very close to control group along time points, there was no significant difference at any time point for either cactus or WntD (Figure 4.4-4, A). Interestingly, it is possible to observe a tendency to increase in dorsal and AMPs mRNA levels 24 hours after injection, returning to control levels at 48 and 72 hours (Figure 4.4-4, B, D), however it was not possible to find significant differences along the test. General microbiota load is very similar when compared to control (Figure 4.4-4, D).

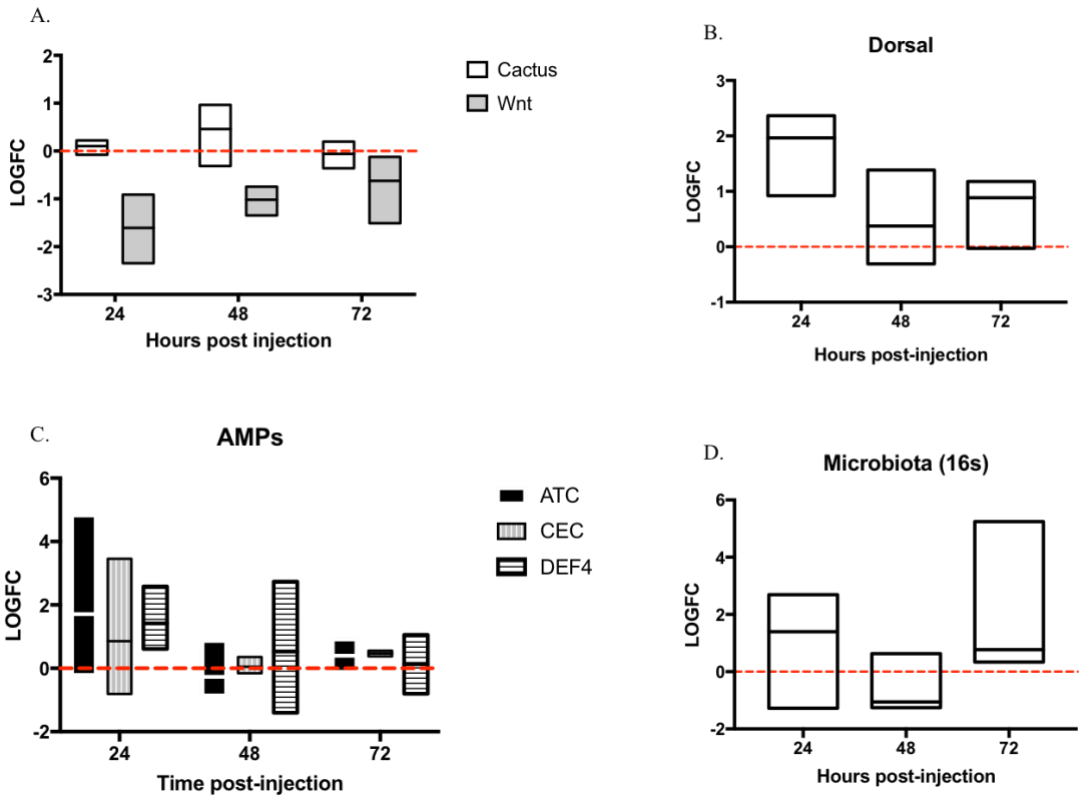

Figure 4.4-4 Gene expression of Toll pathway molecules and microbiota after dsCactus and dsWntD mix injection in *L. longipalpis* females. (A) Log fold change of WntD and cactus gene expression in female *L. longipalpis* at different timepoints after injection with mix dsRNA (cactus+WntD), (B) Log fold change of transcription factor Dorsal (C) Log fold change of gene expression of three AMPs, (D) Log fold change of microbiota load represented by gene expression of bacterial 16S. All graphs Y-axis represent log2(x) of fold change between test group injected with dsCactus versus control group injected with dsβGal, both previously normalized by reference gene (GAPDH) expression values from qPCR data. The X-axis represent timepoints of sample collection 24, 48 and 72 hours after injection with dsRNA. Boxes represent mean with maximum and minimum values from three biological replicates. Student's T test with Welch's correction was performed using log2(x) data from each group for each timepoint.

4.5 DISCUSSION

It is well known that *L. longipalpis* is the vector of *L. infantum (Syn. chagasi)* species. Nevertheless, the mechanisms of interaction between *Leishmania* and the immune system of sand flies are still not well defined. In the last couple of decades RNAi silencing has been used as an important tool to investigate the role of certain immune molecules in adult sand flies (Sant'Anna et al. 2008; Sant'anna et al. 2009; Telleria et al. 2012). Results from those studies have shown that depletion in caspar gene expression, negative regulator of the IMD pathway, can reduce *Leishmania* infection in *L. longipalpis* blocking parasite transmission by the vector, showing the importance of immune pathways in infection control (Telleria et al. 2012). Furthermore, it has been demonstrated that bacterial and *Leishmania* infections elicit defensin expression in adult sand flies, presenting once more an immunological response to the parasite (Telleria et al. 2013). A study was published recently associating activation of the Toll and IMD pathways in *L. longipalpis* LL5 cells after challenges with different bacteria, yeast and *Leishmania*, with upregulation of AMP genes (Tinoco-Nunes et al. 2016). In the same study and through gene silencing of cactus or caspar, negative regulators of Toll and IMD pathway respectively, it was possible to link cecropin and defensin modulation to these pathways. Previous studies in our laboratory have shown upregulation of cactus gene expression during *Leishmania* infection in adult sand flies, suggesting involvement of this pathway in parasite-vector interaction (Tinoco-Nunes 2014). Studies on cactus silenced sand flies suggested also that Toll pathway regulation could include a negative loop in adults by a secondary regulator, WntD, contrary to results in cell line LL5 where the action of a secondary negative regulator was not evident (Tinoco-Nunes 2014).

Our results showed that it was possible to reduce relative expression of cactus only at 24 and 72 hours after injection, at the same time points it was possible to see that AMPs expression had a tendency to reduction when compared to control group (Figure 4.4-1A,C). Even though this result does not have a statistical significance, expression trend is in line with early results from Tinoco-Nunes (2014) where depletion of cactus in adult flies induced downregulation of at least three AMPs (cecropin, defensin 4 and attacin) instead of generating the effect reported for cactus silencing in cell cultures, that was the increase of AMPs expression (Tinoco-Nunes et al. 2016). Also, it was possible to observe that at time points where cactus expression was silenced, transcription factor dorsal also tend to diminish, indicating a possible reduction in dorsal protein available to be translocated to the nucleus and therefore may affect activation of effector genes like AMPs as seen in Figure 4.4-1B and C. Curiously, time points 24 and 72 hours post-injection also

presented significant decrease in general bacterial microbiota load (Figure 4.4-1E). A hypothesis that could explain this result, is the possibility that other AMPs not identified yet or not studied here could have been induced through pathways different from Toll and reduce bacterial load. It could also be proposed that, due to the fact that expression of bacterial 16S gene was used as a reporter for microbiota relative quantities, results only showed general load and not diversity of the microbiota. This diversity could have been changed due to unbalance in the pathway favouring the growth of certain taxa or harshening the environment for other, showing only a general decline in total bacteria. Alterations in midgut environment can certainly affect the equilibrium of microbiota (Engel and Moran 2013). Studies showing the diversity of these interactions microbiota-insect were revised for *L. longipalpis* model by Telleria et al. 2018. It is also important to call attention to the fact that microbiota in insects are not only composed by bacteria, but also by fungi and yeast (Engel and Moran 2013; Telleria et al. 2018), which increase the complexity of the midgut environment and its relationship with the immune system to keep homeostasis.

According to the literature in *Drosophila* Toll pathway regulation, the transcription factor dorsal regulates its own rate of nuclear translocation by activating WntD gene expression, that in conjunction with its receptor Frizzled4 will prevent the extracellular domain of Toll receptor from adopting a productive conformation that is required for the activation of the pathway (Figure 4.1-3 and Figure 4.1-4) (Rahimi et al. 2016). Mutant *Drosophila* flies for WntD gene showed and aberrant expression of some, but not all, AMPs after septic injury, diptericin being the most severely affected. WntD mutant flies displayed dramatically elevated basal levels of diptericin expression, and significantly higher mRNA levels of this AMP following infection, showing WntD as a negative regulator molecule for the pathway (Gordon et al. 2005). Our results showed that silencing of WntD expression was possible in adult sand flies for the first 24h after dsRNA injection (Figure 4.4-2A), yet expression of the gene is restored to levels similar to control in the following two days. For WntD silenced sand flies it was possible to observe an increment trend in dorsal expression at 24 hours post-silencing. Then, with the recovery of WntD expression, dorsal RNA levels seem to diminish. Even though dorsal expression was not differential enough to have statistical significance, the trend is in line with what is described in the literature as a negative regulatory loop in *Drosophila*, where reduction in WntD levels initially increase dorsal translocation to the nucleus which can upregulate effector genes, including WntD, that in turn will bring dorsal expression down or to control levels as seen at 48 and 72 hours post-injection (Figure 4.4-2A, B). The occurrence of autoregulation has been documented for the c-rel (Hannink and Temin 1990) and p50 (Ten et al. 1992; Cogswell et al. 1993) genes in humans, two type of NF-kB

transcription factors. Results from early studies in *Drosophila* dorsal mutants, where biosynthesis of a functional protein is affected, lends strong support to the idea that the dorsal protein is required for full inducibility of the transcription of the dorsal gene itself, in response to immune challenge (Lemaitre et al. 1995). The trend for increase in dorsal expression at 24 hours was not enough to induce AMPs upregulation in WntD silenced sand flies.

It is important to highlight that an interesting synchronicity of cactus and dorsal gene expressions was observed in both single silencing experiments (Figure 4.4-1 A, B and Figure 4.4-2B, D). Studies in the *L. longipalpis* embryonic cell line LL5, have also reported a synchronic expression between cactus and dorsal, and an increase in cactus mRNA levels after several pathogens challenge (Tinoco-Nunes et al. 2016). Kubota and Gay (1995) indicated that the dorsal protein enhances the biosynthesis and stability of the *Drosophila* IkB homologue cactus, proposing an initial theory where dorsal protein is able, directly or indirectly, to stimulate translation of the cactus mRNA.

Subsequent studies of *in vivo* regulation of cactus during immune response of *Drosophila* showed that cactus gene is upregulated in response to immune challenge and that the expression of the cactus gene is controlled by the spätzle/Toll/cactus gene pathway, indicating that the cactus gene is autoregulated. This study also showed the presence of several sequence motifs homologous to insect and/or mammalian binding sites for Rel (NF-kB family) protein in the upstream region of cactus gene sequence (Nicolas et al. 1998). More recently, studies of cactus gene from *Litopenaeus vannamei* (shrimp) reported that the promoter of Lvcactus was predicted to contain five putative NF-kB binding motifs, among which four were proved to be bound by Lvdorsal by chromatin immunoprecipitation assays. Dual-luciferase reporter assays also showed that transcription of Lvcactus was promoted by Lvdorsal but inhibited by Lvcactus itself, indicating a feedback regulatory pathway between Lvcactus and Lvdorsal. This process repeated and made the expression of Lvcactus showing periodic fluctuations during challenge (Li et al. 2012). Considering that the cactus gene in *L. longipalpis* could also exert autoregulation mediated by dorsal and thus explain in part the tendency to synchrony between cactus and dorsal expression and the fluctuation of cactus expression in dsCactus only treated flies, an *in silico* analysis, looking for possible NF-kB binding sites in cactus gene sequence (gene ID: LLOJ004612) was made. A 2000nt section upstream of the beginning of transcription was searched for transcription factor binding sites using JASPAR 2018 program. This region was predicted to include four putative NF-κB/Rel homology region (RHR) factor binding sites (Table 4.5-1, Figure 4.5-1, ANNEX-E). Interestingly, one of the

putative binding sites sequence recognises one of dorsal binding specificity models from *D. melanogaster*.

This finding suggests that cactus and dorsal could be regulating each other through the Toll pathway in our sand fly model as has been reported in other invertebrates, indicating a tighter regulation in the pathway between cactus and dorsal. It is clear that this theory requires experimental follow up to prove that dorsal protein is actually binding to the cactus promoter in *L. longipalpis* and regulating its transcription. For that purpose techniques like using inhibitors for cactus and/or dorsal, gene silencing for dorsal or chromatin immunoprecipitation (ChIP) assays could be carried out, nevertheless this late finding gives us a hint of the kind of interactions might be happening in the pathway regulation.

Matrix ID	Name	Score	Relative score	Start	End	Predicted sequence	Sequence logo
MA0105,3	**NFKB1**	14,969	0,967	1586	1596	TGGAATTTCCT	
MA0105,3	**NFKB1**	12,404	0,930	1231	1241	TGGATTTCCCT	
MA0023,1	**dl(var,2)**	10,664	0,894	1230	1239	CTGGATTTCC	
MA1117,1	**RELB**	9,660	0,874	718	728	GTATTCCACTG	

Table 4.5-1 Putative transcription factor binding sites in cactus gene promoter region in *L. longipalpis.* Generated using JASPAR Database (http://jaspar.genereg.net/)

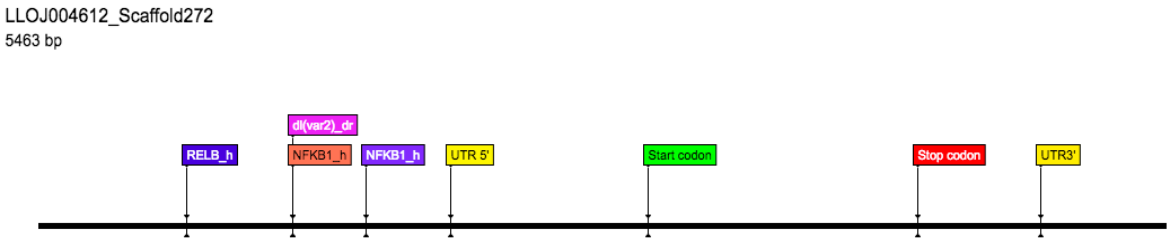

Figure 4.5-1 Map of putative transcription factor binding sites in cactus gene (LLOJ004612) plus 2000nt upstream of UTR5'. Total length=546bpt Graph generated using JASPAR database (http://jaspar.genereg.net/). Refer to ANNEX-E for detail in gene sequence.

Regulation of the Toll pathway is a constant research field, especially in *Drosophila* model, with obvious repercussions in the understanding of mammalian Toll signalling. Recently, Cardoso

et al. (2017) using quantitative analysis in *Drosophila* embryo showed that under specific circumstances, loss of cactus flattens the nDl (nuclear dorsal) gradient, implying that cactus is able to augment dorsal (Dl) nuclear accumulation, acting as a positive regulator, in addition to its widely established role in inhibiting Toll signals. This study proposed a model in which free cactus (unbound to dorsal) is modified by the action of Calpain A protease (CalpA) into Cact[E10] (N-terminal truncated cactus) through a Toll independent pathway to enhance Toll signals in the embryo by replenishing Cact:2Dl (one molecule of cactus bound to two molecules of dorsal) complexes (Figure 4.5-2). Compatible with that hypothesis, CalpA activity is extremely sensitive to Dl and cactus levels, as it is reduced in *dl*$^{-}$ and *cactus*$^{-}$ mutant flies (Fontenele et al. 2009, 2013) - reminiscent of the positive cactus effects described by Cardoso et al (2017). The ability of Cact[E10] to alter Toll signals is strongest in the presence of reduced Dl background, a condition that also reduces endogenous cactus levels (Whalen and Steward 1993; Bergmann et al. 1996). Although further research is required to understand how cactus enhances nDl levels in the *Drosophila* embryo and consequently Dl-target gene expression, it was clearly shown that cactus exerts a positive effect on Dl nuclear uptake, that this effect is strongest when Dl levels are limiting, and that Cact[E10] modifies an essential process responsible for generating this positive effect (Figure 4.5-2). These studies provide a complementary theory about mechanisms of pathway regulation involving cactus and dorsal directly, showing once more signs of heavy regulation in this signal cascade. It also brings into consideration that cactus can have a positive role in the pathway under certain circumstances, therefore the interpretation of the role of cactus in immune responses must be consider depending on the gene expression background in the cell and not only on the premise of cactus as negative regulator. Results from cactus silenced sand flies show us that diminishing cactus does not generate the expected response in dorsal and possible dorsal-activated genes under the idea of cactus as exclusively negative regulator. It would be fascinating to continue studying Toll pathway in *L. longipalpis* to unravel regulation mechanisms and more specifically cactus role(s) in the immune response.

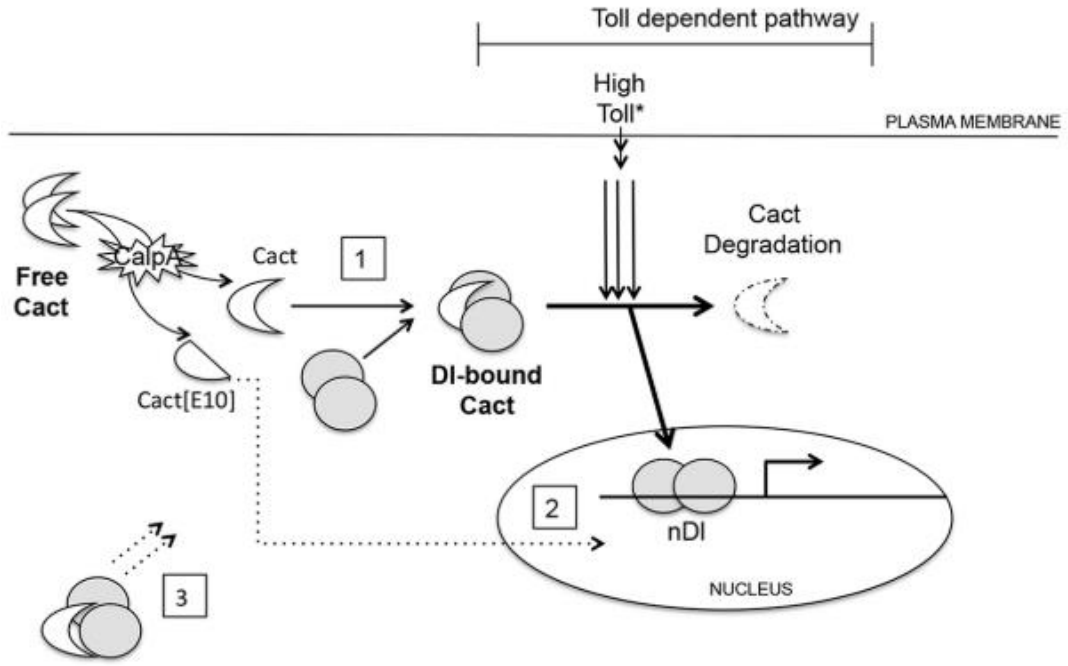

Figure 4.5-2 Three possible mechanisms for positive cactus function, based on deploying a Toll-independent pathway: (1) CalpA activity releases Cact[E10] and free full-length cactus, replenishing Dl:Cact signalling complexes that respond to Toll; (2) nuclear Cact[E10], generated by CalpA, increases Dl resident time at promoters; and (3) a flux of free Cact[E10] or free full-length cactus increases Dl diffusion from dorsal to ventral regions of the embryo over time. From Cardoso M.A et al, 2017

With the intention of better understanding the role of cactus in Toll pathway regulation in the presence of challenge, female sand flies were micro-injected with cactus dsRNA then fed 24 hours later with blood containing *L. infantum (Syn. chagasi)* (Figure 4.4-3). Results from these experiments showed a fast recovery of cactus expression to control levels after infection, possible due to a compensation response to blood meal ingestion and parasite presence as has been shown in other studies (Ribeiro 2003; Jochim et al. 2008; Pitaluga et al. 2009; Hussain et al. 2013; Tinoco-Nunes et al. 2016). Reduction in cactus expression in these experiments was not enough to show statistical significance, like it was shown in previous only silenced flies experiments. Either parasite or microbiota load did not have a significant difference between the groups suggesting that the initial tendency to reduction in cactus expression did not affect positive or negatively *Leishmania* infection or microbiota in the insect gut. WntD showed also a tendency to increase at 24 hours post infection but it was not significant. It is important to highlight that a statistically significant increase in cecropin and defensin4 gene expression occurs at 24 hours post-infection, which could be a late effect from apparent low levels of cactus and WntD before infection (Figure 4.4-3, F). The increment in AMPs expression cannot be linked for certain to the Toll pathway due to the relatively stable expression of dorsal along infection time points (Figure 4.4-3, C). However, this is not unusual, since in general all pathways (Toll, IMD and JAK/STAT) share some common

target genes (Boutros et al. 2002) and Tinoco-Nunes et al (2016) already showed upregulation of relish - transcription factor of IMD pathway – in LL5 cells challenged with live *Leishmania*, proposing participation of this pathway in the immune response against this parasite. Additionally, modifications in time retention of dorsal in the nucleus or ratio of activated dorsal were not evaluated and could modify AMPs gene expression without modification of dorsal mRNA levels.

In an attempt to understand the combined effect of diminishing both cactus and WntD transcripts, micro-injections with mixed dsRNA of cactus and WntD were performed. In these experiments a trend to reduction in WntD transcripts when compared to control was observed, but not in cactus (Figure 4.4-4A) that appears to allow a tendency to increase in dorsal expression (Figure 4.4-4, B). If we compare these results with those obtained in WntD single silencing experiments (Figure 4.4-2), it is possible to correlate the reduction in WntD with the trend to increase in dorsal expression at 24 hours (Figure 4.4-2, A and B respectively), with the difference that in single WntD silenced flies cactus presents a trend to increase at the same time point (Figure 4.4-2, D). In contrast with the experiments with mixed dsRNA, cactus keeps expression levels very close to control group, which could be a consequence of dsCactus having been previously injected in these flies; it is possible that the effect of cactus dsRNA was to prevent any compensatory increase in cactus transcripts in an environment low in WntD.

Low effect of dsRNA in reducing cactus and WntD transcripts could be attributed to the fact that in order to maintain the overall dsRNA concentration of 4,5μg/μL and same volume of injection (32nL per insect), like in previous single silencing experiments, the dsRNA mix of cactus+WntD at a ratio of 1:1 ended with a concentration of 2,25μg/μL for each specific gene dsRNA, possibly giving a short-lasting silencing, therefore not possible to detect in the timepoints selected in these experiments. This theory can also explain in part the tendency for an increased expression of AMPs at 24 hours as a partial delay effect of short co-silencing of cactus and WntD before 24 hour time point analysis, nevertheless this theory need to be evaluated in new injected flies with either higher concentration or volume of mix dsRNA, and the inclusion of earlier timepoints. Microbiota general load varies greatly along the experiment, consequently there is not significant difference when compared to control group, it would be important to evaluate other pathways in order understand it.

4.6 CONCLUSION

-Silencing of cactus or WntD alone is not enough to activate the Toll pathway, evaluated as up regulation of AMPs.

-Toll pathway in *L. longipalpis* appears to be tightly regulated, and difficult to be activated which may suggest that involve more than one control mechanism involving cactus, WntD and dorsal.

- *L. longipalpis* cactus gene contain 4 putative NF-kB binding sites, upstream of start of transcription, that could be related to cactus autoregulation through dorsal.

-Mix of dsCactus + dsWntD was not sufficient to silence both genes simultaneously in adult female sand flies.

5 CHAPTER 3. *L. LONGIPALPIS* IMMUNOLOGICAL RESPONSE TO *LEISHMANIA* POSITIVE OR NEGATIVE FOR LEISHMANIA RNA VIRUS 1 (LRV1).

5.1 INTRODUCTION

Viruses are obligate intracellular parasites having no metabolism of their own. Instead, they use resources from their hosts. Because of their high adaptability and diversity, viruses are the most abundant biological units on Earth (Forterre 2010) and they can parasitize all cellular types. Comprehensibly, virus research is frequently focused on the disease-causing agents of humans and livestock. However, the rise of methods for massively parallel nucleic acid sequencing allowed broad-scale studies of viral ecology and diversity in those groups of hosts, which were previously neglected (Cook et al. 2013; Li et al. 2015; Shi et al. 2016; Aswad and Katzourakis 2017). This lead to the significant progress in the study of viruses in protists (La Scola et al. 2003; Blanc et al. 2015; Maumus and Blanc 2016; Schulz et al. 2017). One of the well studied groups in this respect are trypanosomatids, flagellate parasites of vertebrates (Maslov et al. 2013; Lukeš et al. 2014).

5.1.1 Leishmania RNA Virus

In the late 1980s and early 1990s, dsRNA viruses of the family Totiviridae were discovered in different *Leishmania* spp. (Tarr et al. 1988; Widmer et al. 1989; Guilbride et al. 1992). *Leishmania* RNA virus 1 (LRV1) from *L. guyanensis* M4147 was the first virus from kinetoplastids fully characterized in molecular terms and only four years later the sequencing of the full LRV1 genome was completed (Stuart et al. 1992). Similar viruses were descried from other isolates of *L. guyanensis*, and one isolated of *L. brasiliensis* (Widmer et al. 1989; Guilbride et al. 1992). All these viruses from New World *Leishmania* originating from the Amazon basin were assigned to the genus *Leishmaniavirus* within the family Totiviridae (Patterson and Larsen 1992). Totiviruses are known to infect a wide range of hosts, including protozoa [*T. vaginialis* and *G. lamblia* (Wang and Wang 1991)], yeast (Wickner 1996), fungi, plants, arthropods (Wu et al. 2010; Zhai et al. 2010; Isawa et al. 2011), penaeid shrimp (Poulos et al. 2006) and even vertebrates [salmon (Løvoll et al. 2010)].

Members of the family Totiviridae are characterized by isometric virions 40nm in diameter that are composed of a non-segmented dsRNA genome between 4 and 8kb in length, encoding a major capsid protein (CP) and a capsid-RNA-dependent RNA polymerase (RDRP) fusion protein, essential for the replication of the dsRNA virus (Figure 5.1-1). In 1995 the complete sequence of a new totivirus from the Old World *L. major* was reported (Scheffter et al. 1995). The virus was

evidently related to LRV1, however, it was divergent in terms of amino acid sequences (only 38% and 47% identity in the capsid and RDRP proteins, respectively). It also lacked the overlap between ORF2 and ORF3, suggesting either different mechanism of fusion protein translation or independent initiation of RDRP synthesis (Scheffter et al. 1995). The virus from *L. major* was assigned to the genus *Leishmaniavirus* as LRV2 (Figure 5.1-2). Due to these differences in sequences and genome organizations of LRV1 and LRV2, it was proposed that these viruses diverged upon separation of Old and New World *Leishmania* (Widmer and Dooley 1995; Grybchuk et al. 2018a).

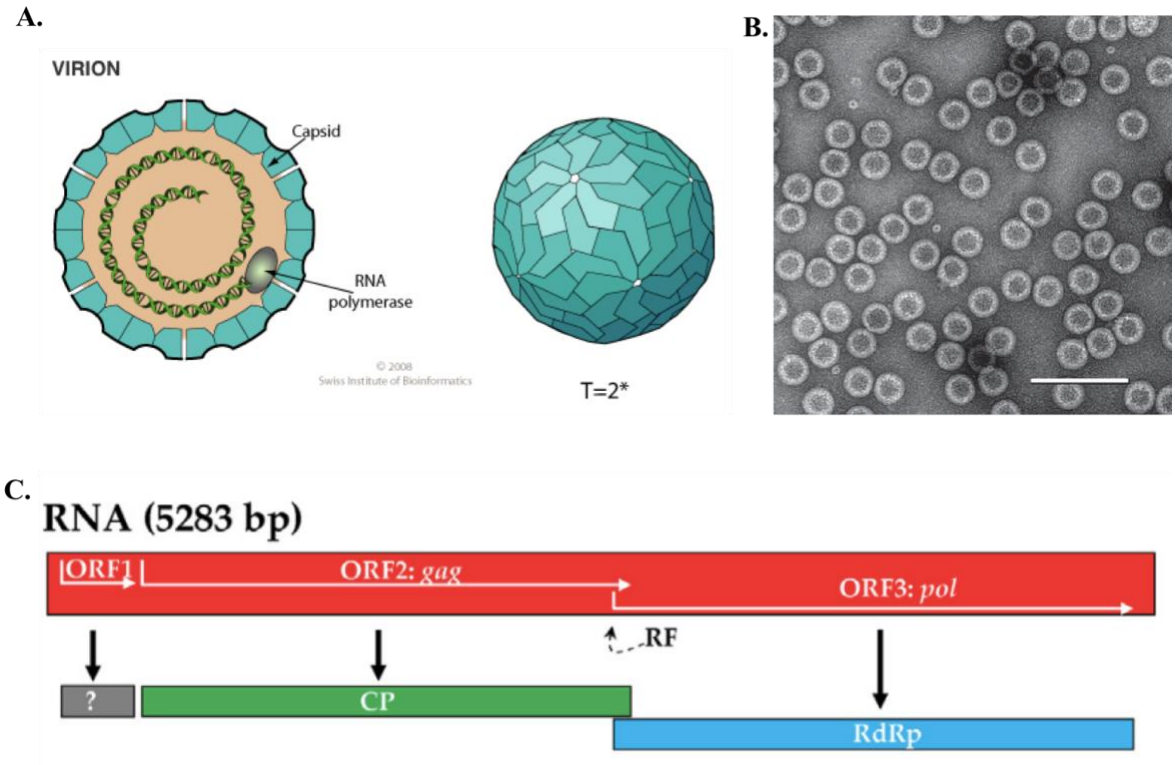

Figure 5.1-1 Totiviridae, *Leishmania*virus 1. A. Schematic representation of the totiviridae virion structure . B. Negative contrast of micron photograph of particles of an isolate of LRV1-1, bar represents 100nm C. Genome organization of LRV1. Taken from https://viralzone.expasy.org/161?outline=all_by_species, 2012; Fermin et al. 2018.

LRV follows the generic Totiviridae conformation described earlier. The 5.3kb dsRNA genome is never completely uncoated within the host cell. Viral polymerase synthesizes mRNA, which is translocated to the cell cytoplasm. There, transcripts are equipped with cap structures derived from host mRNAs by a cap-snatching mechanism mediated by the virus capsid protein. Plus strand viral transcripts direct the translation of ORF2, major CP, and the minor fusion protein of ORF3 CP-RDRP via ribosomal frameshift. Mature visions are transmitted to new cells during cell division (Fermin et al. 2018).

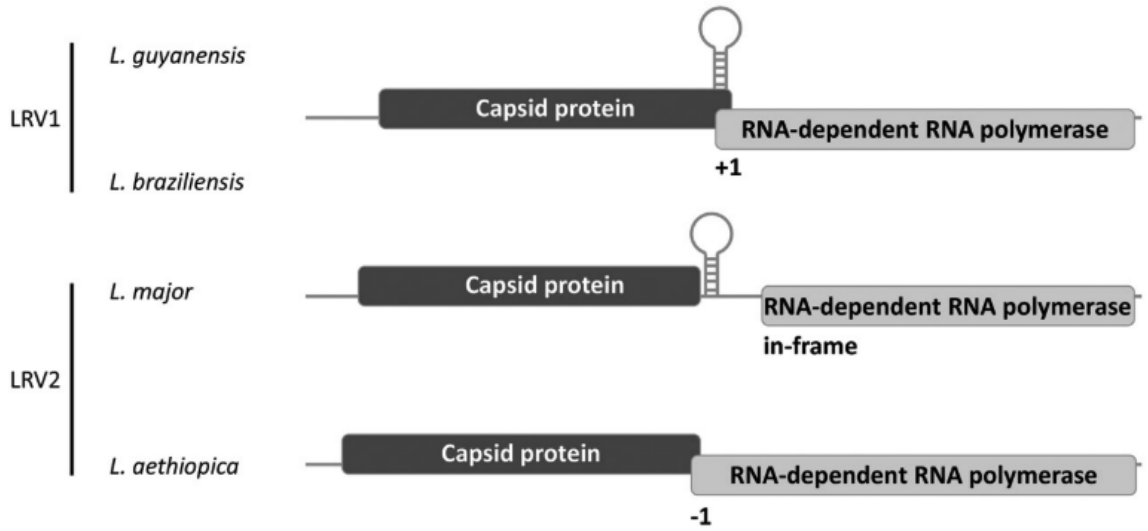

Figure 5.1-2 Genome organization of LRV1/2 from various *Leishmania* spp. All leishmaniaviruses have two ORFs coding for capsid protein and RNA- dependent RNA polymerase (RDRP). The overlaps, putative secondary structures between the ORFs, and the reading frame of RDRP relative to capsid are indicated. Role of LRV1 in pathogenesis of *Leishmania*. Taken from (Grybchuk et al. 2018b)

5.1.2 Advantage of Leishmania LRV1 retention in mammalian host infection

The apparent evolutionary reason for virus retention was discovered almost two decades after its discovery, when it was demonstrated that LRV1 (strain LRV1-LgyM4147 (Adams et al. 2014)) interferes with vertebrate host immune response against *L. guyanensis* (Ives et al. 2011). This is the most studied model for LRV1 function. Viral dsRNA stimulates the expression of pro-inflammatory interferon-β through the interaction with endosomal TLR3. This, in consequence, tilt the balance toward T-helper1 mediated immune response leading to chronic inflammation and increased metastatic potential of *L. guyanensis* (Hartley et al. 2012, 2014). This results in enhanced dissemination and parasite resistance, which eventually increases the possibility of both *Leishmania* and its virus to be picked up by a sand fly and successfully complete their life-cycles (Márquez and Roossinck 2012). Eren et al. (2016) showed that virus-containing *Leishmania* exploits mammalian innate immune signalling pathways at a microRNA level to promote macrophage survival and consequently enhance parasite persistence through a TLR-3/ miR-155/Akt signalling axis (Figure 5.1-3). Thus, virus bearing presents a clear survival advantage in dixenous trypanosomatids. Even though Leishmaniaviruses have been identified in main metastatic strains of *L. braziliensis* and *L. guyanensis*, metastasis can occur in absence of LRV, like in the case for *L. panamensis*. Therefore, LRV may have a variable contribution to this phenotype, acting

alone or in coordination with other factors, such as the host genetic background or species-specific parasite virulence factors (Hartley et al. 2012).

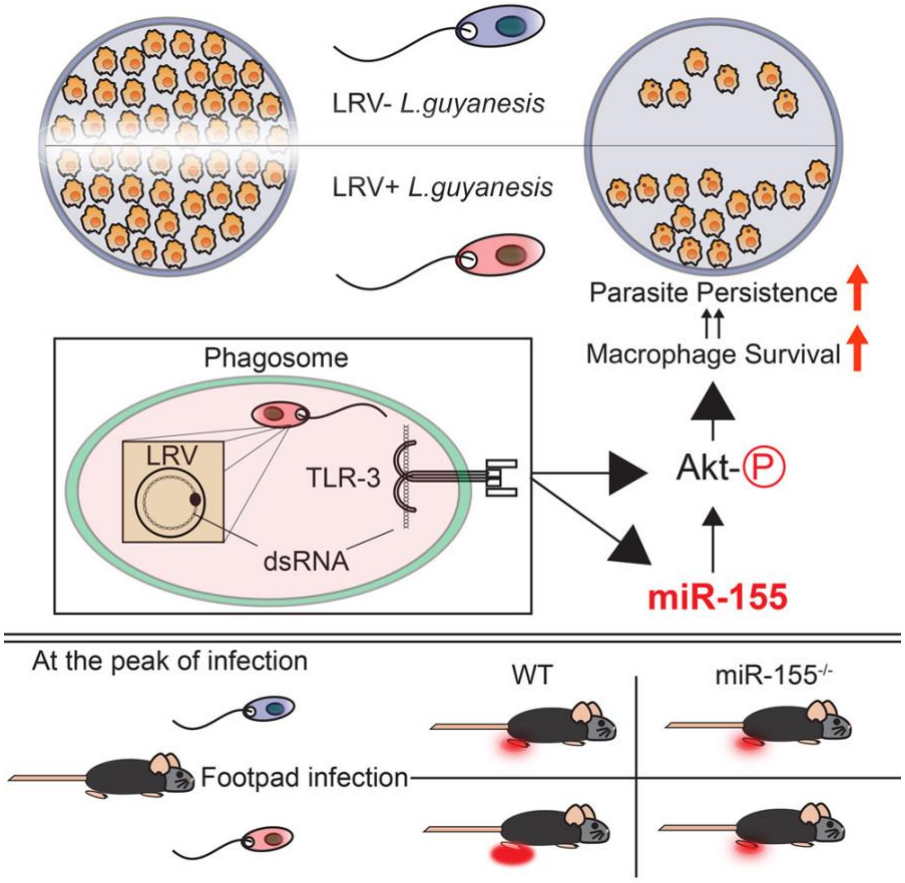

Figure 5.1-3 The viral endosymbiont of *Leishmania* enhances parasite virulence by promoting hyperinflammation in the mammalian host through TLR-3. TLR-3 recognition of *Leishmania* RNA virus 1 (LRV1) induces miR-155 expression. MiR-155-/- mice show a decrease in pathogenesis of LRV1+ *Leishmania* infection. LRV1 induces the activation of PI3K/Akt signalling through TLR3 and miR-155. LRV1 promotes parasite persistence by inducing host survival via Akt. Taken from (Eren et al. 2016)

Concerning the response of the parasite to LRV infection, parasite's genes controlling RNA-mediated interference (RNAi) have been also of interest. The nucleic acid of LRV is potentially recognized by this parasite defence mechanism targeting foreign RNA. Although *Leishmania* are not known to express RNA sensors like those seen in mammals (PKR, RIGH-I, MDA-5), some *Leishmania* species express a strong RNAi activity (Lye et al. 2010). Functional RNAi machinery is generally absent in the *L. leishmania* subgenera (*L. major, L. donovani, L. mexicana*) but has been conserved in the major metastatic parasites of the *L. (Viannia)* subgroup (*L. braziliensis*, *L. panamensis* and *L. guyanensis*) (Lye et al. 2010). Curiously, LRV1 survives in the presence of an active RNAi pathway, where significant levels (0.4 to 2.5%) of small RNAs derived from LRV1 in both *L. braziliensis* and *L. guyanensis*, and with properties consistent with

Dicer-mediated cleavage of the dsRNA genome were found. LRV1 lacks RNAi inhibitory activities, suggesting that a balance may exist between the antiviral response and the replication of the virus (Brettmann et al. 2016). Nevertheless, it was demonstrated that RNAi can be used to eliminate virus from the infected New World *Leishmania* by introducing small hairpin RNAs against viral genome, disrupting in this way the pre-existing balance. This confirmed that virus and RNAi are not mutually exclusive but instead are able to coexist in dynamical equilibrium (Brettmann et al. 2016).

Seeing that retention of LRV in some *Leishmania* species seems to offer advantages while infecting the vertebrate host, it was of interest in this project to investigated if LRV presence may also provide some sort of benefit when infecting the sand fly vector.

5.2 CHAPTER 3 SPECIFIC OBJECTIVES

-Investigate immune responses to *Leishmania guyanensis* LRV1+ or - in *L. longipalpis* LL5 embryonic cell line.

-Evaluate immune responses to *Leishmania guyanensis* LRV1+ or - in the insect vector, *L.longipalpis.*

5.3 METHODS

5.3.1 Parasite culture

L. (V). guyanensis 3539 strain MHOM/BR/2014/271 (Mucocutaneus isolate), positive for LRV1 and *L. (V). guyanensis* 3624 strain MHOM/BR/2015/RO349 (Cutaneous isolate), negative for LRV1, were maintain at 26ºC in Schneider's insect medium (SIGMA-Aldrich) supplemented with 20% foetal bovine serum (FBS), 2% sterile male human urine and 1% antibiotics (Penicillin 100U/ml and Streptomycin 100mg/ml -Sigma). Passages were performed every two - five days.

5.3.2 LRV1 presence confirmation (Nested PCR)

Extraction of RNA and cDNA synthesis (as describe in section 3.3.6 for cell culture) was carried out for each *L. (V). guyanensis* strain, plus using strain MHOM/BR/2014/251 (number 3538) as positive control for the PCR reaction only. Nested PCR was performed using LRV1-pair1 and LRV1-pair2 (ANNEX-A). PCR was performed including a cycle of 95ºC for 3min; 35 cycles of 95ºC for 30 sec, 55ºC for 30 sec and 72ºC for 30 sec (Pereira et al. 2013). The amplified fragments were 125bp and 90bp for first and second round respectively. As negative control was used distilled water for the first round and 2uL of the first reaction for the second round. The reactions from the second round of PCR were visualized in 2% agarose gel (Figure 5.3-1)

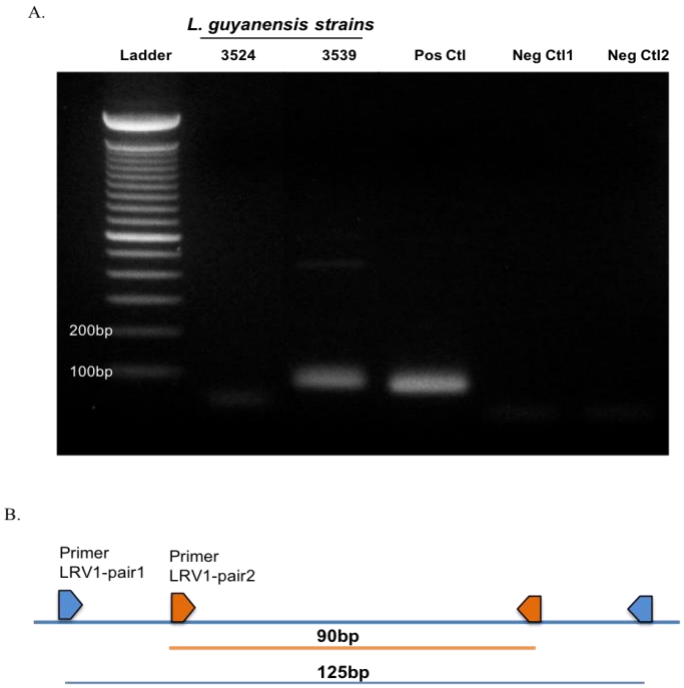

Figure 5.3-1 PCR for LRV1 detection. A. Electrophoresis gel of last round of nested PCR to detect LRV1 presence in *L. (V). guyanensis* strains, Ladder = Molecular size marker; 3524 =*L. (V). guyanensis* negative for LRV1; 3539 = *L. (V). guyanensis* positive for LRV1; Pos Ctl = positive control; Neg Ctl 1= negative control from first round of nested PCR; Neg Ctl2 = Negative control from second round of nested PCR. B. Schematic diagram of nested PCR fragments showing position of each pair of primers used and estimated size of amplicons in each round.

5.3.3 LL5 cell culture (see section 3.3.1)

5.3.4 Insects(see section 4.3.2)

5.3.5 Infection (see section 4.3.3)

5.3.6 LL5 cells challenge with L. (V). guyanensis

LL5 cells were counted in a Neubauer chamber and $2x10^7$ cells were seeded in a $25cm^2$ canted neck flask with L15 complemented medium (10% FBS, 20 TPB, 1% Antibiotics, for more detail see section 3.3.1). After 24h, *L. (V). guyanensis LRV1+* or – were added to the flasks at a ratio 5:1 (parasites : LL5 cells) and maintain at 26ºC for 24h. Then medium of each flask was discarded and TRIzol reagent was added to proceed with LL5 cells RNA extraction.

5.3.7 RNA extraction and cDNA synthesis from LL5 cells (see section 3.3.6) and adult females (see section 4.3.6)

5.4 RESULTS

5.4.1 Immunological state of LL5 challenged with L. (V.) guyanensis LRV1+ or - .

In order to evaluate if canonical innate immune pathways of LL5 cells were modulated during challenge with *L. (V.) guyanensi*s with LRV1 (Lg(LRV1+)), gene expression of molecules belonging to Toll, IMD and JAK/STAT pathway were evaluated. Transcriptional levels were measured 24 hours post challenge and normalized by GAPDH gene expression (Figure 5.4-1). From the transcription factors dorsal (Toll pathway) and Relish (IMD) pathway, only Relish reported a significant down regulation when compared with cells challenged with *L. (V.) guyanensis* LRV1- (Lg(LRV1-)) (Figure 5.4-1, A). Vago and vir-1 genes which, as mentioned before, are related to INF type antiviral response that involves a crosstalk between RNAi and JAK/STAT pathways were also studied. Only vir-1 showed a down regulation when compared with control cells (Figure 5.4-1, B). Additionally, transcriptional levels of AMP genes were measured, showing that only attacin was down regulated significantly in cells challenged with Lg(LRV1+), Defensin 4 and cecropin were not modulated Figure 5.4-1, C).

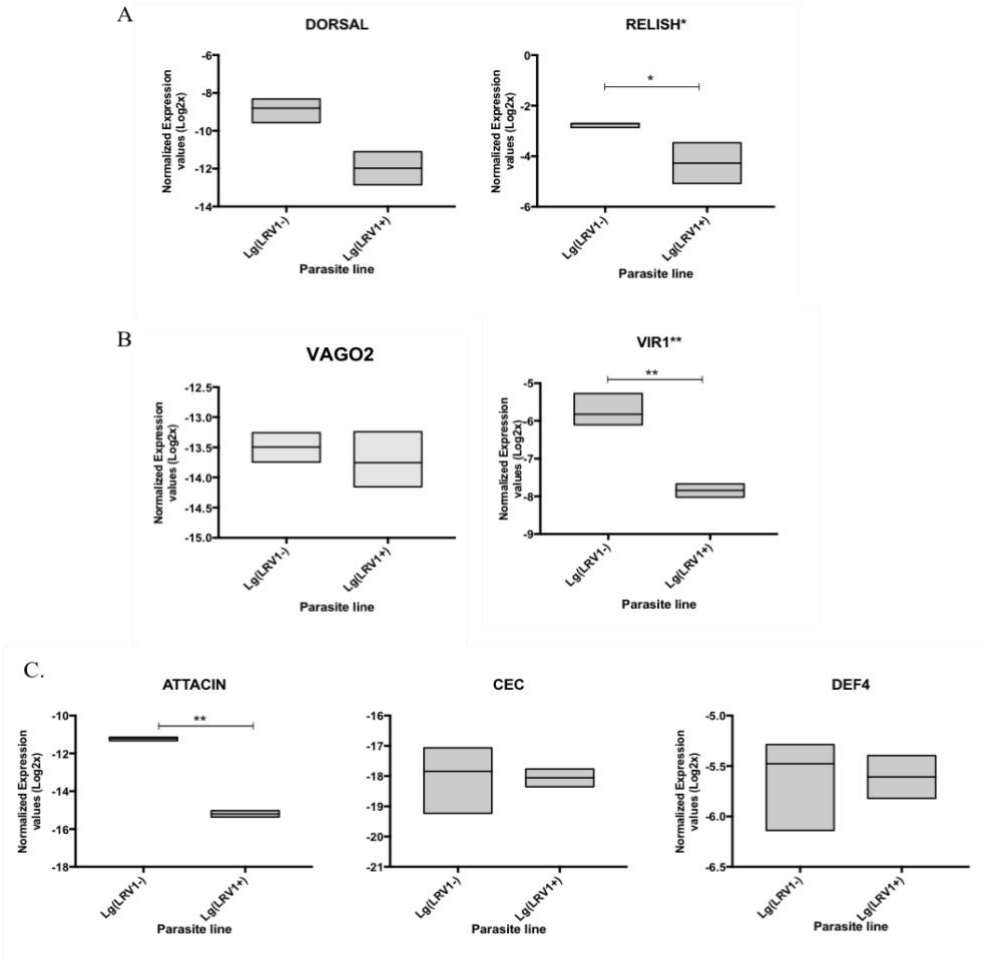

Figure 5.4-1 Gene expression of molecules from canonical innate immune response pathways in LL5 exposed to Lg(LRV1-) or Lg(LRV1+). A. mRNA levels of transcription factors dorsal (Toll pathway) and Relish (IMD pathway) in LL5 cells exposed to Lg(LRV1-) and Lg(LRV1+), B. mRNA levels of effector genes Vago and vir-1 in LL5 cells exposed to Lg(LRV1-) and Lg(LRV1+). C. mRNA levels of AMPs in LL5 cells exposed to Lg(LRV1-) and Lg(LRV1+). Al graphs Y-axis represent log2(x) of normalized by reference gene (GAPDH) expression values from qPCR data. The X-axis represent two parasite lines to which LL5 cells were exposed at MOI 5:1 (parasite:cells). Lg(LRV1-) = L. (v.) guyanensis without LRV1 virus; Lg(LRV1+) = L. (v.) guyanensis with LRV1 virus. Boxes represent mean with maximum and minimum values from three biological replicates for Lg(LRV1-) and two biological replicates for Lg(LRV1+). Student's T test with Welch's correction was performed. *p≤0.05, **p≤0.01,

To further evaluate if IFN-like antiviral response could be elicited by the presence of LRV1 in *L. (V). guyanensis* strain, the transcription of 21 molecules detected in Martins-da-Silva et al. (2018) study, where an initial proteomic and transcriptional analysis was made in the conditioned media of LL5 cells challenged with Poly(I:C), were chosen to be assessed in this experiment (Figure 5.4-2 and Figure 5.4-3). From those 21 molecules, 6 were modulated in this test. *LCAT* and *Transk* (Transketolase) expression was up regulated significantly in cells challenged with Lg(LRV1+) (Figure 5.4-2, A). Four molecules, *Repressor splicing factor* (RRM), *Coronin-6* (WD40-2), *SRC Substrate cortactin* (SH3) and *Tyrosine-protein kinase-like otk* (TYRK) were significantly down regulated in Lg(LRV1+) stimulated cells (Figure 5.4-2, B).

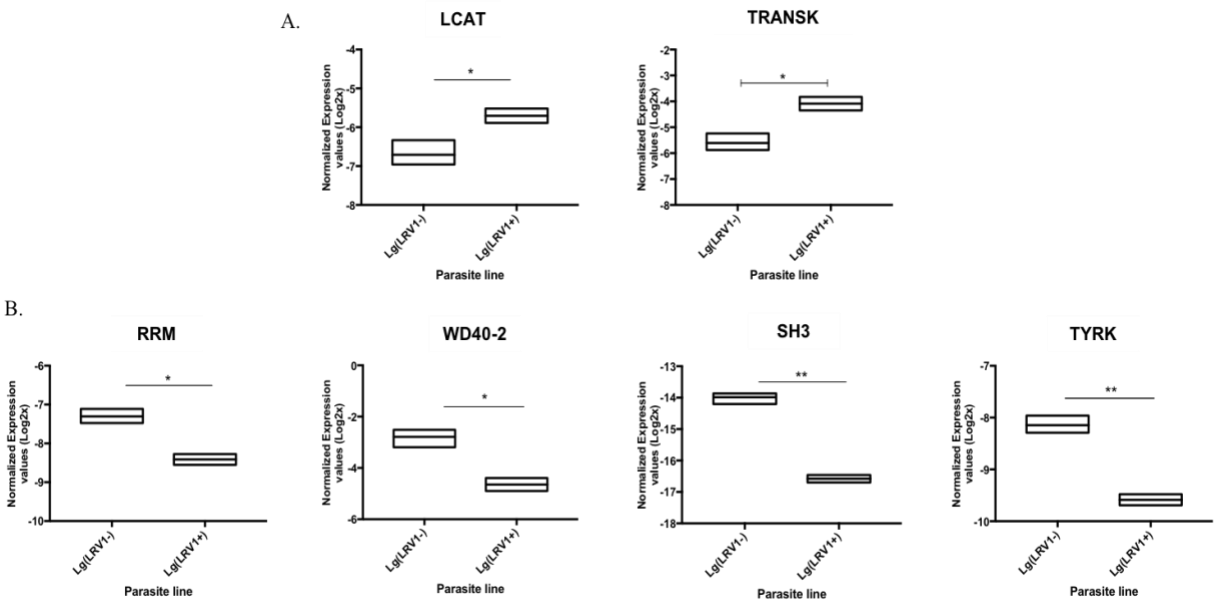

Figure 5.4-2 Modulated genes related to non-specific antiviral response in LL5 cells exposed to Lg(LRV1-) or Lg(LRV1+). A. mRNA levels of LCAT and Tranketolase in LL5 cells exposed to Lg(LRV1-) and Lg(LRV1+), B. mRNA levels of RRM, WD40-2, SH3 and TYRK in LL5 cells exposed to Lg(LRV1-) and Lg(LRV1+). Al graphs Y-axis represent log2(x) of normalized by reference gene (GAPDH) expression values from qPCR data. The X-axis represent two parasite lines to which LL5 cells were exposed at MOI 5:1 (parasite:cells). Lg(LRV1-) = L. (v.) guyanensis without LRV1 virus; Lg(LRV1+) = L. (v.) guyanensis with LRV1 virus. Boxes represent mean with maximum and minimum values from three biological replicates for both challenges. Student's T test with Welch's correction was performed. *p≤0.05, **p≤0.01.

The other 15 molecules tested did not show significant variation when compared with control group cells (Figure 5.4-3), *Tubulin-specific chaperon A* (TBCA), *Proliferating cell nuclear antigen* (PCNA), *FK506 binding protein* (FKPB), *Coatomer delta subunit* (ClatAdapt), *Scramblase* (SCR), *Kinesin, Basic transcription factor 3* (BTF3), *Transmembrane protease serine 9-like* (TPser9*), Actin-interacting protein 1* (WD40-1), *Thioredoxin* (THRX), *Phosphoinositide-binding protein* (PIBP), *Vigilin, Valine-tRNA ligase* (VTRNALI), *Barrier-to-autointegration factor* (BAUTF) and *Regulator of chromosome condensation* (RCCGj1).

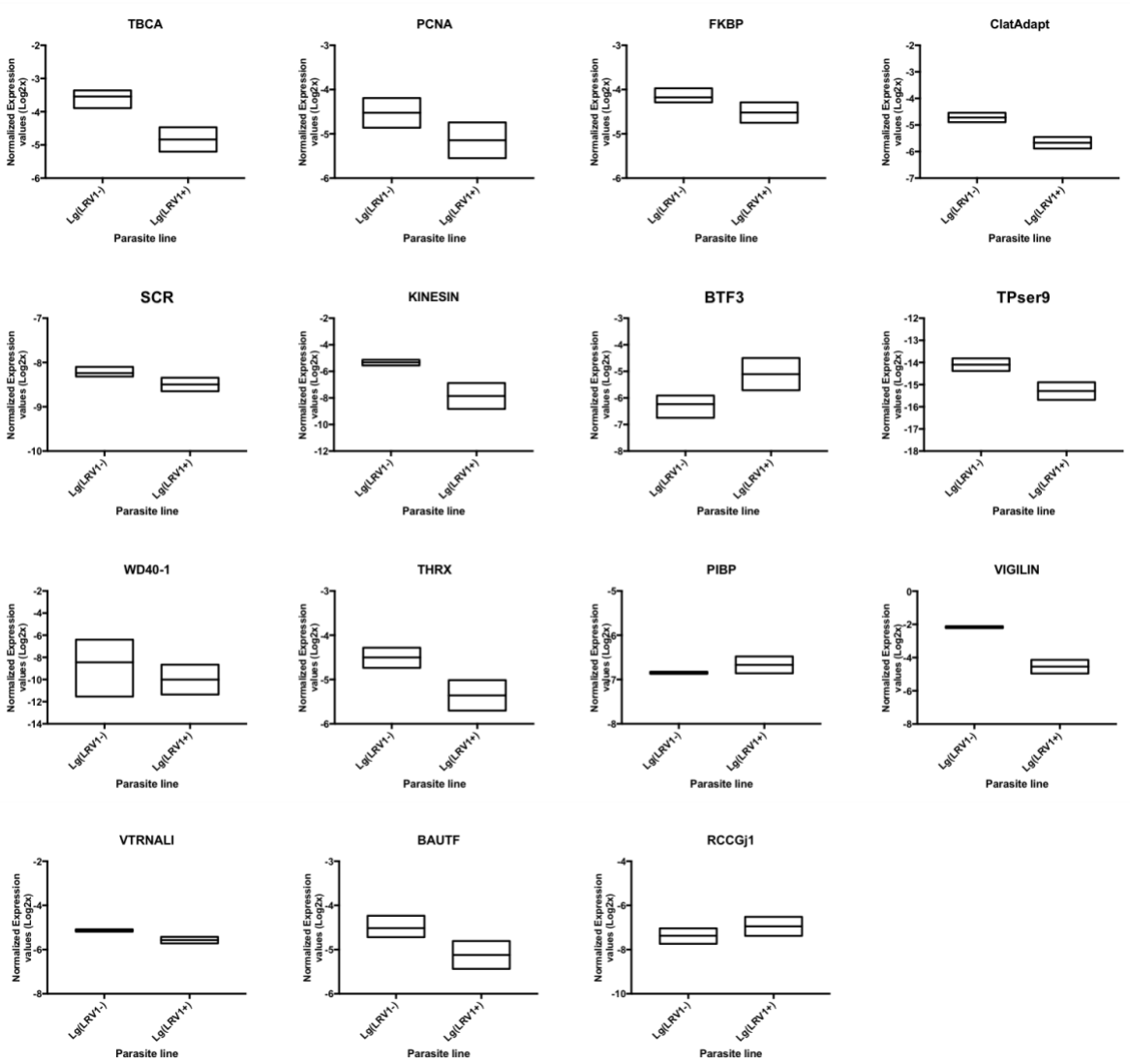

Figure 5.4-3 Gene expression of molecules related to non-specific antiviral response in LL5 exposed to Lg(LRV1-) or Lg(LRV1+). All graphs Y-axis represent log2(x) of normalized by reference gene (GAPDH) expression values from qPCR data. The X-axis represent two parasite lines to which LL5 cells were exposed at MOI 5:1 (parasite : cells). Lg(LRV1-) = *L. (v.) guyanensis* without LRV1 virus; Lg(LRV1+) = *L. (v.) guyanensis* with LRV1 virus. Boxes represent mean with maximum and minimum values. Student's T test with Welch's correction was performed.

5.4.2 Immune state of adult female L. longipalpis infected with L.(V.) guyanensis LRV1+/-.

Adult sand flies were infected with *L. (V.). guyanensis* LRV1+ or - to assess possible influence of the virus in the infection establishment and immunology response in the *in vivo* model.

5.4.2.1 Parasite and microbiota load

Assessment of parasite load in insect pools at each timepoint was performed using the expression of actin from *Leishmania.* Results showed that there is a significant increase in parasite load at 144 hours post infection (hpi) in those insects infected with Lg(LVR+) when compared with insects infected with Lg(LRV1-). While there was no significant difference in parasite load at

earlier timepoints (Figure 5.4-4, A),), Lg(LRV1+) parasites generally exhibited higher prevalence than their Lg(LRV1-) counterparts.

Bacterial microbiota load was also measured during infection by evaluating expression of 16S. No significant difference between groups was found at any time point (Figure 5.4-4, B).

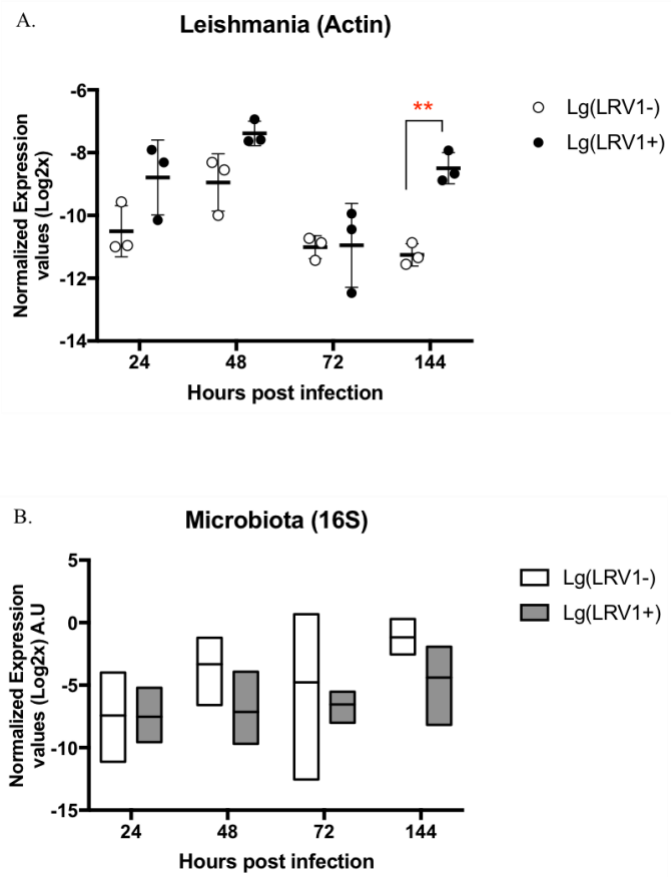

Figure 5.4-4 Parasite and microbiota load in female sand flies infected with Lg(LRV1-) or Lg(LRV1+). A. *Leishmania* actin gene mRNA levels in female sand flies infected Lg(LRV1-) and Lg(LRV1+). B. Bacterial16S gene mRNA levels in female sand flies infected with Lg(LRV1-) and Lg(LRV1+). Al graphs Y-axis represent log2(x) of normalized by sand fly reference gene (GAPDH) expression values from qPCR data. The X-axis represent timepoints of sample collection at 24, 48, 72 and 144 hours after infected blood meal. Lg(LRV1-) = *L. (v.) guyanensis* without LRV1 virus; Lg(LRV1+) = *L. (v.) guyanensis* with LRV1 virus. Boxes represent mean with maximum and minimum values of three experiments, pools of 10 insects per timepoint, per experiment. A Student's T test with Welch's correction was performed for each timepoint. **p≤0.01.

5.4.2.2 Gene expression of canonical pathways (Toll, IMD, JAK/STAT) components

Some regulatory molecules from the canonical pathways were evaluated in order to elucidate if the increment in Lg(LRV1+) load observed previously was regulating any of the three pathways (Toll, IMD and JAK/STAT), (Figure 5.4-5).

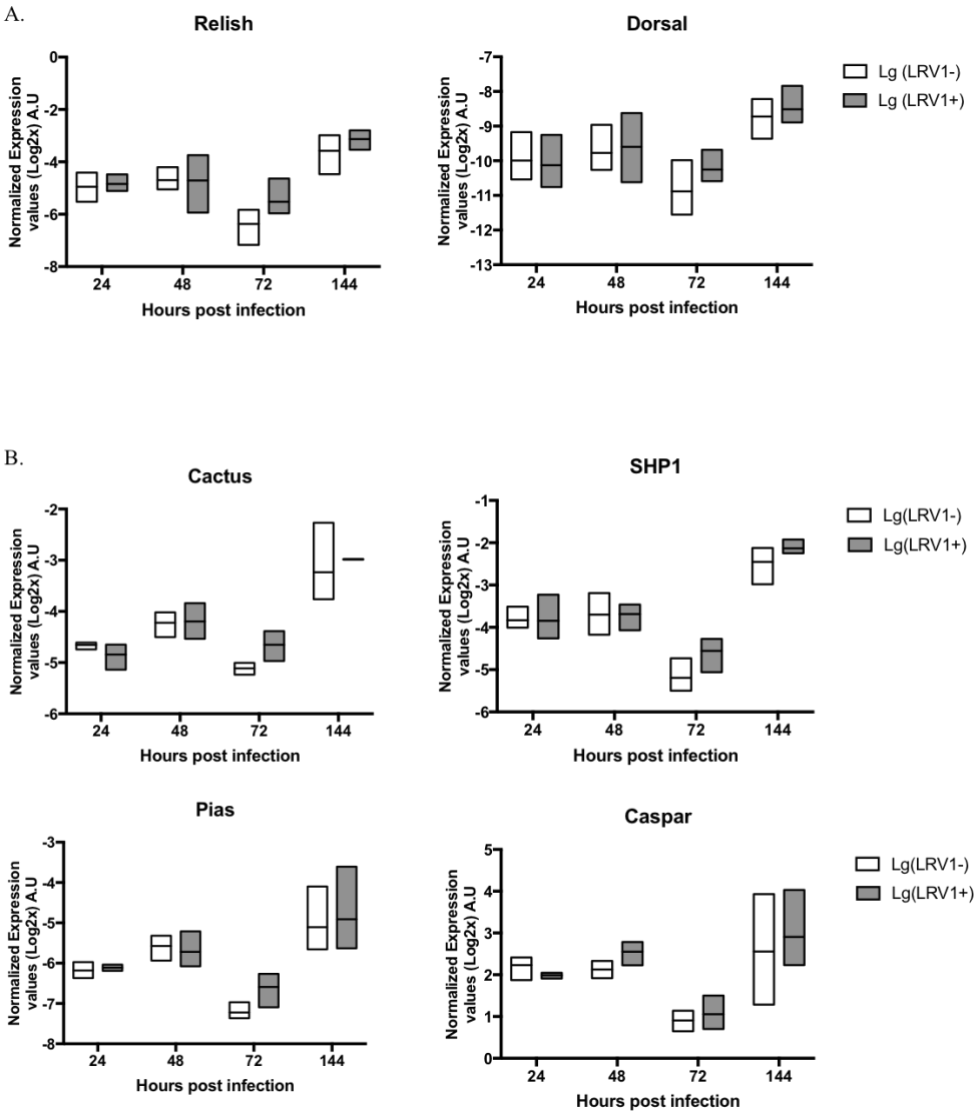

Figure 5.4-5 Gene expression of regulatory molecules from Toll, IMD and JAK/STAT pathways in female sand flies infected with Lg(LRV1-) or Lg(LRV1+). A. mRNA levels of transcription factors Relish (IMD pathway) and dorsal (Toll pathway) in female sand flies infected with Lg(LRV1-) and Lg(LRV1+). B. mRNA levels of negative regulator genes, cactus and SHP1 (Toll pathway), Pias (JAK/STAT pathway) and Caspar (IMD pathway) in female sand flies infected with Lg(LRV1-) and Lg(LRV1+). All graphs Y-axis represent log2(x) of normalized by sand fly reference gene (GAPDH) expression values from qPCR data. The X-axis represent timepoints of sample collection at 24, 48, 72 and 144 hours after infected blood meal. Lg(LRV1-) = *L. (v.) guyanensis* without LRV1 virus; Lg(LRV1+) = *L. (v.) guyanensis* with LRV1 virus. Boxes represent mean with maximum and minimum values. A Student's T test with Welch's correction was performed for each timepoint.

Positive regulators like transcription factors Relish and dorsal from IMD and Toll pathway respectively, did not show important regulation through infection experiments (Figure 5.4-5, A). Several negative regulators were evaluated too, cactus (Toll pathway), Pias (JAK/STAT pathway), Caspar (IMD pathway) and SHP1 that has been associated as regulator of Toll and JAK/STAT pathway. None of the mentioned negative regulators showed any significant modulation along the infection (Figure 5.4-5, B).

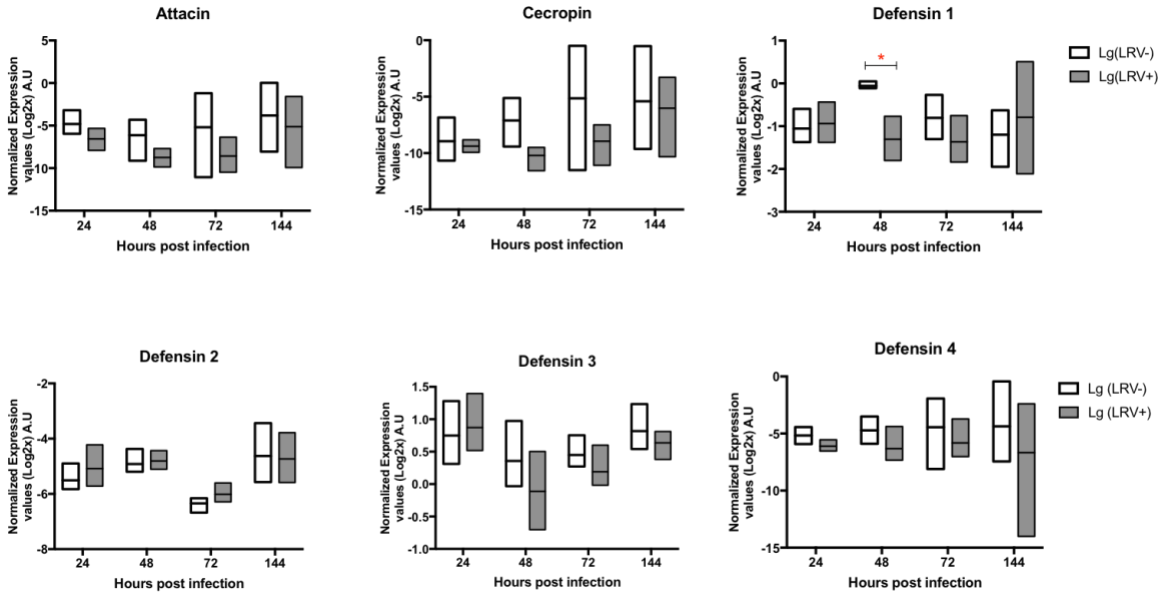

Figure 5.4-6 Gene expression of AMPs in female sand flies infected with Lg(LRV1-) or Lg(LRV1+).mRNA levels of antimicrobial peptides in female sand flies infected with Lg(LRV1-) and Lg(LRV1+). Al graphs Y-axis represent log2(x) of normalized by sand fly reference gene (GAPDH) expression values from qPCR data. The X-axis represent timepoints of sample collection at 24, 48, 72 and 144 hours after infected blood meal. Lg(LRV1-) = *L. (v.) guyanensis* without LRV1 virus; Lg(LRV1+) = *L. (v.) guyanensis* with LRV1 virus. Boxes represent mean with maximum and minimum values. A Student's T test with Welch's correction was performed for each timepoint. *p≤0.05.

Gene expression of attacin, cecropin and four different defensins were measured, (Figure 5.4-6), only Defensin1 showed significant down regulation at 48hpi in insects infected with Lg(LRV1+).

5.4.2.3 RNAi pathway and other antiviral related molecules

To investigate if LRV1 was detected directly by the immune system of the insect possibly triggering an antiviral response, several component from the RNAi pathway and other antiviral response associated molecules were studied (Figure 5.4-7 and Figure 5.4-8). Gene expression of Argonaute, Dicer2, R2D2 and the cytokine-like molecule, Vago, did not show substantial regulation at any time point after infection when compared with control group (Figure 5.4-7). Transcription levels of *Transketolase*, one of the non-specific antiviral response related molecules that was up regulated in the in vitro model, did not vary in infected adult flies when compared with control group (Figure 5.4-8).

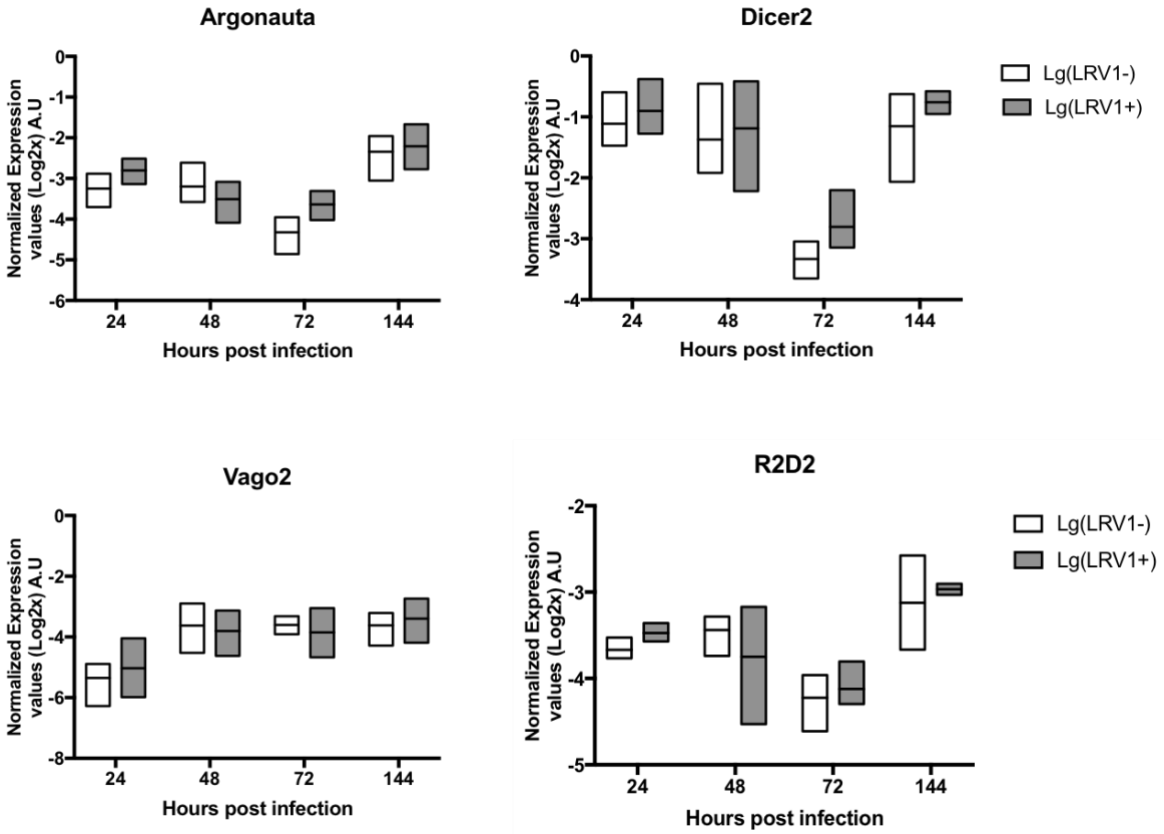

Figure 5.4-7 Gene expression of RNAi pathway related molecules in female sand flies infected with Lg(LRV1-) or Lg(LRV1+). mRNA levels of RNAi pathway related genes in female sand flies infected with Lg(LRV1-) and Lg(LRV1+). Al graphs Y-axis represent log2(x) of normalized by sand fly reference gene (GAPDH) expression values from qPCR data. The X-axis represent timepoints of sample collection at 24, 48, 72 and 144 hours after infected blood meal. Lg(LRV1-) = *L. (V.) guyanensis* without LRV1 virus; Lg(LRV1+) = *L. (V.) guyanensis* with LRV1 virus. Boxes represent mean with maximum and minimum values. A Student's T test with Welch's correction was performed for each time point.

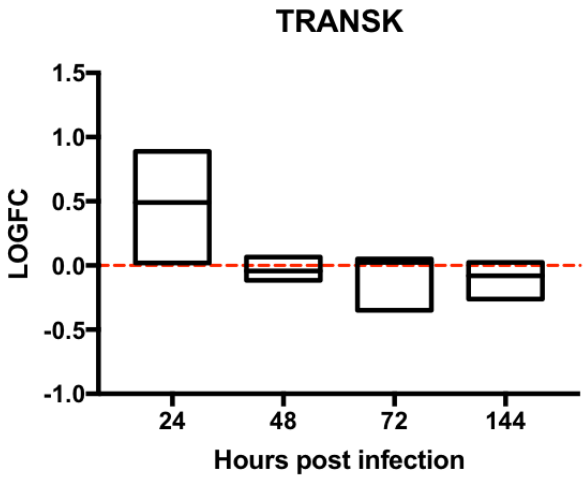

Figure 5.4-8 Gene expression of Transketolase in female sand flies infected with Lg(LRV1+) vs Lg(LRV1-). Graph's Y-axis represent log2(x) of fold change between test group insects infected with (LRV1+) versus control group infected with (LRV1-), both previously normalized by reference gene (GAPDH) expression values from qPCR data. The X-axis represent timepoints of sample collection at 24, 48, 72 and 144 hours after infected blood meal. Lg(LRV1-) = *L. (v.) guyanensis* without LRV1 virus; Lg(LRV1+) = *L. (v.) guyanensis* with LRV1 virus. Boxes represent mean with maximum and minimum values. A Student's T test with Welch's correction was performed using log2(x) data from each group for each timepoint.

5.5 DISCUSSION

5.5.1 Immunological state of LL5 cells challenged with Lg(LRV1+)

Recent studies have shown that LL5 cells have active innate immune responses when challenged with killed bacteria, yeast and *L. infantum (Syn. chagasi),* more specifically canonical Toll and IMD pathways presented transcriptional upregulation of transcription factors and AMPs (Tinoco-Nunes et al. 2016). Similarly, findings from our group revealed that the JAK/STAT pathway is modulated under *L. infantum (Syn. chagasi)* challenge in *in vitro* and *in vivo* models; in this case the presence of the parasite seems to downregulate some pathway molecules in LL5 cells and less drastically in adult females (Azevedo-Brito 2018). In addition to innate immune canonical pathways, a non-specific antiviral response interferon-like was reported in LL5 cells (Pitaluga et al. 2008), that was further studied at a proteomic and transcriptional level by Martins-da-Silva et al. (2018) and discussed in chapter 1 of the present work. All these previous finding support LL5 cells as a good model for study immune responses to several pathogens, especially when they hold similarities with mammalian mechanisms of antiviral response. In line with this idea, the first set of experiments was directed to evaluate the immune state of LL5 cells challenged with either Lg(LRV1+) or Lg(LRV1-). Transcriptional analyses of molecules from all three canonical pathways showed that Relish, transcription factor of IMD pathway was significantly downregulated in LL5 cells exposed to Lg(LRV1+) (Figure 5.4-1, A). Likewise, vir-1 an effector molecule of JAK/STAT pathway closely related to antiviral response in *Drosophila* and mosquitoes (Fullaondo and Lee 2012; Merkling and van Rij 2013; Prasad et al. 2013) and attacin, an antimicrobial peptide that can be regulated either by IMD or JAK/STAT pathways (De Gregorio et al. 2002; Huang et al. 2013) were downregulated in cells challenged by Lg(LRV1+) (Figure 5.4-1B,C). Our results seem to indicate that LRV1 presence in *L. (V.) guyanensis* can contribute to regulate negatively IMD and JAK/STAT pathways in LL5 cells that in itself could provide an advantage to the parasite in the insect due to a diminished immune response. The majority, if not all the studies about LRV1 role in *Leishmania* infection have been based in the mammalian host, where it was reported that recognition of the viral RNA by TLR3 induced proinflammatory mediators like type I interferons, subverting the immune response to infection to promote parasite persistence (Ives et al. 2011; Rossi et al. 2017). Our results contrast with those reported in humans, showing a reduction in immune response instead. It is important to highlight that in the sand fly, *Leishmania* parasites have extracellular stages and a short phase of direct interaction with the midgut epithelium (Figure 1.2-2) which means that different immune evasion mechanisms may be

needed. In the insect the majority of the interaction with the parasite is through secreted molecules, like AMPs and ROS, hence the need of the parasite to reduce this kind of "aggressions" by regulating immune pathways. There are reports of inhibition of IFN production through impaired JAK/STAT signalling in different viral infections in mammalian cell lines (Muñóz-Jordán et al. 2003; Lin et al. 2004; Fros et al. 2010).

As mentioned before, LL5 cells present a non-specific antiviral response that is similar to mammalian IFN type response and knowing that LRV1 detection in macrophages can elicit type I INF production that increase inflammation and helps with parasite persistence, we evaluated if LRV1 could stimulate the non-specific antiviral response in LL5 cells at a transcriptional level. Several candidates that were regulated after Poly(I:C) stimulation, either at protein or at transcriptional level (Martins-da-Silva et al. 2018) were assessed in LL5 challenged with Lg(LRV1+) or Lg(LRV1-). Interestingly, LCAT and TRANSK, were up regulated in cells stimulated with Lg(LRV1+). LCAT (Lecithin cholesterol acyltransferase) is a plasma enzyme which esterifies free cholesterol (FC) to cholesteryl ester (CE), forming mature HDL (High density lipoprotein) as part of Reverse cholesterol transport (RCT), (Azzam and Fessler 2012; Saeedi et al. 2015). It has been reported that HDL suppresses the type I interferon response in mammals (Suzuki et al. 2010). Studies in mammalian cells have also shown the cross talk between cholesterol metabolism and innate immunity pathways. Cholesterol and its mobilization by RCT can regulate innate immune response at several levels: a) cell (plasma and endosomal) membranes; b) intracellular signalling pathways; and c) extracellularly, through effects of HDL (Azzam and Fessler 2012). Castrillo et al. (2003) showed that activation of TLR 3 and 4 by viral and bacterial pathogens, having a greater effect with specific ligands like Poly (I:C), strongly inhibits cholesterol efflux from macrophages- *in vitro* and *in vivo*- by downregulating LXR (Liver X receptors) dependent genes. Accumulation of cholesterol in macrophages and other immune cells results in amplification of inflammatory responses (Tall and Yvan-Charvet 2015). In humans, during TLR activation and acute phase response (APR), decreased LCAT activity contributes to cause changes in HDL composition that therefore impair its cholesterol-transport and anti-inflammatory functions. One of the hypotheses raised by Castillo et al. (2013) is that LRX activation could interfere with the expression of one or more genes important for mounting an appropriate antimicrobial response, and therefore an activation of this pathway – in our case upregulation of LCAT – could be beneficial to LRV1 and *Leishmania* in the insect. LCAT was found to be down regulated in Poly(I:C) transfected LL5 cells (Martins-da-Silva et al. 2018) suggesting that reduction in this enzyme's transcripts may be a characteristic of these cells antiviral response to dsRNA

structure; it is possible that the stimuli from live LRV1 and *Leishmania* may diminished antiviral response through upregulation of LCAT.

Transketolase was also reported down regulated at protein level 24 hours post challenge with Poly(I:C) (Martins-da-Silva et al. 2018). Transketolase is the key rate-limitating enzyme of the non-oxidative branch of the pentose phosphate pathway of the carbohydrate transformation, which is involved in energy generation and nucleic acid synthesis (Kochetov and Solovjeva 2014). Increase in TRANSK activity has been associated with high rate of nucleic acid ribose synthesis necessary for tumour cell survival, chemotherapy resistance and proliferation (Cascante et al. 2000; Kochetov and Solovjeva 2014); also was reported unregulated in Kaposi's sarcoma-associated herpesvirus (KSHV) or human herpes virus 8 (HHV-8) infected cells through Nrf2 (nuclear factor erythroid 2 related factor 2), that together with up regulation of other molecules and pentose phosphate pathway enzymes, all contribute to establishment of infection and KSHV oncogenesis (Ramezani et al. 2018). A proteomic study in *Drosophila* larvae, TRANSK was reported up regulated after 6h of recovery from bacterial extract challenge, in this study up regulation of molecules from the carbohydrate metabolism pathways was related more to ATP synthesis than biosynthesis of fatty acids or amino acids. At the cellular level, ATP depletion results in proteotoxic stress that can lead to dysfunction, destabilization and aggregation of many cellular proteins including enzymes and constituents of cytoskeletal structures (Kabakov et al. 2002; De Morais Guedes et al. 2005). Together, literature findings about these two molecules, suggest that up regulation of LCAT could impaired the establishment of an appropriate antiviral response in LL5 cells by improving cholesterol transport and anti-inflammatory functions of HDL; and increase in TRANSK may contribute to cell survival and replication, that altogether could play in favour of Lg(LRV1+) establishment.

From the associated non-specific antiviral response evaluated in LL5 cells challenged with either Lg(LRV1+) or Lg(LRV1-), four of them were significantly down regulated (Figure 5.4-2B). Interestingly, molecules RRM and Coronin, were found to be upregulated at a protein level in the secretome of LL5 cells stimulated with Poly(I:C) (Martins-da-Silva et al. 2018). The *Repressor splicing factor* (RRM), is a molecule that comprises an N-terminal RRM-type RNA-binding domain and a C-terminal part enriched with glycine (G), arginine (R),and serine (S) residues (GRS domain), (Labourier et al. 1999b, 1999a). *Drosophila*'s homolog, repressor splicing factor 1 (RSF1) has been shown to antagonize splicing factors of the serine/arginine-rich (SR) family (Labourier et al. 1999a). A study in mammalian cells and mice showed that stimulation with pro-inflammatory cytokines like interleukin1(IL-1), tumour necrosis factor (TNFa) and IFN induce

downregulation in several genes, including Repressor splicing factor-1 (*zfm1*). Antisense oligonucleotide suppression of *zfm1* protein synthesis resulted in an increase in expression of pro-inflammatory effector genes and an increase in the rate of cell proliferation (Cattaruzza et al. 2001).

Coronin-6 was also down regulated in LL5 cells challenged with Lg(LRV1+). The coronin family is one of the WD (tryptophan-aspartate)-repeat domain containing families that are diverse both in structures and functions (Liu et al. 2016). Coronins form one of the many groups of actin cytoskeleton regulators. *Drosophila* has a coronin-like protein (*coro*) that has been found to mediate trafficking and fusion of F-actin coated vesicles with the membrane (Bharathi et al. 2004). In mammals, 7 coronin have been identified to date. Although some studies showed that mammalian coronins regulate the actin dynamics, later many other functions such as calcium signalling regulation, cAMP signalling regulation, have been also reported beyond the actin modulation (Liu et al. 2016). Coronin 1C was found down regulated in Adenovirus (Hartman et al. 2007) and Cytomegalovirus infections (Hertel and Mocarski 2004) in mammals. Interestingly, several cases of immunodeficiencies have been associated with mutation in coronin1,(review in (Pieters et al. 2013)); one of these cases was a homozygous missense mutation in coronin 1 in three people with a combined immunodeficiency that is associated with a particular vulnerability to Epstein-Barr virus (EBV) infection (Moshous et al. 2013) showing the crucial role of this gene in shaping appropriate immune responses in humans.

SRC Substrate cortactin (SH3) and *Tyrosine-protein kinase-like otk* (TYRK) were also down regulated at a transcriptional level in LL5 cells challenged with Lg(LRV1+), interestingly these proteins were also down regulated at a protein level in the secretome of Poly(I:C) challenged LL5 cells by Martins da Silva et al (2018), and may be associated with antiviral response to detection of LRV1 from dead parasites. *SRC Substrate Cortactin* (SH3) is a ubiquitously-expressed protein and is expressed in most eukaryotic cells. Named after its cortical intracellular localization and binding to actin, cortactin is a central regulator of filamentous-actin, which maintains cell shape and integrity and it is important for many cellular functions including cell migration and endocytosis (Wu and Parsons 1993; van Rossum et al. 2006; Kirkbride et al. 2011). Due to its role in cell migration, cortactin is associated with several types of cancers, and the upregulation of this molecules is a marker for cancer progression (MacGrath and Koleske 2012). Additionally, cortactin has also been associated with some bacterial and virus infections (Varon et al. 2014; Woollard et al. 2014; Kenney and Meng 2015). Initially identified as the substrate of Src-tyrosine kinase, cortactin is also one of the substrates of multi-substrate deacetylase, histone deacetylase 6 (HDAC6) in mammalian cells (Zhang et al. 2007; Li et al. 2013), which was recently identified as

an antiviral host factor of Influenza A Virus (IAV) by negative regulating trafficking of viral components to the plasma membrane via its substrate activated microtubules (Husain and Cheung 2014), later was show that caspase mediated degradation of host cortactin favours IAV infection in epithelial cells. Further studies showed that cortactin polypeptide level was down regulated in IAV infected cells and its silencing reduce the percentage of released virions (Chen and Husain 2016).

Tyrosine-protein kinase like otk, also known as off-track (*otk*) in *Drosophila* and Protein Tyrosine Kinase 7 (PTK7) in humans, is an evolutionarily conserved transmembrane receptor with a broad range of functions in tissue development and homeostasis (Berger et al. 2017). Initially it was identified as a gene unregulated in colon carcinoma cells (Mossie et al. 1995); later it was shown to affect various aspects of cell-cell communication and movement. PTK7 controls tissue morphogenesis and patterning by affecting cell polarity, migration as well as tissue regeneration and wound healing (Lu et al. 2004; Shnitsar and Borchers 2008; Caddy et al. 2010; Lander and Petersen 2016). Additionally its function in adult tissue homeostasis is demonstrated by the fact that misregulation of PTK7 expression correlates with development of cancer and its progression to metastasis in various cellular contexts (reviewed in (Dunn and Tolwinski 2016).

All together, these modulated molecules are associated one way or another with response to viral infection, cytoskeletal modification, cell proliferation and division; that is yet to be determined if it is part of the antiviral response to fight against LRV1 or modulation elicit by the virus in order to provide an advantage for the parasite and itself.

5.5.2 Immunology of adult L. longipalpis infected with Lg(LRV1+) vs Lg(LRV1-).

After observing that LRV1 presence in *L. guyanensis* seems to elicit regulation of several genes related to antiviral response and cell proliferation in LL5 cells, the next step was to test the possible role of LRV1 as a bias to the parasite in the insect's midgut. Results from sand flies infected either with Lg(LRV1+) or Lg(LRV1-) showed an important increase in parasite load at 144h post infection in insects infected with Lg(LRV1+) (Figure 5.4-4A). This result could be an evidence that maintaining its viral endosymbiont, will benefit *Leishmania* establishment and propagation not only in its mammalian hots but also in its insect vector. Knowing that microbiota could influence the insect immune response and interaction with *Leishmania* during infection, bacterial microbiota load was also assed. Despite the absence of statistical significance, results presented a slight trend to total microbiota reduction in insects infected with Lg(LRV1+) (Figure

5.4-4B), which could indicate a competition scenario taking into account that *L. guyanensis* with LRV1 appears to replicate better in the insect gut than the parasite without the virus.

Taking as reference our previous results in challenged LL5 cells with *L. guyanensis* that have or not the virus, several molecules from the canonical pathways were assessed, with particular emphasis in their positive and negative regulators (Figure 5.4-5) as well as some AMPs (Figure 5.4-6). Interestingly, despite the difference in parasite load at 144h, neither dorsal or relish, transcription factors of Toll and IMD pathways respectively, showed different gene expression from control group (Figure 5.4-5A). Similarly, negative regulators cactus and SHP1 (Toll pathway), pias (JAK/STAT pathway) and caspar (IMD pathways) did not present significant difference when compared to control group (Figure 5.4-5B). It is clear that due to the difference in complexity between a cell culture and a whole organism (insect), not always the modulations observed in *in vitro* model can be reproduce in *in vivo* model. In the challenged cells experiments, *L. guyanensis* had a direct interaction with LL5 cells generating modulation of certain molecules as it was discuss previously; on the contrary, in the sand fly midgut, the parasites – and the virus for that matter - do not have a direct contact with the epithelium until approximately 72h after infection, when the digestion ends and the parasite load is the lowest. Curiously, even in 144h when Lg(LRV1+) parasites are in grater quantity than control group, it was not enough to elicit a differential regulation of *L. longipalpis* immune system, could be that the presence of LRV1 help *L. guyanensis* to replicate faster while keeping insect immunity undisturbed – at least compared to infection with Lg(LRV1-)- this could translate in an advantage to favour transmission of the parasite.

In order to assess further if the canonical pathways could be modulated by the presence of LRV1, several AMP genes were evaluated (Figure 5.4-6). Out of the six AMP genes tested, only defensin 1 was found downregulated at 48h post infection, if we compare this result with *Leishmania* load at the same time point it is possible to see a trend to increase in Lg(LRV1+) load that may not be enough to show statistical difference in parasite abundance but could have had influenced in the modulation in this defensin gene.

To evaluate if LRV1 could have being detected by RNAi pathway, some of the molecules of this pathway were evaluated (Figure 5.4-7). However, none of them showed any significant variation, suggesting that the presence of LRV1 did not elicit RNAi pathway activation.

Taking into account results from LL5 cells challenged with Lg(LRV1+) discussed earlier, where molecules associated to non-specific antiviral response were modulated, one of the molecules that showed upregulation was Transketolase. This gene was chosen to be assessed in

infected flies (Figure 5.4-8), where adult females infected with Lg(LRV1+) did not modulate this gene significantly when compared with flies infected with Lg(LRV1-). Nevertheless, it is possible to see a slight increased expression of transketolase at 24h post infection in insects infected with Lg(LRV1+). This trend could reflect in part the modulation observed in the *in vitro* experiments, where TRANSK was found upregulated (Figure 5.4-2A), possibly by the presence of LRV1. It is difficult to assess to what extend this slight variation could favour Lg(LRV1+) to later stablish a more intense infection.

Altogether, results obtained from *L. longipalpis in vitro* and *in vivo* models after challenge with Lg(LRV1+) or Lg(LRV1-), suggest that the viral endosymbiont of *L. guyanensis* could be modulating several genes related to antiviral response and cell division that may bring an advantage in the insect, as observed in the increase in parasite load at late times of infection. To better understand the role of LRV1 in the establishment of *L. guyanensis* in *L. longipalpis* midgut, further studies are needed. Incrementing the number of *in vivo* infections analysed could strengthen the difference in gene expression to more significant values. Additionally, other molecules that were found to be modulated in LL5 cells should be evaluated next.

5.6 CONCLUSIONS

- LL5 cells challenged with *L. (V). guyanensis* LRV1+ modulated significantly immune molecules related to canonical pathways and non-specific antiviral response: relish, attacin, LCAT, TRANSK, RRM, WD40-2, SH3 and TYRK when compared to *L. (V). guyanensis* LRV1-

-*L.(v). guyanensis* LRV1+ established a stronger infection than *L. (V). guyanensis* LRV1- in *L. longipalpis* adult females.

-Presence of LRV1 in adult sand flies infected with *L. (V). guyanensis* downregulate significantly defensin 1 gene out of 16 immune genes assessed.

6 GENERAL CONCLUSIONS

-Exosomes from Poly(I:C) stimulated LL5 cells contain exclusive proteins that support the theory that the non-specific antiviral response previously discovered in these cells is INF-like type and exosomes may be part of this response mechanisms to protect neighbour cells from infection. This antiviral response involve new and different molecules that those reported for canonical innate immune pathways.

-The Toll pathway hold stronger regulation in adult sand flies avoiding activation of effector genes after silencing independently two of its known negative regulators, cactus and WntD and attempts to silence both genes simultaneously was unsuccessful. New mechanisms of autoregulation in Toll pathway in *L. longipalpis* or different roles of cactus as a regulator were proposed, yet they need further investigation.

-Presence of LRV1 in a *L.(V.) guyanensis* strain appears to favour parasite survival and establish a heavier infection in *L. longipalpis* midgut, without eliciting an important activation of any of the immune pathways evaluated. On the other hand, *L. (V.) guyanensis* strain with LRV1 downregulate molecules from canonical innate pathways and modulate some related to IFN- like antiviral response and cell division in LL5 linage, suggesting that the viral endosymbiont may also offer benefits for the parasite persistence not only in the mammalian host but also in the insect vector, with important consequences in disease transmission and public health.

7 REFERENCES

Adams MJ, Lefkowitz EJ, King AMQ, Carstens EB. Ratification vote on taxonomic proposals to the International Committee on Taxonomy of Viruses. Arch Virol. 2014 Oct 7;159(10):2831–41.

Agaisse H, Perrimon N, Agaisse H, Perrimon N. The roles of JAK/STAT signaling in Drosophila immune responses. Immunol Rev. 2004;198(1):72–82.

Aggarwal K, Silverman N. Positive and negative regulation of the Drosophila immune response. BMB Rep. 2008;41(4):267–77.

Agrawal N, Dasaradhi PVN, Mohmmed A, Malhotra P, Bhatnagar RK, Mukherjee SK. RNA Interference: Biology, Mechanism, and Applications. Microbiol Mol Biol Rev. 2003;67(4):657–85.

Akhoundi M, Kuhls K, Cannet A, Votýpka J, Marty P, Delaunay P, et al. A Historical Overview of the Classification, Evolution, and Dispersion of Leishmania Parasites and Sandflies. PLoS Negl Trop Dis. 2016;10(3):1–40.

Akira S, Kiyoshi T. Toll-like receptor signalling. Nat Rev Immunol. 2004;4(July).

Akira S, Uematsu S, Takeuchi O. Pathogen Recognition and Innate Immunity. Cell. 2006 Feb 24;124(4):783–801.

Alborzi A, Rasouli M, Shamsizadeh A. Leishmania tropica–isolated patient with visceral leishmaniasis in southern Iran. Am J Trop Med Hyg. 2006;74(2):306–7.

Alvar J, Vélez ID, Bern C, Herrero M, Desjeux P, Cano J, et al. Leishmaniasis worldwide and global estimates of its incidence. Vol. 7, PLoS ONE. 2012.

An C, Kanost MR. Manduca sexta serpin-5 regulates prophenoloxidase activation and the Toll signaling pathway by inhibiting hemolymph proteinase HP6. Insect Biochem Mol Biol. 2010;40(9):683–9.

Angelakis E, Raoult D. Pathogenicity and treatment of Bartonella infections. Int J Antimicrob Agents. 2014 Jul;44(1):16–25.

Arbouzova N, Zeidler M. JAK/STAT signalling in Drosophila: insights into conserved regulatory and cellular functions. Development. 2006;133(14):2605–16.

Arnot CJ, Gay NJ, Gangloff M. Insights into the molecular mechanism that induces activation of Spatzle, the ligand for the Drosophila Toll receptor. J Biol Chem. 2010;jbc-M109.

Aswad A, Katzourakis A. A novel viral lineage distantly related to herpesviruses discovered within

fish genome sequence data. Virus Evol. 2017 Jul 1;3(2).

Avadhanula V, Weasner BP, Hardy GG, Kumar JP, Hardy RW. A novel system for the launch of alphavirus RNA synthesis reveals a role for the Imd pathway in arthropod antiviral response. PLoS Pathog. 2009 Sep 18;5(9):e1000582.

Ayhan N, Charrel RN. Of phlebotomines (sandflies) and viruses: a comprehensive perspective on a complex situation. Curr Opin Insect Sci. 2017 Aug 1;22:117–24.

Azevedo-Brito DA. Investigação da resposta imune inata relacionada à via JAK-STAT em Lutzomyia longipalpis infectada com Leishmania infantum chagasi. Oswaldo Cruz Institute; Tese de mestrado. 2018.

Azzam KM, Fessler MB. Crosstalk between reverse cholesterol transport and innate immunity. Trends Endocrinol Metab. 2012;23(4):169–77.

Barbalat R, Ewald SE, Mouchess ML, Barton GM. Nucleic Acid Recognition by the Innate Immune System. Annu Rev Immunol. 2011 Apr 23;29(1):185–214.

Barillas-Mury C, Han Y-S, Seeley D, Kafatos FC. Anopheles gambiae Ag-STAT, a new insect member of the STAT family, is activated in response to bacterial infection. Vol. 18, The EMBO Journal. 1999.

Bartholome O, Van den Ackerveken P, Sánchez Gil J, de la Brassinne Bonardeaux O, Leprince P, Franzen R, et al. Puzzling Out Synaptic Vesicle 2 Family Members Functions. Front Mol Neurosci. 2017;10(May):1–15.

Basak S, Mondal A, Polley S, Mukhopadhyay S, Chattopadhyay D. Reviewing Chandipura: a vesiculovirus in human epidemics. Biosci Rep. 2007 Oct 6;27(4–5):275–98.

Bauzer LG, Souza NA, Maingon RD, Peixoto AA. Lutzomyia longipalpis in Brazil: a complex or a single species? A mini-review. Mem Inst Oswaldo Cruz. 2007 Feb;102(1):1–12.

Berger H, Wodarz A, Borchers A. PTK7 Faces the Wnt in Development and Disease. Front Cell Dev Biol. 2017 Apr 5;5:31.

Bergmann A, Stein D, Geisler R, Hagenmaier S, Schmid B, Fernandez N, et al. A gradient of cytoplasmic Cactus degradation establishes the nuclear localization gradient of the dorsal morphogen in Drosophila. Mech Dev. 1996 Nov 1;60(1):109–23.

Bharathi V, Pallavi SK, Bajpai R, Emerald BS, Shashidhara LS. Genetic characterization of the Drosophila homologue of coronin. J Cell Sci. 2004 Apr 15;117(Pt 10):1911–22.

Blanc G, Gallot-Lavallée L, Maumus F. Provirophages in the Bigelowiella genome bear testimony to past encounters with giant viruses. Proc Natl Acad Sci U S A. 2015 Sep 22;112(38):E5318-26.

Bocock JP, Carmicle S, Sircar M, Erickson AH. Trafficking and proteolytic processing of RNF13, a model PA-TM-RING family endosomal membrane ubiquitin ligase. FEBS J. 2011 Jan;278(1):69–77.

Booth K, Cambron L, Fisher N, Greenlee KJ. Immune Defense Varies within an Instar in the Tobacco Hornworm, Manduca sexta. Physiol Biochem Zool. 2015 Mar;88(2):226–36.

Boulanger N, Lowenberger C, Volf P, Ursic R, Sigutova L, Sabatier L, et al. Characterization of a Defensin from the Sand Fly Phlebotomus duboscqi Induced by Challenge with Bacteria or the Protozoan Parasite Leishmania major. Infect Immun. 2004;72(12):7140–6.

Boutros M, Agaisse H, Perrimon N. Sequential activation of signaling pathways during innate immune responses in Drosophila. Dev Cell. 2002;3(5):711–22.

Breitschwerdt EB. Bartonellosis, One Health and all creatures great and small. Vet Dermatol. 2017;28(1):96-e21.

Brettmann EA, Shaik JS, Zangger H, Lye L-F, Kuhlmann FM, Akopyants NS, et al. Tilting the balance between RNA interference and replication eradicates Leishmania RNA virus 1 and mitigates the inflammatory response. Proc Natl Acad Sci U S A. 2016 Oct 25;113(43):11998–2005.

Brown KL, Hancock RE. Cationic host defense (antimicrobial) peptides. Curr Opin Immunol. 2006;18:24–30.

Bryceson ADM. Diffuse cutaneous leishmaniasis in Ethiopia I. The clinical and histological features of the disease. Trans R Soc Trop Med Hyg. 1969 Jan 1;63(6):708–37.

Bulet P, Stocklin R. Insect Antimicrobial Peptides: Structures, Properties and Gene Regulation. Protein Pept Lett. 2005 Jan 1;12(1):3–11.

Bulet P, Stöcklin R, Menin L. Anti-microbial peptides: from invertebrates to vertebrates. Immunol Rev. 2004 Apr;198:169–84.

Caddy J, Wilanowski T, Darido C, Dworkin S, Ting SB, Zhao Q, et al. Epidermal wound repair is regulated by the planar cell polarity signaling pathway. Dev Cell. 2010;19(1):138–47.

Calderwood SK. Cdc37 as a Co-chaperone to Hsp90. In: Sub-cellular biochemistry. 2015. p. 103–12.

Campbell CL, Keene KM, Brackney DE, Olson KE, Blair CD, Wilusz J, et al. Aedes aegypti uses RNA interference in defense against Sindbis virus infection. BMC Microbiol. 2008 Mar 17;8(1):47.

Camuset G, Remy V, Hansmann Y, Christmann D, Gomes de Albuquerque C, Sena Casseb G-A. Leishmaniose cutanéomuqueuse en Amazonie brésilienne. Médecine Mal Infect. 2007 Jun

1;37(6):343–6.

Cardoso MA, Fontenele M, Lim B, Bisch PM, Shvartsman SY, Araujo HM. A novel function for the IκB inhibitor Cactus in promoting Dorsal nuclear localization and activity in the Drosophila embryo. Co Biol. 2017;144:2907–13.

Cascante M, Centelles JJ, Veech RL, Lee W-NP, Boros L. Role of Thiamin (Vitamin B-1) and Transketolase in Tumor Cell Proliferation. Nutr Cancer. 2000;36(2):150–4.

Castillo JC, Robertson AE, Strand MR. Characterization of hemocytes from the mosquitoes Anopheles gambiae and Aedes aegypti. Insect Biochem Mol Biol. 2006 Dec 1;36(12):891–903.

Castrillo A, Joseph SB, Vaidya SA, Haberland M, Fogelman AM, Cheng G, et al. Crosstalk between LXR and Toll-like Receptor Signaling Mediates Bacterial and Viral Antagonism of Cholesterol Metabolism. Mol Cell. 2003 Oct 1;12(4):805–16.

Cattaruzza M, Schä Fer § K, Hecker M. Cytokine-induced Down-regulation of zfm1/Splicing Factor-1 Promotes Smooth Muscle Cell Proliferation. J Biol Chem. 2001;277(8):6582–9.

Chen D-YY, Husain M. Caspase-mediated degradation of host cortactin that promotes influenza A virus infection in epithelial cells. Virology. 2016 Oct 1;497:146–56.

Chen W, White MA, Cobb MH. Stimulus-specific requirements for MAP3 kinases in activating the JNK pathway Downloaded from. J Biol Chem. 2002;6.

Chiu H, Ring BC, Sorrentino RP, Kalamarz M, Garza D, Govind S. dUbc9 negatively regulates the Toll-NF-κB pathways in larval hematopoiesis and drosomycin activation in Drosophila. Dev Biol. 2005 Dec 1;288(1):60–72.

Choudhary S, Lee H-C, Maiti M, He Q, Cheng P, Liu Q, et al. A Double-Stranded-RNA Response Program Important for RNA Interference Efficiency. Mol Cell Biol. 2007;27(11):3995–4005.

Christensen BM, Li J, Chen C-C, Nappi AJ. Melanization immune responses in mosquito vectors. Trends Parasitol. 2005 Apr 1;21(4):192–9.

Christophides GK, Vlachou D, Kafatos FC. Comparative and functional genomics of the innate immune system in the malaria vector Anopheles gambiae. Immunol Rev. 2004 Apr;198(1):127–48.

Cogswell PC, Scheinman RI, Baldwin AS. Promoter of the human NF-kappa B p50/p105 gene. Regulation by NF-kappa B subunits and by c-REL. J Immunol. 1993;150(7):2794–804.

Cook S, Chung BY-W, Bass D, Moureau G, Tang S, McAlister E, et al. Novel Virus Discovery and Genome Reconstruction from Field RNA Samples Reveals Highly Divergent Viruses in Dipteran Hosts. Attoui H, editor. PLoS One. 2013 Nov 18;8(11):e80720.

Costa A, Jan E, Sarnow P, Schneider D. The Imd Pathway Is Involved in Antiviral Immune Responses in Drosophila. Sommer P, editor. PLoS One. 2009 Oct 15;4(10):e7436.

Cupolillo E, Medina-Acosta E, Noyes H, Momen H, Grimaldi G. A revised classification for Leishmania and Endotrypanum. Parasitol today. 2000;16(4):142–4.

Deddouche S, Matt N, Budd A, Mueller S, Kemp C, Galiana-Arnoux D, et al. The DExD/H-box helicase Dicer-2 mediates the induction of antiviral activity in drosophila. Nat Immunol. 2008;9(12):1425–32.

DeLotto Y, DeLotto R. Proteolytic processing of the Drosophila Spätzle protein by Easter generates a dimeric NGF-like molecule with ventralising activity. Mech Dev. 1998 Mar 1;72(1–2):141–8.

Depaquit J, Grandadam M, Fouque F, Andry P, Peyrefitte C. Arthropod-borne viruses transmitted by Phlebotomine sandflies in Europe: a review. Eurosurveillance. 2010 Mar 11;15(10):19507.

Desjeux P. Leishmaniasis: current situation and new perspectives. Comp Immunol Microbiol Infect Dis. 2004 Sep 1;27(5):305–18.

Detrait E, Maurice T, Hanon E, Leclercq K, Lamberty Y. Lack of synaptic vesicle protein SV2B protects against amyloid-β25–35-induced oxidative stress, cholinergic deficit and cognitive impairment in mice. Behav Brain Res. 2014 Sep 1;271:277–85.

Dillon RJ, Ivens AC, Churcher C, Holroyd N, Quail MA, Rogers ME, et al. Analysis of ESTs from Lutzomyia longipalpis sand flies and their contribution toward understanding the insect–parasite relationship. Genomics. 2006 Dec 1;88(6):831–40.

Dimopoulos G. Insect immunity and its implication in mosquito-malaria interactions. Cell Microbiol. 2003 Jan 1;5(1):3–14.

Döflein F. Die Protozoen als Parasiten und Krankheitserreger nach biologischen Gesichtspunkten dargestellt. Fischer; 1901.

Dong Y, Das S, Cirimotich C, Souza-Neto JA, McLean KJ, Dimopoulos G. Engineered Anopheles Immunity to Plasmodium Infection. Vernick KD, editor. PLoS Pathog. 2011 Dec 22;7(12):e1002458.

Dostert C, Jouanguy E, Irving P, Troxler L, Galiana-Arnoux D, Hetru C, et al. The Jak-STAT signaling pathway is required but not sufficient for the antiviral response of drosophila. Nat Immunol. 2005;6(9):946–53.

Dujardin J, Torrez ME, Pont F L, Hervas D, Sossa D. Isozymic and metric variation in the Lutzomyia longipalpis complex. Med Vet Entomol. 2008 Jun 28;11(4):394–400.

Dunn NR, Tolwinski NS. Ptk7 and Mcc, unfancied components in non-canonical Wnt signaling

and cancer. Cancers (Basel). 2016;8(7).

Dvorak V, Shaw J, Volf P. Parasite Biology: The Vectors. In: The Leishmaniases: Old Neglected Tropical Diseases. Springer; 2018. p. 31–77.

Ekengren S, Hultmark D. Drosophila cecropin as an antifungal agent. Insect Biochem Mol Biol. 1999 Nov 1;29(11):965–72.

Engel E, Viargues P, Mortier M, Taillebourg E, Couté Y, Thevenon D, et al. Identifying USPs regulating immune signals in Drosophila: USP2 deubiquitinates Imd and promotes its degradation by interacting with the proteasome. Cell Commun Signal. 2014;12(1):41.

Engel P, Moran NA. The gut microbiota of insects - diversity in structure and function. FEMS Microbiol Rev. 2013 Sep 1;37(5):699–735.

Eren RO, Reverte M, Rossi M, Hartley M-AA, Castiglioni P, Prevel F, et al. Mammalian Innate Immune Response to a Leishmania-Resident RNA Virus Increases Macrophage Survival to Promote Parasite Persistence. Cell Host Microbe. 2016 Sep 14;20(3):318–28.

Esch KJ, Petersen CA. Transmission and epidemiology of zoonotic protozoal diseases of companion animals. Clin Microbiol Rev. 2013 Jan;26(1):58–85.

Fermin G, Mazumdar-Leighton S, Tennant P. Chapter 9 - Viruses of Prokaryotes, Protozoa, Fungi, and Chromista. In: Tennant P, Fermin G, Foster JEBT-V, editors. Viruses. Academic Press; 2018. p. 217–44.

Fernandez NQ, Grosshans J, Goltz JS, Stein D. Separable and redundant regulatory determinants in Cactus mediate its dorsal group dependent degradation. Development. 2001;128(15):2963–74.

Ferrandon D, Imler JL, Hetru C, Hoffmann JA. The Drosophila systemic immune response: Sensing and signalling during bacterial and fungal infections. Nat Rev Immunol. 2007;7(11):862–74.

Flenniken ML, Andino R. Non-Specific dsRNA-Mediated Antiviral Response in the Honey Bee. PLoS One. 2013;8(10):1–16.

Fontenele M, Carneiro K, Agrellos R, Oliveira D, Oliveira-Silva A, Vieira V, et al. The Ca2+-dependent protease Calpain A regulates Cactus/IκB levels during Drosophila development in response to maternal Dpp signals. Mech Dev. 2009 Aug 1;126(8–9):737–51.

Fontenele M, Lim B, Oliveira D, Buffolo M, Perlman DH, Schupbach T, et al. Calpain A modulates Toll responses by limited Cactus/IκB proteolysis. 2013;

Forterre P. Defining Life: The Virus Viewpoint. Orig Life Evol Biosph. 2010 Apr 3;40(2):151–60.

Fragkoudis R, Chi Y, Siu RWC, Barry G, Attarzadeh-Yazdi G, Merits A, et al. Semliki Forest virus

strongly reduces mosquito host defence signaling. Insect Mol Biol. 2008;17(6):647–56.

França C, Parrot L. Essai de classification des Phlebotomes. Arch Inst Pasteur Afr Nord. 1921;1:279–84.

Fros JJ, Liu WJ, Prow NA, Geertsema C, Ligtenberg M, Vanlandingham DL, et al. Chikungunya Virus Nonstructural Protein 2 Inhibits Type I/II Interferon-Stimulated JAK-STAT Signaling †. J Virol. 2010;84(20):10877–87.

Fullaondo A, Lee SY. Regulation of Drosophila-virus interaction. Dev Comp Immunol. 2012;36(2):262–6.

Gaidamovich SI, Obukhova VR, Sveshnikova NA, Cherednichenko IN, Kostiukov MA. Natural foci of viruses borne by Phlebotomus papatasi in the USSR according to a serologic study of the population. Vopr Virusol. 1978;(5):556–60.

Galati EAB. Classificação, morfologia, terminologia e identificação de Adultos: Bioecologia e Identificação de Phlebotominae. Flebotomíneos do Bras FIOCRUZ, Río. 2014;367.

Galati EAB, Rangel EF, Lainson R. Flebotomíneos do Brasil. Rangel EF, Lainson R Morfol e Taxon Rio Janeiro Fiocruz. 2003;23–51.

Gangloff M, Murali A, Xiong J, Arnot CJ, Weber AN, Sandercock AM, et al. Structural insight into the mechanism of activation of the Toll receptor by the dimeric ligand Spatzle. J Biol Chem. 2008;

Ganguly A, Jiang J, Ip YT. Drosophila WntD is a target and an inhibitor of the Dorsal/Twist/Snail network in the gastrulating embryo. Development. 2005;132(15):3419–29.

Garver LS, Bahia AC, Das S, Souza-Neto JA, Shiao J, Dong Y, et al. Anopheles Imd Pathway Factors and Effectors in Infection Intensity-Dependent Anti-Plasmodium Action. Schneider DS, editor. PLoS Pathog. 2012 Jun 7;8(6):e1002737.

Georgel P, Naitza S, Kappler C, Ferrandon D, Zachary D, Swimmer C, et al. Drosophila Immune Deficiency (IMD) Is a Death Domain Protein that Activates Antibacterial Defense and Can Promote Apoptosis. Dev Cell. 2001 Oct 1;1(4):503–14.

Goihman-Yahr M. American mucocutaneous leishmaniasis. Dermatol Clin. 1994;12(4):703–12.

Gordon MD, Ayres JS, Schneider DS, Nusse R. Pathogenesis of Listeria-Infected Drosophila wntD Mutants Is Associated with Elevated Levels of the Novel Immunity Gene edin. Ausubel FM, editor. PLoS Pathog. 2008 Jul 25;4(7):e1000111.

Gordon MD, Dionne MS, Schneider DS, Nusse R. WntD is a feedback inhibitor of Dorsal/NF-kappaB in Drosophila development and immunity. Nature. 2005;437(7059):746–9.

Goto H, Lindoso JAL. Current diagnosis and treatment of cutaneous and mucocutaneous

leishmaniasis. Expert Rev Anti Infect Ther. 2010 Apr 10;8(4):419–33.

Gouveia C, Asensi MD, Zahner V, Rangel EF, Oliveira SMP de. Study on the bacterial midgut microbiota associated to different Brazilian populations of Lutzomyia longipalpis (Lutz & Neiva) (Diptera: Psychodidae). Neotrop Entomol. 2008 Oct;37(5):597–601.

Green TJ, Montagnani C. Poly I:C induces a protective antiviral immune response in the Pacific oyster (Crassostrea gigas) against subsequent challenge with Ostreid herpesvirus (OsHV-1 μvar). Fish Shellfish Immunol. 2013;35(2):382–8.

De Gregorio E, Spellman PT, Tzou P, Rubin GM, Lemaitre B. The Toll and Imd pathways are the major regulators of the immune response in Drosophila. EMBO J. 2002 Jun 3;21(11):2568–79.

Grybchuk D, Akopyants NS, Kostygov AY, Konovalovas A, Lye L-F, Dobson DE, et al. Viral discovery and diversity in trypanosomatid protozoa with a focus on relatives of the human parasite Leishmania. Proc Natl Acad Sci. 2018a Jan 16;115(3):E506–15.

Grybchuk D, Kostygov AY, Macedo DH, D'Avila-Levy CM, Yurchenko V, Grybchuk D, et al. RNA viruses in trypanosomatid parasites: a historical overview. Mem Inst Oswaldo Cruz. 2018b Feb 19;113(4).

Guilbride L, Myler P, Stuart K. Distribution and sequence divergence of LRV1 viruses among different Leishmania species. Mol Biochem Parasitol. 1992;54(1):101–4.

Handler MZ, Patel PA, Kapila R, Al-Qubati Y, Schwartz RA. Cutaneous and mucocutaneous leishmaniasis: Clinical perspectives. J Am Acad Dermatol. 2015;73(6):897–908.

Hannink M, Temin HM. Structure and autoregulation of the c-rel promoter. Oncogene. 1990;5(12):1843–50.

Hartley M-A, Ronet C, Zangger H, Beverley SM, Fasel N. Leishmania RNA virus: when the host pays the toll. Front Cell Infect Microbiol. 2012 Jul 12;2:99.

Hartley MA, Drexler S, Ronet C, Beverley SM, Fasel N. The immunological, environmental, and phylogenetic perpetrators of metastatic leishmaniasis. Trends Parasitol. 2014;30(8):412–22.

Hartman ZC, Kiang A, Everett RS, Serra D, Yang XY, Clay TM, et al. Adenovirus infection triggers a rapid, MyD88-regulated transcriptome response critical to acute-phase and adaptive immune responses in vivo. J Virol. 2007 Feb 15;81(4):1796–812.

Hedengren M, Borge K, Hultmark D. Expression and Evolution of the Drosophila Attacin/Diptericin Gene Family. Biochem Biophys Res Commun. 2000 Dec 20;279(2):574–81.

Hedges LM, Johnson KN. Induction of host defence responses by Drosophila C virus. J Gen Virol.

2008;89(6):1497–501.

Heerman M, Weng J-L, Hurwitz I, Durvasula R, Ramalho-Ortigao M. Bacterial Infection and Immune Responses in Lutzomyia longipalpis Sand Fly Larvae Midgut. Acosta-Serrano A, editor. PLoS Negl Trop Dis. 2015 Jul 8;9(7):e0003923.

Hertel L, Mocarski ES. Global analysis of host cell gene expression late during cytomegalovirus infection reveals extensive dysregulation of cell cycle gene expression and induction of Pseudomitosis independent of US28 function. J Virol. 2004;78(21):11988–2011.

Hillyer JF. Insect immunology and hematopoiesis. Dev Comp Immunol. 2016 May 1;58:102–18.

Hoffmann JA. The immune response of Drosophila. Nature. 2003 Nov 6;426(6962):33–8.

Horng T, Medzhitov R. Drosophila MyD88 is an adapter in the Toll signaling pathway. Proc Natl Acad Sci. 2001;98(22):12654–8.

Huang Z, Kingsolver MB, Avadhanula V, Hardy RW. An antiviral role for antimicrobial peptides during the arthropod response to alphavirus replication. J Virol. 2013 Apr;87(8):4272–80.

Hultmark D, Engstrom' A, Andersson K, Steiner H, Bennich1 H, Boman HG. Insect immunity. Attacins, a family of antibacterial proteins from Hyalophora cecropia. Vol. 2, The EMBO Journal. 1983.

Husain M, Cheung C-Y. Histone deacetylase 6 inhibits influenza A virus release by downregulating the trafficking of viral components to the plasma membrane via its substrate, acetylated microtubules. J Virol. 2014 Oct 16;88(19):11229–39.

Hussain M, Walker T, O'Neill SL, Asgari S. Blood meal induced microRNA regulates development and immune associated genes in the Dengue mosquito vector, Aedes aegypti. Insect Biochem Mol Biol. 2013 Feb 1;43(2):146–52.

Husseneder C, Park J-S, Howells A, Tikhe C V., Davis JA. Bacteria Associated With Piezodorus guildinii (Hemiptera: Pentatomidae), With Special Reference to Those Transmitted by Feeding. Environ Entomol. 2016 Dec 26;46(1):nvw112.

Isawa H, Kuwata R, Hoshino K, Tsuda Y, Sakai K, Watanabe S, et al. Identification and molecular characterization of a new nonsegmented double-stranded RNA virus isolated from Culex mosquitoes in Japan. Virus Res. 2011 Jan 1;155(1):147–55.

Ives A, Ronet C, Prevel F, Ruzzante G, Fuertes-marraco S, Schutz F, et al. Leishmania RNA Virus Controls the Severity of Mucocutaneous Leishmaniasis. Science (80-). 2011;331(11):775–8.

Ji S, Sun M, Zheng X, Li L, Sun L, Chen D, et al. Cell-surface localization of Pellino antagonizes Toll-mediated innate immune signalling by controlling MyD88 turnover in Drosophila. Nat Commun. 2014 Dec 17;5(1):3458.

Jiang R, Kim E-H, Gong J-H, Kwon H-M, Kim C-H, Ryu K-H, et al. Three pairs of protease-serpin complexes cooperatively regulate the insect innate immune responses. J Biol Chem. 2009;284(51):35652–8.

Jiravanichpaisal P, Lee BL, Söderhäll K. Cell-mediated immunity in arthropods: Hematopoiesis, coagulation, melanization and opsonization. Immunobiology. 2006 Jun 2;211(4):213–36.

Jirků M, Yurchenko VY, Lukeš J, Maslov DA. New Species of Insect Trypanosomatids from Costa Rica and the Proposal for a New Subfamily within the Trypanosomatidae. J Eukaryot Microbiol. 2012;59(6):537–47.

Jochim RC, Teixeira CR, Laughinghouse A, Mu J, Oliveira F, Gomes RB, et al. The midgut transcriptome of Lutzomyia longipalpis: comparative analysis of cDNA libraries from sugar-fed, blood-fed, post-digested and Leishmania infantum chagasi-infected sand flies. BMC Genomics. 2008 Jan 14;9(1):15.

Jupatanakul N, Dimopoulos G. Molecular interactions between arboviruses and insect vectors: insects' immune responses to virus infection. In: Vasilakis, Nikos; Gubler D, editor. Arboviruses. Norfolk, UK: Caister Academic Press; 2016. p. 107.

Kabakov AE, Budagova KR, Latchman DS, Kampinga HH. Stressful preconditioning and HSP70 overexpression attenuate proteotoxicity of cellular ATP depletion. Am J Physiol Physiol. 2002 Aug;283(2):C521–34.

Kang D, Gopalkrishnan R V, Wu Q, Jankowsky E, Pyle AM, Fisher PB. mda-5: An interferon-inducible putative RNA helicase with double-stranded RNA-dependent ATPase activity and melanoma growth-suppressive properties. Proc Natl Acad Sci U S A. 2002 Jan 22;99(2):637–42.

Keita S, Masuzzo A, Royet J, Kurz CL. Drosophila larvae food intake cessation following exposure to Erwinia contaminated media requires odor perception, Trpa1 channel and evf virulence factor. J Insect Physiol. 2017 May 1;99:25–32.

Kelly PH, Bahr SM, Serafim TD, Ajami NJ, Petrosino JF, Meneses C, et al. The Gut Microbiome of the Vector Lutzomyia longipalpis Is Essential for Survival of Leishmania infantum. 2017;

Kenney SP, Meng X-J. An SH3 binding motif within the nucleocapsid protein of porcine reproductive and respiratory syndrome virus interacts with the host cellular signaling proteins STAMI, TXK, Fyn, Hck, and cortactin. Virus Res. 2015;204:31–9.

Killick-Kendrick R. The biology of Leishmainia in Phlebotomine sandflies. In: Lumsden W, Evans D, editors. In Biology of the Kinetoplastida. London: Academic Press, London/New York; 1979. p. 395–460.

Killick-Kendrick R, Lainson R, Rioux J-A, Sar'janova VM. The taxonomy of Leishmania-like parasites of reptiles. 1986;

Kim M, Hee Lee J, Young Lee S, Kim E, Chung J. Caspar, a suppressor of antibacterial immunity in Drosophila. PNAS. 2006;103(44):16358–63.

King AMQ, Adams MJ, Carstens EB, Lefkowitz EJBT-VT, editors. Family - Totiviridae. In: Virus Taxonomy Ninth Report of the International Committee on Taxonomy of Viruses Classification and Nomenclature of Viruses. San Diego: Elsevier; 2012. p. 639–50.

Kingsolver MB, Huang Z, Hardy RW. Insect antiviral innate immunity: Pathways, effectors, and connections. J Mol Biol. 2013;425(24):4921–36.

Kirkbride KC, Sung BH, Sinha S, Weaver AM. Cortactin: a multifunctional regulator of cellular invasiveness. Cell Adh Migr. 2011;5(2):187–98.

Kleino A, Valanne S, Ulvila J, Kallio J, Myllymä Ki H, Enwald H, et al. Inhibitor of apoptosis 2 and TAK1-binding protein are components of the Drosophila Imd pathway. EMBO J. 2005;24:3423–34.

Kobe B, Kajava A V. The leucine-rich repeat as a protein recognition motif. Curr Opin Struct Biol. 2001 Dec 1;11(6):725–32.

Kochetov GA, Solovjeva ON. Structure and functioning mechanism of transketolase. Biochim Biophys Acta - Proteins Proteomics. 2014;1844(9):1608–18.

Kounatidis I, Ligoxygakis P. Drosophila as a model system to unravel the layers of innate immunity to infection. Open Biol. 2012;2(5):120075–120075.

Kubota K, Gay NJ. The dorsal protein enhances the biosynthesis and stability of the Drosophila IkB homologue cactus. Nucleic Acids Res. 1995 Aug 25;23(16):3111–8.

Kumar A, Srivastava P, Sirisena P, Dubey SK, Kumar R, Shrinet J, et al. Mosquito Innate Immunity. Insects. 2018;9(95).

Kuttenkeuler D, Pelte N, Ragab A, Gesellchen V, Schneider L, Blass C, et al. A Large-Scale RNAi Screen Identifies Deaf1 as a Regulator of Innate Immune Responses in Drosophila. J Innate Immun. 2010;2:181–94.

Labourier E, Allemand E, Brand S, Fostier M, Tazi J, Bourbon H-M. Recognition of exonic splicing enhancer sequences by the Drosophila splicing repressor RSF1. Nucleic Acids Res. 1999a;27(11).

Labourier E, Bourbon HM, Gallouzi IE, Fostier M, Allemand E, Tazi J. Antagonism between RSF1 and SR proteins for both splice-site recognition in vitro and Drosophila development. Genes Dev. 1999b;13(6):740–53.

Lainson R, Shaw JJ, Ryan L, Ribeiro RSM, Silveira FT. Leishmaniasis in Brazil. XXI. Visceral leishmaniasis in the Amazon Region and further observations on the role of Lutzomyia longipalpis (Lutz & Neiva, 1912) as the vector. Trans R Soc Trop Med Hyg. 1985 Jan 1;79(2):223–6.

Lainson R, Ward RD, Shaw JJ. Experimental transmission of leishmania chagasi, causative agent of neotropical visceral leishmaniasis, by the sandfly lutzomyia longipalpis [18]. Nature. 1977a;266(5603):628–30.

Lainson R, Ward RD, Shaw JJ. Leishmania in phlebotomid sandflies: VI. Importance of hindgut development in distinguishing between parasites of the Leishmania mexicana and L. braziliensis complexes. Proc R Soc London Ser B, Biol Sci. 1977b Nov 14;199(1135):309–20.

Lamiable O, Kellenberger C, Kemp C, Troxler L, Pelte N, Boutros M, et al. Cytokine Diedel and a viral homologue suppress the IMD pathway in Drosophila. Proc Natl Acad Sci. 2016a;113(3):201516122.

Lamiable O, Meignin C, Imler J-L. WntD and Diedel: Two immunomodulatory cytokines in Drosophila immunity. Fly (Austin). 2016b;10(4):187–94.

Lander R, Petersen CP. Wnt, Ptk7, and FGFRL expression gradients control trunk positional identity in planarian regeneration. Elife. 2016;5:e12850.

Lane RP. Sandflies (Phlebotominae). In: Lane RP, Crosskey R., editors. Medical Insects and Arachnids. Dordrecht: Springer Netherlands; 1993. p. 78–119.

Lanot R, Zachary D, Holder F, Meister M. Postembryonic hematopoiesis in Drosophila. Dev Biol. 2001;230(2):243–57.

Lanzaro GC, Ostrovska K, Herrero M V., Lawyer PG, Warburg A. Lutzomyia longipalpis is a species complex: Genetic divergence and interspecific hybrid sterility among three populations. Am J Trop Med Hyg. 1993;48(6):839–47.

Lee MN, Roy M, Ong S-E, Mertins P, Villani A-C, Li W, et al. Identification of regulators of the innate immune response to cytosolic DNA and retroviral infection by an integrative approach. Nat Immunol. 2013 Feb 23;14(2):179–85.

Van der Lee R, Feng Q, Langereis MA, ter Horst R, Szklarczyk R, Netea MG, et al. Integrative Genomics-Based Discovery of Novel Regulators of the Innate Antiviral Response. Peters B, editor. PLOS Comput Biol. 2015 Oct 20;11(10):e1004553.

Lella F Di, Vincenti V, Zennaro D, Afeltra A, Baldi A, Giordano D, et al. Case Report Oral Medicine Mucocutaneous leishmaniasis: report of a case with massive involvement of nasal,

pharyngeal and laryngeal mucosa. J Oral Maxillofac Surg. 2006;35:870–2.

Lemaitre B, Hoffmann J. The Host Defense of Drosophila melanogaster. Annu Rev Immunol. 2007;25:697–743.

Lemaitre B, Meister M, Govind S, Georgel P, Steward R, Reichhart J-M, et al. Functional analysis and regulation of nuclear import of dorsal during the immune response in Drosophila. EMBO J. 1995;14(3):536–45.

Lemaitre B, Nicolas E, Michaut L, Reichhart J-M, Hoffmann JA. The Dorsoventral Regulatory Gene Cassette spätzle/Toll/cactus Controls the Potent Antifungal Response in Drosophila Adults. Cell. 1996 Sep 20;86(6):973–83.

Letchworth GJ, Rodriguez LL, Del CBarrera J. Vesicular Stomatitis. Vet J. 1999 May 1;157(3):239–60.

Leulier F, Rodriguez A, Khush RS, Abrams JM, Lemaitre B. The Drosophila caspase Dredd is required to resist Gram-negative bacterial infection. Vol. 1, EMBO Reports. 2000.

Li C-X, Shi M, Tian J-H, Lin X-D, Kang Y-J, Chen L-J, et al. Unprecedented genomic diversity of RNA viruses in arthropods reveals the ancestry of negative-sense RNA viruses. Elife. 2015;4:e05378.

Li C, Chen Y-X, Zhang S, Lü L, Chen Y-H, Chai J, et al. Identification, Characterization, and Function Analysis of the Cactus Gene from Litopenaeus vannamei. Meijler MM, editor. PLoS One. 2012 Nov 21;7(11):e49711.

Li Y, Shin D, Kwon SH. Histone deacetylase 6 plays a role as a distinct regulator of diverse cellular processes. FEBS J. 2013;280(3):775–93.

Lin R-J, Liao C-L, Lin E, Lin Y-L. Blocking of the Alpha Interferon-Induced Jak-Stat Signaling Pathway by Japanese Encephalitis Virus Infection. J Virol. 2004;78(17):9285–94.

Liu X, Gao Y, Lin X, Li L, Han X, Liu J. The Coronin Family and Human Disease. Curr Protein Pept Sci. 2016;17:603–11.

Løvoll M, Wiik-Nielsen J, Grove S, Wiik-Nielsen CR, Kristoffersen AB, Faller R, et al. A novel totivirus and piscine reovirus (PRV) in Atlantic salmon (Salmo salar) with cardiomyopathy syndrome (CMS). Virol J. 2010 Nov 10;7(1):309.

Lu X, Borchers AGM, Jolicoeur C, Rayburn H, Baker JC, Tessier-Lavigne M. PTK7/CCK-4 is a novel regulator of planar cell polarity in vertebrates. Nature. 2004;430(6995):93.

Lu Y, Wu LP, Anderson K V. The antibacterial arm of the Drosophila innate immune response requires an IB kinase. Genes Dev. 2001;15:104–10.

Lukeš J, Skalický T, Týč J, Votýpka J, Yurchenko V. Evolution of parasitism in kinetoplastid

flagellates. Mol Biochem Parasitol. 2014 Jul 1;195(2):115–22.

Luplertlop N, Surasombatpattana P, Patramool S, Dumas E, Wasinpiyamongkol L, Saune L, et al. Induction of a Peptide with Activity against a Broad Spectrum of Pathogens in the Aedes aegypti Salivary Gland, following Infection with Dengue Virus. Diamond MS, editor. PLoS Pathog. 2011 Jan 13;7(1):e1001252.

Lutz A, Neiva A. Contribution to the recognition of the species of the genus Phlebotomus in Brazil. Mem Inst Oswaldo Cruz. 1912;4(1):84–95.

Lye L-F, Owens K, Shi H, Murta SMF, Vieira AC, Turco SJ, et al. Retention and Loss of RNA Interference Pathways in Trypanosomatid Protozoans. Ullman B, editor. PLoS Pathog. 2010 Oct 28;6(10):e1001161.

MacGrath SM, Koleske AJ. Cortactin in cell migration and cancer at a glance. J Cell Sci. 2012;125(7):1621–6.

Maguiña C, Gotuzzo E. Bartonellosis: New and Old. Infect Dis Clin North Am. 2000 Mar 1;14(1):1–22.

Maguiña C, Guerra H, Ventosilla P. Bartonellosis. Clin Dermatol. 2009 May 1;27(3):271–80.

Maroli M, Feliciangeli MD, Bichaud L, Charrel RN, Gradoni L. Phlebotomine sandflies and the spreading of leishmaniases and other diseases of public health concern. Med Vet Entomol. 2013 Jun;27(2):123–47.

Márquez LM, Roossinck MJ. Do persistent RNA viruses fit the trade-off hypothesis of virulence evolution? Curr Opin Virol. 2012 Oct 1;2(5):556–60.

Martins-da-Silva A, Telleria EL, Batista M, Marchini FK, Traub-Csekö YM, Tempone AJ. Identification of secreted proteins involved in nonspecific dsRNA-mediated Lutzomyia longipalpis LL5 cell antiviral response. Viruses. 2018;10(1):1–17.

Maslov DA, Votýpka J, Yurchenko V, Lukeš J. Diversity and phylogeny of insect trypanosomatids: all that is hidden shall be revealed. Trends Parasitol. 2013 Jan 1;29(1):43–52.

Maumus F, Blanc G. Study of Gene Trafficking between Acanthamoeba and Giant Viruses Suggests an Undiscovered Family of Amoeba-Infecting Viruses. Genome Biol Evol. 2016 Nov 1;8(11):3351–63.

Meekins DA, Kanost MR, Michel K. Serpins in arthropod biology. In: Seminars in cell & developmental biology. Elsevier; 2017. p. 105–19.

Meister S, Kanzok SM, Zheng X, Luna C, Li T-R, Hoa NT, et al. Immune signaling pathways regulating bacterial and malaria parasite infection of the mosquito Anopheles gambiae. PNAS. 2005;102(32):11420–5.

Merkling SH, van Rij RP. Beyond RNAi: Antiviral defense strategies in Drosophila and mosquito. J Insect Physiol. 2013;59(2):159–70.

Minnick MF, Anderson BE, Lima A, Battisti JM, Lawyer PG, Birtles RJ. Oroya Fever and Verruga Peruana: Bartonelloses Unique to South America. Vinetz JM, editor. PLoS Negl Trop Dis. 2014 Jul 17;8(7):e2919.

Moncrieffe MC, Grossmann JG, Gay NJ. Assembly of oligomeric death domain complexes during Toll receptor signaling. J Biol Chem. 2008;283(48):33447–54.

Moore AJ, Beazley WD, Bibby MC, Devine DA. Antimicrobial activity of cecropins. Vol. 37, Journal of Antimicrobial Chemotherapy. 1996.

De Morais Guedes S, Vitorino R, Domingues R, Tomer K, Correia AJF, Amado F, et al. Proteomics of immune-challenged Drosophila melanogaster larvae hemolymph. Biochem Biophys Res Commun. 2005;328(1):106–15.

Moriconi M, Rugna G, Calzolari M, Bellini R, Albieri A, Angelini P, et al. Phlebotomine sand fly–borne pathogens in the Mediterranean Basin: Human leishmaniasis and phlebovirus infections. Warburg A, editor. PLoS Negl Trop Dis. 2017 Aug 10;11(8):e0005660.

Moshous D, Martin E, Carpentier W, Lim A, Callebaut I, Canioni D, et al. Whole-exome sequencing identifies Coronin-1A deficiency in 3 siblings with immunodeficiency and EBV-associated B-cell lymphoproliferation. J Allergy Clin Immunol. 2013 Jun 1;131(6):1594–1603.e9.

Mossie K, Jallal B, Alves F, Sures I, Plowman GD, Ullrich A. Colon carcinoma kinase-4 defines a new subclass of the receptor tyrosine kinase family. Oncogene. 1995;11(10):2179–84.

Muñóz-Jordán JL, Sánchez-Burgos GG, Laurent-Rolle M, García-Sastre A. Inhibition of interferon signaling by dengue virus. PNAS. 2003;100(24):14333–8.

Mylonakis E, Podsiadlowski L, Muhammed M, Vilcinskas A. Diversity, evolution and medical applications of insect antimicrobial peptides. Philos Trans R Soc Lond B Biol Sci. 2016 May 26;371(1695):20150290.

Nettles VF, Comer JA, Erickson GA, Corn JL. Isolation of Vesicular Stomatitis Virus New Jersey Serotype from Phlebotomine Sand Flies in Georgia. Am J Trop Med Hyg. 1990 May 1;42(5):476–82.

Nicolas E, Reichhart JM, Hoffmann J a., Lemaitre B. In Vivo Regulation of the IkB Homologue cactus during the Immune Response of Drosophila. J Biol Chem. 1998;273(17):10463–9.

Niu J, Meeus I, Smagghe G. Differential expression pattern of Vago in bumblebee (Bombus terrestris), induced by virulent and avirulent virus infections. Sci Rep. 2016 Dec

29;6(1):34200.

Oliveira SMP de, Moraes BA de, Gonçalves CA, Giordano-Dias CM, d'Almeida JM, Asensi MD, et al. Prevalência da microbiota no trato digestivo de fêmeas de Lutzomyia longipalpis (Lutz & Neiva, 1912) (Diptera: Psychodidae) provenientes do campo. Rev Soc Bras Med Trop. 2000 Jun;33(3):319–22.

de Oliveira SMP, de Morais BA, Gonçalves CA, Giordano-Dias CM, Vilela ML, Brazil RP, et al. Digestive tract microbiota in female Lutzomyia longipalpis (Lutz & Neiva, 1912)(Diptera: Psychodidae) feeding on blood meal and sacarose plus blood meal. Cad Saude Publica. 2001;17(1):229–32.

Oshiumi H, Matsumoto M, Seya T. Ubiquitin-mediated modulation of the cytoplasmic viral RNA sensor RIG-I. J Biochem. 2012 Jan 1;151(1):5–11.

Osta MA, Christophides GK, Kafatos FC. Effects of Mosquito Genes on Plasmodium Development. Science (80-). 2004;303:2030–2.

PAHO/WHO. Leishmaniasis Informe Epidemiológico de las Américas. Panamerican Health Organization. www.paho.org. 2018.

Paradkar PN, Duchemin JB, Voysey R, Walker PJ. Dicer-2-Dependent Activation of Culex Vago Occurs via the TRAF-Rel2 Signaling Pathway. PLoS Negl Trop Dis. 2014;8(4).

Paradkar PN, Trinidad L, Voysey R, Duchemin J-B, Walker PJ. Secreted Vago restricts West Nile virus infection in Culex mosquito cells by activating the Jak-STAT pathway. Proc Natl Acad Sci. 2012;1–6.

Patterson D, Larsen J. A perspective on protistan nomenclature. J Protozool. 1992;39(1):125–31.

Peralta PH, Tesh RB, Johnson KM, Chaniotis BN. Ecology of Viruses Isolated from Panamanian Phlebotomine Sandflies. Am J Trop Med Hyg. 1974 Mar 1;23(2):258–69.

Pereira L de OR, Maretti-Mira AC, Rodrigues KM, Lima RB, de Oliveira-Neto MP, Cupolillo E, et al. Severity of tegumentary leishmaniasis is not exclusively associated with Leishmania RNA virus 1 infection in Brazil. Mem Inst Oswaldo Cruz. 2013;108(5):665–7.

Perkins P V., Sacks DL. Development of Infective Stage Leishmania Promastigotes within Phlebotomine Sand Flies. Am J Trop Med Hyg. 1985 May 1;34(3):456–9.

Pfaffl MW. A new mathematical model for relative quantification in real-time RT-PCR. Nucleic Acids Res. 2001 May 1;29(9):45e–45.

Pieters J, Müller P, Jayachandran R. On guard: Coronin proteins in innate and adaptive immunity. Nat Rev Immunol. 2013;13(7):510–8.

Piot N, Snoeck S, Vanlede M, Smagghe G, Meeus I, Piot N, et al. The Effect of Oral Administration

of dsRNA on Viral Replication and Mortality in Bombus terrestris. Viruses. 2015 Jun 18;7(6):3172–85.

Pires ACAM, Villegas LEM, Campolina TB, Orfanó AS, Pimenta PFP, Secundino NFC. Bacterial diversity of wild-caught Lutzomyia longipalpis (a vector of zoonotic visceral leishmaniasis in Brazil) under distinct physiological conditions by metagenomics analysis. Parasit Vectors. 2017 Dec 29;10(1):627.

Pitaluga AN, Beteille V, Lobo AR, Ortigão-Farias JR, Dávila AMR, Souza AA, et al. EST sequencing of blood-fed and Leishmania-infected midgut of Lutzomyia longipalpis, the principal visceral leishmaniasis vector in the Americas. Mol Genet genomics. 2009;282(3):307–17.

Pitaluga AN, Mason PW, Traub-Csekö YM. Non-specific antiviral response detected in RNA-treated cultured cells of the sandfly, Lutzomyia longipalpis. Dev Comp Immunol. 2008;32(3):191–7.

Pons MJ, Udia Gomes C, Del Valle-Mendoza J, Ruiz J. Carrion's Disease: More Than a Sand Fly–Vectored Illness. PLoS Pathog. 2016;12(10).

Poulos BT, Tang KFJ, Pantoja CR, Bonami JR, Lightner D V. Purification and characterization of infectious myonecrosis virus of penaeid shrimp. J Gen Virol. 2006 Apr 1;87(4):987–96.

Prasad AN, Brackney DE, Ebel GD. The role of innate immunity in conditioning mosquito susceptibility to West Nile virus. Viruses. 2013;5(12):3142–70.

Pretzel J, Mohring F, Rahlfs S, Becker K. Antiparasitic Peptides. In: Vilcinskas A, editor. Yellow Biotechnology I Advances in Biochemical Engineering/Biotechnology. Springer, Berlin, Heidelberg; 2013. p. 157–92.

Pruzinova K, Sadlova J, Seblova V, Homola M, Votypka J, Volf P. Comparison of Bloodmeal Digestion and the Peritrophic Matrix in Four Sand Fly Species Differing in Susceptibility to Leishmania donovani. Oliveira PL, editor. PLoS One. 2015 Jun 1;10(6):e0128203.

Qiu X-B, Shao Y-M, Miao S, Wang L. The diversity of the DnaJ/Hsp40 family, the crucial partners for Hsp70 chaperones. Cell Mol Life Sci. 2006 Nov 4;63(22):2560–70.

Rahimi N, Averbukh I, Haskel-Ittah M, Degani N, Schejter ED, Barkai N, et al. A WntD-Dependent Integral Feedback Loop Attenuates Variability in Drosophila Toll Signaling. Dev Cell. 2016 Feb 22;36(4):401–14.

Ramalho-Ortigão JM, Kamhawi S, Joshi MB, Reynoso D, Lawyer PG, Dwyer DM, et al. Characterization of a blood activated chitinolytic system in the midgut of the sand fly vectors Lutzomyia longipalpis and Phlebotomus papatasi. Insect Mol Biol. 2005 Nov 9;14(6):703–

12.

Ramalho-Ortigão JM, Traub-Csekö YM. Molecular characterization of Llchit1, a midgut chitinase cDNA from the leishmaniasis vector Lutzomyia longipalpis. Insect Biochem Mol Biol. 2003 Mar 1;33(3):279–87.

Ramezani A, Nahad MP, Faghihloo E. The role of Nrf2 transcription factor in viral infection. J Cell Biochem. 2018;119(8):6366–82.

Ramirez JL, Dimopoulos G. The Toll immune signaling pathway control conserved anti-dengue defenses across diverse Ae. aegypti strains and against multiple dengue virus serotypes. Dev Comp Immunol. 2010;34(6):625–9.

Randall RE, Goodbourn S, Richard Randall CE, Goodbourn sgoodbourn S. Interferons and viruses: an interplay between induction, signalling, antiviral responses and virus countermeasures. J Gen Virol. 2008;89:1–47.

Raposo G, Stoorvogel W. Extracellular vesicles: Exosomes, microvesicles, and friends. J Cell Biol. 2013;200(4):373–83.

Ratcliffe NA, Gagen SJ. Studies on the in vivo cellular reactions of insects: an ultrastructural analysis of nodule formation in Galleria mellonella. Tissue Cell. 1977;9(1):73–85.

Ready PD. Epidemiology of visceral leishmaniasis. Clin Epidemiol. 2014;6:147–54.

Reichhart J-M. Tip of another iceberg: Drosophila serpins. Trends Cell Biol. 2005;15(12):659–65.

Reichhart J-M, Georgel P, Meister M, Lemaitre B, Kappler C, Hoffmann JA. Expression and nuclear translocation of the rel/NF-kappa B-related morphogen dorsal during the immune response of Drosophila. Comptes rendus l'' Académie des Sci Série III, Sci la vie. 1993;316(EPFL-ARTICLE-151760):1218–24.

Ribeiro JMC. A catalogue of Anopheles gambiae transcripts significantly more or less expressed following a blood meal. Insect Biochem Mol Biol. 2003 Sep 1;33(9):865–82.

Robalino J, Bartlett T, Shepard E, Prior S, Jaramillo G, Scura E, et al. Double-stranded RNA induces sequence-specific antiviral silencing in addition to nonspecific immunity in a marine shrimp: convergence of RNA interference and. J …. 2005;79(21):13561–71.

Robalino J, Browdy CLC, Prior S, Metz A, Parnell P, Gross P, et al. Induction of antiviral immunity by double-stranded RNA in a marine invertebrate. J …. 2004;78(19):10442–8.

Rodrigues SG, da Rosa T, Vasconcelos PFC, Travassos da Rosa ES, Tesh RB. Characterization of two new phleboviruses associated with human illness from the Amazon region of Brazil. In: An overview of arbovirology in Brazil and neighbouring countries. 1998. p. 100–6.

Rogers ME, Chance ML, Bates PA. The role of promastigote secretory gel in the origin and

transmission of the infective stage of Leishmania mexicana by the sandfly Lutzomyia longipalpis. Parasitology. 2002 May 5;124(05):495–507.

Ross R. Further notes on Leishman's bodies. Br Med J. 1903;2(2239):1401.

Rossi M, Castiglioni P, Hartley M-A, Eren RO, Prével F, Desponds C, et al. Type I interferons induced by endogenous or exogenous viral infections promote metastasis and relapse of leishmaniasis. Proc Natl Acad Sci. 2017 Apr 9;114(19):4987–92.

van Rossum AGSH, Moolenaar WH, Schuuring E. Cortactin affects cell migration by regulating intercellular adhesion and cell spreading. Exp Cell Res. 2006;312(9):1658–70.

Rutschmann S, Jung AC, Zhou R, Silverman N, Hoffmann JA, Ferrandon D. Role of Drosophila IKKγ in a Toll-independent antibacterial immune response. Nat Immunol. 2000 Oct 1;1(4):342–7.

Rutschmann S, Kilinc A, Ferrandon D. Cutting Edge: The Toll pathway is required for resistance to Gram-Positive bacterial infections in Drosophila. J Immunol. 2002;168:1542–6.

Sacks D, Kamhawi S. Molecular aspects of parasite-vector and vector-host interactions in Leishmaniais. Annu Rev Microbiol. 2001;55:453–83.

Sádlová J, Volf P. Peritrophic matrix of Phlebotomus duboscqi and its kinetics during Leishmania major development. Cell Tissue Res. 2009 Aug 27;337(2):313–25.

Saeedi R, Li M, Frohlich J. A review on lecithin:cholesterol acyltransferase deficiency. Clin Biochem. 2015 May 1;48(7–8):472–5.

Sagan SM, Sarnow P. RNAi, antiviral after all. Science (80-). 2013;342(6155):207–8.

Sánchez-Vargas I, Scott JC, Poole-Smith BK, Franz AWE, Barbosa-Solomieu V, Wilusz J, et al. Dengue Virus Type 2 Infections of Aedes aegypti Are Modulated by the Mosquito's RNA Interference Pathway. Rice CM, editor. PLoS Pathog. 2009 Feb 13;5(2):e1000299.

Sanchez-Vargas I, Travanty EA, Keene KM, Franz AWE, Beaty BJ, Blair CD, et al. RNA interference, arthropod-borne viruses, and mosquitoes. Virus Res. 2004;102:65–74.

Sanchez Clemente N, Ugarte-Gil CA, Solórzano N, Maguiña C, Pachas P, Blazes D, et al. Bartonella bacilliformis: A Systematic Review of the Literature to Guide the Research Agenda for Elimination. Walker DH, editor. PLoS Negl Trop Dis. 2012 Oct 25;6(10):e1819.

Sanders HR, Foy BD, Evans AM, Ross LS, Beaty BJ, Olson KE, et al. Sindbis virus induces transport processes and alters expression of innate immunity pathway genes in the midgut of the disease vector, Aedes aegypti. Insect Biochem Mol Biol. 2005 Nov 1;35(11):1293–307.

Sant'Anna MR, Diaz-Albiter H, Aguiar-Martins K, Al Salem WS, Cavalcante RR, Dillon VM, et al. Colonisation resistance in the sand fly gut: Leishmania protects Lutzomyia longipalpis

from bacterial infection. Parasit Vectors. 2014 Jul 23;7(1):329.

Sant'anna MR, Diaz-Albiter H, Mubaraki M, Dillon RJ, Bates P a. Inhibition of trypsin expression in Lutzomyia longipalpis using RNAi enhances the survival of Leishmania. Parasit Vectors. 2009;2(1):62.

Sant'Anna MRV, Alexander B, Bates PA, Dillon RJ. Gene silencing in phlebotomine sand flies: Xanthine dehydrogenase knock down by dsRNA microinjections. Insect Biochem Mol Biol. 2008;38(6):652–60.

Satoh T, Kato H, Kumagai Y, Yoneyama M, Sato S, Matsushita K, et al. LGP2 is a positive regulator of RIG-I- and MDA5-mediated antiviral responses. Proc Natl Acad Sci U S A. 2010 Jan 26;107(4):1512–7.

Saville-Kent W. A manual of the Infusoria: including a description of all known flagellate, ciliate, and tentaculiferous protozoa, British and foreign, and an account of the organization and the affinities of the sponges. Vol. 1. D. Bogue; 1880.

Scheffter SM, Ro YT, Chung IK, Patterson JL. The Complete Sequence of Leishmania RNA Virus LRV2-1, a Virus of an Old World Parasite Strain. Virology. 1995 Sep 10;212(1):84–90.

Schlein Y, Jacobson RL, Messer G. Leishmania Infections Damage the Feeding Mechanism of the Sandfly Vector and Implement Parasite Transmission By Bite. Proc Natl Acad Sci U S A. 1992;89(20):9944–8.

Schoggins JW, Rice CM. Interferon-stimulated genes and their antiviral effector functions. Curr Opin Virol. 2011;1(6):519–25.

Schulz F, Yutin N, Ivanova NN, Ortega DR, Lee TK, Vierheilig J, et al. Giant viruses with an expanded complement of translation system components. Science. 2017 Apr 7;356(6333):82–5.

La Scola B, Audic S, Robert C, Jungang L, de Lamballerie X, Drancourt M, et al. A giant virus in amoebae. Science (80-). 2003;299(5615):2033.

Serafim TD, Coutinho-Abreu I V., Oliveira F, Meneses C, Kamhawi S, Valenzuela JG. Sequential blood meals promote Leishmania replication and reverse metacyclogenesis augmenting vector infectivity. Nat Microbiol. 2018;3(5):548–55.

Shaw JJ, de Rosa AT, Cruz AC, Vasconcelos PF da C. Brazilian Phlebotomines as Hosts and Vectors of Viruses, Bacteria, Fungi, Protozoa (Excluding Those Belonging to the Genus Leishmania) and Nematodes. In: Brazilian Sand Flies. Springer; 2018. p. 417–41.

Sheldon TJ, Miguel-Aliaga I, Gould AP, Taylor WR, Conklin D. A novel family of single VWC-domain proteins in invertebrates. 2007;

Shi M, Lin X-D, Tian J-H, Chen L-J, Chen X, Li C-X, et al. Redefining the invertebrate RNA virosphere. Nature. 2016 Dec 23;540(7634):539–43.

Shnitsar I, Borchers A. PTK7 recruits dsh to regulate neural crest migration. Development. 2008;135(24):4015–24.

Silaghi C, Pfeffer M, Kiefer D, Kiefer M, Obiegala A. Bartonella, Rodents, Fleas and Ticks: a Molecular Field Study on Host-Vector-Pathogen Associations in Saxony, Eastern Germany. Microb Ecol. 2016 Nov 24;72(4):965–74.

Silverman N, Zhou R, Erlich RL, Hunter M, Bernstein E, Schneider D, et al. Immune Activation of NF-κB and JNK Requires Drosophila TAK1. J Biol Chem. 2003;

Sim S, Jupatanakul N, Dimopoulos G. Mosquito immunity against arboviruses. Viruses. 2014;6(11):4479–504.

Simpson RJ, Jensen SS, Lim JWEE. Proteomic profiling of exosomes: Current perspectives. Proteomics. 2008;8(19):4083–99.

Sluss HK, Han Z, Barrett T, Goberdhan DC, Wilson C, Davis RJ, et al. A JNK signal transduction pathway that mediates morphogenesis and an immune response in Drosophila. Genes Dev. 1996 Nov 1;10(21):2745–58.

Souza-Neto JA, Sim S, Dimopoulos G. An evolutionary conserved function of the JAK-STAT pathway in anti-dengue defense. Proc Natl Acad Sci U S A. 2009;106(42):17841–6.

Steimer L, Klostermeier D. RNA helicases in infection and disease. RNA Biol. 2012 Jun 27;9(6):751–71.

Stierhotf Y-D, Bates PA, Lacobson RL, Rogers ME, Schlein Y, Handman E, et al. Filamentous proteophosphoglycan secreted by Leishmania promastigotes forms gel-like three-dimensional networks that obstruct the digestive tract of infected sandfly vectors. Eur J Cell Biol. 1999;78:675–89.

Stöven S, Silverman N, Junell A, Hedengren-Olcott M, Erturk D, Engströ Y, et al. Caspase-mediated processing of the Drosophila NF-B factor Relish. PNAS. 2003;100(10):5991–6.

Strand MR. The insect cellular immune response. Insect Sci. 2008;15(1):1–14.

Strazzulla A, Cocuzza S, Pinzone MR, Postorino MC, Cosentino S, Serra A, et al. Mucosal leishmaniasis: an underestimated presentation of a neglected disease. Biomed Res Int. 2013 Jun 18;805108.

Stuart KD, Weeks R, Guilbride L, Myler PJ. Molecular organization of Leishmania RNA virus 1. Proc Natl Acad Sci U S A. 1992 Sep 15;89(18):8596–600.

Sun H, Bristow BN, Qu G, Wasserman SA. A heterotrimeric death domain complex in Toll

signaling. Proc Natl Acad Sci. 2002;99(20):12871–6.

Sun S-C, Ltndstrom I, Lee J-Y, Faye I. Structure and expression of the attacin genes in Hyalophora cecropia. Vol. 196, Eur. J. Biochem. 1991.

Suzuki M, Pritchard DK, Becker L, Hoofnagle AN, Tanimura N, Bammler TK, et al. HDL suppresses the type I interferon response, a family of potent antiviral immunoregulators, in macrophages challenged with lipopolysaccharide. Circulation. 2010;122(19):1919.

Takeuchi O, Akira S. RIG-I-like antiviral protein in flies. Nat Immunol. 2008;9(12):1327–8.

Tall AR, Yvan-Charvet L. Cholesterol, inflammation and innate immunity. Nat Rev Immunol. 2015;15(2):104–16.

Tarr PI, Aline RF, Smiley BL, Scholler J, Keithly J, Stuart K. LR1: a candidate RNA virus of Leishmania. Proc Natl Acad Sci U S A. 1988 Dec 1;85(24):9572–5.

Tauszig-Delamasure S, Bilak H, Capovilla M, Hoffmann JA, Imler J-L. Drosophila MyD88 is required for the response to fungal and Gram-positive bacterial infections. Nat Immunol. 2002;3(1):91.

Telleria EL, Martins-da-Silva A, Tempone AJ, Traub-Csekö YM. Leishmania, microbiota and sand fly immunity. Parasitology. 2018 Jun 20;1–18.

Telleria EL, Sant'Anna MR V, Ortigão-Farias JR, Pitaluga AN, Dillon VM, Bates PA, et al. Caspar-like gene depletion reduces leishmania infection in sand fly host Lutzomyia longipalpis. J Biol Chem. 2012;287(16):12985–93.

Telleria EL, Sant'Anna MRV, Alkurbi MO, Pitaluga AN, Dillon RJ, Traub-Csekö YM. Bacterial feeding, Leishmania infection and distinct infection routes induce differential defensin expression in Lutzomyia longipalpis. Parasit Vectors. 2013;6(1):12.

Ten RM, Payal C V, Israel1 N, Le Bail O, Mattei2 M-G, Virelizierl J-L, et al. The characterization of the promoter of the gene encoding the p50 subunit of NF-xB indicates that it participates in its own regulation. Vol. 1, The EMBO Journal. 1992.

Tesh R, Saidi S, Javadian E, Loh P, Nadim A. Isfahan virus, a new vesiculovirus infecting humans, gerbils, and sandflies in Iran. Am J Trop Med Hyg. 1977;26(2):299–306.

Tesh RB. The genus Phlebovirus and its vectors. Annu Rev Entomol. 1988;33:169–81.

Tesh RB, Boshell SJ, Modi GB, Morales AA, Young DG, Corredor AA, et al. Natural Infection of Humans, Animals, and Phlebotomine Sand Flies with the Alagoas Serotype of Vesicular Stomatitis Virus in Colombia. Am J Trop Med Hyg. 1987 May 1;36(3):653–61.

Théry C, Clayton A, Amigorena S, Raposo G. Isolation and characterization of exosomes from cell culture supernatants and biological fluids. Curr Protoc Cell Biol. 2006;Chapter 3(Supplement

30).

Tinoco-Nunes B. Caracterização de vias de imunidade em Lutzomyia longipalpis (Diptera: Psychodidae). Instituto Oswaldo Cruz, Tese de mestrado. Fiocruz; 2014.

Tinoco-Nunes B, Telleria EL, Silva-neves M, Marques C, Azevedo-brito DA. The sandfly Lutzomyia longipalpis LL5 embryonic cell line has active Toll and Imd pathways and shows immune responses to bacteria , yeast and Leishmania. Parasit Vectors. 2016;9(222).

Tipping M, Kim Y, Kyriakakis P, Tong M, Shvartsman SY, Veraksa A. β-arrestin Kurtz inhibits MAPK and Toll signalling in Drosophila development. EMBO J. 2010;29(19):3222–35.

Towb P, Bergmann A, Wasserman SA. The protein kinase Pelle mediates feedback regulation in the Drosophila Toll signaling pathway. Development. 2001;128(23):4729–36.

Valanne S. Functional genomic analysis of the Drosophila immune response. Dev Comp Immunol. 2014;42(1):93–101.

Valanne S, Myllymäki H, Kallio J, Schmid R, Kleino A, Murumägi A, et al. Genome-Wide RNA Interference in Drosophila Cells Identifies G Protein-Coupled Receptor Kinase 2 as a Conserved Regulator of NF-κB Signaling. J Immunol. 2010;184.

Valanne S, Wang J-H, Rämet M. The Drosophila Toll signaling pathway. J Immunol. 2011;186(2):649–56.

Vale N, Aguiar L, Gomes P. Antimicrobial peptides: a new class of antimalarial drugs? Front Pharmacol. 2014 Dec 19;5:275.

Varon C, Mocan I, Mihi B, Péré-Védrenne C, Aboubacar A, Moraté C, et al. Helicobacter pullorum cytolethal distending toxin targets vinculin and cortactin and triggers formation of lamellipodia in intestinal epithelial cells. J Infect Dis. 2014;209(4):588–99.

Vilcinskas A. ANTI-infective Therapeutics from the Lepidopteran Model Host Galleria mellonella. Curr Pharm Des. 2011 May 1;17(13):1240–5.

Vizioli J, Bulet P, Charlet M, Lowenberger C, Blass C, Müller H-M, et al. Cloning and analysis of a cecropin gene from the malaria vector mosquito, Anopheles gambiae. Vol. 9, Insect Molecular Biology. 2000.

Volf P, Kiewegová A, Nemec A. Bacterial colonisation in the gut of Phlebotomus duboscqi (Diptera: Psychodidae): Transtadial passage and the role of female diet. Folia Parasitol (Praha). 2002;49:73–7.

Walters LL, Irons KP, Guzman H, Tesh RB. Formation and Composition of the Peritrophic Membrane in the Sand Fly, Phlebotomus perniciosus (Diptera: Psychodidae). J Med Entomol. 1993 Jan 1;30(1):179–98.

Wang AL, Wang CC. Viruses of the Protozoa. Annu Rev Microbiol. 1991;45:251–63.

Wang F, Xia Q. Back to homeostasis: negative regulation of NF-κB immune signaling in insects. Dev Comp Immunol. 2018 Jun 14;

Wang H, Smagghe G, Meeus I. The role of a single gene encoding the Single von Willebrand factor C-domain protein (SVC) in bumblebee immunity extends beyond antiviral defense. Insect Biochem Mol Biol. 2017 Dec 1;91:10–20.

Wang P-H, Weng SP, He JG. Nucleic acid-induced antiviral immunity in invertebrates: An evolutionary perspective. Dev Comp Immunol. 2015;48(2):291–6.

Wang P-H, Yang L-S, Gu Z-H, Weng S-P, Yu X-Q, He J-G. Nucleic acid-induced antiviral immunity in shrimp. Antiviral Res. 2013;99(3):270–80.

Wang X-H, Aliyari R, Li W-X, Li H-W, Kim K, Carthew R, et al. RNA interference directs innate immunity against viruses in adult Drosophila. Science. 2006;312(5772):452–4.

Weber A, Tauszig-Delamasure S, Gascan H. Binding of the Drosophila cytokine Spätzle to Toll is direct and establishes signaling. Nat Immunol. 2003;4(8):794–800.

Weber ANR, Moncrieffe MC, Gangloff M, Imler J-L, Gay NJ. Ligand-receptor and receptor-receptor interactions act in concert to activate signaling in the Drosophila toll pathway. J Biol Chem. 2005;280(24):22793–9.

Wertheim B, Kraaijeveld AR, Schuster E, Blanc E, Hopkins M, Pletcher SD, et al. Genome-wide gene expression in response to parasitoid attack in Drosophila. Genome Biol. 2005 Oct 31;6(11):R94.

Whalen AM, Steward R. Dissociation of the Dorsal-Cactus Complex and Phosphorylation of the Dorsal Protein Correlate with the Nuclear Localization of Dorsal. J Cell Biol. 1993;123(3):523–34.

WHO. WHO | Epidemiological situation [Internet]. WHO. World Health Organization; 2017 [cited 2018 Aug 10]. Available from: http://www.who.int/leishmaniasis/burden/en/

Wickner RB. Double-stranded RNA viruses of Saccharomyces cerevisiae. Microbiol Rev. 1996 Mar;60(1):250–65.

Widmer G, Comeau AM, Furlong DB, Wirth DF, Patterson JL. Characterization of a RNA virus from the parasite Leishmania. Proc Natl Acad Sci U S A. 1989 Aug 1;86(15):5979–82.

Widmer G, Dooley S. Phylogenetic analysis of Leishmania RNA virus and leishmania suggests ancient virus-parasite association. Nucleic Acids Res. 1995 Jun 25;23(12):2300–4.

Wiesner J, Vilcinskas A. Antimicrobial peptides: The ancient arm of the human immune system. Virulence. 2010;1(5):440–64.

Wilkins C, Gale M. Recognition of viruses by cytoplasmic sensors. Curr Opin Immunol. 2010 Feb 1;22(1):41–7.

Woollard SM, Li H, Singh S, Yu F, Kanmogne GD. HIV-1 induces cytoskeletal alterations and Rac1 activation during monocyte-blood–brain barrier interactions: modulatory role of CCR5. Retrovirology. 2014;11(1):20.

Wu H, Parsons JT. Cortactin, an 80/85-kilodalton pp60src substrate, is a filamentous actin-binding protein enriched in the cell cortex. J Cell Biol. 1993;120(6):1417–26.

Wu LP, Anderson K V. Regulated nuclear import of Rel proteins in the Drosophila immune response. Nature. 1998;392(6671):93.

Wu Q, Luo Y, Lu R, Lau N, Lai EC, Li W-X, et al. Virus discovery by deep sequencing and assembly of virus-derived small silencing RNAs. Proc Natl Acad Sci U S A. 2010 Jan 26;107(4):1606–11.

Xi Z, Ramirez JL, Dimopoulos G. The Aedes aegypti toll pathway controls dengue virus infection. Schneider DS, editor. PLoS Pathog. 2008 Jul 4;4(7):e1000098.

Xiao T, Towb P, Wasserman SA, Sprang SR. Three-dimensional structure of a complex between the death domains of Pelle and Tube. Cell. 1999;99(5):545–55.

Yi H-Y, Chowdhury M, Huang Y-D, Yu X-Q. Insect antimicrobial peptides and their applications. Appl Microbiol Biotechnol. 2014 Jul 9;98(13):5807–22.

Yoneyama M, Kikuchi M, Matsumoto K, Imaizumi T, Miyagishi M, Taira K, et al. Shared and unique functions of the DExD/H-box helicases RIG-I, MDA5, and LGP2 in antiviral innate immunity. J Immunol. 2005;175(5):2851–8.

Young DG, Duncan MA. Guide of the identification and geografic distribution of Lutzomyia Sand Flies in Mexico, West Indies, Central and South America (Diptera: Psychodidae). Mem Am Entomol Inst. 1994;54(54):1–881.

Zambon R a, Nandakumar M, Vakharia VN, Wu LP. The Toll pathway is important for an antiviral response in Drosophila. Proc Natl Acad Sci U S A. 2005;102(20):7257–62.

Zambon RA, Vakharia VN, Wu LP. RNAi is an antiviral immune response against a dsRNA virus in Drosophila melanogaster. Cell Microbiol. 2006;8(5):880–9.

Zhai Y, Attoui H, Mohd Jaafar F, Wang H -q., Cao Y -x., Fan S -p., et al. Isolation and full-length sequence analysis of Armigeres subalbatus totivirus, the first totivirus isolate from mosquitoes representing a proposed novel genus (Artivirus) of the family Totiviridae. J Gen Virol. 2010 Nov 1;91(11):2836–45.

Zhang X, Yuan Z, Zhang Y, Yong S, Salas-Burgos A, Koomen J, et al. HDAC6 modulates cell

motility by altering the acetylation level of cortactin. Mol Cell. 2007;27(2):197–213.

Zhang Y, Li L-F, Munir M, Qiu H-J. RING-Domain E3 Ligase-Mediated Host-Virus Interactions: Orchestrating Immune Responses by the Host and Antagonizing Immune Defense by Viruses. Front Immunol. 2018;9:1083.

ANNEX-A. PRIMERS LIST

GENE NAME	PRIMER ID	SEQUENCE (5'-3')
Actin (Leishmania)	ACTIN_LEISH-F	GTC GTC GAT AAA GCC GAA GGT GGT T
	ACTIN_LEISH-R	TTG GGC CAG ACT CGT CGT ACT CGC T
Actin interacting protein-1	WD40-1-F	GAATTCCGGAAATGGTGTAA
	WD40-1-R	TATCTTCGCCCATTGCTTTA
Argonaute2	AGO2-F	GACGCACCCGAGTCCAGAT
	AGO2-R	CCCGTATAGCGGAACCCA
Attacin	ATTACIN-F	AGGCTGATCCTCTGGGTCCTGT
	ATTACIN-R	ATGGGCATGGCAGCGTCTCT
B Galactosidase (for dsRNA)	DSBGAL-F	**TGG CGC CCC TAG ATG** TGA TGG CAC CCT GAT TGA
	DSBGAL-R	**TGG CGC CCC TAG ATG** TCA TTG CCC AGA GAC CAG A
Barrier-to-autointegration factor	BAUTF-F	GAGAGAAGTCGGTGACAGAATTGG
	BAUTF-R	ACACGGAGTAGGCCTTGTCAAATC
Basic transcription factor 3	BTF3-F	TCGATAGGCATCTCACGTTTCCAC
	BTF3-R	TCTTCCCCACTGTATCCAGGATGT
Cactus	CACTUS-F	CTAATCCGAATGAATCCCTACCC
	CACTUS-R	GACCCACGATCACGGCTAGA
Cactus (for dsRNA)	DSCAC-F	**TGG CGC CCC TAG ATG** CGG TGA TTC GGG CTT TAT
	DSCAC-R	**TGG CGC CCC TAG ATG** GCA GGG GTA GGG ATT CAT T
Caspar	CASPAR-F	CCAAAGAGGAGGCAAGAAAGA
	CASPAR-R	TTCCGCTTCAAGACGCATA
Cecropin	CECROPIN-F	TGGCAGTCCTGACCACTGGA
	CECROPIN-R	CTTCTCCACTGAACGGTGAACG
Coatomer delta subunit	CLATADAP-F	TAGCCGATGAGAAGTTCGGGAAGA
	CLATADAP-R	CAAACGCACCCCAATGTCGATAAG
Coronin-6	WD40-2-F	GGTCATATGGAATGTGGGTA
	WD40-2-R	AGTTTCGATCCATCCCAAT
Defensin 1	DEF1-F	GCTGCAAATCCTGCAAAGA
	DEF1-R	CCCAAGGAGGTCACAGGTTA
Defensin 2	DEF2-F	TGAAGAGATTCCTGAAGCACC
	DEF2-R	TGAAGAGATTCCTGAAGCACC
Defensin 3	DEF3-F	TGAAGAGATTCCTGAAGCACC
	DEF3-R	TGAAGAGATTCCTGAAGCACC
Defensin4	DEF4-F	ATCCATCCTTTATGCAACCG
	DEF4-R	GCCTTTGAGTCGCAGTATCC
Dicer2	DICER2-F	AGGATGGTGGGAAGCGCAGT
	DICER2-R	TCCACCTGCATGTCTCCCGT
Dorsal	DORSAL-F	CAATCTCGTGGGAAAGGATG
	DORSAL-R	ACCCGGAGAGCTTCTTCAAT

FK506 binding protein	FKBP-F	TGAGTTTGAACGTGCCCAGGAT
	FKBP-R	AAGGGTGCCAAGTACATCAAGGAG
Glyceraldehide-3-phosphate dehydrogenase (*L.longipalpis*)	GAPDH-F	TTCGCAGAAGACAGTGATGG
	GAPDH-R	CCCTTCATCGGTCTGGACTA
Glyceraldehide-3-phosphate dehydrogenase (*Leishmania*)	GAPDH_LEISH-F	TCGTGTCTTCGGACTTCAAC
	GAPDH_LEISH-R	ACCCGTTTCGTTGTCGTAC
Hemocytin	VWC_FOW	TTGCCTGAATCTCATTTGC
	VWC_REV	TGTAGCCAATTTTGCACTG
Histone	HISTONE-F	GAAAAGCAGGCAAAGACTCC
	HISTONE-R	GAAGGATGGGTGGAAAGAAG
Kinesin	KINESIN-F	GCGCGATCGTAAACGGTACCAATA
	KINESIN-R	TCCAGCACGAATTGGCTTAGCA
Lecithin cholesterol acyltransferase	LCAT-F	AGCCGTGAAGGTCTTTGCCATT
	LCAT-R	CAAATTACATCCCCATCCCTGGCA
Leishmania RNA virus_pair1	LRV1-PAIR1-F	CTGACTGGACGGGGGGTAAT
	LRV1-PAIR1-R	CAAAACACTCCCTTACGC
Leishmania RNA virus_pair2	LRV1-PAIR2-F	GGTAATCGAGTGGGAGTCC
	LRV1-PAIR2-R	GCGGCAGTAACCTGG
Phosphoinositide-binding protein	PIBP-F	TGTGAATGCGGCCTGCTTGATA
	PIBP-R	TGACAAATACTCGGCCAGTACTGC
Pias	PIAS-F	GCCACAAGGGTTGAGCACAT
	PIAS-R	GACACTGCTTCCCGTTGACTTT
Proliferating cell nuclear antigen	PCNA-F	CATGAATCTCGACCAGGAGCACTT
	PCNA-R	TTTGCACGCATTTGCCGTGA
R2D2	R2D2-F	CTGAAACAGACTACGTTGGCACA
	R2D2-R	AGGCATCCACCTGCACAAA
Regulator of chromosome condensation	RCCGJ1-F	AGACTTGGGTTGGGTGAAAAGACG
	RCCGJ1-R	GTGAGGGCAAAGCTCTGAGAAT
Relish2	RELISH2-F	ACGGGATTGCTCTGACTACG
	RELISH2-R	ACGGCTTGTAGGTGAAGTGC
Repressor splicing factor1	RRM-F	GAAGCTCAATAGCGTGT
	RRM-R	CGAGAACTTCGCTGCCATTGA
Ribosomal 16S	16S-F	TCCTACGGGAGGCAGCAGT
	16S-R	GGAGTACCAGGGTATCTAATCCTGTT
RP49	RP49-F	GACCGATATGCCAAGCTAAAGCA
	RP49-R	GGGGAGCATGTGGCGTGTCTT
Signal Transducer and Activator of Transcription proteins	STAT-F	GGCTCCAAAGATTCCGACAA
	STAT-R	AGGAAGAGAAAGAAGCGGGATGTCG

Src substrate cortactin	SH3-F	TCAAAGCGGTAGCCTTGTA
	SH3-R	CATTTCAATGTGCGTGATG
T7	T7	TAA TAC GAC TCA CTA TAG GG
T7+Adaptor sequence	T7+ ADAPTOR	**CCG TAA TAC GAC TCA CTA TAG GGT GGC GCC CCT AGA TG**
Thioredoxin	THRX-F	GCTTTCTGTGGCAATTTTC
	THRX-R	CAGCATATTCAGGCTTTCCT
Transketolase	TRANSK-F	TGTTAGCTGCGAACGTGCTGTA
	TRANSK-R	CATTCGCACATCCCGACCAAATAC
Transmembrane protease serine9-like	TPSER9-F	TCCACAATCCGGATGCAGACATAG
	TPSER9-R	TTCTGAGATCGTCAATCGGGTTGG
Tubulin	TBCA-F	CGTACGAAAAGGAAGCAGATCAGCA
	TBCA-R	ATGAACACGTGATCCGGAAGGAAG
Tyrosine-specific protein phosphatase	SHP1-R	TAC GTC TCT CCT CCT TGC CA
	SHP1-F	TCA GAC ACA GGA ATG GGG AC
Tyrosine kinase	TYRK-F	GAATGCCTCAAACCCATCCTGACA
	TYRK-R	AGAGCAACGGTGAGTTGGCTAA
Vago2	VAGO2-F	CGGGAAAATGCTGGGATGAAACAC
	VAGO2-R	CACCGGATATTCCGAGGTCTTTGT
Valine-tRNA ligase	VTRNALI-F	GCCCATGATAAAGCCACAGTGGTA
	VTRNALI-R	TGGGCTTCCGGAAGGATTTTGA
Vigilin	VIGILIN-F	TACGCATCTATCCGCGTCTCATTG
	VIGILIN-R	CACCTGTCTTGGGGAATTTCACCT
Vir-1	VIR-1-F	TAGTCCCGGATTTGACTTGG
	VIR-1-R	GTGTCAGGGGTTCATTCGTT
Wnt inhibitor of Dorsal	WNTD-F	CGTGTTCCATTCAAACATGC
	WNTD-R	GCGTCCACTATTATCAATGGC
WntD (for dsRNA)	DSWNTD-F	TAA TAC GAC TCA CTA TAG GG TTTTCCCGAAATAACCAGTGA
	DSWNTD-R	TAA TAC GAC TCA CTA TAG GG TAATTCCGAGCATTTTTCGC

***Sequences in blue** represent the T7 sequence required for dsRNA synthesis

***Sequences in red** represent adaptor sequences between gene and T7 sequences (require and extra PCR step for template preparation before dsRNA synthesis)

ANNEX-B. LIST OF PROTEINS PRESENT IN POLY(I:C) TRANSFECTED CELLS ONLY

Average of intensity	Mol. weight [kDa]	Protein IDs	Gene name	Pfam
32731000	36,507	LLOJ001758-PA	**Leucine-rich repeat protein / carboxypeptidase N subunit 2-like**	Leucin-rich repeat
29965000	111,55	LLOJ006761-PA	**ATP-dependent RNA helicase A**	DEAD/DEAH box helicase domain/ RWD domain (Zinc finger, CCCH-type)
9693900	32,669	LLOJ000307-PA	**Alpha-tocopherol transfer protein-like**	CRAL-TRIO lipid binding domain
6111800	15,162	LLOJ005291-PA	**Putative peptidyl-trna hydrolase PTRHD1**	Peptidyl-tRNA hydrolase, PTH2
5178800	59,56	LLOJ001309-PA	**Synaptic vesicle glycoprotein 2B-like**	Major facilitator, sugar transporter-like
1431700	82,102	LLOJ009642-PA	**Leucine zipper putative tumor suppressor 2 homolog**	Family Fez1 (contains a leucine-zipper region)
1106500	64,395	LLOJ003029-PA	**Elongation factor Tu, mitochondrial**	Transcription factor, GTP-binding domain/SUPERFAMILY Translation elongation factor EF1A/initiation factor IF2gamma, C-terminal
857690	279,77	LLOJ007948-PA	**Protein unc-80 homolog**	Cation channel complex component UNC80, N-terminal
559570	18,292	LLOJ007947-PA	**Myosin light chain alkali**	Myosin light chain alkali
538690	121,42	LLOJ005689-PA	**Isovaleryl-coa dehydrogenase, mitochondrial**	Acyl-CoA dehydrogenase, conserved site/ Isovaleryl-CoA dehydrogenase/ Proteasome beta-type subunit, conserved site
520320	211,33	LLOJ007856-PA	**Glutamate synthase**	Dihydroprymidine dehydrogenase domain II/FAD/NAD(P)-binding domain/Glutamate synthase, alpha subunit, C-terminal
506730	55,832	LLOJ000817-PA	**E3 ubiquitin-protein ligase RNF13**	PA domain/Zinc finger, RING-type
501760	22,391	LLOJ001625-PA	**60S ribosomal protein L11**	Ribosomal protein L5 domain superfamily
413300	34,93	LLOJ001875-PA	**Cell division cycle 37**	Cdc37, Hsp90 binding
399030	20,108	LLOJ006348-PA	**Arf3: ADP-ribosylation factor 3**	Small GTPase superfamily, ARF/SAR type
397040	53,248	LLOJ009369-PA	**S-adenosylhomocysteine hydrolase-like protein**	Adenosylhomocysteinase-like
276350	81,979	LLOJ008241-PA	**Sphingomyelin phosphodiesterase**	Calcineurin-like phosphoesterase domain, ApaH type/Sphingomyelin phosphodiesterase

225500	12,685	LLOJ001189-PA	**Vesicle transport v-SNARE 12**	Family V-SNARE_C (SNARE region achored in the vesicule membrane c-terminus)
212860	22,794	LLOJ003622-PA	**Flavin reductase (NADPH)**	NAD(P)-binding domain
209680	16,48	LLOJ004428-PA	**Protein NPC2 homolog**	MD-2-related lipid-recognition domain
182270	367,59	LLOJ001307-PA	**Ankyrin-3 isoform**	Death domain
172480	44,422	LLOJ001204-PA	**DNAJ-like protein 2**	Chaperone DnaJ/Heat shock protein DnaJ, cysteine-rich domain
164180	22,819	LLOJ005349-PA	**Vacuolar protein sorting-associated protein 37B**	Modifier of rudimentary, Modr/Vacuolar protein sorting-associated protein 37 VPS?
147320	63,832	LLOJ000061-PA	**Ionotropic receptor 21a-like [Aedes albopictus]**	domain superfamily
145980	33,116	LLOJ006682-PA	**Golgi phosphoprotein 3 homolog sauron [Aedes albopictus]**	Golgi phosphoprotein 3-like
145360	27,818	LLOJ004857-PA	**Guanylate kinase**	Guanylate kinase/L-type calcium channel beta subunit
144650	23,607	LLOJ009131-PA	**SH3 domain-binding glutamic acid-rich protein**	SH3-binding, glutamic acid-rich protein
137340	16,03	LLOJ003521-PA	**V-type proton atpase proteolipid subunit [Lutzomyia longipalpis]**	V-ATPase proteolipid subunit C-like domain
119910	66,388	LLOJ009718-PA	**Integrin alpha-PS1 [Culex quinquefasciatus]**	Integrin alpha-2
114500	16,533	LLOJ000883-PA	**Coactosin-like protein [Drosophila busckii]**	Actin-depolymerising factor homology domain
110230	14,784	LLOJ008434-PA	**Putative nuclear transport factor 2 [Anopheles darlingi]**	Nuclear transport factor 2
103770	56,586	LLOJ001580-PA	**Ubqn: ubiquilin**	Ubiquitin family/ UBA domain
86529	44,306	LLOJ009328-PA	**Probable isoaspartyl peptidase/L-asparaginase GA20639 [Aedes aegypti]**	Peptidase T2, asparaginase 2
77600	44,194	LLOJ005310-PA	**Vacuolar atpase subunit C [Lutzomyia longipalpis]/ Vha44: vacuolar H+ atpas 44kd subunit**	ATPase, V1 complex, subunit C
77250	12,837	LLOJ005181-PA	**Elongin-C [Drosophila willistoni]/transcription elongation factor B polypeptide 1**	SKP1 component, POZ domain (tetramerisation domain)
72515	4,2241	LLOJ003536-PA	**Camp-dependent protein kinase catalytic subunit [Anopheles darlingi]**	Phosphorilase kinase; domain1.
70178	37,95	LLOJ000658-PA	**26S proteasome non-atpase regulatory subunit 7 [Drosophila serrata]**	JAB1/MPN/MOV34 metalloenzyme domain
69580	208,12	LLOJ007054-PA	**Uncharacterized protein**	PDZ domain/Sterile alpha motif domain

68567	51,637	LLOJ001587-PA	**Sorting nexin [Anopheles darlingi]**	Sorting nexin Vps5-like, C-terminal/Phox homologous domain
62652	84,096	LLOJ005056-PA	**Lamin [Anopheles darlingi]**	Ribosome binding protein-1

Note: Proteins in this table are organized in a descendant manner according to the intensity values in mass spectrometry data (First colum)

ANNEX-C. LIST OF PROTEINS PRESENT IN MOCK-TRANSFECTED CELLS ONLY

Average of intensity	Mol. weight [kDa]	Protein IDs	Gene name
85802000	21,301	LLOJ000465-PA	**Transcriptional repressor protein YY1 isoform X2 [Bombus terrestris]**
20404000	451,82	LLOJ004905-PA	**Cytoplasmic dynein heavy chain [Culex quinquefasciatus]**
15129000	287,89	LLOJ004049-PA	**Trehalose-6-phosphate synthase [Anopheles darlingi]**
14929000	161,26	LLOJ005958-PA	**Scavenger receptor class B member 1 isoform X2 [Aedes aegypti]**
2578400	292,64	LLOJ006837-PA	**Serine/threonine-protein kinase ATR-like [Aedes aegypti]**
1461580	34,99	LLOJ009492-PA	**60S ribosomal protein L22 [Anopheles darlingi]**
1164000	45,703	LLOJ008699-PA	**Putative protein**
1020700	21,523	LLOJ005293-PA	**ADP ribosylation factor [Culex quinquefasciatus]**
933300	19,412	LLOJ000706-PA	**Serine protease inhibitor 88Ea isoform X2 [Aedes aegypti]**
864130	5,0738	LLOJ006630-PA	**Ras-associated protein 2-like, isoform A [Drosophila melanogaster]**
846010	37,184	LLOJ004963-PA	**Tetraspanin**
778315	22,788	LLOJ000216-PA	**Proteasome subunit beta type**
757567	430,49	LLOJ006928-PA	**Multidrug resistance-associated protein 1 [Culex quinquefasciatus]**
748820	18,8	LLOJ004479-PA	**Uncharacterized protein**
664130	29,773	LLOJ000528-PA	**Histone H2B**
625760	15,682	LLOJ002153-PA	**Putative protein**
615210	34,432	LLOJ008664-PA	**Putative protein**
592665	30,682	LLOJ005519-PA	**Putative protein**
584170	68,231	LLOJ001958-PA	**Putative protein**
582660	35,593	LLOJ004001-PA	**Putative protein**
557580	61,976	LLOJ007792-PA	**Polypeptide N-acetylgalactosaminyltransferase**
521140	22,714	LLOJ004050-PA	**Prx6: peroxiredoxin**
512410	147,52	LLOJ006834-PA	**Putative protein**
510630	47,022	LLOJ008118-PA	**Putative protein**
502305	36,41	LLOJ001680-PA	**Cn-IIIB: pyrimidine 5-nucleotidase**
495350	45,087	LLOJ008920-PA	**Putative protein**
470960	73,902	LLOJ000284-PA	**Putative protein**
453360	9,8967	LLOJ000837-PA	**Putative protein**
450790	89,92	LLOJ008986-PA	**Putative protein**

428120	46,984	LLOJ005751-PA	**Putative protein**
416590	64,406	LLOJ008211-PA	**Putative protein**
384015	68,542	LLOJ002061-PA	**Putative protein**
349980	7,2714	LLOJ009846-PA	**Putative protein**
343430	44,244	LLOJ009318-PA	**Clathrin light chain**
332840	68,089	LLOJ003921-PA	**Putative protein**
315320	30,07	LLOJ003779-PA	**Proteasome subunit beta type**
303120	53,467	gi|28863959	**Midgut chitinase [Lutzomyia longipalpis]**
298940	25,503	LLOJ005369-PA	**Putative protein**
291425	63,78	LLOJ009502-PA	**Putative protein**
233070	13,41	LLOJ002783-PA	**Putative protein**
228940	38,61	LLOJ008404-PA	**Sptr: sepiapterin reductase**
185620	88,063	LLOJ000629-PA	**Putative protein**
143850	13,625	LLOJ008203-PA	**Putative protein**
140990	38,731	LLOJ006277-PA	**Putative protein**
139370	12,199	LLOJ010480-PA	**Putative protein**
133050	52,442	LLOJ004613-PA	**Putative protein**
126200	85,497	LLOJ010074-PA	**Putative protein**
120460	17,574	LLOJ002171-PA	**Rpl26: 60S ribosomal protein L26**
120270	9,9363	LLOJ002348-PA	**Putative protein**
106410	47,489	LLOJ006694-PA	**Pain: transient receptor potential channel**
105230	26,386	LLOJ005434-PA	**Putative protein**
103050	12,849	LLOJ003411-PA	**Tubulin-specific chaperone A**
97565	24,066	LLOJ000618-PA	**Putative protein**
91641	12,698	LLOJ004934-PA	**Putative protein**
86135	11,561	LLOJ006494-PA	**Rps23: 40S ribosomal protein S23**
79418	7,4795	LLOJ001477-PA	**Adenylosuccinate synthetase**
70609	39,966	LLOJ007893-PA	**Putative protein**
59573	42,232	LLOJ004507-PA	**Putative protein**
58189	11,055	LLOJ008457-PA	**Putative protein**
50104	65,73	LLOJ008900-PA	**Serine/threonine protein phosphatase 2 alpha**

Note: Putative proteins sequences were not blast against NCBI data base to find possible homologs, it was given priority to T only proteins. Proteins in this table are organized in a descendant manner according to the intensity values in mass spectrometry data (First colum)

ANNEX-D. LIST OF SHARED PROTEINS BETWEEN M AND T GROUP

Average of Intensity	Mol. weight [kDa]	LOGFC	Protein ID	Gene name	Pfam
120701444	158,64	0,503	LLOJ001742-PA	**Phenoloxidase 2**	
112575750	109,47	0,406	LLOJ008861-PA	**T-complex protein 1 subunit beta**	Chaperonin Cpn60/TCP-1 family/TCP-1-like chaperonin intermediate domain superfamily
85947556	41,82	0,578	LLOJ009270-PA	**Actin-4 [Bombyx mori]**	Actin family
67783462	15,933	-0,100	LLOJ005027-PA	**Deoxyuridine 5'-triphosphate nucleotidohydrolase [Culex quinquefasciatus]**	Dutpase-like
47551611	47,414	0,012	LLOJ000006-PA	**Cht1: chitinase**	
45120882	61,398	-0,038	LLOJ004160-PA	**Papilin-like isoform X2 [Aedes albopictus]**	Immunoglobulin-like domain superfamily
44381812	36,334	-0,054	LLOJ002072-PA	**Salivary apyrase [Phlebotomus papatasi]/SP36 [Phlebotomus papatasi]**	Apyrase
40723667	11,545	0,432	LLOJ002693-PA	**Uncharacterized protein**	
40527094	77,102	-0,089	LLOJ004330-PA	**Histone deacetylase 3 [Aedes aegypti]**	Histone deacetylase domain
37501833	56,29	-0,003	LLOJ001225-PA	**Annexin**	
37379422	36,22	0,298	LLOJ003303-PA	**Annexin**	
30030728	36,149	-0,450	LLOJ010018-PA	**Aldose reductase isoform X1 [Aedes aegypti]**	NADP-dependent oxidoreductase domain
27791789	8,1242	0,271	LLOJ000880-PA	**14-3-3zeta, isoform C [Drosophila melanogaster]**	14-3-3 domain superfamily
27318941	10,872	-0,140	LLOJ003574-PA	**Tetraspanin 39D [Anopheles darlingi]**	Tetraspanin/Peripherin
26903578	50,67	0,156	LLOJ001538-PA	**49 kda salivary protein [Lutzomyia longipalpis]**	Serpin superfamily
26624494	208,7	-0,104	LLOJ007577-PA	**Hemocytin isoform X1 [Stomoxys calcitrans]**	Trypsin Inhibitor-like, cysteine rich domain/von Willebrand factor, type D domain
25676067	23,883	-0,327	LLOJ008576-PA	**Ferritin**	
21812978	64,75	0,112	LLOJ009018-PA	**Leucine-rich repeat-containing protein 15-like isoform X2 [Branchiostoma belcheri]**	Leucine rich repeat 5
21380511	86,874	0,034	LLOJ008981-PA	**Elongation factor 1-alpha [Aedes aegypti]**	Transcription factor, GTP-binding domain
20661639	64,181	0,424	LLOJ010025-PA	**Regucalcin [Papilio xuthus]/anterior fat body protein [Anopheles darlingi]**	

20172237	26,075	0,387	LLOJ005427-PA	**Hsp22: heat shock protein**	SMP-30/Gluconolactonase/LRE-like region
18347050	10,614	0,842	LLOJ006936-PA	**Synaptic vesicle membrane protein VAT-1 homolog-like [Aedes aegypti]/vesicle amine transport protein [Bombyx mori]**	Groes-like superfamily
18271589	24,019	0,881	LLOJ000655-PA	**Failed axon connections isoform X2 [Ceratitis capitata]**	
17502361	39,411	-0,057	LLOJ003112-PA	**Aldo: fructose biphosphate aldolase**	
15785256	72,95	0,703	LLOJ002147-PA	**Hsc70-3: heat shock protein 70 cognate**	
15629772	20,818	0,122	LLOJ004815-PA	**Transgelin**	Calponin homology domain
15605167	52,591	0,371	LLOJ006317-PA	**Plasma glutamate carboxypeptidase [Culex quinquefasciatus]**	Peptidase M28/ PA domain
15289976	20,906	0,236	LLOJ003420-PA	**Uncharacterized protein**	
14433141	46,658	-0,537	LLOJ008989-PA	**Tetraspanin**	Tetraspanin/Peripherin
14366329	175,17	0,190	LLOJ006405-PA	**Laminin subunit beta-1 [Aedes aegypti]**	Laminin EGF domain
14296211	80,725	-0,271	LLOJ000636-PA	**Deoxyhypusine hydroxylase**	WD40 repeat/WD40/YVTN repeat-like-containing domain superfamily
14077578	43,028	-0,473	LLOJ001405-PA	**Pvr: PDGF/VEGF-receptor related**	
14004339	26,317	-0,418	LLOJ008575-PA	**Ferritin**	
13634422	42,404	0,358	LLOJ003329-PA	**Lysosomal aspartic protease [Culex quinquefasciatus]**	
13158689	37,47	0,398	LLOJ006821-PA	**Hsc70-4: heat shock protein cognate**	Heat shock protein 70 family
13072906	17,631	-0,422	LLOJ000654-PA	**Failed axon connections, isoform E [Drosophila melanogaster]**	Metaxin, glutathione S-transferase domain
12769683	176,8	-0,164	LLOJ002686-PA	**Laminin subunit gamma-1**	
12014600	23,298	0,070	LLOJ009037-PA	**GSTS1: glutathione S-transferase (GSTS1)**	
11851508	21,588	-0,131	LLOJ001554-PA	**Prx-2540-2: peroxidredoxin**	Small gtpase superfamily
10987417	98,761	0,590	LLOJ004224-PA	**Hsp83: heat shock protein 83**	Heat shock protein Hsp90 family
10773022	49,898	0,448	LLOJ000326-PA	**Tubulin beta chain**	Tubulin/ftsz, gtpase domain
10476667	93,557	0,698	LLOJ004225-PA	**Multiple inositol polyphosphate phosphatase 1 [Culex quinquefasciatus]**	Histidine phosphatase superfamily
9900299	56,881	0,019	LLOJ004346-PA	**Cystathionine beta-synthase [Musca domestica]**	Pyridoxal-phosphate dependent enzyme
9764778	35,236	-0,032	LLOJ001891-PA	**Glyceraldehyde-3-phosphate dehydrogenase [Lutzomyia longipalpis]**	Glyceraldehyde 3-phosphate dehydrogenase, catalytic domain
9696039	19,161	-0,548	LLOJ002211-PA	**Actin-depolymerizing factor 1**	Actin-depolymerising factor homology domain

9493783	20,791	0,082	LLOJ005152-PA	**Ras-like protein 3 [Ceratitis capitata, Apis melifera, Aedes albopictus]**	Small gtpase superfamily, Ras-type
9362789	40,831	0,528	LLOJ005808-PA	**IST1 homolog isoform X1 [Aedes albopictus]**	Vacuolar protein sorting-associated protein Ist1
9270288	65,858	-0,020	LLOJ008774-PA	**Tubulin alpha-1A chain [Aedes aegypti]**	Tubulin/ftsz, 2-layer sandwich domain
8720250	37,842	0,195	LLOJ007240-PA	**Cathepsin L**	Peptidase C1A, papain C-terminal
8512874	14,909	-0,400	LLOJ009052-PA	**Lipocalin**	Lipocalin/cytosolic fatty-acid binding domain
7951435	70,086	0,184	LLOJ001213-PA	**Hsc70-2: heat shock protein 70 cognate 2**	Heat shock protein 70 family
7186665	100,04	0,247	LLOJ010503-PA	**Peroxidasin isoform X2 [Aedes aegypti]**	Haem peroxidase, animal type
7048668	69,904	0,808	LLOJ006803-PA	**Putative protein**	
7000417	198,23	0,541	LLOJ003616-PA	**Putative protein**	
6922849	46,762	0,064	LLOJ000219-PA	**Putative enolase [Lutzomyia longipalpis]**	
6826661	45,342	0,672	LLOJ000425-PA	**Putative protein**	
6630488	38,828	-0,336	LLOJ007578-PA	**Hemocytin**	
6355144	74,859	-0,205	LLOJ005278-PA	**Putative protein**	
6308722	73,975	0,466	LLOJ008657-PA	**Putative protein**	
5717223	260,25	-0,852	LLOJ001484-PA	**Putative protein**	
5689163	13,191	-0,780	LLOJ005281-PA	**Putative protein**	
5642118	70,422	0,116	LLOJ003590-PA	**Programmed cell death protein 6/Juvenile hormone-inducible protein**	Pacifastin domain/VWFC domain
5519911	101,59	-0,086	LLOJ001772-PA	**Putative protein**	
5332682	57,697	0,129	LLOJ007605-PA	**Cat: catalase**	
5247857	34,179	0,261	LLOJ010472-PA	**Rplp0: 60S ribosomal protein LP0 ¡**	
5229013	33,976	1,149	LLOJ006374-PA	**Putative protein**	
5174389	24,245	-0,321	LLOJ004462-PA	**GSTD: glutathione S-transferase**	
5139278	66,068	0,604	LLOJ007632-PA	**Putative protein**	
5118287	61,409	0,444	LLOJ007425-PA	**Putative protein**	
5055028	22,353	0,046	LLOJ007174-PA	**Peptidyl-prolyl cis-trans isomerase**	
4889435	11,592	-0,245	LLOJ003617-PA	**Peptidylprolyl isomerase**	
4838023	25,699	-1,050	LLOJ001992-PA	**Putative protein**	
4733808	11,81	0,253	LLOJ005819-PA	**Thioredoxin**	
4433171	46,369	-0,160	LLOJ008432-PA	**Putative protein**	
4380280	70,948	-0,249	LLOJ008388-PA	**Hsc70-1: heat shock protein**	
4353710	50,954	-0,061	LLOJ008139-PA	**Isocitrate dehydrogenase [NADP]**	
4324591	150,6	-0,250	LLOJ000639-PA	**Mrp4: multidrug resistance protein 4**	
4298906	39,251	-0,405	LLOJ005964-PA	**Putative protein**	

4234820	406,11	-0,344	LLOJ003765-PA	**Putative protein**	
4147503	19,827	-0,431	LLOJ008093-PA	**Putative protein**	
4028488	24,873	0,404	LLOJ001363-PA	**Putative protein**	
4016709	12,129	0,173	LLOJ006559-PA	**Gprmys2: myosuppressin receptor (gprmys2)**	
4008512	21,132	0,979	LLOJ005598-PA	**Putative protein**	
3999806	24,708	0,647	LLOJ003421-PA	**Putative protein**	
3806674	40,168	0,336	LLOJ002349-PA	**Putative protein**	
3690338	25,754	0,233	LLOJ009854-PA	**Gprstn: starry night receptor**	
3445852	44,698	0,567	LLOJ004653-PA	**Putative protein**	
3421222	15,385	-0,348	LLOJ008594-PA	**SOD: superoxide dismutase**	
3416998	94,581	0,305	LLOJ002108-PA	**Putative protein**	
3404917	68,202	0,503	LLOJ009754-PA	**Vha68-1: vacuolar H+ atpase subunit**	
3334075	34,624	-0,662	LLOJ007648-PA	**Putative protein**	
3328710	31,335	0,042	LLOJ001349-PA	**Putative protein**	
3292083	114,79	0,278	LLOJ003807-PA	**Putative protein**	
3189358	64,68	0,154	LLOJ009332-PA	**Putative protein**	
3181091	9,4817	0,168	LLOJ001002-PA	**Putative protein**	
3110397	54,968	0,737	LLOJ005573-PA	**ATP synthase subunit beta**	
3067532	66,348	-0,469	LLOJ002582-PA	**Putative protein**	
3027704	46,658	0,093	LLOJ001720-PA	**Putative protein**	
3022824	24,506	-0,812	LLOJ007234-PA	**Putative protein**	
3010413	11,506	0,070	gi|157674445	**60S acidic ribosomal protein P1-like protein [Lutzomyia longipalpis]**	
3006164	33,039	-0,102	LLOJ008278-PA	**Putative protein**	
2990396	88,469	-0,142	LLOJ008702-PA	**Putative protein**	
2945054	42,716	0,387	LLOJ000130-PA	**Tubulin alpha chain**	
2942801	107,23	-0,452	LLOJ002510-PA	**Putative protein**	
2925213	135,35	0,116	LLOJ004968-PA	**Putative protein**	
2881608	110,59	-0,159	LLOJ003941-PA	**Putative protein**	
2813041	35,639	0,332	LLOJ007897-PA	**Putative protein**	
2812084	49,925	0,057	LLOJ001263-PA	**Rab GDP dissociation inhibitor**	
2786120	86,052	-0,278	LLOJ007339-PA	**Hsp70C: heat shock protein 70C**	
2766985	22,921	0,295	LLOJ003036-PA	**Putative protein**	
2731646	44,933	0,220	LLOJ010023-PA	**Putative protein**	
2689068	45,197	-0,053	LLOJ001445-PA	**Aminoacylase**	
2672241	28,403	0,208	LLOJ006182-PA	**Putative protein**	

2669299	23,041	-0,601	LLOJ007340-PA	**Putative protein**	
2630117	104,52	-0,454	LLOJ001459-PA	**Putative protein**	
2598971	22,635	-0,470	LLOJ009243-PA	**PHGP: phospholipid hydroperoxide glutathione peroxidase**	
2587764	26,124	-0,532	LLOJ001624-PA	**Ubiquitin carboxyl-terminal hydrolase**	
2585973	20,388	-0,904	LLOJ009449-PA	**Lactoylglutathione lyase**	
2397047	93,171	-0,194	LLOJ007144-PA	**Sodium/potassium-transporting atpase subunit alpha**	
2366102	42,15	0,205	LLOJ008844-PA	**Putative serine protease inhibitor 4 [Lutzomyia longipalpis]**	
2359631	37,144	0,537	LLOJ001626-PA	**Putative protein**	
2329722	49,955	-0,592	LLOJ006833-PA	**Putative protein**	
2283469	11,812	-0,385	LLOJ009657-PA	**Putative protein**	
2273000	23,011	0,597	LLOJ006663-PA	**Putative protein**	
2230293	83,772	0,700	LLOJ004656-PA	**Putative protein**	
2226769	68,383	-0,128	LLOJ010108-PA	**Putative protein**	
2208978	48,412	-0,276	LLOJ008678-PA	**Phosphoglycerate kinase**	
2187320	19,976	0,436	LLOJ007279-PA	**Putative protein**	
2183298	19,978	0,425	LLOJ010504-PB	**Putative protein**	
2176539	23,76	0,255	LLOJ007786-PA	**Putative protein**	
2145300	32,165	0,284	LLOJ002524-PA	**Putative protein**	
2136266	40,459	0,442	LLOJ008960-PA	**Putative protein**	
2120067	18,693	0,127	LLOJ006207-PA	**Putative protein**	
2077975	216,54	-1,211	LLOJ008763-PA	**Putative protein**	
2077260	150,91	0,492	LLOJ005904-PA	**Putative protein**	
2074618	26,038	0,251	LLOJ003270-PA	**Putative protein**	
2064768	15,567	-0,114	LLOJ000043-PA	**Putative protein**	
2032440	30,023	-0,588	LLOJ002936-PA	**Proteasome subunit alpha type**	
2031076	53,653	-0,431	LLOJ001957-PA	**Putative protein**	
2013036	26,212	-0,357	LLOJ004308-PA	**Tpi: triosephosphate isomerase**	
1997507	29,057	0,200	LLOJ006091-PA	**Proliferating cell nuclear antigen**	
1984403	91,324	0,683	LLOJ009711-PA	**Endoplasmin [Aedes aegypti]**	HSP90 Superfamily
1954960	37,108	-0,535	LLOJ009644-PA	**Putative protein**	
1938956	23,74	0,916	LLOJ004292-PA	**Putative protein**	
1935300	15,618	-0,121	LLOJ005078-PA	**Myosin light chain, partial [Lutzomyia longipalpis]**	
1919457	32,486	0,908	LLOJ003450-PA	**Putative protein**	

1906069	71,395	0,664	LLOJ010833-PA	**Putative protein**	
1898645	186,78	0,448	LLOJ003927-PA	**Integrin beta**	
1841990	23,399	-0,113	LLOJ002554-PA	**Gprccp: CCAP receptor**	
1825169	34,563	-0,453	LLOJ005822-PA	**Rpsa: 40S ribosomal protein SA**	
1744356	131,19	-0,016	LLOJ002785-PA	**Putative protein**	
1742633	219,22	-0,520	LLOJ005706-PA	**Putative protein**	
1742632	25,484	-0,860	LLOJ002085-PA	**Putative protein**	
1741899	24,334	-0,156	LLOJ004146-PA	**Putative protein**	
1695511	54,169	0,015	LLOJ005862-PA	**Putative protein**	
1690964	203,06	0,643	LLOJ007261-PA	**Putative protein**	
1688386	11,22	0,453	LLOJ010037-PA	**Putative protein**	
1663019	14,42	-0,395	LLOJ005926-PA	**Putative protein**	
1656996	21,442	-0,450	LLOJ006486-PA	**Putative protein**	
1655864	27,264	-0,170	LLOJ003382-PA	**Putative protein**	
1649169	32,147	-0,235	LLOJ000921-PA	**Putative protein**	
1648415	23,223	-0,532	LLOJ009761-PA	**Rps28: 40S ribosomal protein S28**	
1644347	70,9	0,203	LLOJ008964-PA	**Putative protein**	
1641089	20,688	-0,173	LLOJ004768-PA	**Putative protein**	
1627819	9,7251	0,160	LLOJ004619-PA	**Putative protein**	
1569960	14,998	-0,473	LLOJ009317-PA	**Putative protein**	
1566101	55,198	0,786	LLOJ004383-PA	**Putative protein**	
1546400	18,035	-0,828	LLOJ002288-PA	**Putative protein**	
1499328	41,614	0,468	LLOJ001895-PA	**Rps9: 40S ribosomal protein S9**	
1477532	28,476	-0,996	LLOJ005433-PA	**Phosphoglycerate mutase**	
1474406	61,717	0,995	LLOJ000862-PA	**SH3PX1: sortin nexin**	
1471071	94,588	-0,453	LLOJ002539-PA	**Putative protein**	
1451163	27,887	0,374	LLOJ008889-PA	**Putative protein**	
1445526	28,093	-0,745	LLOJ003612-PA	**Prosalpha7: 26S proteasome alpha 7 subunit**	
1429048	48,85	0,928	LLOJ002673-PA	**Putative protein**	
1410536	42,655	0,448	LLOJ010805-PA	**Putative protein**	
1410456	35,376	-0,224	LLOJ000319-PA	**Putative protein**	
1399134	22,902	0,136	LLOJ001836-PA	**Putative protein**	
1393054	32,795	0,414	LLOJ006748-PA	**Putative protein**	
1392312	15,74	0,046	LLOJ007676-PA	**Rps18: 40S ribosomal protein S18**	

1368852	69,763	0,650	LLOJ006488-PA	**Hsp70A: heat shock protein 70A/LLOJ005732-PA Hsp70Bb: heat shock protein 70 Bb**	
1361786	37,93	-0,130	LLOJ005520-PA	**Putative protein**	
1341338	15,285	-1,926	LLOJ004724-PA	**Rps12: 40S ribosomal protein S12**	
1328385	24,53	-0,757	LLOJ002611-PA	**Ribosomal protein**	
1324433	119,62	-0,705	LLOJ009367-PA	**ATP-citrate synthase**	
1299311	96,105	0,384	LLOJ009390-PA	**Putative protein**	
1297669	27,501	-0,172	LLOJ001686-PA	**Putative protein**	
1272369	29,249	0,312	LLOJ009873-PA	**Putative protein**	
1272059	57,858	1,339	LLOJ006795-PA	**Putative protein**	
1269542	47,667	-0,180	LLOJ002615-PA	**Putative protein**	
1255770	131,71	-1,849	LLOJ007767-PA	**Putative protein**	
1254626	158,9	0,430	LLOJ008918-PA	**Putative protein**	
1244165	10,172	0,786	LLOJ002439-PA	**Putative protein**	
1238309	54,46	-0,228	LLOJ005262-PA	**Putative protein**	
1237421	130,27	-0,233	LLOJ009050-PA	**Putative protein**	
1237189	22,449	-0,131	LLOJ002096-PA	**Putative protein**	
1235043	44,725	0,276	LLOJ000349-PA	**Putative protein**	
1196018	16,253	0,003	LLOJ004944-PA	**Putative protein**	
1195928	23,615	-0,264	LLOJ006846-PA	**40S ribosomal protein S8-like protein [Lutzomyia longipalpis]**	
1162837	48,492	-0,413	LLOJ002130-PA	**Putative protein**	
1145581	55,892	-0,768	LLOJ007890-PA	**Putative protein**	
1137886	26,744	-0,249	LLOJ004493-PA	**Putative protein**	
1129084	186,59	0,650	LLOJ003092-PA	**Putative protein**	
1126569	57,53	0,337	LLOJ006531-PA	**Putative protein**	
1123784	66,492	0,460	LLOJ010006-PA	**Putative protein**	
1112351	18,072	-0,169	LLOJ001627-PA	**Putative protein**	
1110395	8,5621	-0,739	gi|459667238	**Ribosomal protein L17, partial [Lutzomyia longipalpis]**	
1107344	13,433	-0,441	LLOJ000995-PA	**Rps20: 40S ribosomal protein S20**	
1104677	58,137	-0,575	LLOJ006842-PA	**Putative protein**	
1103342	119,12	0,390	LLOJ007298-PA	**Putative protein**	
1088753	29,511	0,163	LLOJ009006-PA	**Putative protein**	
1082465	40,058	-0,479	LLOJ008999-PA	**Putative protein**	
1065406	30,74	-0,189	LLOJ003652-PA	**Putative protein**	

1064708	118,27	0,316	LLOJ007481-PA	**Putative protein**	
1064234	128,44	-0,350	LLOJ004030-PA	**Putative protein**	
1058223	16,88	-0,577	LLOJ009173-PA	**Putative protein**	
1048645	75,52	0,806	LLOJ001603-PA	**Putative protein**	
1036083	25,171	-0,096	LLOJ008417-PA	**Putative protein**	
1033604	205,14	-1,268	LLOJ007680-PA	**Putative protein**	
1024474	30,837	-0,143	LLOJ009478-PA	**Putative protein**	
1010477	37,77	-0,411	LLOJ002507-PA	**Putative protein**	
1007504	55,082	-0,050	LLOJ009957-PA	**Putative protein**	
1000925	173,96	-0,489	LLOJ007761-PA	**Putative protein**	
982568	26,548	0,133	LLOJ000104-PA	**Putative protein**	
973848	7,1223	-0,573	LLOJ009641-PA	**Putative protein**	
972049	53,312	0,835	LLOJ010053-PA	**Putative protein**	
970838	119,56	0,167	LLOJ004461-PA	**Putative protein**	
963638	294,95	-0,692	LLOJ008380-PA	**Rhea: rhea-like talin protein**	
961222	34,551	-0,577	LLOJ008719-PA	**Putative protein**	
957485	40,313	0,740	LLOJ009748-PA	**Putative protein**	
954851	55,17	0,287	LLOJ002675-PA	**Putative protein**	
951237	76,337	0,099	LLOJ002104-PA	**Putative protein**	
948708	86,189	-0,623	LLOJ009987-PA	**Putative protein**	
939417	64,989	-0,453	LLOJ002457-PA	**Putative protein**	
939160	58,519	0,795	LLOJ000477-PA	**Putative protein**	
935234	101,59	0,049	LLOJ004342-PA	**Putative protein**	
932288	16,565	-0,223	LLOJ006446-PA	**Putative protein**	
916632	41,388	0,070	LLOJ004650-PA	**Putative protein**	
911748	30,306	0,508	LLOJ001775-PA	**Putative protein**	
905720	18,145	-0,895	LLOJ010468-PA	**Putative protein**	
905324	52,369	-0,148	LLOJ009531-PA	**Putative protein**	
895111	29,479	0,364	LLOJ010076-PA	**Putative protein**	
878599	232,07	1,127	LLOJ008853-PA	**Putative protein**	
869181	29,388	0,519	LLOJ006893-PA	**Putative protein**	
864627	17,547	-0,750	LLOJ004058-PA	**Putative protein**	
860810	25,17	-0,047	LLOJ000831-PA	**Putative protein**	
855978	13,943	-0,351	LLOJ008472-PA	**Putative protein**	
855362	21,985	-1,242	gi|157674475	**40S ribosomal protein S7-like protein [Lutzomyia longipalpis]**	
852010	42,55	-0,049	LLOJ003917-PA	**Putative protein**	

851779	29,035	-0,488	LLOJ010473-PA	**Putative protein**	
835494	48,934	0,119	LLOJ002819-PA	**Putative protein**	
830898	42,217	0,707	LLOJ002254-PA	**Putative protein**	
830881	52,93	-1,129	LLOJ002203-PA	**Putative protein**	
824182	28,6	0,273	LLOJ004953-PA	**Putative protein**	
819095	46,223	0,134	LLOJ003829-PA	**Putative protein**	
794269	56,703	-0,345	LLOJ007347-PA	**Putative protein**	
793827	45,644	0,684	LLOJ006309-PA	**Putative protein**	
785141	75,197	-0,283	LLOJ009985-PA	**Putative protein**	
779230	63,705	0,976	LLOJ004501-PA	**Putative protein**	
769793	53,782	0,190	LLOJ008890-PA	**Putative protein**	
767368	47,394	0,542	LLOJ003577-PA	**Putative protein**	
763334	34,319	-0,066	LLOJ000816-PA	**Rpl5: 60S ribosomal protein L5**	
757221	71,774	0,300	LLOJ001655-PA	**Putative protein**	
754109	53,726	0,071	LLOJ002102-PA	**Putative protein**	
740491	56,001	-0,205	LLOJ007938-PA	**Trxr1: thioredoxin reductase 1**	
738951	51,073	-0,075	LLOJ007844-PA	**Acid phosphatase activity**	
736548	21,907	0,279	LLOJ008460-PA	**Prdx1: thioredoxin peroxidase**	
736177	14,112	-1,674	LLOJ004093-PA	**Putative protein**	
735006	30,469	-0,771	LLOJ004907-PA	**Putative protein**	
728531	28,776	-0,834	LLOJ005377-PA	**Pmm: phophomannomutase**	
727009	19,516	0,154	LLOJ000429-PA	**Putative protein**	
724535	23,376	0,006	LLOJ005693-PA	**Putative protein**	
720501	61,596	-0,063	LLOJ007397-PA	**Putative protein**	
701866	39,282	-0,482	LLOJ005753-PA	**Putative protein**	
689125	11,097	-0,046	LLOJ008701-PA	**Putative protein**	
688238	24,071	-0,222	LLOJ009569-PA	**Putative protein**	
688026	24,071	0,668	LLOJ004361-PA	**60S ribosomal protein L19-like protein [Lutzomyia longipalpis]**	
676986	54,745	-0,101	LLOJ003593-PA	**Putative protein**	
671739	21,941	-0,345	LLOJ001103-PA	**Putative protein**	
670459	138,77	1,550	LLOJ003719-PA	**Putative protein**	
661667	47,95	-0,379	LLOJ001817-PA	**Putative protein**	
655062	29,405	1,287	LLOJ005905-PA	**Putative protein**	
642102	54,602	0,286	LLOJ000074-PA	**Putative protein**	
634093	32,61	0,887	LLOJ005028-PA	**Putative protein**	
632713	30,421	-0,427	LLOJ007991-PA	**Putative protein**	

631323	140,42	-0,363	LLOJ006593-PA	**Putative protein**	
628142	8,4024	-0,441	LLOJ008771-PA	**Putative protein**	
624064	47,538	-0,551	LLOJ009981-PA	**Putative protein**	
619470	26,593	-0,672	LLOJ007171-PA	**Putative protein**	
613208	28,069	0,442	LLOJ008505-PA	**Putative protein**	
611973	23,965	0,479	LLOJ004816-PA	**Putative protein**	
610191	15,699	-0,983	LLOJ008039-PA	**Putative protein**	
608851	46,749	-0,477	LLOJ009319-PA	**Putative protein**	
607423	141,18	-0,409	LLOJ004435-PA	**Putative protein**	
603683	33,256	-0,962	LLOJ002357-PA	**Putative protein**	
603367	21,559	-0,571	LLOJ001196-PA	**Dhfr: dihydrofolate reductase**	
600106	75,754	2,108	LLOJ003101-PA	**Hsc70-5: heat shock protein 70 cognate 5**	
588102	43,938	-0,270	LLOJ008886-PA	**Putative protein**	
578312	25,776	-0,017	LLOJ001526-PA	**Putative protein**	
577689	73,95	0,278	LLOJ009194-PA	**Putative protein**	
573765	19,215	-0,751	LLOJ006805-PA	**Putative protein**	
571507	42,521	-0,564	LLOJ008859-PA	**Putative protein**	
570126	69,078	-0,902	LLOJ008973-PA	**Putative protein**	
565262	33,531	-0,102	LLOJ001289-PA	**Putative protein**	
563333	133,67	-0,135	LLOJ001308-PA	**Putative protein**	
558638	10,75	-0,570	LLOJ009182-PA	**Putative protein**	
557543	41,843	0,346	LLOJ001447-PA	**Putative protein**	
555657	145,13	0,809	LLOJ001959-PA	**Putative protein**	
554679	27,735	-0,790	LLOJ000464-PA	**Putative protein**	
553907	40,378	-0,034	LLOJ002845-PA	**Putative protein**	
553358	22,017	-1,334	LLOJ005969-PA	**Putative protein**	
549245	29,335	1,188	LLOJ009864-PA	**Putative protein**	
547297	29,6	1,417	LLOJ009181-PA	**Putative protein**	
547214	40,62	-1,079	LLOJ006084-PA	**Putative protein**	
546890	60,079	0,098	LLOJ009635-PA	**Putative protein**	
545135	43,847	0,612	LLOJ008037-PA	**Putative protein**	
541488	34,278	-0,581	LLOJ004923-PA	**Putative protein**	
532280	39,883	1,694	LLOJ001031-PA	**Putative protein**	
530304	30,553	-1,130	LLOJ009136-PA	**GSTO2: glutathione S-transferase omega class**	
529842	10,053	-0,286	LLOJ001230-PA	**Putative protein**	
529325	58,385	-0,715	LLOJ000116-PA	**Putative protein**	

527568	9,844	-1,089	LLOJ008958-PA	**Putative protein**	
524862	13,36	-0,875	LLOJ008353-PA	**Putative protein**	
521939	52,149	-0,573	LLOJ002598-PA	**Putative protein**	
519939	17,246	-1,424	LLOJ002231-PA	**Putative protein**	
514671	25,444	-0,624	LLOJ008028-PA	**Clic: chloride intracellular channel**	
504441	36,006	0,193	LLOJ002807-PA	**Tumor susceptibility gene 101 [Drosophila melanogaster]**	
502357	15,986	-0,824	LLOJ004534-PA	**Putative protein**	
501545	26,647	-0,590	LLOJ005041-PA	**Putative protein**	
500201	29,938	0,336	LLOJ007871-PA	**Putative protein**	
497599	30,927	-0,222	LLOJ008611-PA	**Putative protein**	
497364	44,178	-1,218	LLOJ008643-PA	**Putative protein**	
496788	15,159	-0,521	LLOJ005039-PA	**Putative protein**	
494148	52,292	0,065	LLOJ006529-PA	**Putative protein**	
483890	242,53	-0,310	LLOJ005315-PA	**Putative protein**	
482378	27,507	0,098	LLOJ009574-PA	**Putative protein**	
481760	17,175	-0,832	LLOJ003081-PA	**Putative protein**	
481440	75,775	-0,867	LLOJ001890-PA	**Putative protein**	
481302	60,751	0,817	LLOJ007357-PA	**Putative protein**	
477300	77,236	-0,170	LLOJ006104-PA	**Putative protein**	
469767	148,61	-0,545	LLOJ007941-PA	**Putative protein**	
467828	43,912	-1,192	LLOJ004444-PA	**Putative protein**	
466865	64,51	-0,112	LLOJ005914-PA	**Putative protein**	
464577	38,903	-0,643	LLOJ008755-PA	**Putative protein**	
460773	17,783	-0,994	LLOJ005725-PA	**Putative protein**	
460049	67,267	-1,032	LLOJ006328-PA	**Putative protein**	
457870	25,366	0,625	LLOJ006059-PA	**Putative protein**	
457784	18,27	-0,447	LLOJ009148-PA	**Putative protein**	
454842	44,873	-0,295	LLOJ007146-PA	**Putative protein**	
453081	106,44	-0,231	LLOJ006000-PA	**Putative protein**	
452196	149,59	0,612	LLOJ002424-PA	**Putative protein**	
449303	57,604	-0,255	LLOJ000821-PA	**Putative protein**	
442912	56,613	0,095	LLOJ000961-PA	**Putative protein**	
429990	31,866	-1,044	LLOJ003671-PA	**Putative protein**	
427499	47,293	0,736	LLOJ005445-PA	**Putative protein**	
426948	55,763	-0,586	LLOJ000530-PA	**Putative protein**	
426388	13,67	-0,687	LLOJ007881-PA	**Putative protein**	

425803	26,526	-1,203	LLOJ009551-PA	**Putative protein**	
422072	18,432	-0,588	LLOJ001899-PA	**Skpa: S-phase kinase associate protein A**	
415004	29,876	-0,513	LLOJ001075-PA	**Putative protein**	
413683	56,897	0,707	LLOJ004952-PA	**Putative protein**	
400369	22,337	-0,965	LLOJ009742-PA	**Putative protein**	
399983	45,995	1,167	LLOJ000813-PA	**Putative protein**	
396020	24,909	-0,247	LLOJ007032-PA	**Putative protein**	
394801	26,55	-0,588	LLOJ003971-PA	**Putative protein**	
391721	50,11	-0,143	LLOJ004453-PA	**Putative protein**	
391130	119,75	1,690	LLOJ009512-PA	**Putative protein**	
390445	42,877	-0,258	LLOJ000726-PA	**Putative protein**	
384649	149,15	-0,883	LLOJ010544-PA	**Putative protein**	
383962	35,21	0,497	LLOJ006516-PA	**Mitochondrial malate dehydrogenase 2 [Anopheles darlingi]**	
381945	42,678	0,395	LLOJ000900-PA	**Putative protein**	
381677	87,982	-1,425	LLOJ008378-PA	**Putative protein**	
379225	72,644	0,374	LLOJ008282-PA	**Putative protein**	
368650	164,93	-0,383	LLOJ004993-PA	**Putative protein**	
368635	157,8	-1,741	LLOJ005841-PA	**Putative protein**	
366827	42,699	-0,949	LLOJ007086-PA	**Putative protein**	
366540	120,04	0,701	LLOJ003089-PA	**Putative protein**	
363277	44,067	-0,134	LLOJ007043-PA	**Putative protein**	
360308	29,974	0,234	LLOJ004499-PA	**Rpl6: 60S ribosomal protein L6**	
342227	44,261	-1,597	LLOJ009460-PA	**Putative protein**	
340731	32,424	-0,318	LLOJ002671-PA	**Putative protein**	
335079	44,771	-0,200	LLOJ003103-PA	**Putative protein**	
332505	121,28	-0,114	LLOJ002775-PA	**Putative protein**	
323960	46,958	-0,070	LLOJ007365-PA	**Putative protein**	
318614	37,34	0,063	LLOJ005605-PA	**Putative protein**	
318290	154,29	-0,859	LLOJ000218-PA	**Putative protein**	
317805	45,355	-0,086	LLOJ000150-PA	**Putative protein**	
315251	27,659	-0,464	LLOJ007262-PA	**Putative protein**	
314305	178,76	-0,311	LLOJ000928-PA	**Putative protein**	
311644	71,594	-0,172	LLOJ005451-PA	**Putative protein**	
308893	45,492	-0,069	LLOJ002023-PA	**Putative protein**	
303343	39,894	0,102	LLOJ009129-PA	**Putative protein**	
297576	16,963	-1,083	LLOJ009767-PA	**Putative protein**	

293900	87,682	-1,378	LLOJ008558-PA	**Putative protein**	
293891	34,271	-0,870	LLOJ003787-PA	**Putative protein**	
293367	23,879	-0,550	LLOJ010466-PA	**Putative protein**	
293108	13,217	-0,674	LLOJ008491-PA	**Putative protein**	
289656	139,44	-0,593	LLOJ003812-PA	**Putative protein**	
285974	20,985	-1,590	LLOJ009564-PA	**Putative protein**	
277915	77,48	-0,036	LLOJ005659-PA	**Putative protein**	
277207	70,393	1,640	LLOJ002103-PA	**Phb-2: prohibitin**	
276998	41,657	0,403	LLOJ009719-PA	**Putative protein**	
269369	36,514	0,224	LLOJ008752-PA	**Putative protein**	
257093	14,71	-0,136	LLOJ000161-PA	**Putative protein**	
254276	119,26	-0,150	LLOJ002327-PA	**Putative protein**	
242773	51,752	-0,752	LLOJ000823-PA	**Putative protein**	
241218	41,84	-0,756	LLOJ004103-PA	**Putative protein**	
241154	39,482	-1,216	LLOJ008670-PA	**Putative protein**	
233997	16,546	-2,035	LLOJ002776-PA	**Putative protein**	
229330	23,203	-1,288	LLOJ003102-PA	**Putative protein**	
223621	35,847	-0,721	LLOJ004163-PA	**Putative protein**	
210490	42,638	-0,473	LLOJ006769-PA	**Putative protein**	
210374	26,967	-0,856	LLOJ003920-PA	**Putative protein**	
199521	63,461	-1,611	LLOJ001370-PA	**Putative protein**	
198944	20,493	-0,968	LLOJ006270-PA	**Peptidyl-prolyl cis-trans isomerase**	
185705	49,339	-0,343	LLOJ009468-PA	**Putative protein**	
184507	43,778	1,434	LLOJ009261-PA	**Putative protein**	
169412	53,733	-1,315	LLOJ004694-PA	**Putative protein**	
166988	97,552	-1,184	LLOJ008540-PA	**Putative protein**	
166911	119,86	-1,048	LLOJ003926-PA	**Putative protein**	
160382	241,76	-0,266	LLOJ002388-PA	**Putative protein**	
153890	47,224	-0,518	LLOJ003299-PA	**Putative protein**	
151804	113,9	-1,522	LLOJ003132-PA	**Putative protein**	
150184	10,765	-0,507	LLOJ007979-PA	**Putative protein**	
119241	187,83	-0,382	LLOJ002484-PA	**Clathrin heavy chain**	

Note: Putative proteins sequences were not blast against NCBI data base to find possible homologs, it was given priority to T only proteins. Proteins in this table are organized in a descendant manner according to the intensity values in mass spectrometry data (First colum)

ANNEX-E. DETAIL OF *L. LONGIPALPIS* CACTUS GENE SEQUENCE SHOWING TFBS

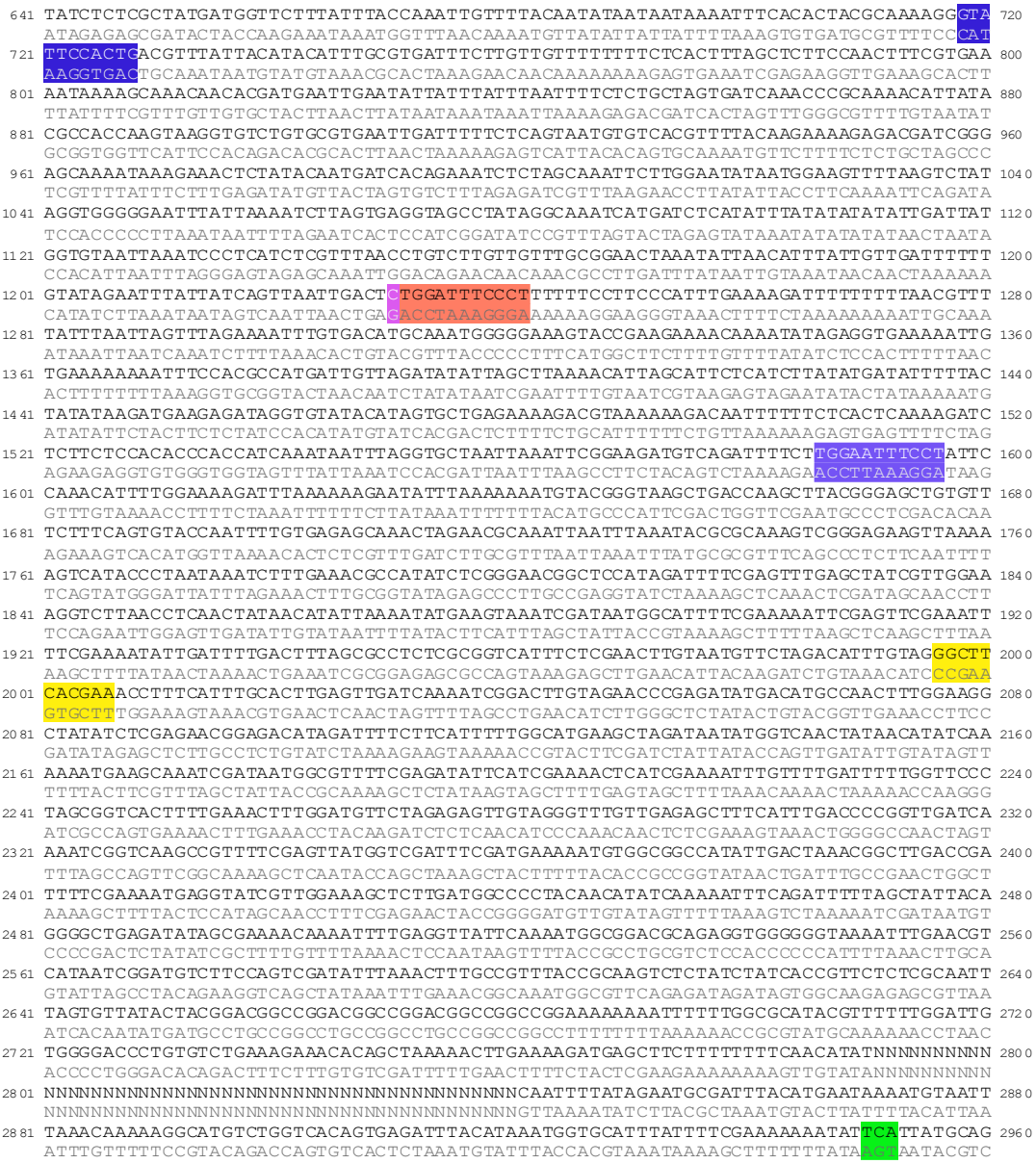

Note: Segment of Cactus gene sequence showing the four transcription factor binding sites (See colour guides below), start of transcription and start of translation (See colour guides below).

Colour guide for features in the sequence.